INTESTINAL CALCIUM ABSORPTION: MECHANISMS OF ABSORPTION AND ADAPTATIONS TO DIET- INDUCED IRON DEFICIENCY

BY

OLUWATOBI IFE-OLUWA OLUSANYA

Thesis submitted for the degree of Doctor of Philosophy in the Division of Biosciences, School of Life and Medical Sciences University College London, London, United Kingdom

Epithelial Physiology Group
Department of Neuroscience, Physiology & Pharmacology
University College London
Royal Free Campus
Rowland Hill Street
London
NW3 2PF

August 2022

Declaration

I, Oluwatobi Olusanya, confirm that the work presented in this thesis is my own. Where information has been derived from other sources, I confirm that this has been indicated in the thesis.

Signed: Oluwatobi Ife-Oluwa Olusanya

Conference Abstract and Publications

1. Olusanya O., Asowata E., Chichger H., Marks J. (2019)

Iron deficiency impacts duodenal paracellular calcium absorption via a mechanism involving claudin 2. *Future Physiology, Liverpool, UK.* ***Proc Physiol Soc*** *45, PC88.*

2. Shil A, Olusanya O, Ghufoor Z, Forson B, Marks J, Chichger H (2020).

Artificial Sweeteners Disrupt Tight Junctions and Barrier Function in the Intestinal Epithelium through Activation of the Sweet Taste Receptor, T1R3. ***Nutrients***. 22;12(6):1862. doi: 10.3390/nu12061862. PMID: 32580504; PMCID: PMC7353258.

3. Asowata EO*, Olusanya O*, Abaakil K, Chichger H, Srai SKS, Unwin RJ, Marks J (2021)

Diet-induced iron deficiency in rats impacts small intestinal calcium and phosphate absorption**.** ***Acta Physiol*** *(Oxf)*. 232(2): e13650. doi: 10.1111/apha.13650. Epub 2021 Mar 31. PMID: 33749990.

***Authors contributed equally.**

Abstract

To maintain calcium homeostasis, controlling intestinal calcium absorption is vital, and the paracellular pathway is known to predominantly mediate calcium absorption under normal dietary conditions. While the segmental profile of the transcellular pathway has provided important insights into the mechanisms of calcium absorption in the different segments of the small intestine, there is limited information regarding the paracellular pathway. In the current study, the segmental profile of paracellular calcium absorption and the underlying mechanisms were investigated *in vivo*. Paracellular calcium absorption was shown to be highest in the duodenum, however, the expression profile of the calcium-permeable claudin-2 and -12 were similar in all segments of the small intestine. Interestingly, the expression profile of claudin-15, speculated to mediate solvent drag-induced calcium absorption, mirrored the segmental differences in paracellular calcium transport. Additionally, based on the inverse relationship between iron and calcium transport, the impact of diet-induced iron deficiency on the intestinal and renal mechanisms of calcium homeostasis was investigated. Iron deficiency increased paracellular calcium absorption in the duodenum, and this was associated with upregulated duodenal claudin-2 and vitamin D receptor (VDR) expression. In addition, renal claudin-2 levels were upregulated in iron-deficient animals, even though urinary calcium excretion or serum calcium levels were unchanged. Since intestinal iron absorption mainly occurs in the duodenum, it is speculated that low cellular iron or high divalent metal transporter 1 (DMT1) levels may be linked to the increase in duodenal calcium absorption in iron deficiency. To test this speculation, deferoxamine, known to reduce cellular iron levels, resulted in upregulated VDR protein, while erythropoietin-

induced increase in DMT1 protein had no impact on VDR in Caco-2 cells. Therefore, it is hypothesised that reduced cellular iron increases VDR-mediated paracellular calcium absorption via claudin-2. This mechanism may be targeted to increase intestinal calcium absorption in patients with hypocalcaemia or bone disease.

Impact statement

To identify novel targets to control intestinal calcium absorption, this study aimed to investigate the mechanisms underlying the differences in paracellular calcium absorption across the 3 segments of the small intestine. The paracellular pathway is known to predominantly mediate calcium absorption under normal or high dietary calcium conditions, therefore, understanding the mechanisms underlying this pathway will be essential in controlling overall intestinal calcium absorption. The findings of this doctoral research showed that the duodenum has the highest capacity for paracellular calcium absorption. Surprisingly, the regional expression of the known mediators of paracellular calcium absorption in the small intestine, claudin-2 and-12, was unchanged, while claudin-15, speculated to mediate solvent drag-induced paracellular calcium absorption, showed significant segmental differences, with the highest levels seen in the duodenum. These findings provide the first evidence suggesting that claudin-15 may be an important mediator of paracellular calcium absorption in the small intestine. Importantly, because claudin-15 is not a calcium pore, it has been speculated that this claudin may be mediating solvent drag-induced calcium absorption via claudin-2. Therefore, targeting claudin-2 and claudin-15 in the duodenum may be an effective approach to increase intestinal calcium absorption in conditions associated with negative calcium balance. There is growing evidence that conditions associated with iron metabolism such as iron overload and iron deficiency are linked to increased risk of developing osteoporosis and osteopenia. However, the link between iron and calcium metabolism is poorly understood. The findings of this study demonstrate for the first time that diet-induced iron deficiency enhances duodenal paracellular calcium

absorption via a mechanism involving VDR and claudin-2. Based on this finding and the recent report that low intracellular iron results in increased cellular calcium uptake in vitro, it is speculated that intracellular iron impacts both transcellular and paracellular calcium absorption. Therefore, targeting intracellular iron levels in duodenal enterocytes may be a potentially novel approach for controlling intestinal calcium absorption in conditions associated with dysfunctional mineral metabolism. For example, reduced intracellular iron levels following hepcidin administration is now being explored as a potential therapy for increasing duodenal calcium absorption to correct bone disease in patients with β-thalassaemia and iron overload.

In addition, this is the first study to show that diet-induced iron deficiency upregulates renal claudin-2 protein levels. Claudin-2 is the major protein mediating proximal tubular calcium reabsorption, which is responsible for over 60% of total renal calcium reabsorption, and mutation in this claudin is associated with kidney stones in patients. Understanding the mechanisms by which iron deficiency upregulates renal claudin-2 will be essential in controlling excessive renal calcium excretion in these patients. Nevertheless, the findings of this study suggest that targeting claudin-2 using iron-related approaches may be an effective way of increasing proximal tubular calcium reabsorption to prevent kidney stone formation in high-risk patients.

Acknowledgement

First, I thank God Almighty, in whom is hidden all treasures of wisdom and knowledge, for surrounding me with several extraordinary individuals without whom this research project would have been impossible. I specifically wish to acknowledge my supervisors, Dr Joanne Marks and Dr Havovi Chichger for their motivation and painstaking guidance from the inception of this work till submission of the thesis. Their dedication and drive to bring out the best in me was exceptional and I hope their confidence in me was worthwhile.

I would like to thank all the staff at the Centre for Nephrology and my colleagues, specifically, Dr Anselm Zdebik, Dr Lucile Figures and Dr Anne Kesselheim for their technical assistance and encouragement in the laboratory.

The COVID-19 restrictions presented unprecedented logistical challenges during the course of this work. My family members did their utmost to minimise the impact and ensure that the project was completed in time. My husband, Dr Evans Asowata was right by my side throughout to guide and support me. I am eternally grateful to my parents for their financial support and for being an unfailing source of inspiration throughout my academic career. Finally, I thank my siblings, Yemisi, Seyi and Fikayo, wholeheartedly for their moral support and encouragement at every critical stage.

Abbreviations

$1,25(OH)_2D_3$	1,25 dihydroxyvitamin D3
ATP	Adenosine triphosphate
BBM	Brush border membrane
BSA	Bovine serum albumin
CaCA	Ca^{2+}/cation antiporter
CaM	Calmodulin
cAMP	Cyclic adenosine monophosphate
CaSR	Calcium sensing receptor
CaT	Calcium transport protein
Ca_V	Voltage-gated calcium channel
CBD	Calcium binding domain
CD	Collecting duct
cDNA	Complementary deoxyribonucleic acid
CKD	Chronic kidney disease
CNT	Connecting tubule
CTX-1	Carboxy terminal telopeptide of type I collagen
DBP	Vitamin D binding protein
DCT	Distal convoluted tubule
DCT	Divalent cation transporter 1
DcytB	Duodenal cytochrome b
DFO	Deferoxamine
DMT1	Divalent metal transporter 1
DNA	Deoxyribonucleic acid
ECaC	Epithelial calcium channel
ECF	Extracellular fluid
ECL	Extracellular loop
ECP	Exchangeable calcium pool
EDTA	Ethylenediaminetetraacetic acid
ELISA	Enzyme-linked immunosorbent assay
EPO	Erythropoietin
FGF	Fibroblast growth factor

FPN	Ferroportin
GTP	Guanosine triphosphate
HIF	Hypoxia Inducible factor
HO	Haem oxygenase
HRP	House radish peroxidase
IDA	Iron deficiency anaemia
IP3	Inositol triphosphate
IRE	Iron-regulatory element
IRP	Iron-regulatory protein
MDCK	Madin-Darby Canine kidney
mRNA	Messenger ribonucleic acid
NCX	Sodium calcium exchanger
NHE	Sodium hydrogen exchanger
NKCC	Sodium, potassium, and chloride co-transporter
Nramp	Natural resistance-associated macrophage protein
O.D	Optical density
PCBP	Poly(rC)-binding protein
PCT	Proximal convoluted tubule
PHD	Propyl-hydroxylase domain
PHD	Propyl-hydroxylase domain
PKA	Protein kinase A
PKC	Protein kinase C
PL-BD	Phospholipid binding domain
PLC	Phospholipase C
PMCA	Plasma membrane calcium ATP-ase
PTH	Parathyroid hormone
PTHR	Parathyroid hormone receptor
RNA	Ribonucleic acid
ROMK	Renal outer medullary potassium channel
RT-PCR	Reverse-transcription polymerase chain reaction
RXR	Retinoid X receptor
SEM	Standard error of mean

SGLT	Sodium-glucose transporter
SLC	Solute carrier
tAL	Thin ascending limb
TAL	Thick ascending limb
tDL	Thin descending limb
TEER	Transepithelial electrical resistance
TMB	3,3′,5,5′-Tetramethylbenzidine
TRPV	Transient receptor potential vanilloid
UIBC	Unsaturated iron binding capacity
UVB	Ultraviolent B
VDR	Vitamin D receptor
VDRE	Vitamin D response element
XIP	Exchanger inhibitory peptide

Table of Contents

List of Figures

List of Tables

Chapter 1 - Introduction

1.1. Overview of calcium homeostasis

Calcium is an essential element required for several physiological process in the body. In particular, calcium is vital for bone formation, where over 99% of calcium in the body is stored in the form of hydroxyapatite [1]. The remaining <1%, found in the soft tissues, blood and extracellular fluid, is tightly regulated and utilised for other functions such as cell signalling, muscle contraction, enzyme activation, cell differentiation and nerve impulse transmission [2]. Serum calcium exists in three forms; a free ionic form (~ 51%), a protein-bound form (~ 40%), which binds mainly to albumin and globulins, and an ionic bound form (~ 9%) complexed with small anions such as phosphate and carbonate [1]. Ionic calcium is physiologically active, and is the only form which can enter cells to carry out its characteristic functions listed above [3]. Intracellular calcium levels are maintained at ~ 0.1μM by calcium transporters (including channels, ATPases and exchangers) and the endoplasmic reticulum [4,5]. In contrast, total calcium concentrations in the extracellular fluid are maintained within 2.2mM - 2.6mM (or 1.10 - 1.35mM in the ionic form) by the intestine, kidney, and bone (**Figure 1.1)** [1]. The small intestine, and the large intestine to a lesser extent, provide the major source of calcium through absorption from the diet, with the small intestine contributing ~ 90% of total calcium absorption, while the large intestine (caecum and colon) contributes ~ 10% [6]. The kidney is the major organ responsible for calcium regulation as it responds to changes in extracellular calcium levels by altering the degree of calcium reabsorption during hypocalcaemia or hypercalcaemia. Additionally, the bone is also involved in maintaining extracellular calcium levels. When extracellular calcium levels are low the bone can restore calcium levels by increasing the rate of bone resorption, resulting in an increase in

calcium release into the circulation [1]. Furthermore, the presence of an exchangeable calcium pool (ECP) in the bone allows for the rapid exchange of calcium between the circulatory system and the bone to restore small changes in extracellular calcium levels [7]. Alongside the kidney, bone and intestine, the calcium regulating hormones: calcitriol ($1,25(OH)_2D_3$), parathyroid hormone (PTH) and fibroblast growth factor-23 (FGF23) play a crucial role in maintaining calcium balance by regulating the activity of their target organs [8].

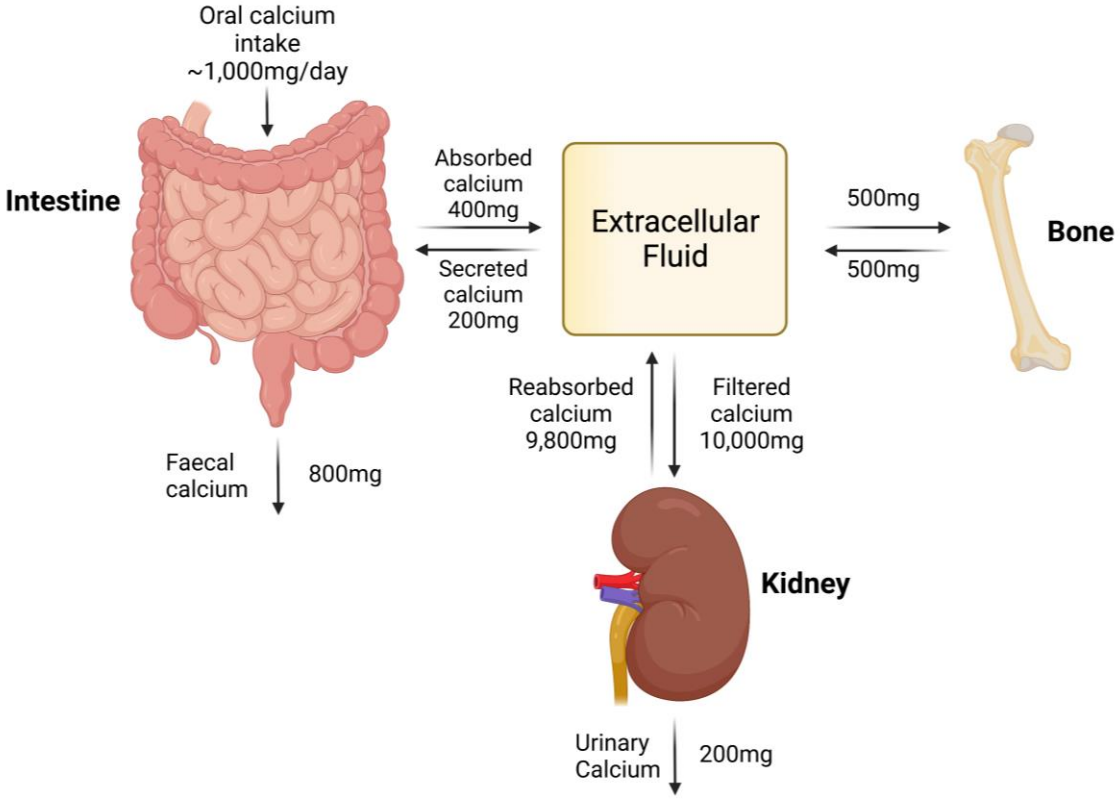

Figure 1.1. Organs involved in calcium homeostasis. To maintain calcium homeostasis, net intestinal calcium absorption (200mg) is excreted by the kidney under normal conditions. The bone acts as a storage pool for calcium from which calcium is constantly mobilised into the extracellular fluid when required and subsequently replenished when calcium is available in the circulation, thus, 500mg of calcium is constantly exchanged between the bone and extracellular fluid. *Created with BioRender.com.*

1.2. General overview of the mechanisms underlying calcium transport in the small intestine and kidney

In mammals, calcium entry into the blood and extracellular fluid occurs mainly through calcium absorption and reabsorption in the small intestine and the kidney, respectively. The mechanism of calcium transport has been extensively studied over the past 56 years and is generally accepted to occur via 2 major pathways, an active saturable (transcellular) pathway and a passive unsaturable (paracellular) pathway [9]. The transcellular pathway is a 3-step process consisting of calcium entry via the apical cell membrane into the cells, cytosolic translocation of calcium from the apical to basolateral region of the cell, and calcium extrusion across the basolateral membrane into the extracellular fluid. In the small intestine, calcium entry into the cell is mainly mediated by the transient receptor potential vanilloid 6 (TRPV6) located on the apical membrane; calbindin-D9k then shuttles calcium ions to the basolateral membrane, where calcium is transported into the circulation via the plasma membrane calcium ATP-ase type 1 (PMCA1) and the sodium calcium exchanger 1 (NCX1) [10–12] (**Figure 1.2**). Transcellular calcium transport in the distal tubular cells of the kidney is similar to the small intestine, however, TRPV5 is mainly responsible for calcium entry, calbindin-D28k shuttles calcium to the basolateral membrane where NCX1 and PMCA1 actively extrude calcium into the circulation [13–15] (**Figure 1.3**). Compared to NCX1, PMCA1 mediates a greater proportion of basolateral calcium transport in the small intestine [12,16], while the reverse is the case in the kidney where NCX1 is known to be the major basolateral calcium exporter [9,17,18]. Additionally, there is speculation that calcium transport via voltage-gated calcium

channels (e.g. Cav1.3) and vesicular calcium transport processes also contribute to the transcellular pathway for calcium absorption [19–21].

In contrast to the transcellular pathway, the paracellular pathway is a passive process that allows calcium movement between cells via tight junction proteins (**Figure 1.2 and 1.3**). There are 2 proposed mechanisms for paracellular calcium transport: simple diffusion and solvent drag. Simple diffusion occurs in the presence of an electrochemical gradient that drives the flow of free calcium ions across the intercellular space. On the other hand, solvent drag occurs in a sodium enriched intercellular space, caused by the Na+/K+-ATPase-mediated extrusion of sodium across the lateral membrane. The accumulation of sodium in this space results in the movement of water containing dissolved electrolytes including calcium through the tight junction [22,23]. There is evidence that paracellular calcium transport is controlled by various tight junction proteins present in the small intestine, including occludins and claudins. The involvement of claudins in calcium transport has been more extensively studied than occludins, with claudin-2, -12, -14, -15, -16 and -19 reported to be involved in renal and intestinal epithelial calcium transport [24–28].

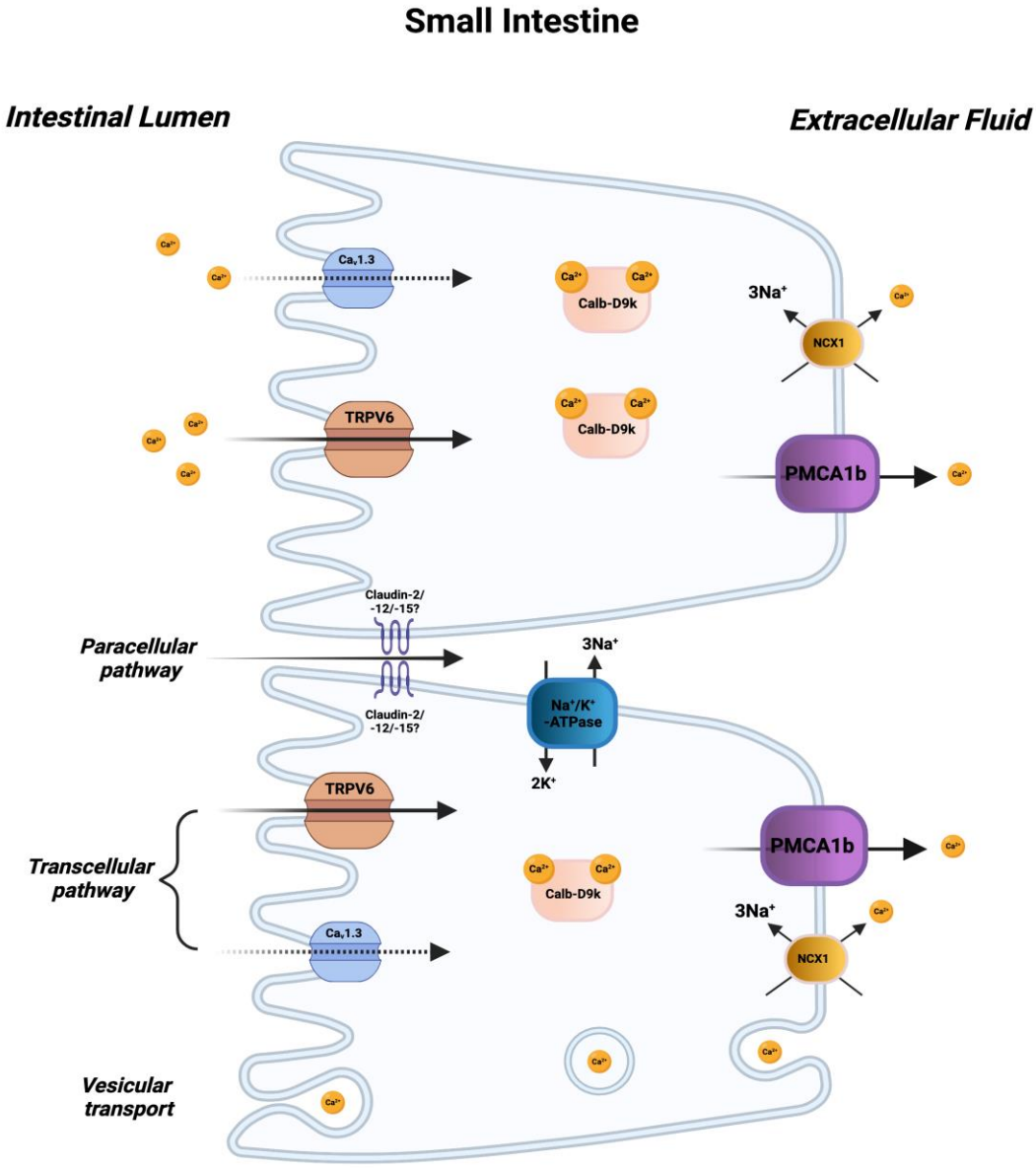

Figure 1.2. Mechanisms of intestinal calcium absorption. The intestinal epithelia absorb calcium via a transcellular and paracellular pathway. The transcellular pathway involves a three-step process; the apical entry of calcium through TRPV6 and $Ca_v1.3$, cytoplasmic translocation of calcium via calbindin-D9k (calb-D9k) and the basolateral extrusion of calcium into the extracellular fluid via PMCA1 and NCX1. The paracellular pathway occurs via the passive diffusion of calcium through claudin-2 and -12 and solvent drag, driven by the osmotic gradient created by Na^+/K^+ATPase and potentially, claudin-15. Alternatively, calcium absorption can also occur via the vesicular transport pathway. *Created with BioRender.com.*

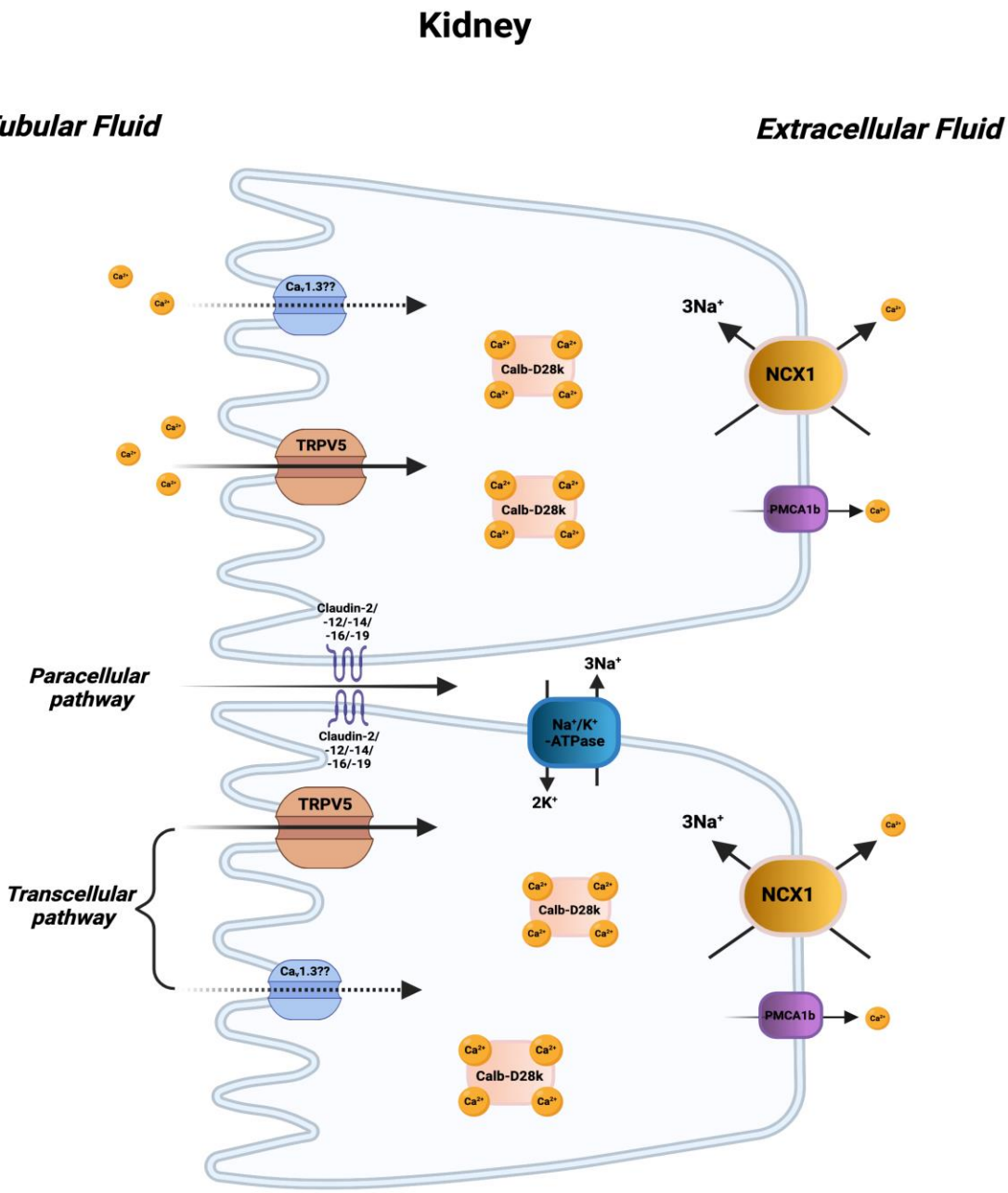

Figure 1.3. Mechanisms of renal calcium reabsorption. Renal calcium reabsorption occurs via a transcellular and paracellular pathway. The transcellular pathway is a three-step process that involves the apical entry of calcium through TRPV5 and potentially $Ca_v1.3$, followed by the cytoplasmic translocation of calcium via calbindin-D28k (calb-D28k) and the extrusion of calcium into the extracellular fluid via NCX1 and PMCA1. The paracellular pathway occurs via the passive diffusion of calcium through claudin-2, -12, -16 and -19 or solvent drag, driven by the osmotic gradient created by Na^+/K^+ATPase. *Created with BioRender.com.*

1.2.1. Calcium entry: epithelial calcium channels (ECaC)

Two epithelial calcium selective channels have been identified to play a role in the entry of calcium ions into epithelial cells, TRPV5 and TRPV6. TRPV5 (also known as ECaC1 and CaT2) and TRPV6 (also called ECaC2 and CaT1) are members of the transient receptor potential vanilloid family, which is a subfamily of the transient receptor potential (TRP) cation channel superfamily.

1.2.1.1. Structure of transient receptor potential cation channels

The TRP family consists of 28 members and are categorised into six subfamilies including the vanilloid subfamily. The vanilloid family consists of six isoforms in which TRPV1-4 are identified as heat sensitive ion channels, while, TRPV5 and TRPV6 are involved in cellular calcium uptake [29]. The human TRPV5 and TRPV6 proteins consist of 729 amino acid residues and 725 amino acid residues, respectively, with a predicted molecular weight of 83kDa [30,31]. While these channels show 75% amino acid homology, their differences are mainly located within the N- and C-terminal tails [30]. Both isoforms consist of 4 identical subunits, with each subunit containing 6 transmembrane spanning domains and a hydrophobic putative loop structure located between domain 5 and 6, predicted to form the calcium pore **(Figure 1.4)** [32]. Within the pore region, a single negatively charged aspartic acid (Asp^{542}) residue is located, which determines the calcium permeability function of the channel [32,33]. Each subunit also contains an intracellular N- and C- terminal, containing binding sites that modulate the activity and trafficking of the channel [32].

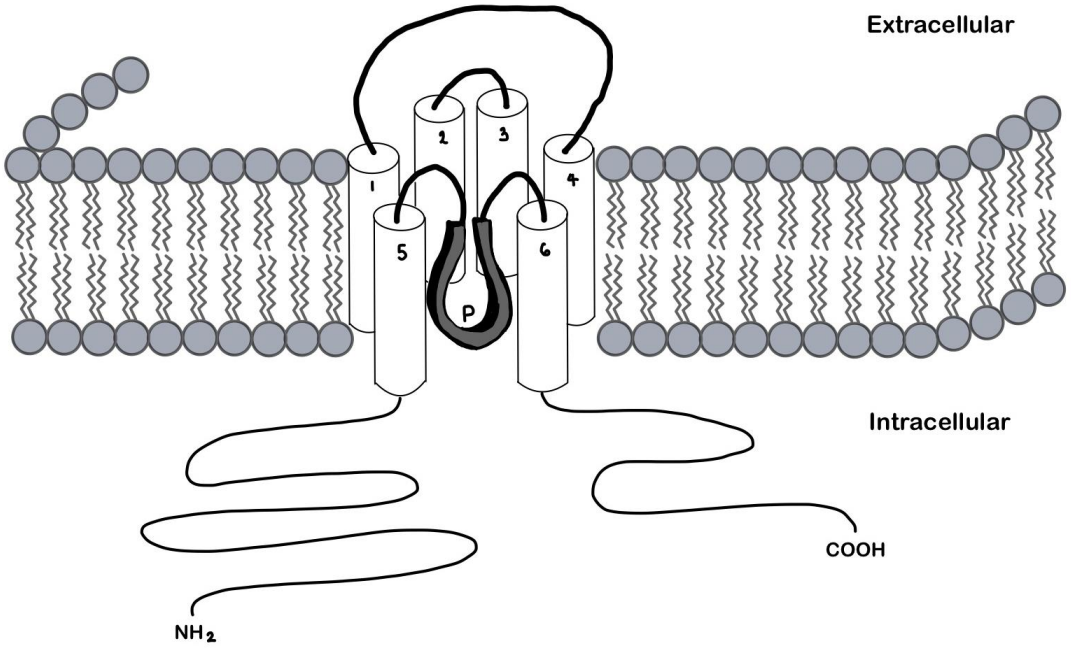

Figure 1.4. General structure of a TRPV5 or TRPV6 subunit. TRPV5/6 is made up of 6 transmembrane spanning domains, with the intracellular amino- (NH_2) and carboxyl- (COOH) tails indicated, along with the putative loop located between transmembrane domain 5 and 6, which form the calcium pore.

1.2.1.2. Tissue distribution and localisation of TRPV5 and TRPV6

TRPV5 and 6 are broadly expressed in several tissues such as the brain, pancreas, prostate and testis [32]. PCR and Northern blot analyses have detected human TRPV5 and 6 mRNA in the apical membrane of intestinal and renal epithelial cells [34–36]. However, studies have reported conflicting results on the relative abundance of these isoforms in the two tissues. Peng *et al.* [34,35] demonstrated that TRPV6 expression is higher than TRPV5 in the human small intestine (particularly the duodenum) compared to the kidney. In contrast, Hoenderop *et al.* [36] identified TRPV5 as the most abundant epithelial calcium channel in the human small intestine and kidney. Although the reason for these discrepancies is unclear, the characteristics of the human donors such as their medical history was not specified,

and therefore could contribute to the differences observed. Contrary to the human studies, reports on the relative abundance of these channels in the small intestine and kidney of rats and mice are more consistent. In rodents, particularly mice, TRPV6 mRNA is more abundant in the small intestine and therefore, considered the major isoform mediating the first step of transcellular intestinal calcium absorption, while TRPV5 expression is higher in the kidney and hence, considered the major calcium channel responsible for transcellular calcium reabsorption [36–38]. Furthermore, TRPV5 and 6 are predominantly localised in the proximal region of the small intestine and distal parts of the nephron [32,38].

1.2.1.3. Function and importance of TRPV5 and TRPV6

Out of the six TRPV isoforms identified, TRPV5 and TRPV6 have the highest selectivity for calcium (P_{Ca}:P_{Na} >100) [39] and are therefore thought to play a major role in mediating apical calcium influx in renal and intestinal epithelial cells, respectively. Consistent with this finding, studies using TRPV6 knockout mice fed a low calcium diet, showed a significant reduction in intestinal calcium absorption when compared to wild type [40,41]. Moreover, transgenic mice expressing human TRPV6 in intestinal epithelial cells exhibited a significant increase in calcium absorption [42], thus, demonstrating an important role for TRPV6 in mediating calcium transport in the small intestine. Furthermore, studies investigating the importance of this transporter to calcium homeostasis have demonstrated a decrease in serum calcium levels in TRPV6 knockout mice fed a low calcium diet compared to wild type [40,41]. In contrast, serum calcium levels in TRPV6 knockout mice fed a normal/high calcium diet were unaffected in both studies [40,41]. This confirms the importance of TRPV6 in mediating transcellular calcium transport particularly under low dietary calcium

conditions. Although TRPV6 is also expressed in the kidney, information on the impact of TRPV6 knockout on renal calcium reabsorption is limited. However, Bianco *et al.* [40] have reported a strong trend for an increase in urine calcium levels in TRPV6 knockout mice fed a normal calcium diet, suggesting a potential role in renal calcium reabsorption. The function of TRPV5 in mediating renal calcium transport on the other hand has been more extensively studied. Hoenderop *et al.* [43] demonstrated renal calcium wasting in TRPV5 knockout mice, which persisted under calcium deficient diets, highlighting the importance of TRPV5 in renal calcium transport. Interestingly, serum calcium levels were unaffected in these animals, which was speculated to be due to the compensatory increase in intestinal calcium absorption proposed to be mediated by the upregulation of TRPV6 expression observed in these mice [43].

1.2.1.4. Regulation of TRPV5 and TRPV6 in intestinal and renal epithelia

Previous studies have identified the regulatory role of $1,25(OH)_2D_3$ on TRPV5 and TRPV6 expression. The administration of $1,25(OH)_2D_3$ in C57BL6 mice causes the upregulation of TRPV5 and TRPV6 mRNA expression and protein levels in the kidney [38]. Furthermore, incubation of human duodenal biopsies with $1,25(OH)_2D_3$ results in higher TRPV6 expression [44]. The direct action of $1,25(OH)_2D_3$ on TRPV5/6 is proposed to occur via the activation of $1,25(OH)_2D_3$-response elements (VDRE) located in the promoter regions of the TRPV5 and TRPV6 gene [38,45]. In addition to the hormonal regulation, TRPV5 and TRPV6 can also be regulated by associated proteins that interact with the N- and C- terminals. For example, S100A10-annexin 2 protein-complex is an auxiliary protein that interacts with the C-terminal region of TRPV6 to facilitate the translocation of cytosolic TRPV6 to the plasma membrane

and in order to enhance its channel activity [46]. Also, Rab11a has been shown to be involved in promoting the trafficking of TRPV5 and TRPV6 to the plasma membrane by binding to the C-terminal [47]. Furthermore, in response to high serum calcium levels, cytosolic calcium binds to the calcium-sensing protein, calmodulin, and this has been reported to regulate TRPV5 and TRPV6 by inactivating their activity upon binding to their high affinity binding site, located on the C-terminal [48,49].

1.2.2. Cytosolic calcium diffusion: calbindin

Following the entry of calcium into the cell, its translocation from the apical region to the basolateral region is required to facilitate the extrusion of Ca^{2+} into the circulation. This process has been proposed to occur either through diffusion, vesicular trafficking or mediated by the calcium-binding protein, calbindin [9].

1.2.2.1. Structure of calbindin

Calbindin is categorised into 2 major classes, calbindin-D9k and calbindin-D28k. Calbindin-D9k is a small acidic protein consisting of 79 amino acid residues encoded by the S100G gene, with a molecular weight of 9kDa [50,51]. This protein consists of four alpha helices making up a pair of calcium binding EF hands, with each EF hand containing 2 helices linked by a stretch of 10 amino acids [52]. Since each EF hand binds to one Ca^{2+}, a single calbindin-D9k protein binds to 2 calcium ions [52]. In comparison, calbindin-D28k is made up of 261 amino acid residues and is encoded by the CALB1 gene, with a molecular weight of approximately 28kDa [51,52]. Although this protein is made up of 6 EF hands and therefore, 6 calcium binding sites, only 4 of the EF domains are functional, with EF-2 and EF-6 being non-functional [52,53]. Therefore, each Calbindin-D28k protein binds to 4 calcium ions.

1.2.2.2. Tissue distribution and localisation of calbindin

Calbindin-D9k and -D28k are expressed in a range of tissues including the kidney, intestine, bone and placenta [51]. In humans and rodents, calbindin-D9k expression is localised in the proximal small intestine, particularly the duodenum, and the distal part of the nephron in rodents [23,54–56]. Calbindin-D28k, first identified in the avian small intestine and kidney [51,57,58], is also expressed in the distal part of the human and rodent nephron, however, it is undetected in the small intestine of these species [54,59,60]. Calbindin-D9k and -D28k are widely accepted as the major calcium binding protein in the mammalian intestine and kidney, respectively [51].

1.2.2.3. Function of calbindin-D9k and -D28k

The major function of calbindin is to bind to intracellular calcium ions, however, it has also been shown to bind to other metal cations with reduced affinity: $Ca^{2+} > Cd^{2+} > Sr^{2+} > Mn^{2+} > Zn^{2+} > Ba^{2+}$ [61]. The calcium binding function of calbindin is important in buffering intracellular calcium levels within normal limits (0.1μM) preventing complications such as apoptotic cell death, which is induced by high intracellular Ca^{2+} levels [62,63]. In addition to its buffering capacity, using mathematical modelling, calbindin has also been proposed to act like an intracellular calcium ferry, facilitating the transport of Ca^{2+} ions from the apical to basolateral regions of the cell during $1,25(OH)_2D_3$-dependent transcellular calcium absorption [64]. This model is supported by early studies that have demonstrated a correlation between an increase in $1,25(OH)_2D_3$-induced intestinal calcium transport and calbindin-D28K and -D9k levels in chick and rats, respectively [65,66]. Furthermore, hypocalcaemia and skeletal abnormalities observed in 25(OH)D-1α-hydroxylase (1α-OHase) knockout mice (an

enzyme necessary for the synthesis of 1,25-dihydroxyvitamin D from 25-hydroxyvitamin D) was accompanied by the complete ablation of intestinal calbindin-D9k expression and a reduction in renal calbindin-D28k and -D9k expression [67]. Additionally, PTH stimulation of transepithelial calcium transport in rabbit connecting tubule/cortical collecting duct (CNT/CCD) primary cells was accompanied by an upregulation of calbindin-D28k [68]. Taken together, based on the mathematical studies and the regulation of calbindin during hormone-induced transepithelial calcium transport, it was generally accepted that calbindin played an important role in mediating transcellular calcium transport. However, more recently, the direct investigation of calbindin function in studies involving calbindin knockout animals has challenged the importance of calbindin to calcium transport and homeostasis. Lee *et al.* [69] demonstrated that there was no notable difference in calcium absorption or serum and urine calcium levels in calbindin-D9k knockout mice compared to wild-type. Consistent with this finding, Benn *et al.* [41] also reported no change in calcium absorption in calbindin-D9k knockout mice fed either a low or a high calcium diet compared to wild type, providing further evidence to question the importance of calbindin in transcellular calcium transport. Similarly, calbindin-D28k knockout mice did not exhibit any calcaemic abnormalities [70]. Collectively, these studies suggest that calbindin may not be a key component of transcellular calcium transport.

1.2.2.4. Regulation of calbindin-D9k and -D28k in intestinal and renal cells

It is well established that calbindin-D9k is regulated by $1,25(OH)_2D_3$ in intestinal and renal epithelial cells. Dupret *et al.* [71] reported a 2-fold increase in duodenal calbindin-D9k expression upon administration of $1,25(OH)_2D_3$ in rats. This action of $1,25(OH)_2D_3$ on calbindin-D9k is explained by the identification of a $1,25(OH)_2D_3$-

response element in the promoter region of the S100G gene, which is directly activated by the 1,25$(OH)_2D_3$-vitamin D receptor (VDR) complex [72]. Consistent with this finding, Li *et al.* [73] demonstrated a significant reduction in intestinal and renal calbindin-D9k expression in VDR knockout mice. In addition to 1,25$(OH)_2D_3$ regulation, glucocorticoids have also been reported to regulate calbindin-D9k expression. Studies have shown differential modulation of duodenal calbindin-D9k expression by dexamethasone in mice and rats, where calbindin-D9k expression was inhibited in mice and upregulated in rats following 3 or 7 days of treatment respectively [74,75]. This may be attributed to the differences in the length of treatment. Similar to calbindin-D9k, the regulation of calbindin-D28k by 1,25$(OH)_2D_3$ has been reported following the activation of a 1,25$(OH)_2D_3$-response element in the gene [76]. Furthermore, a study carried out by Varghese *et al.* [77] using rat kidneys, demonstrated an increase in calbindin-D28k expression in response to 1,25$(OH)_2D_3$ administration. Other regulators of Calbindin-D28k include glucocorticoids and PTH, where studies have reported an upregulation of calbindin-D28k expression in rat and rabbit renal epithelial cells treated with dexamethasone and PTH, respectively [68,75].

1.2.3. Calcium extrusion at the basolateral membrane

Calcium efflux at the basolateral membrane is an active process that occurs against an electrochemical gradient, whereby, calcium is pumped out from the intracellular compartment (containing ~ 0.1μM Ca^{2+}), to the extracellular fluid (containing ~ 1mM Ca^{2+}) [78]. The extrusion of calcium from the cytoplasm to the circulation is mediated by two calcium-specific transporters, PMCA1 and NCX1.

1.2.3.1. Structure of PMCA

PMCAs are calcium-specific efflux pumps that belong to the type 2B subfamily of the P-type ATPase superfamily, encoded by ATP2b [79]. There are 4 major isoforms of PMCA: PMCA1, PMCA2, PMCA3 and PMCA4, along with several splice variants that differ mainly in their C-terminal amino acid sequence [79]. The amino acid length ranges from 1103-1220 residues with a molecular weight of 120-140kDa [80,81]. PMCA is predicted to be made up of 10 transmembrane domains, 2 intracellular loops and a cytosolic amino- (NH_2) and carboxyl- (COOH) tail (**Figure 1.5**). Additionally, 2 intracellular loops are located between the transmembrane domain 2 and 3, and 4 and 5 as shown in **Figure 1.5**.

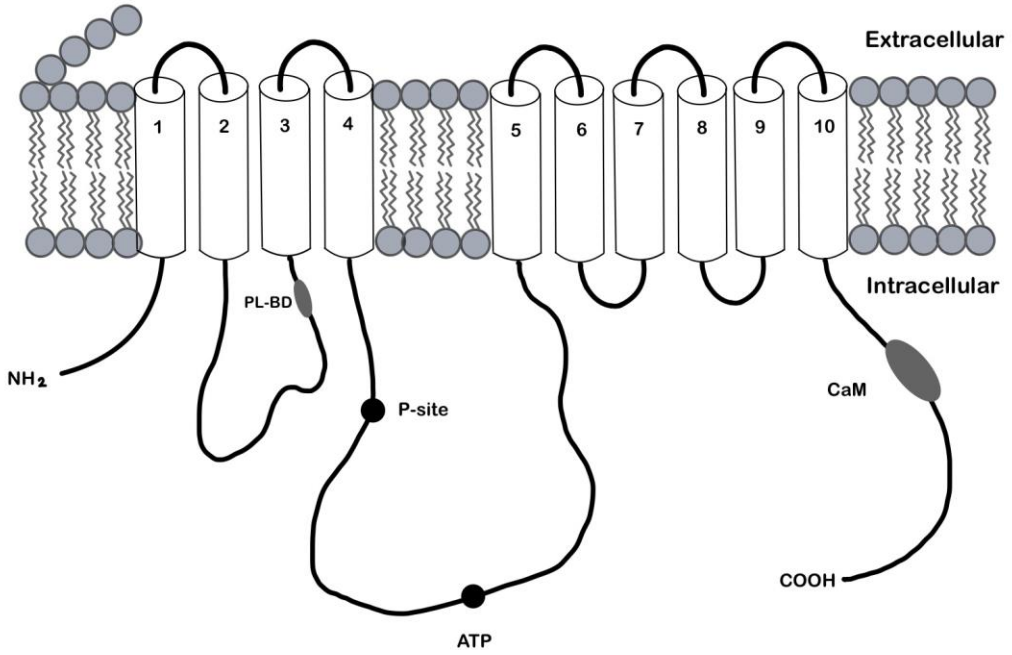

Figure 1.5. General structure of PMCA. The amino- (NH_2) and carboxyl- (COOH) tails are indicated in the intracellular compartment, along with the phospholipid binding domain (PL-BD), the aspartyl-phosphate intermediate (P-site), the region of (ATP) binding and the calmodulin (CaM) binding site.

The first intracellular loop is a smaller loop located between transmembrane domain 2 and 3. This loop contains a phospholipid binding domain (PL-BD) and is thought to play a role in the conformational changes that occur during the PMCA activation. The second intracellular loop is the catalytic region of the protein containing an ATP binding site and a site for the aspartyl-phosphate intermediate formed during ATP hydrolysis (P-site) [80].

1.2.3.2. Tissue distribution and localisation of PMCA

PMCA1 and 4 are considered to be ubiquitously expressed across human adult tissues, while the expression of PMCA2 and 3 are more restricted and are predominantly found in the brain [82]. Although reports have detected all four isoforms in the small intestine and kidney with varying levels of abundance (reviewed in [80]), PMCA1 is the most extensively studied isoform in relation to intestinal and renal calcium transport. PMCA1b is the predominant isoform in the small intestine and kidney of rodents and humans [83,84]. PMCA1b has been reported to be most highly expressed in the duodenum of human and rodents compared to other segments of the small intestine [84–87]. Furthermore, previous studies have detected PMCA1b in both the proximal and distal nephron of rodents and humans, with stronger signals observed in the distal segments [18,88–90].

1.2.3.3. Function of PMCA

As mentioned previously, PMCA1 is involved in the final step of transcellular calcium transport, exporting Ca^{2+} ions from the cytosol to the extracellular compartment. PMCA is a primary active transporter with a stoichiometry of 1:1 Ca^{2+}/ATP meaning that it binds and exports a single intracellular Ca^{2+} utilising the energy generated

from the hydrolysis of an ATP molecule [91]. The current kinetic model proposes that PMCA exists in 2 conformations; E_1, which has a high calcium affinity and can easily be phosphorylated by ATP, and E_2, which has low Ca^{2+} affinity and can be phosphorylated by inorganic phosphate (P_i). Following cytosolic Ca^{2+} binding to the high affinity binding site, ATP phosphorylates E_1 resulting in a conformational change (E_1P). Subsequently, E_1P transitions to E_2P, allowing for the release of Ca^{2+} to the extracellular space from the low affinity site. E_2P is then hydrolysed to E_2 and transitions back to its original E_1 confirmation [92]. Based on studies showing reduced serum calcium levels, bone mineral density and increase urinary calcium levels in PMCA1 knockout mice, it has been concluded that PMCA1 is essential to calcium homeostasis [93,94]. Since PMCA1 is ubiquitously expressed, it has also been regarded as a housekeeping gene, supported by gene knockout studies that showed embryo lethality in PMCA1 homozygous knockout mice [95].

1.2.3.4. Regulation of PMCA

Similar to the other components of transcellular calcium transport, PMCA1b is primarily regulated by $1,25(OH)_2D_3$, evidenced by increased PMCA1b expression and activity in human duodenal explants and Madin-Darby canine kidney (MDCK) cells, in response to $1,25(OH)_2D_3$ treatment [44,96]. In addition to hormonal regulation, PMCA is highly regulated by calmodulin and acidic phospholipids [91]. Calmodulin has been demonstrated to increase the binding affinity for calcium by binding to the calmodulin-binding domain located on the C-terminal, and disrupting its autoinhibitory interactions [97]. As a result, calmodulin interaction was shown to reduce the dissociation constant (K_d) of PMCA from 10μM to less than 0.8μM [97]. Similarly, acidic phospholipids have also been reported to increase the binding affinity of

PMCA by interacting with its calmodulin-binding domain and PL-BD, thus, reducing the K_d to less than 0.9μM [97].

1.2.4.1. Structure of NCX1

The Na^+/Ca^{2+} exchanger is a member of the Ca^{2+}/cation antiporter (CaCA) super-family and is encoded by the solute carrier 8 (SLC8) gene family. Three NCX isoforms have been identified in mammals encoded by three separate SLC8 genes. SLC8A1 gene encodes NCX1, SLC8A2 encodes NCX2, while, SLC8A3 encodes NCX3 [98]. Although a fourth NCX isoform has been also discovered, its expression is only detected in fish species, not in mammals [99]. NCX protein consists of an amino- (NH_2) and carboxyl- (COOH) tail located in the extracellular space, and 10 transmembrane (TM) helices with a large intracellular loop between TM5 and TM6 (**Figure 1.6**) [100,101].

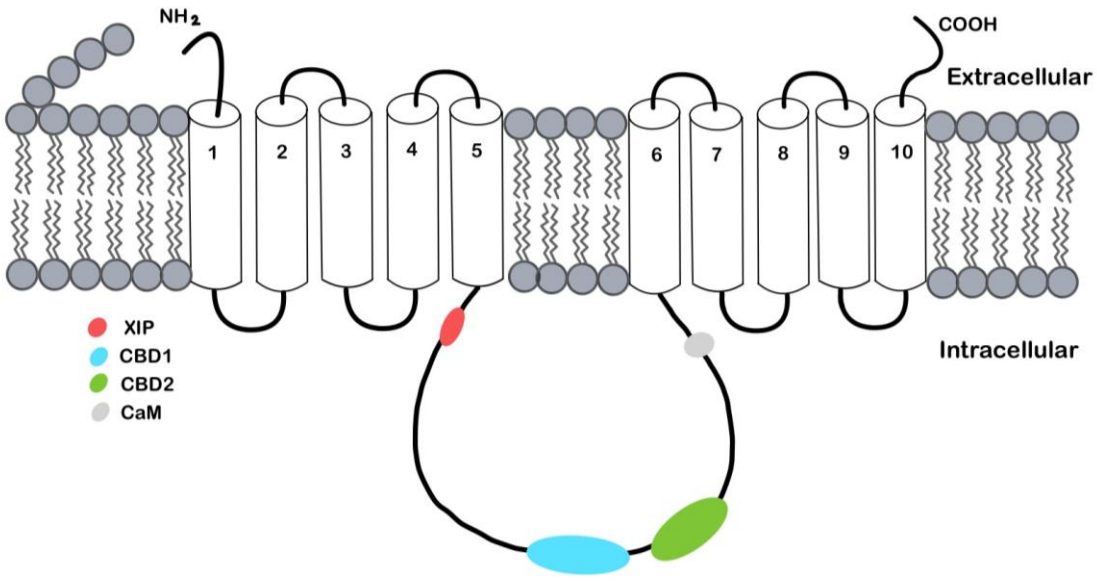

Figure 1.6. General structure of NCX. The amino- (NH_2) and carboxyl- (COOH) tails are present in the extracellular compartment while the exchanger inhibitory peptide (XIP), calcium binding domain-1 (CBD1) and -2 (CBD2), and a calmodulin (CaM) binding site are located on the intracellular loop.

The intracellular loop contains regulatory sites including 2 regulatory calcium binding domains (CBD1 and CBD2) and a calmodulin (CaM) binding site that allows for the modulation of NCX function [102]. Additionally, an endogenous exchanger inhibitory peptide (XIP) has been identified in the intracellular loop and is thought to be involved in Na^+-dependent NCX inactivation [103].

1.2.4.2. Tissue distribution and localisation of NCX1

While NCX1 is ubiquitously expressed [104], NCX2 and NCX3 expression is restricted to the skeletal muscle and brain (reviewed in [105]). PCR techniques have identified NCX1 transcripts in all 3 segments of rat and mouse small intestine, while there is a paucity of information regarding the expression of NCX1 in the human small intestine, [23,106]. Moreover, NCX1 has been detected in the distal portion of the human and rodent nephron using immunolocalization techniques [107,108].

1.2.4.3. Function of NCX1

NCX1 is a secondary active transporter that utilises the energy generated from the influx of three Na^+ ions down its electrochemical gradient to export one Ca^{2+} ion out of the cell, which makes the NCX1 transport process electrogenic in nature [109]. NCX is coupled with Na^+/K^+ ATPase which is involved in generating a sodium gradient necessary for NCX-mediated calcium extrusion. This function of NCX is reversible depending on the electrochemical gradient of Na^+ and Ca^{2+} ions, and the membrane potential [110]. While NCX-mediated calcium exit is the predominant mode, NCX-mediated calcium entry has also been reported in cardiac cells triggered by membrane depolarisation and elevated intracellular Na^+ ions [111]. Alongside PMCA1, NCX1 is also involved in the extrusion of calcium ions during transcellular calcium

transport. Consistent with this, Khuituan *et al.* [112] reported an inhibition of 1,25$(OH)_2D_3$-enhanced calcium transport in response to NCX1 inhibition in mouse duodenum [112]. Although both PMCA1 and NCX1 are involved in calcium extrusion in the small intestine and kidney, findings from calcium transport studies have shown that PMCA-dependent calcium transport is higher than NCX-mediated calcium transport in the rat small intestine, with PMCA activity demonstrated to be 5-fold higher in the duodenum [16]. Based on this report it is generally accepted that PMCA1 is the major basolateral calcium extrusion mechanism in the small intestine [12,16]. In contrast, NCX1 is the predominant calcium exporter in the kidney and therefore responsible for the majority of renal calcium extrusion in the distal tubule [9,17,18,23].

1.2.4.4. Regulation of NCX1

A number of studies have shown that NCX1 is regulated by 1,25$(OH)_2D_3$. Centeno *et al.* [113] demonstrated a downregulation and an upregulation of duodenal NCX1 expression in 1,25$(OH)_2D_3$-deficient and 1,25$(OH)_2D_3$-treated chicks, respectively. Furthermore, Hoenderop *et al.* [114] reported a downregulation of renal NCX1 gene expression in 1α-OHase knockout mice and an increase in its expression in response to 1,25$(OH)_2D_3$ treatment. In addition to 1,25$(OH)_2D_3$, PTH has also been shown to regulate NCX1 expression. Van *et al.* [68] reported an upregulation of renal NCX expression in PTH-treated rabbits and Riccardi *et al.* [115] showed a downregulation of NCX in parathyroidectomized rats. The action of PTH on renal NCX1 expression is thought to occur directly through the activation of PTH receptors located on the membrane of renal epithelial cells [115]. Unlike 1,25$(OH)_2D_3$ and PTH, there is a paucity of information regarding the impact of calcitonin on NCX1 expression and other transcellular calcium transporters.

Apart from the hormonal regulation, NCX1 is also regulated by intracellular Ca^{2+} and Na^{+} levels. Under high intracellular Ca^{2+} concentration, calcium ions can bind to CBD1 and CBD2 located in the cytosolic loop of the NCX1 protein resulting in conformational changes that lead to an increase in NCX1 activity [102]. In contrast, an increase in intracellular Na^{+} ions has been reported to inhibit the calcium transport activity of NCX1 [116]. Furthermore, calmodulin is also known to modulate NCX1 activity when bound to the calmodulin (CaM) binding site identified in the intracellular loop of NCX [101,117]. Chou *et al.* [101] noted a reduction in NCX1 activity and membrane localisation in HEK293T cells when the CaM binding region was deleted from the cytosolic loop, thus, confirming the regulatory role of calmodulin on the function of NCX1.

1.2.5. Alternative routes for transcellular calcium transport

1.2.5.1. $Ca_V1.3$

In addition to TRPV6, $Ca_V1.3$ has been identified as an alternative route for apical calcium entry and has been proposed by Kellett [19] to play a complementary role alongside TRPV6 in calcium entry into the enterocytes. $Ca_V1.3$ is an L-type voltage gated channel encoded by the CACNA1D gene and has been detected in the kidney, small intestine, and colon of rodents and humans [118,119]. The expression of $Ca_V1.3$ has been reported to be similar across the segments of the human and mouse small intestine [118,120], while its expression is highest in the jejunum and proximal ileum of rats compared to the other segments [119]. $Ca_V1.3$ activity is activated by glucose-induced membrane depolarisation and has been proposed to be involved in mediating intestinal calcium absorption [119]. However, there has been contrasting

evidence regarding this function. In rat jejunum perfused with 20mM glucose and 1.25mM Ca^{2+} *in vivo*, Morgan *et al.* [119] demonstrated an inhibition in the rate of transcellular calcium absorption in response to nifedipine (an L-type voltage-gated calcium channel antagonist) and an increase in absorption in response to Bay K 8644 (an L-type voltage-gated calcium channel agonist). Due to the lack of evidence showing the presence of any other known L-type voltage-gated calcium channel in the small intestine, it was concluded that transcellular calcium transport was driven by $Ca_v1.3$ in these experiments. Therefore, this channel was suggested to play a role in mediating intestinal calcium absorption under depolarising conditions induced by high luminal glucose levels following a meal [119]. However more recently, a study carried out in 9-week-old mice failed to show enhanced calcium absorption in the presence of luminal glucose, suggesting that $Ca_v1.3$ plays little or no role in active intestinal calcium absorption [120]. The discrepancies between the 2 findings suggest that the importance of $Ca_v1.3$ in mediating glucose-induced calcium absorption may be different in rats and mice. Consistent with this finding, while $Ca_v1.3$-mediated transport was seen in adult rats, Beggs *et al.* [121] reported an inhibition in transcellular calcium transport in the jejunum of pre-weaned $Ca_v1.3$ knockout mice, but not in adult mice. This suggests that $Ca_v1.3$ plays a more important role during growth and development in mice [121]. This may explain why Reyes-Fernandez and Fleet were unable to demonstrate an increase in glucose-induced calcium absorption in adult mice [120]. Despite the growing interest in identifying alternative mediators of apical calcium absorption, the importance of $Ca_v1.3$ in calcium homeostasis remains unclear. Additionally, the lack of a $Ca_v1.3$ specific inhibitor makes it difficult to confirm the importance of this channel to transcellular calcium absorption. Moreover, despite

the detection of $Ca_v1.3$ gene expression in the human and mouse kidney [118], its role in renal calcium reabsorption is yet to be established.

1.2.5.2. Vesicular transport

In addition to protein-mediated active calcium transport, transcellular calcium transport has also been proposed to occur via vesicular trafficking [21,122,123]. This model has been speculated to occur via endocytotic calcium internalisation, intracellular shuttling of calcium-containing lysosomes, and the subsequent release of calcium into the circulation via exocytosis (**Figure 1.2**). During calcium absorption, the presence of ^{45}Ca within lysosomal and endosomal fractions in chick duodenal cells [124,125] support the vesicular transport model. Furthermore, the increase in lysosomal proliferation [126] and intracellular calcium content [125] in response to $1,25(OH)_2D_3$ treatment highlights the existence of $1,25(OH)_2D_3$-dependent vesicular calcium absorption in this model. However, more studies are required to delineate the contribution of this model of transport to overall intestinal calcium absorption and homeostasis.

1.2.6. Paracellular calcium transport

Calcium transport via the paracellular pathway is a passive process, which is driven by an electrochemical calcium gradient or solvent drag. This process is considered to be the major pathway for calcium absorption under a normal or high calcium diet [127]. Paracellular calcium transport occurs in all three segments of the small intestine, and in the renal proximal tubules and thick ascending limb of the loop of Henle [128]. Paracellular calcium transport requires both a driving force and a paracellular pore [24]. Two mechanisms mediate paracellular calcium transport; an electrochemical

gradient-dependent mechanism and a solvent drag mechanism. The electrochemical gradient-dependent route is the simple diffusion of calcium ions, while the solvent drag mechanism involves the transport of calcium driven by water movement, with both mechanisms occurring via the tight junction between epithelial cells. Freeze-fracture electron microscopy shows that tight junctions are made up of multiple proteins including occludins, tricellulin and claudins, which maintain membrane barrier integrity [129]. Of these proteins, claudins are considered the major determinant of tight junction permeability to ions including calcium [130].

1.2.6.1. Structure of claudins involved in paracellular calcium transport (claudin-2, -12, -14, -15, -16 and -19)

Claudins are integral membrane proteins consisting of four transmembrane (TM) domains, an intracellular NH_2 and COOH termini, a large extracellular loop (ECL1), a small extracellular loop (ECL2) and an intracellular loop (**Figure 1.7**) [130]. In rodents, a total of 27 claudins have been identified, while 26 claudins (excluding claudin-13) have been detected in humans [131,132]. The molecular weight of these proteins range from 21-34kDa with an amino acid sequence between 207 and 305 [132]. Of the claudins identified, claudin-2 and -12 have been demonstrated to mediate intestinal calcium absorption [25], while claudin-15 has been speculated to also contribute to this process [128]. In the kidney, claudin-2, -12, -14, -16 and -19 have been reported to play a role in paracellular calcium transport across different segments of the nephron [26,128]. The molecular weight and the number of amino acid residues of the claudins involved in paracellular calcium transport in the intestine and kidneys are shown in **Table 1.1**

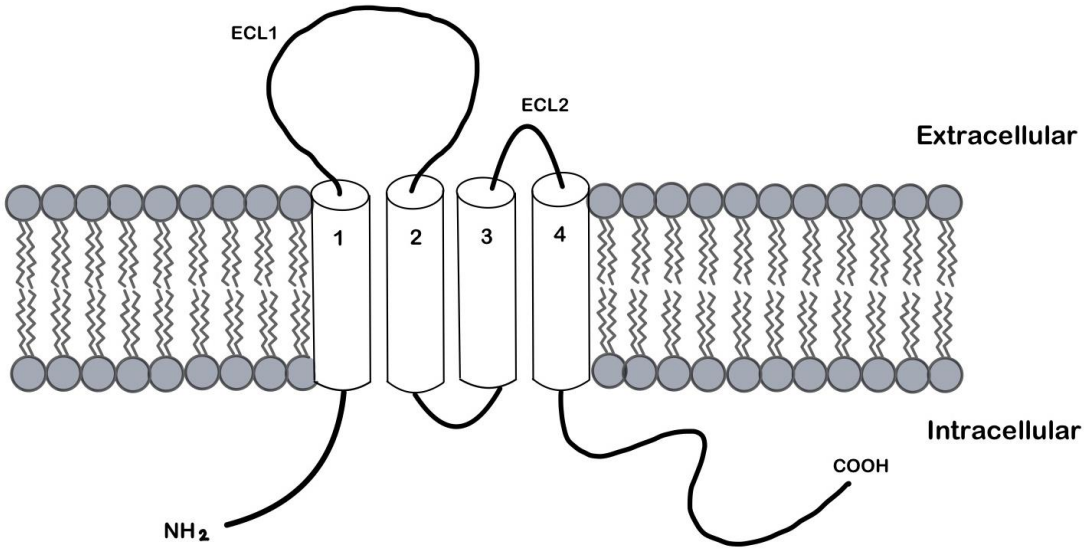

Figure 1.7. General structure of claudins. Claudins are predicted to have 4 transmembrane domains, with the amino- (NH_2) and carboxyl- (COOH) tails are localised in the intracellular compartment, while the extracellular loops; extracellular loop 1 (ECL1), and extracellular loop 2 (ECL2) are indicated in the extracellular compartment.

Table 1.1: Molecular weight and number of amino acid residues of calcium-associated claudins [133,134].

Claudin	Molecular weight (kDa)	Amino Acid residues
2	24.5	230
12	27.1	244
14	25.7	239
15	24.4	228
16	33.8	305
19	22.1-23.2	211-224

1.2.6.2. Intestinal and renal localisation and distribution of claudin-2, -12, -14, -15, -16 and -19

Claudin-2, -12, and -15 are differentially localised in the small intestine. Using immunolocalization techniques, it has been demonstrated that claudin-2 expression is restricted to the crypt epithelium while claudin-12 and -15 expression is detected along the crypt to villus axis of the mouse small intestine [135,136]. In addition to the differences in localisation, differential expression patterns of claudin-2, -12 and -15 have been reported along the segments of human and rodent small intestine (**Figure 1.8**). The mRNA expression of claudin-2 has been shown to be the highest in the human, rat and mouse ileum [137,138]. On the other hand, while claudin-12 mRNA expression is greatest in the rat jejunum [139], in mice, claudin-12 expression was highest in the ileum [137]. Although the regional profile of claudin-15 has not been characterised in rats, high claudin-15 expression exists in the human duodenum [138] and mouse proximal small intestine (duodenum and jejunum) [137]. The mRNA expression profile of the claudins involved in calcium absorption in rodent and human small intestine is summarised in **Figure 1.8.**

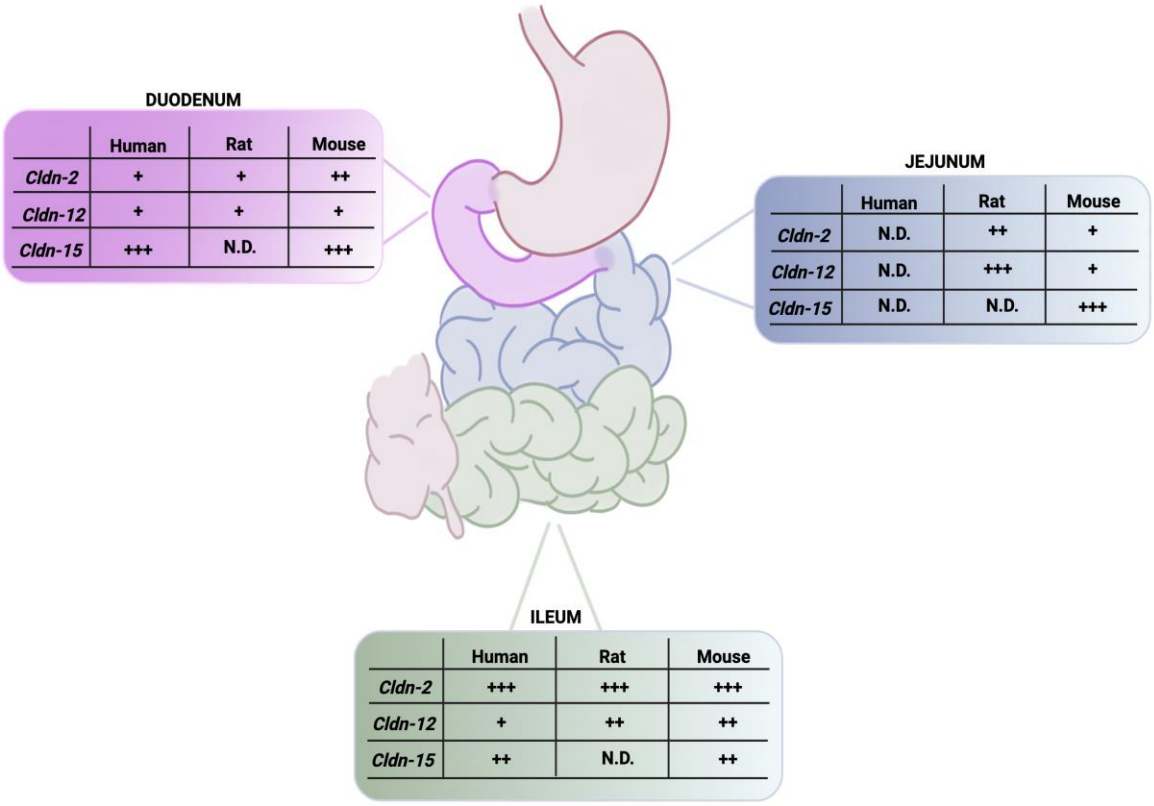

Figure 1.8. Relative mRNA expression of claudin-2, -12 and -15 in the segments of the human, rat and mouse small intestine [136–139]. Cldn represents claudin, +++ represents high expression, ++ represents moderate expression, + represents low expression and N.D. represents not determined. *Created with BioRender.com.*

Like the small intestine, claudins are differentially distributed along the segments of the nephron (**Figure 1.9**). In humans and rodents, claudin-2 is localised in the proximal convoluted tubule (PCT) [140–144]. Additionally, this claudin has also been detected in the thin descending limb (tDL) of mice [140,141]. Claudin-12 has been shown to be expressed in the proximal tubule of mice [26,145], while information regarding the tubular expression of this claudin in rats and humans is limited. Claudin-14, has been identified in the thick ascending limb (TAL) of rodents [146,147] and distal convoluted tubule (DCT) of humans [142]. Previous studies have detected claudin-16 in the TAL

and DCT of the human and rodent nephron [140,142,147–150], with evidence in rats demonstrating that this claudin is also expressed in the thin ascending limb (tAL) and the collecting duct (CD) [149,151]. Claudin-19 has been reported to be expressed in the TAL, DCT and CD of human and rodent nephron [147,150,152,153]. Additionally, there is evidence that claudin-19 is also expressed in the tAL and connecting tubule (CNT) of rodents [150,151,153]. The renal localisation and segmental distribution of claudins involved in calcium transport in rodents and humans is summarised in **Figure 1.9**.

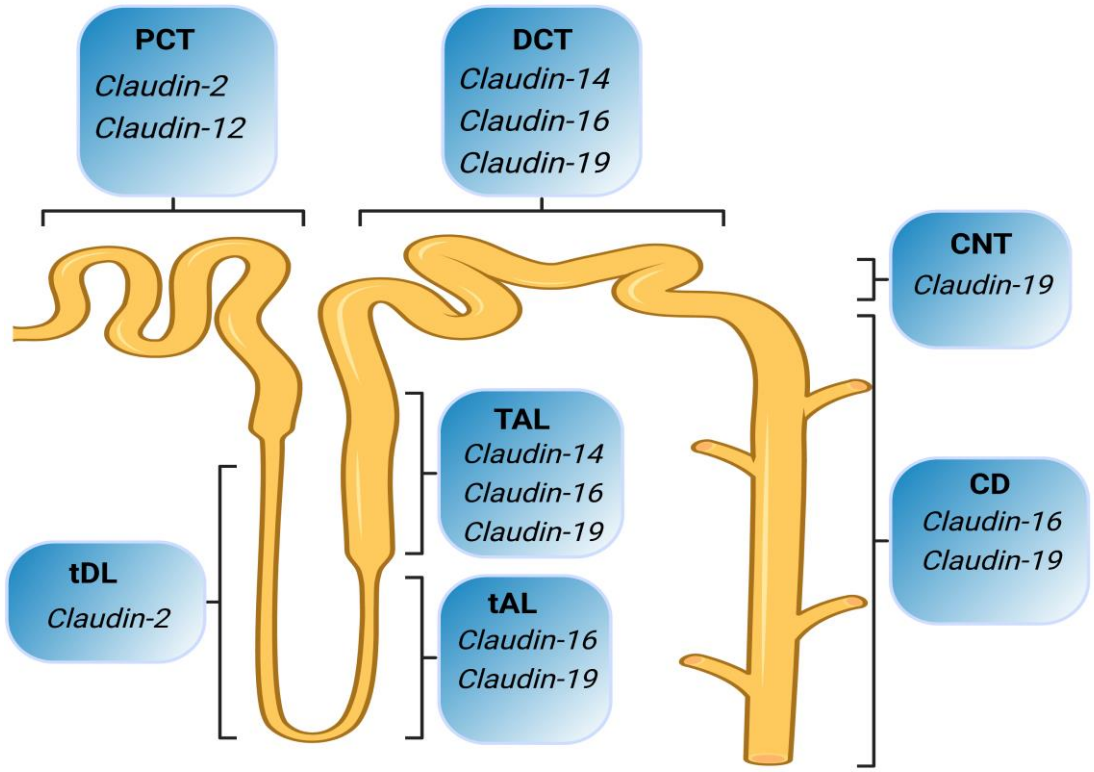

Figure 1.9. Localisation of claudin-2,-12,-14,-16,-19 detected in human and rodent nephron [26,140,150,152,153,141–144,146–149]. The renal claudins are localised as follows: claudin-2 and -12 are detected in the proximal convoluted tubule (PCT), claudin-2 in the thin descending limb (tDL), claudin-16 and -19 in the thin ascending limb (tAL), claudin-14, -16 and -19 in the thick ascending limb (TAL) and distal convoluted tubule (DCT), claudin-19 in the connecting tubule (CNT) and claudin-16 and -19 in the collecting duct (CD). *Created with BioRender.com.*

1.2.6.3. Function of claudins involved in intestinal and renal paracellular calcium transport

Claudins are commonly categorised as either pore-forming or barrier-forming proteins for small cations and anions [132]. However, the majority of the calcium mediating claudins are classed as pore-forming claudins. The electrogenic property of the extracellular loops, mainly ECL1, and the pore size of claudins, determine the charge and size selectivity of specific ions across the tight junction [154]. For example, claudin-2, -12 and -15 have been demonstrated to contain negatively-charged amino acid residues in the ECL loops that attract cations including calcium [136,155,156]. Furthermore, the pore size of claudin-2 has been reported to be approximately 6.5Å, which is larger than the ionic radius of Ca^{2+} (1Å) [157,158] suggesting that this claudin allows the passive diffusion of calcium. In keeping with this suggestion, claudin-2 has been implicated in the paracellular calcium transport process in the small intestine. In addition, while claudin-12 has also been shown to mediate calcium transport, evidence suggests that claudin-15 is not a calcium-selective pore [25]. Fujita *et.al* [25] was the first to directly demonstrate this function *in vitro*. Using Caco-2 cells as a human model for the small intestine, Fujita *et.al* [25] showed that the overexpression of either claudin-2 or claudin-12 resulted in an increase in paracellular calcium flux, while knockdown of these claudins caused a reduction in $1,25(OH)_2D_3$-induced paracellular calcium flux *in vitro*. To confirm the role of claudin-2 and -12 in mediating intestinal calcium transport *in vivo*, the knockout of claudin-2 has recently been shown to only decrease colonic calcium permeability, with no effect on paracellular calcium flux in the duodenum and ileum of mice [159]. Like claudin-2, claudin-12 has also been demonstrated to mediate colonic calcium

permeability [26,27]. Moreover, claudin-2 and -12 are also known to mediate paracellular sodium transport [25–27,160,161], a function that implicates these claudins as important mediators of solvent drag mediated calcium absorption. Claudin-15 has also been speculated to be involved in mediating calcium flux due to its ability to mediate the transport of other cations such as sodium and potassium [162]. Even though Fujita *et.al* [25] showed that the overexpression of claudin-15 in Caco-2 cells had no impact on calcium permeability, there is evidence that this claudin may indirectly mediate calcium transport via solvent drag due to its role in regulating the absorption of osmotically active electrolytes (e.g. sodium) and solutes (e.g. glucose) [163–165].

In the kidney, evidence from claudin-2 or -12 knockout animals has shown that these claudins mediate proximal tubular (PT) calcium reabsorption [26,27,159]. However, while claudin-2 knockout animals showed significant loss of calcium in urine (hypercalciuria) [159], urinary calcium excretion was not impacted in claudin-12 knockout mice [26], suggesting that claudin-2 is the major claudin responsible for the bulk of PT calcium reabsorption in mice. In humans, genetic mutation in the claudin-2 gene has been shown to be associated with impaired renal calcium reabsorption and kidney stones, thus demonstrating the importance of this claudin in renal calcium transport [159]. Knockout of both claudin-2 and -12 has been shown to exhibit a more significant renal calcium excretion compared to single knockout of claudin-2 or -12, suggesting that claudin-2 and -12 may play a complementary role in mediating renal calcium transport [26,27,159,161]. Claudin-14, -16 and -19 have been reported to also play a role in renal paracellular calcium transport [146,148,166–169]. In the distal nephron, claudin-16 and -19 have been shown to assemble in the tight junction to form a

cation selective complex that mediates calcium transport [169,170]. Furthermore, the knockdown of both claudin-16 and -19 in mice results in chronic calcium wasting, highlighting their importance in mediating paracellular calcium reabsorption in the kidney [168,169]. In contrast to claudin-16 and -19, claudin-14 has been shown to play an inhibitory role in renal calcium transport by interacting with claudin-16 to reduce the transport function of the claudin-16 and -19 pore-forming complex [146]. Consistent with this finding, claudin-14 knockout mice developed significant hypocalciuria, suggesting that the loss of this claudin increases calcium reabsorption in the distal nephron [146]. In addition to the calcium transport function of these claudins, claudin-14, -16 and -19 play an important role in renal magnesium transport [168,169,171,172].

1.2.6.4. Regulation of claudins involved in mediating paracellular calcium transport

Intestinal and renal claudins involved in paracellular calcium transport are regulated by a range of cellular and hormonal factors. $1,25(OH)_2D_3$ is known to be the major regulator of the claudins mediating intestinal calcium absorption i.e. claudin-2, -12 and -15 [25,173], while extracellular calcium levels and PTH are important regulators of renal claudin-14, -16 and -19 [174]. The overexpression of VDR or $1,25(OH)_2D_3$ administration has been shown to increase the levels of claudin-2, -12 and -15 [25,173]. $1,25(OH)_2D_3$ has also been demonstrated to regulate claudin-16 and -19 by down-regulating their mRNA expression in the mouse kidney [175]. The regulatory role of $1,25(OH)_2D_3$ on renal claudin-16 and -19 is speculated to compensate for the vitamin D-induced increase in intestinal calcium absorption, thus, controlling calcium homeostasis [156]. Extracellular calcium levels regulate the expression of claudin-14, -16 and -19 via stimulation of the basolateral membrane calcium sensing receptor

(CaSR) in the cells of TAL of the loop of Henle [176–178]. Activation of CaSR by high levels of extracellular calcium causes the upregulation of claudin-14 [146,166]. In contrast, PTH interacts with its receptor, PTH type 1 receptor (PTHR1), located on both the apical and basolateral membrane, to directly downregulate the levels of claudin-14 [174]. There is evidence that claudin-14 inhibits the calcium permeability of the paracellular pore formed by claudin-16 and-19 [146]. Based on this finding, extracellular calcium levels and PTH indirectly regulate the calcium transport function of claudin-16 and -19.

Since the localisation of intestinal and renal claudins to the tight junction membrane is necessary for their function, claudin activity may also be regulated by proteins involved in membrane trafficking [179]. For example, Rab proteins are GTPases that regulate the budding, delivery, tethering and fusion of vesicles to their target compartments [180]. Studies have demonstrated the regulatory function of Rab proteins on claudin-2 and claudin-16 membrane localisation [175,181]. Rab14 knockdown in MDCK cells has been reported to increase claudin-2 targeting to lysosomes and therefore, decrease its membrane localisation [181]. Additionally, dominant negative Rab11 mutants in MDCK cells show decreased claudin-16 membrane localisation compared to wild-type [182]. The vesicle trafficking protein syntaxin-8 (STX-8) has also been demonstrated to affect claudin-16 membrane localisation [182]. In addition to membrane trafficking proteins, post-translational modifications such as the phosphorylation of claudins by kinases also play a role in regulating claudin expression and localisation [179,183]. For instance, PKA-mediated phosphorylation of claudin-16 has been shown to be vital for its tight junction

localisation [184]. Additionally, the phosphorylation of claudin-2 on the c-terminal tail has also been shown to be important for its membrane retention [185].

Interestingly, claudin localisation can also be regulated by other claudins. The disruption of claudin-19 membrane localisation has been reported in claudin-16 knockdown mice [169]. Similarly, claudin-16 knockdown in mouse kidneys also causes delocalisation of claudin-19 [169]. Moreover, evidence from NHE3 knockout mice demonstrates that NHE3 regulates the expression of claudin-2 in the small intestine and kidney [186]. Low levels of intestinal claudin-15 and renal claudin-19 have also been detected in these mice [186]. Other cellular protein modulators and transcription factors such as guanylyl cyclase C, cathepsin, matriptase, hepatocyte nuclear factor 1α have also been reported to regulate the intestinal expression of claudin-2 (reviewed in [187]). Furthermore, differential levels of intestinal claudin-2 and -15 have been reported in humans and rodents of different ages [187,188]. Relatively high levels of claudin-2 has been detected in young rodents and in children compared to adults, while claudin-15 levels increase with age [137,187,188]. Other factors that regulate the expression of claudins include immune regulators such as interleukin-6 (IL-6); growth factor signalling regulators such as epidermal growth factor (EGF), which have been demonstrated to specifically modulate claudin-2 expression [189,190]; and pH [191,192]. For instance, a low pH has been shown to downregulate claudin-2 expression and upregulate claudin-12 expression in MDCK and Caco-2 cells, respectively [191,192].

1.2.7. Solvent drag

In addition to the passive diffusion of calcium ions, paracellular calcium flux has also been proposed to be driven by a solvent drag mechanism [128,164]. Solvent drag is the

movement of water along with dissolved ions including calcium across the intercellular space, driven by an osmotic gradient, which is created from the sodium-mediated active transport of ions and nutrients [19]. Sodium-coupled transporters such as Na^+/K^+ATPase, NHE3 and SGLT1 are proposed to play a principal role in creating the osmotic driving force for solvent drag [193,194]. Sodium transported into the cell via apical SGLT1, NHE3 and other sodium-dependent transporters is pumped into the intercellular space by the Na^+/K^+ATPase located on the lateral membrane of epithelial cells [195]. The accumulation of sodium in this space creates an osmotic driving force that results in the drag of water along with dissolved solutes from the intestinal lumen to the intercellular space [196]. This process can occur in the absence of a calcium concentration gradient [164] and has therefore been referred to as a secondary active transport process because it depends on cellular energy to create the sodium gradient in the intercellular spaces by the Na^+/K^+ATPase [19,22]. Claudins mediating paracellular sodium transport (claudin-2, -12 and -15), may also contribute to the magnitude of the osmotic driving force for solvent drag mediated calcium transport. Although claudin-2 has been demonstrated to be permeable to sodium, calcium and water [160,197], there is no evidence suggesting that this claudin directly mediates solvent drag. Similarly, the role of claudin-12 in mediating paracellular sodium transport has not been demonstrated to contribute to solvent drag [26,27]. Interestingly, even though it has recently been speculated that claudin-15 is not a drag [198], evidence of impaired intestinal sodium and glucose absorption in claudin-15 knockout mice [199] links this claudin to solvent drag-induced calcium absorption. Moreover, prolactin has been reported to increase solvent drag-mediated calcium

absorption [164,200], a finding that is potentially due to the increase in claudin-15 levels seen in the duodenum of rats [163].

Interestingly, solvent drag-induced calcium transport has also been shown to be significantly higher in the duodenum compared to the jejunum of rats, and is suggested to account for ~30% of active calcium transport in the duodenum [164]. Although solvent drag contributes to total active calcium transport particularly in the duodenum, the importance of this pathway to total intestinal calcium transport is yet to be determined. Solvent drag-induced calcium transport has been shown to be regulated by prolactin, $1,25(OH)_2D_3$ and pH [164,201,202]. Prolactin treatment has been reported to increase solvent drag-induced calcium transport in a dose-dependent manner in the duodenum, but not in the jejunum of female rats [164]. Tudpor *et.al* [201] has demonstrated an increase in solvent drag-induced calcium transport in response to $1,25(OH)_2D_3$ treatment in the duodenum of female rats. Furthermore, pH has also been shown to affect solvent drag-induced calcium absorption, where Charoenphandhu *et.al* [202] demonstrated a decrease in duodenal solvent drag-induced calcium transport in response to acidic extracellular pH.

1.3. Intestinal calcium handling

As previously mentioned in **section 1.2.,** intestinal calcium absorption occurs via both transcellular and paracellular pathways, however, under physiological conditions when dietary calcium is normal or high, the paracellular pathway is dominant [6,12,127,203]. Calcium absorption has been reported to occur in the small intestine, the caecum and the colon [204–207]. Under physiological conditions, it is widely accepted that the small intestine is the major site for calcium absorption,

contributing to about 90% of total calcium absorbed, while the large intestine, particularly the colon, contributes approximately 10% [6,208]. However, in patients where the small intestine has been resected, the colon has been demonstrated to play a more significant role in intestinal calcium absorption [209]. While calcium absorption is absent in the stomach [204], it has been speculated that the acidic environment created through gastric acid secretion solubilises calcium salts, and therefore aids calcium absorption in the subsequent segments of the small intestine, particularly the duodenum [210]. Consistent with this, patients with achlorhydria (absence of gastric acid secretions) have been reported to absorb significantly less calcium from a calcium carbonate solution compared to a healthy control group [211]. Furthermore, when one of these patients was treated with betazole hydrochloride to stimulate gastric acid secretions, the proportion of calcium absorbed increased [211], thus, demonstrating the importance of the gastric acids to intestinal calcium absorption.

From studies investigating the rate of calcium transport using ligated intestinal loop experiments, and the rate of passage of intestinal content through the intact intestinal tract, Cramer and Copp in 1959 [212] showed that the ileum contributes about 65%, jejunum 17%, colon 8% and duodenum 7% to overall intestinal calcium absorption. This finding was confirmed and extended by Marcus and Lengemann in 1962 [204]. They used a solid diet (containing 6.62mg of calcium) or liquid dose (6.62mg calcium in 1ml), to investigate the impact of transit time on regional calcium absorption. Calcium absorption was estimated to be the highest in the ileum (liquid: 88% and solid: 62%), compared to the jejunum (liquid: 23% and solid: 4%) and duodenum (liquid: 15% and solid: 8%) [204]. Based on these findings the relative contribution of

each segment of the intestine to overall calcium absorption is summarised in **Figure 1.10.** The major factors responsible for the high level of ileal calcium absorption is its length and the long intestinal transit time of chyme (141min), compared to the jejunum (43min) and duodenum (~2.5min) [213]. In addition to the intestinal transit time, calcium solubility impacts absorption, as only ionised or dissolved calcium can be absorbed in each intestinal segment [6,213,214]. Since acidic pH has been shown to increase the solubility of calcium salts [215], calcium solubility is expected to be highest in the duodenum compared to the other segments of the small intestine as intestinal pH has been reported to increase from below 6.6 in the duodenum to above 8 in the ileum [213]. In keeping with this suggestion, the duodenum is reported to have the highest rate of overall calcium absorption in the small intestine, while the ileum has the lowest rate of calcium absorption [212,216].

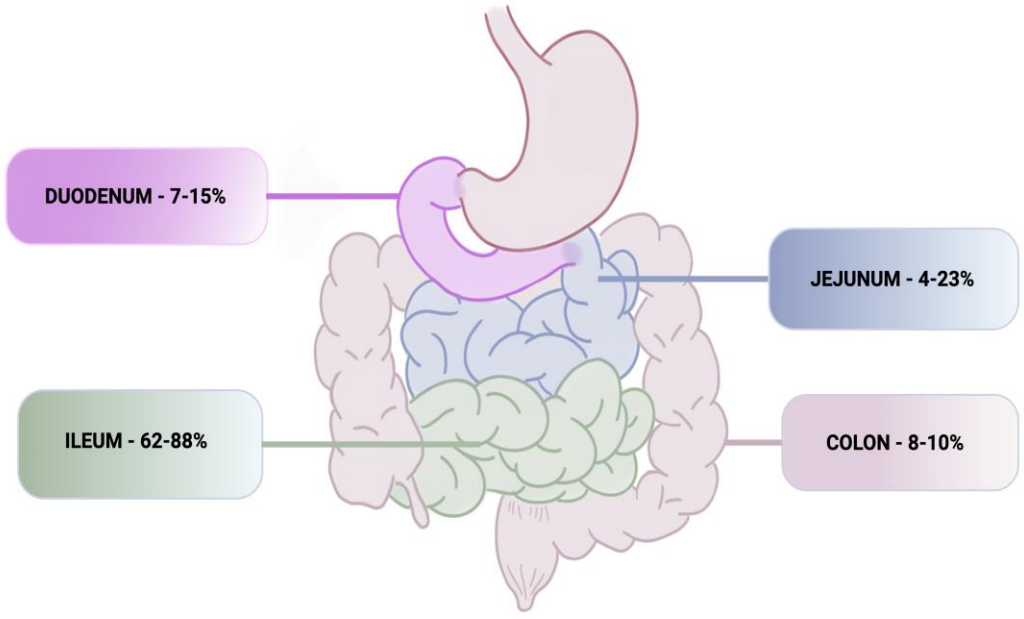

Figure 1.10. Relative contribution of intestinal segments to total calcium absorption [6,204,208,212]. The duodenum contributes 8-15%, the jejunum contributes 4-23%, the ileum contributes 62-88%, while the colon contributes 8-10% to overall calcium absorption across the small intestine. *Created with BioRender.com.*

The capacity of calcium transport in any given intestinal segment is mainly determined by the presence and relative contribution of the saturable (transcellular) and non-saturable (paracellular-passive diffusion and solvent drag) component of calcium absorption. It is widely accepted that the transcellular pathway is confined to the proximal region of the small intestine (i.e. duodenum and to a lesser extent the jejunum), while the paracellular pathway occurs in all three segments [216,217]. Transcellular calcium absorption primarily occurs in the duodenum, where it mediates up to 80% of overall calcium transport under low dietary calcium conditions [11]. In comparison to the duodenum, 20% of overall calcium absorption is believed to be mediated via the transcellular route in the jejunum, while little or no transcellular calcium transport occurs in the ileum [11]. The higher contribution of the transcellular calcium transport pathway to overall calcium transport in the duodenum, compared to the jejunum and ileum, allows for optimal adaptation to changes in dietary calcium levels, particularly when dietary calcium is low. In addition to its presence in the duodenum and jejunum, transcellular calcium transport has been reported in the caecum, and proximal and distal colon [23,202,205,218,219]. Although the relative contribution of the caecum to overall calcium absorption is unclear, the finding that intestinal calcium absorption is unchanged in caecectomized rats suggests that the caecum plays little or no role in overall calcium absorption under physiological conditions [220]. This is likely due to the low bioavailability of absorbable calcium in the caecum [213,214,221]. In the proximal and distal colon, transcellular calcium transporters have been detected, however, the relative contribution of these transporters to overall calcium absorption in the colon is uncertain [23,222].

Nevertheless, the paracellular pathway is believed to mediate the bulk of overall calcium absorption in the colon under normal dietary calcium conditions [23,223].

Paracellular calcium absorption in the intestine has been reported to be mediated via passive diffusion through calcium-specific claudins, and solvent drag. The magnitude of paracellular calcium transport is dependent on the transepithelial calcium concentration gradient along the different segments of the intestine [11,218]. Although, the transepithelial calcium concentration gradient in the intestinal tract is largely dependent on the dietary calcium content, the proportion of the calcium that is available for absorption in each segment has remained uncertain. Findings from studies investigating the solubility and bioavailability of absorbable calcium in the different intestinal segments have shown that the proportion of absorbable calcium is higher in the small intestine compared to the caecum and colon [213,214,221]. Moreover, intestinal paracellular tight junction composition, determined by claudins and occludins, plays an important role in regulating paracellular calcium transport, with the small intestine demonstrated to exhibit a leakier epithelia than the caecum and colon [224]. Taken together, these findings suggest that paracellular calcium absorption is higher in the leakier (more porous) epithelia of the small intestine compared to the caecum and colon. Paracellular calcium transport is regulated by hormones (e.g., $1,25(OH)_2D_3$) and cellular factors (e.g., NHE3) that control the expression of the claudins mediating intestinal calcium absorption (claudin-2, -12 and -15) as described in **section 1.2.6.4.**

1.4. Renal calcium handling

The kidney plays a vital role in maintaining calcium homeostasis by excreting excess calcium when calcium levels in the extracellular fluid (ECF) are high or by reabsorbing almost all the calcium filtered into the renal tubules when the calcium concentration in the ECF is low. Ionised calcium is freely filtered through the glomerulus and ~ 99% of the filtered calcium is reabsorbed by the kidney under normal conditions [225]. Like the intestine, the contribution of the different segments of the nephron to total calcium reabsorption is heterogenous. Approximately two-thirds of filtered calcium is reabsorbed by the proximal tubule, 20-25% by the thick ascending loop of Henle, and 10% by the distal tubule [14,128,225,226] (**Figure 1.11.**). Although some of the proteins involved in calcium transport are expressed in the thin descending and ascending limbs (**see section 1.2.6.2.**), there is currently no evidence of calcium reabsorption in these segments.

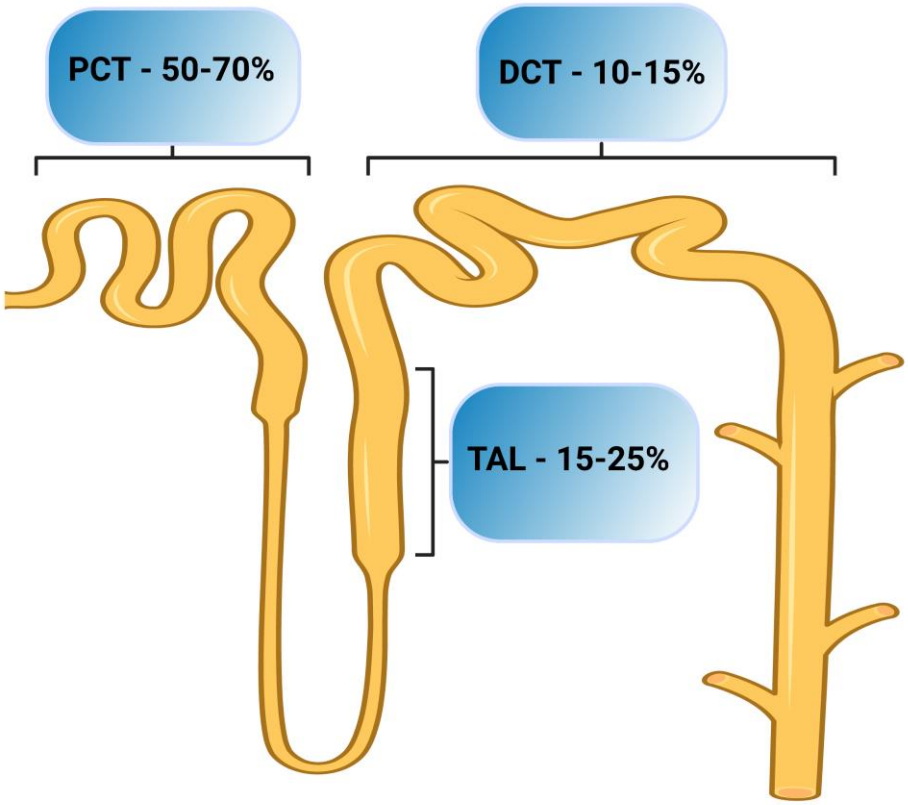

Figure 1.11. Relative contribution of the segments of the nephron to total calcium reabsorption [14,128,225,226]. In the kidney, the proximal convoluted tubule (PCT) contributes about 50-70% to overall calcium reabsorption, while the thick ascending limb (TAL) contributes about 15-25% and the distal convoluted tubule (DCT) contributes 10-15%. *Created using Biorender.com.*

Calcium reabsorption in the proximal tubular segment occurs predominantly via the paracellular pathway by passive diffusion and solvent drag [14,227]. Claudin-2 is known to play a major role in this process based on the evidence that claudin-2 knockout in mice, results in an excess loss of calcium in the urine (hypercalciuria) [159,161,225]. Evidence from claudin-12 knockout mice and the double knockout of claudin-2 and -12 has shown that claudin-12 plays a contributory role in mediating proximal tubular calcium reabsorption [26,27]. Passive diffusion of calcium via claudin-2 and -12 in the

proximal tubule is known to occur in the S2 and S3 segments, driven by the electrochemical gradient of calcium. This electrochemical gradient consists of a concentration gradient generated by the initial transport of sodium and water in the S1 segment [228,229] and an electrical gradient, which is mainly due to the lumen positive transepithelial potential difference generated by the transport of chloride (via claudin-10a and -17 [230,231]) and bicarbonate [227,232]. Calcium reabsorption via solvent drag in the proximal tubule has been reported to be driven by sodium transport mainly via NHE3 [128,186,227]. Interestingly, paracellular calcium transport in the proximal tubule has been speculated to be independent of hormonal regulation [227].

Similar to the proximal tubule, calcium absorption in the TAL occurs mainly via the paracellular pathway [14,225]. This is mainly driven by a lumen positive potential difference generated by the sodium-potassium-chloride co-transporter type 2 (NKCC2) and the renal outer medullary potassium channel (ROMK). While NKCC2 is electroneutral, transporting one Na^+ and K^+ ion along with two Cl^-, the secretion of K^+ back into the lumen via ROMK creates the positive lumen potential difference that drives the paracellular movement of calcium ions via claudin-16 and -19 [128,227]. Paracellular calcium reabsorption in the TAL is regulated by the basolateral CaSR that responds to high dietary calcium load or circulatory calcium infusion [176–178,233,234]. Activation of CaSR regulates calcium transport in the TAL by upregulating the expression claudin-14, which reduces the calcium permeability of claudin-16 and -19 [146,166]. Calcium reabsorption in this segment is also regulated by PTH, which acts via PTH1R to downregulate claudin-14 [174].

It is generally accepted that calcium reabsorption in the distal nephron (DCT and CNT) occurs entirely via the transcellular pathway under physiological conditions [14,227,235]. This is mainly attributed to the fact that the distal tubular calcium concentration is lower compared to serum calcium levels, thus, favouring calcium reabsorption via the active transport pathway [226]. Transcellular calcium reabsorption occurs via the function of TRPV5/6, calbindin-D28k and NCX1 and PMCA [227,236]. Although claudin-14, -16 and -19 expression have been detected in the distal tubule, connecting tubule and collecting ducts of the nephron (**see section 1.2.6.2.**), the contribution of these claudins to calcium reabsorption in these segments is unclear. Interestingly, while the bulk of filtered calcium is reabsorbed in the proximal tubule, urinary calcium excretion is fine-tuned by the distal segments of the nephron, which are considered the main target of the regulatory hormones PTH and $1,25(OH)_2D_3$ [14,236]. The final concentration of urinary calcium is usually determined in the collecting duct, which is the segment where the action of anti-diuretic hormone (vasopressin) results in water reabsorption in order to concentrate urine [227,237,238]. Even though TRPV6 has been shown to be expressed in the collecting duct, there is currently limited evidence as to whether this protein mediates calcium transport in this segment, thus, the contribution of this segment to total calcium reabsorption is uncertain [38,227,236].

1.5. Hormonal regulation of calcium homeostasis

Serum calcium levels are tightly regulated by the interplay between the calciotropic hormones (PTH, vitamin D ($1,25(OH)_2D_3$) and calcitonin) and their target organs (intestine, kidney and bone) [239,240]. When serum calcium levels are low, CaSR located on the parathyroid gland are inactivated resulting in an increase in PTH

secretion [1]. Subsequently, PTH binds to PTHRs in the kidney and bone to increase renal calcium reabsorption and calcium release through osteoclastic bone resorption, respectively [240,241]. Additionally, PTH also increases $1,25(OH)_2D_3$-production in the kidney, which increases serum calcium levels by enhancing intestinal calcium absorption, renal calcium reabsorption and bone resorption, while also supressing further PTH production [241,242]. In contrast, when serum calcium levels are high, these processes are reversed. Circulating calcium activates CaSR to inhibit PTH production, and its stimulatory effect on $1,25(OH)2D_3$ production in the kidney is removed, resulting in a decrease in intestinal calcium absorption, renal calcium reabsorption and bone resorption [1,240]. Furthermore, increase in serum calcium levels also stimulates calcitonin secretion to reduce calcium release by inhibiting the process of bone resorption [241,243]. The major calcium regulatory hormones and mechanisms of calcium homeostasis described above are illustrated in **Figure 1.12**. In addition to PTH, $1,25(OH)_2D_3$ and calcitonin, other hormones such as FGF23, glucocorticoids, prolactin, oestrogen and growth hormone have also been implicated in regulating calcium homeostasis [196,241,242].

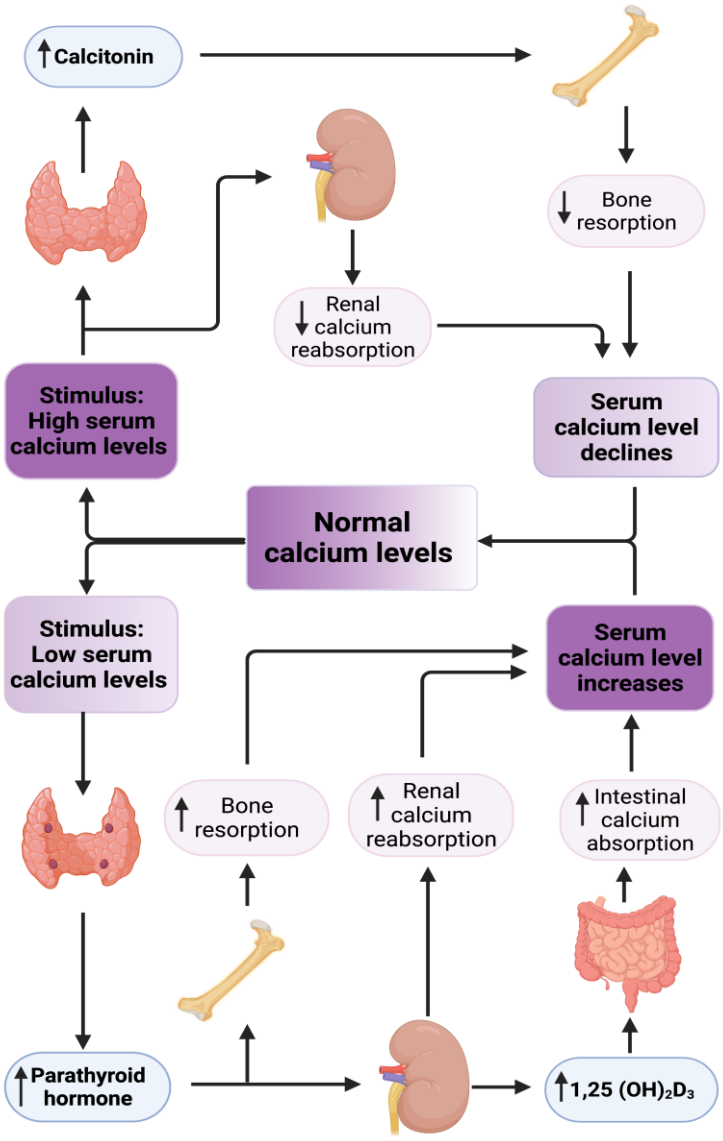

Figure 1.12. Hormonal regulation of calcium homeostasis. Low serum calcium levels stimulate the parathyroid gland to produce PTH, which enhances bone resorption, renal calcium reabsorption and 1,25$(OH)_2D_3$ production to increase intestinal calcium absorption. These result in an increase in serum calcium levels, thus, restoring calcium to normal levels. When serum calcium levels are high, renal calcium reabsorption is reduced and calcitonin production by the thyroid gland is stimulated, resulting in the inhibition of bone resorption and a consequent reduction in serum calcium levels. *Image created using Biorender.com.*

1.5.1. Parathyroid hormone

PTH is a peptide hormone that is produced and secreted by the parathyroid gland in response to low serum calcium levels [225,240,244]. In the kidney, PTH stimulates renal calcium reabsorption in TAL and the DCT by upregulating the proteins mediating the paracellular and transcellular calcium pathways, respectively (described in **section 1.4**). In keeping with this, surgical removal of the parathyroid gland in mice has been reported to result in the downregulation of the renal transcellular calcium proteins, TRPV5, calbindin-D28k and NCX1 [68]. PTH also plays a role in increasing intestinal calcium absorption indirectly by stimulating the production of $1,25(OH)_2D_3$ via its role in activating 1-α-hydroxylase enzyme, which catalyses the conversion of $25(OH)D_3$ (inactive form) to $1,25(OH)_2D_3$ (active form) [8,196,240]. In the skeletal system, PTH has been shown to have a dual effect on calcium release or deposition in bone based on whether there is a continuous or intermittent release of this hormone [245]. During an intermittent or low dose of PTH, bone formation is stimulated by inducing calcium deposition, while calcium release from bone is stimulated by continuous PTH release by enhancing osteoclast activity as seen during primary hyperparathyroidism [246–251]. The physiological function of PTH in the kidney and bone is mediated via the PTH1R [252]. For example, in the TAL of the nephron, the deletion of the PTH1R results in an increase in claudin-14 expression, which is involved in the inhibition of paracellular calcium transport in this segment [174].

The interaction of PTH with PTH1R, a G-protein-coupled receptor, activates either the adenylyl cyclase-cyclic adenosine monophosphate (cAMP)-protein kinase A (PKA) or the phospholipase C (PLC)-inositol triphosphate (IP_3)-protein kinase C (PKC) signalling cascade [252–254]. PTH1R has been identified on the apical and

basolateral membrane of the proximal tubule and TAL, but only on the basolateral membrane of the DCT [255,256]. Additionally, it has been proposed that the activation of apical PTH1R preferentially stimulates the PLC-PKC signalling pathway [257]. PTH has been reported to stimulate calcium uptake in the DCT via the PKC and PKA signalling pathway, while the role of this hormone in mediating calcium uptake in the TAL occurs via PKA signalling [258]. Moreover, the role of PTH in mediating increased expression and activity of 1α-hydroxylase for $1,25(OH)_2D_3$ synthesis in the kidney has been demonstrated to be mediated by cAMP [259,260].

The role of PTH1R in mediating PTH function in bone is not completely understood. However, it is widely accepted that PTH mediates the role of osteoclasts in bone resorption indirectly by activating PTH1R in osteoblasts [256,261,262]. There is evidence that osteoclasts express PTH1R, and the activation of this receptor directly mediates calcium release in the presence or absence of osteoblasts [263,264].

1.5.2. $1,25(OH)_2D_3$

$1,25(OH)_2D_3$ is a steroid hormone that is derived from the diet, supplements or through the conversion of 7-dehydrocholesterol to vitamin D_3 in the skin by ultraviolent B (UVB) radiation [265,266]. $1,25(OH)_2D_3$ is synthesised through a series of metabolic reactions in the liver and kidney. In the liver, vitamin D_3 is converted to $25(OH)D_3$ (inactive form) by the 25-hydroxylase enzyme and is subsequently transported to the kidney by a vitamin D binding protein (DBP) [267]. In response to low serum calcium levels, increased expression of 1α-hydroxylase catalyses the rate-limiting step for the synthesis of $1,25(OH)_2D_3$ (active form) from 25(OH)D3 in the kidney [268]. $1,25(OH)_2D_3$ primarily enhances intestinal calcium absorption via the

transcellular pathway under low serum calcium conditions [196,269]. This has been shown by the upregulation of duodenal TRPV5, calbindin-D9k and PMCA expression following $1,25(OH)_2D_3$ supplementation in 1α-hydroxylase knockout mice [270]. Furthermore, studies using Caco-2 cells treated with $1,25(OH)_2D_3$ have also reported an increase in TRPV5, calbindin-D9k and PMCA expression along with enhanced transcellular calcium flux [271–273]. $1,25(OH)_2D_3$ also enhances paracellular calcium transport via the upregulation of pore forming claudin-2 and -12 [25]. The role of $1,25(OH)_2D_3$ in mediating intestinal calcium absorption requires the interaction of this hormone with its intracellular receptor, VDR [274–276]. Unlike PTH, $1,25(OH)_2D_3$ is a lipophilic steroid hormone that can freely diffuse across the plasma membrane of target cells and binds to VDR located in the cytoplasm [196,269,277]. When VDR is activated, it forms a heterodimer with the retinoid X receptor (RXR) and functions as a transcription factor that binds to VDRE located on the promoter region of target genes in the nucleus to regulate gene expression [278–280]. The loss of the $1,25(OH)_2D_3$ receptor in VDR knockout mice has been shown to result in the downregulation of the mRNA and protein levels of transcellular and paracellular calcium transport proteins [25,276,281].

In addition to the small intestine, $1,25(OH)_2D_3$ has been shown to enhance calcium reabsorption in the DCT by upregulating the proteins involved in transcellular calcium reabsorption (i.e. TRPV5, Calbindin-D28k, NCX1 and PMCA1) [114,227]. There is evidence that $1,25(OH)_2D_3$ affects paracellular calcium transport in the kidney by a mechanism involving CaSR [175]. $1,25(OH)_2D_3$ has been demonstrated to inhibit paracellular calcium transport in the TAL by downregulating the expression of claudin-16 and 19, thus, leading to increased fractional calcium excretion in mice [175].

This action of $1,25(OH)_2D_3$ on renal paracellular calcium absorption has been speculated to be a compensatory mechanism to restore normal serum calcium levels following excessive intestinal calcium absorption in response to this hormone [156].

1.5.3. Calcitonin

Calcitonin is a peptide hormone produced by the parafollicular cells of the thyroid gland, which activates target cells by binding to its receptor [241,242]. Although it is considered one of the hormones regulating calcium homeostasis, very little is known about its effect on calcium homeostasis. While there are no studies indicating a direct effect of calcitonin on intestinal calcium absorption, what is known regarding its effect on calcium absorption is controversial. Some reports suggest that calcitonin increases intestinal calcium absorption indirectly by stimulating 1α-hydroxylase (CYP27B1) expression and $1,25(OH)_2D_3$ production [282,283], while others have reported a decrease in intestinal calcium absorption in response to this hormone [284,285]. More importantly, calcitonin has been reported to have a direct effect on bone by inhibiting osteoclastic bone resorption, which is expected to reduce circulatory calcium levels [286,287]. However, unlike other calcium regulatory hormones, there is a paucity of studies reporting metabolic abnormalities associated with excess levels or deficiency in calcitonin, suggesting that this hormone is unlikely to play a significant role in maintaining calcium homeostasis [243].

1.5.4. Fibroblast growth factor-23

FGF-23 is a glycoprotein that is produced by osteocytes and osteoclasts [288,289]. Although FGF-23 has been established as a phosphaturic hormone that is regulated by phosphate and $1,25(OH)_2D_3$ [290–293], more recent studies have also implicated

calcium as a modulator of FGF-23 secretion [294–296]. Circulatory FGF-23 binds to its receptors on target tissues including the kidney and parathyroid gland, along with α-klotho (a FGF-23 co-factor) to enhance FGF23 binding [297–300]. The action of FGF-23 on the parathyroid gland results in the suppression of PTH production to reduce serum calcium levels [301,302]. In the kidney, FGF23 has been reported to downregulate 1α-hydroxylase expression resulting in the reduction of renal $1,25(OH)_2D_3$ production and subsequently a decrease in intestinal calcium absorption [112,299,300,303].

1.5.5. Dietary calcium

Dietary calcium is thought to be the master regulator of calcium homeostasis since it directly influences serum calcium levels, which subsequently modulates the production of the hormonal regulators [1,9,269]. A low calcium diet results in hypocalcaemia, which has been reported to stimulate PTH secretion in order to enhance calcium release from bone and $1,25(OH)_2D_3$ production in the kidney [196,304,305]. Conversely, a prolonged period of a high calcium diet results in hypercalcaemia, which has been reported to suppress PTH and $1,25(OH)_2D_3$ production [1,305]. Although dietary calcium is known to regulate calcium homeostasis indirectly through the actions of hormones, there is limited information on the direct impact of luminal calcium levels on the regulation of intestinal calcium absorption. Recently, it has been proposed that dietary calcium may directly regulate intestinal calcium absorption due to the presence of CaSR on the intestinal epithelia [306,307]. A study carried out by Lee *et al*. in 2019 [308] demonstrated a decrease in transcellular calcium absorption due to the downregulation of TRPV6 in response to the activation of intestinal CaSR. This effect was stimulated by increased extracellular calcium

levels following dietary calcium intake. The action of CaSR on TRPV6 levels and intestinal calcium flux was demonstrated to be independent of changes in the calciotropic hormones, thus, suggesting that the intestinal epithelia can directly sense extracellular calcium and acutely regulate intestinal calcium absorption [308]. More importantly, there is evidence that increased serum calcium levels, a consequence of increased dietary calcium, directly activates renal CaSR, leading to a PTH-independent upregulation of claudin-14, which inhibits calcium reabsorption in the distal parts of the nephron (**discussed in section 1.4**) [146,166,309,310].

1.5.6. Other regulatory hormones

Other hormones involved in the regulation of calcium homeostasis include oestrogen, which has been shown to increase calcium absorption particularly in postmenopausal women experiencing negative calcium balance [270,311–313]. Prolactin has also been implicated in regulating calcium by stimulating intestinal calcium absorption, particularly during pregnancy and lactation to enhance the calcium available for milk production [165,196,218,314].

1.6. Iron homeostasis

Iron is an essential micronutrient required for several physiological processes within the body, with the most important being erythropoiesis [315–317]. Thus, the majority (approximately 65%) of total body iron (~ 3-5g) is present in the haem component of haemoglobin [315,317,318]. Intestinal iron absorption, iron recycling by macrophages and iron stored in the liver and macrophages play a role in maintaining normal serum iron levels (approximately 14-35μmol/L) [319–321]. Unlike other micronutrients such as calcium and magnesium, there is no known controlled mechanism of excretion for

iron, therefore, iron balance is mainly regulated by intestinal iron absorption from dietary sources [315,322,323]. Under normal conditions, only a small proportion of dietary iron is absorbed daily (~ 1-2mg per day) [323,324]. Therefore, the iron required for erythropoiesis and other metabolic processes is mainly derived from iron recycled by the reticuloendothelial system of the liver and spleen [315,320,325–327].

The adaptation of the small intestine to changes in systemic iron levels is hormonally regulated by the liver derived, 25-amino acid peptide, hepcidin [320,326,327]. When systemic iron levels are high, hepcidin is secreted from the liver, and this hormone lowers serum iron levels by inhibiting intestinal iron absorption and iron release from hepatocytes, and liver (Kupffer cells) or splenic macrophages (**Figure 1.13**) [317,320,328]. When systemic iron levels are low, hepcidin production is suppressed resulting in an increase in intestinal iron absorption and release of iron from its stores to restore normal serum iron levels (**Figure 1.13**) [316,318].

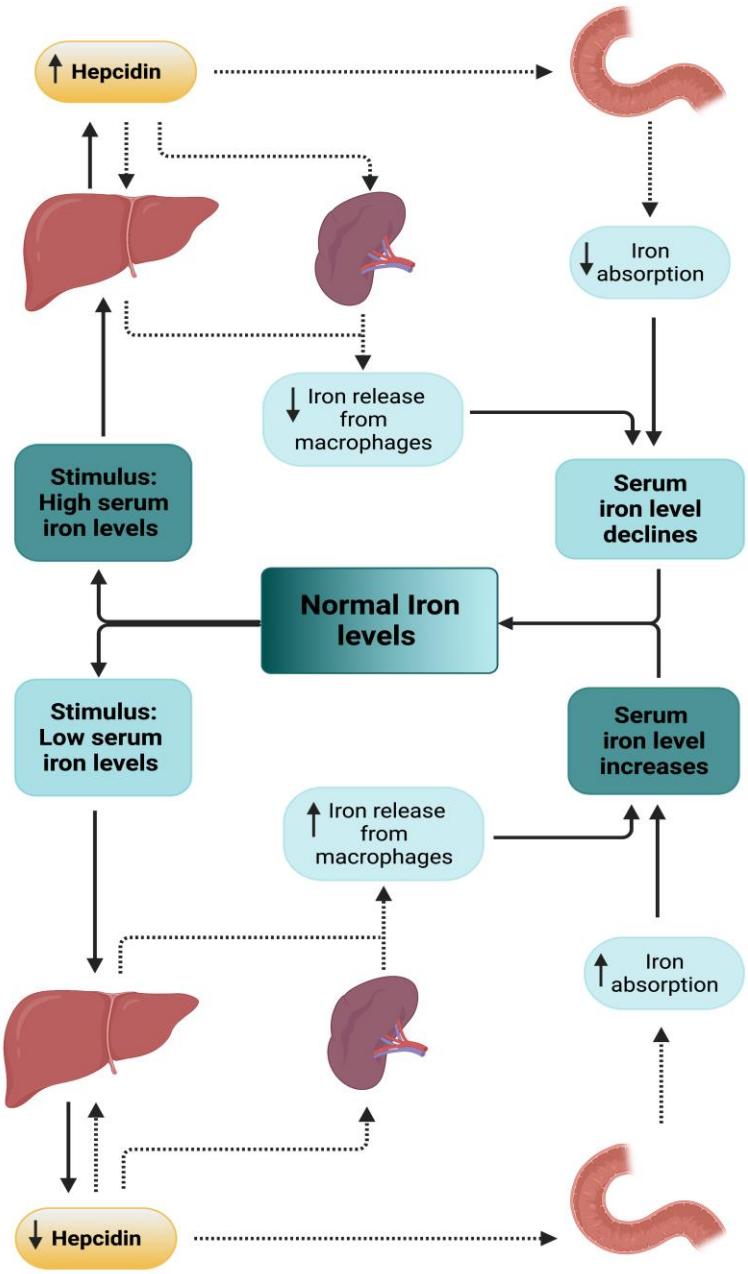

Figure 1.13. Hormonal regulation of iron homeostasis. When serum iron levels are high, hepcidin production and secretion by the liver is enhanced. This results in the reduction of duodenal iron absorption, iron release from hepatocytes and iron release from macrophages of the liver (Kupffer cells) and spleen, thus, reducing serum iron levels. In response to low serum iron levels, hepcidin production and secretion is suppressed resulting in an increase in duodenal iron absorption and iron release from hepatocytes, Kupffer cells and splenic macrophages to increase serum iron levels. Dotted lines represent the effect of hepcidin on its target organs. *Image created using Biorender.com.*

1.6.1. Mechanism of intestinal iron absorption

Intestinal iron absorption occurs in the proximal small intestine (i.e. duodenum and jejunum), of which the duodenum has been reported to be the major site of absorption [329–333]. Dietary iron is available in 2 forms, haem and non-haem iron [316,331,334]. Haem iron is limited to animal sources such as meat, poultry and fish in the form of haemoglobin and myoglobin, and is absorbed more efficiently, however, its mechanisms of absorption are not widely studied [317,323,335]. The apical entry of dietary haem into enterocytes is proposed to occur via a haem carrier protein 1 (HCP1), it is then cleaved by haem oxygenase (HO) in the cytosol to release ferrous iron (Fe^{2+}) that can be exported into the circulation via the basolateral protein, ferroportin (FPN) or stored as ferritin (**Figure 1.14**) [336–338]. In contrast to haem, non-haem iron is found in a wider variety of foods including plant-based foods like legumes, but is absorbed less efficiently [323,335,339,340]. The well-established transport of non-haem iron across the duodenum, begins with the entry of Fe^{2+} through the apical membrane divalent metal transporter 1 (DMT1; also known as Nramp2, SLC11A2 or DCT1) into the enterocyte [330,331,338]. DMT1 acts as a secondary active co-transporter utilising the energy generated from driving protons down its concentration gradient to transport Fe^{2+} into the enterocyte [331,341]. The electrochemical gradient of hydrogen necessary to drive the H^+-coupled Fe^{2+} absorption is created by NHE3, which pumps hydrogen into the intestinal lumen [330,342]. Prior to the entry of iron into the enterocytes, Fe^{3+}, which is the state of most dietary iron, is reduced to Fe^{2+} by duodenal cytochrome b (DcytB) (a reductase enzyme located on the apical membrane), making Fe^{2+} available for DMT1-mediated transport [331,343,344]. Following iron entry into the enterocyte, iron is potentially

chaperoned by the iron trafficking protein, poly(rC)-binding protein 1 (PCBP1) to the basolateral membrane for export into the circulation via FPN or stored as ferritin [331,345,346]. Exported Fe^{2+} is then re-oxidised to Fe^{3+} by hephaestin to enable its binding to circulatory transferrin, which delivers iron to target tissues (**Figure 1.14**) [329,338,347].

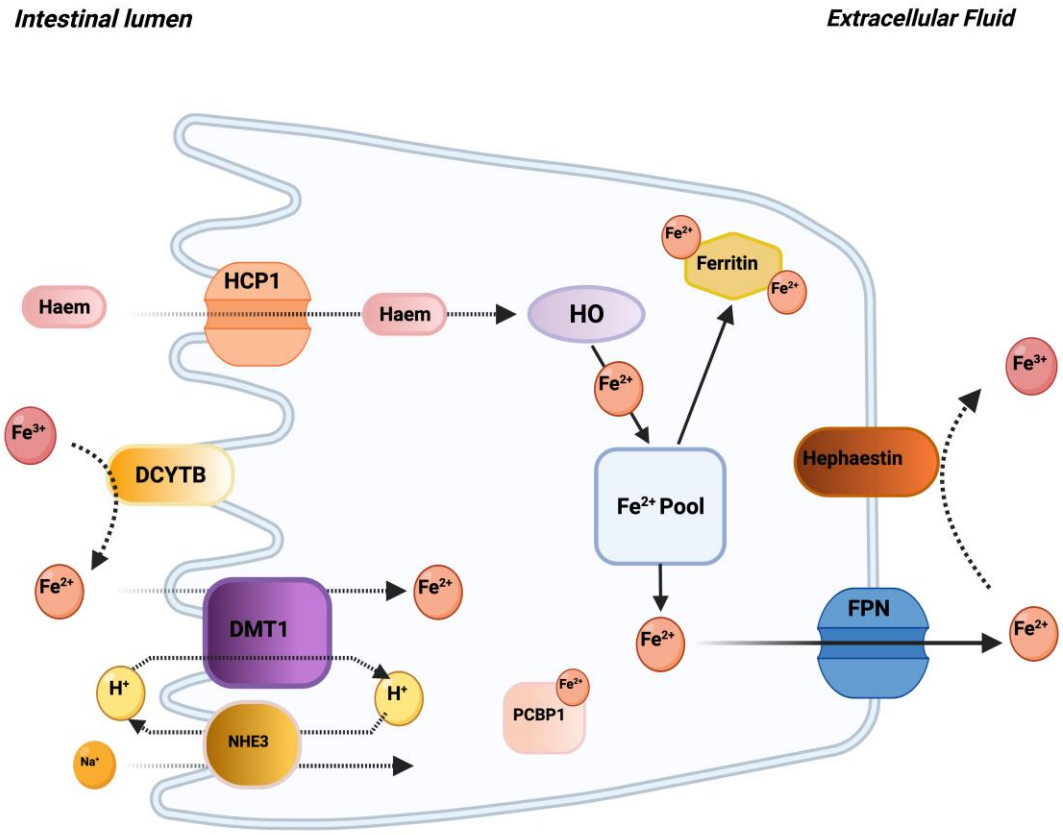

Figure 1.14. Mechanism of intestinal iron absorption. Dietary non-haem Fe^{3+} is first reduced to Fe^{2+} by duodenal cytochrome b to facilitate its apical entry via the divalent metal transporter (DMT1) into the enterocyte. DMT1-mediated Fe^{2+} entry is driven by the transport of H^+ down its concentration gradient which is created by NHE3. Following apical entry, Fe^{2+} can either be delivered by the poly(rC)-binding protein 1 (PCBP1) to the basolateral membrane for FPN-mediated iron export or stored as ferritin. Once exported, Fe^{2+} is re-oxidised to Fe^{3+} by hephaestin to enable binding to transferrin. Dietary haem iron is transported into the cytosol via the haem carrier protein 1 (HCP1), where it is cleaved by haem oxygenase (HO) to release Fe^{2+}, which can then be stored or exported out of the enterocyte. *Image created using Biorender.com*.

1.6.2. Regulation of intestinal iron absorption

Iron absorption is regulated at both cellular and systemic levels. The enterocyte adapts to changes in intracellular iron levels through the post-transcriptional regulation of genes involved in iron metabolism by the iron-regulatory protein (IRP)-iron regulatory element (IRE) system [331,336]. DMT1 and FPN transcripts contain an iron regulatory element in the 3' and 5' untranslated region, respectively [331,348,349]. Under low dietary iron conditions, IRP is activated, which enhances DMT1 transcript stability and translation to protein, while suppressing FPN protein levels, a response that is thought to maintain cellular iron content [331,336,350]. Interestingly, a ferroportin isoform lacking the 5'IRE (FPN1B) has been identified, which is not subjected to repression by the IRP-IRE system during iron deficiency. Therefore, the lack of suppression of FPN1B is proposed to be responsible for the characteristic increase in overall FPN levels during iron deficiency [351].

In addition to the IRP-IRE system, DMT1 and FPN are also transcriptionally regulated by hypoxia-inducible factor-2α (HIF-2α) [331,352,353]. HIF-2α is part of the HIF family consisting of the isoforms, HIF-1, HIF-2 and HIF-3, which are heterodimeric nuclear transcription factors made up of an oxygen sensitive and iron-responsive cytoplasmic α-subunit, and a constitutively expressed β-subunit, found in the nucleus [354,355]. The HIF family are hypoxia responsive transcription factors that regulate the expression of target genes involved in oxygen homeostasis [354,355]. Under a normal oxygen environment, HIF-1α and HIF-2α are hydroxylated by an iron-dependent propyl-hydroxylase domain (PHD) enzymes, which targets them for proteosomal degradation [356,357]. More recently, HIF-2 has also been shown to play a role in iron metabolism [352,353].

Under iron-deficient conditions, the PHD enzymes are suppressed resulting in the accumulation and translocation of HIF-2α into the nucleus where it binds to the constitutively-expressed β-subunit (HIF-2β) [358,359]. The HIF heterodimer, along with the transcriptional co-activators then binds to the hypoxia-responsive-elements (HRE) of target genes resulting in the transcription of genes coding for proteins involved in iron transport, including DMT1, FPN, hepcidin and erythropoietin [360,361]. Targeted deletion of intestinal HIF-2α in mice has been reported to decrease DMT1 and FPN mRNA expression, and causes a reduction in serum iron and liver hepcidin levels [360].

As previously described, hepcidin is the major systemic regulator of intestinal iron absorption, which acts by reducing iron transport when extracellular iron levels are high. Using duodenal segments of mice and Caco-2 cells, hepcidin has been shown to suppress iron absorption by inducing ubiquitin-dependent proteosomal degradation of DMT1 [362–364]. Although there is evidence demonstrating direct downregulation of FPN by hepcidin in macrophages, there are conflicting reports regarding the changes in duodenal FPN levels in response to hepcidin treatment [362,364,365]. While Chung *et al.* [364] reported a decrease in duodenal FPN expression in response to a 72 hour treatment of hepcidin in mice, Chaston *et al.* [365] and Brasse-Lagnel et al. [362] demonstrated no change in FPN levels following a 24 hour and 30 minute hepcidin treatment respectively. The reason for this discrepancy is likely due to the duration of hepcidin treatment, suggesting that the regulation of duodenal FPN by hepcidin requires more than 24 hours of treatment unlike macrophage FPN.

In addition to hepcidin, erythropoietin (EPO) has also been implicated in regulating intestinal iron absorption. EPO is a kidney-derived glycoprotein hormone that stimulates erythropoiesis upon binding to its receptor on erythroid progenitor cells in the bone marrow [317,366,367]. Additionally, EPO has also been reported to increase intestinal iron absorption [368]. Studies in rats and mice have shown that EPO treatment results in the inhibition of hepcidin mRNA expression [369,370]. Moreover, EPO receptor has been detected in the rat duodenum [368], and the treatment of rats with EPO has been shown to increase mRNA and protein levels of DMT1-IRE [370]. Furthermore, an upregulation of FPN mRNA and protein has also been detected in EPO-treated Caco-2 cells [368]. Taken together, these findings suggests that EPO induces intestinal iron transport indirectly by inhibiting hepcidin production and/or directly via its interaction with intestinal EPO receptor to stimulate the upregulation of DMT1 and FPN.

1.7. Relationship between regulators of calcium and iron homeostasis

There is evidence that hepcidin effectively upregulates intestinal calcium transport in a mouse model of dysfunctional iron metabolism (β-thalassaemic mice) [371]. β-thalassemia, a condition characterised by iron overload, has been reported to decrease duodenal calcium absorption and $1,25(OH)_2D_3$ levels in mice [371,372]. Although the decrease in calcium absorption in β-thalassaemic mice could be attributed to the low levels of $1,25(OH)_2D_3$, surprisingly, hepcidin treatment has been reported to increase intestinal calcium absorption in these animals [371]. This suggests a relationship between the iron regulatory hormone and calcium transport [371]. Moreover, an inverse correlation between intestinal iron and calcium absorption has also been speculated [371,373]. Taken together, the role of hepcidin in mediating

intestinal calcium absorption and the inverse relationship between intestinal iron and calcium absorption, suggest that iron and the other regulators of iron homeostasis may be novel regulators of the intestinal transcellular and paracellular calcium transport pathways.

Furthermore, cellular iron levels have been shown to be inversely correlated with cellular calcium levels in Caco-2 cells [374]. Low levels of intracellular iron following hepcidin treatment have been demonstrated to increase calcium uptake in Caco-2 cells [374], suggesting that cellular iron content may locally impact intestinal calcium absorption. Importantly, disorders involving iron overload in humans and rodents (e.g. haemochromatosis and β-thalassemia) have been shown to be associated with altered bone mineral density and osteoporosis [375–380]. Since changes in intestinal calcium absorption was reported under conditions associated with iron overload [371,372,375,381–383], it is possible that the altered bone mineral density and osteoporosis may be linked to iron imbalance. In addition to iron overload, there is a large body of evidence indicating that iron deficiency results in the loss of bone mineral density, and consequently causes bone disease [384–388].

1.8. Hypothesis

Based on the evidence indicating a relationship between iron and calcium homeostasis (**discussed in section 1.7**), the hypothesis of the current study was that iron, or the regulators of iron homeostasis, may play a novel role in regulating the mechanisms of paracellular calcium absorption in the small intestine.

1.9. Aims of thesis

This study builds on a previous study in our laboratory demonstrating a distinct segmental profile of intestinal phosphate absorption and the impact of diet-induced iron deficiency on transepithelial phosphate transport in the different segments of the small intestine *in vivo*. Since phosphate and calcium, which are essential components of bone mineral are replenished by dietary sources, this study focused on intestinal calcium absorption. Since the paracellular pathway is known to predominantly mediate intestinal calcium absorption under normal dietary conditions, this study was carried out using experimental conditions that favour the paracellular pathway. To investigate the hypothesis of the current study, the following aims were established:

1. Since iron absorption is known to occur predominantly in the duodenum, the first aim was to investigate the segmental differences in calcium absorption across the duodenum, jejunum, and ileum of rats, and to compare the intestinal expression profile of calcium transport proteins in rats and humans.
2. Based on the evidence that iron imbalance is associated with altered bone mineral metabolism (**discussed in section 1.7**), the second aim was to examine whether diet-induced iron deficiency affects calcium homeostasis, with particular focus on its impact on intestinal calcium absorption using the *in situ* intestinal loop technique.
3. Using Caco-2 cells, the current study also aimed to understand the potential cellular mechanisms underlying the impact of iron-deficiency on paracellular calcium flux *in vitro*.

The aims of the current study are important because a complete understanding of the mechanisms underlying the segmental differences in calcium absorption will be essential to identify new targets for controlling calcium absorption in specific small intestinal segments. Importantly, unravelling the impact of iron deficiency on intestinal calcium absorption and underlying mechanism will generate novel insights into how iron can be targeted as a regulator of intestinal calcium absorption *in vivo*.

Chapter 2 - Segmental differences in calcium absorption in the small intestine

2.1. Introduction

The regulation of intestinal calcium absorption, renal calcium reabsorption and the release of calcium stored in the bone, collectively play a vital role in tightly regulating calcium levels within normal physiological limits [1]. In humans with renal insufficiency due to kidney disease or hereditary disorders, intestinal absorption becomes the major determinant of the levels of calcium in the circulation. Although calcium stored in the bone can also contribute to the maintenance of normal serum calcium levels, dietary calcium is still required to replenish its stores [225]. Therefore, tightly regulated absorption of calcium from the diet is crucial to maintain calcium levels within normal physiological limits in this scenario. Dietary calcium is absorbed in both the small and large intestine, however, due to the solid state of chyme in the large intestine, the bulk of calcium absorption occurs in the small intestine [6,204]. Small intestinal calcium absorption is mediated via transcellular and paracellular pathways (discussed in detail in **Chapter 1, section 1.2**). While the transcellular calcium absorption pathway is known to be very important during dietary calcium restriction, the paracellular pathway is predominant under a normal or high calcium diet [11]. As described in **Chapter 1, section 1.2**, TRPV6, calbindin-D9k, PMCA1b and NCX1 mediate transcellular calcium transport, while claudin-2 and -12 are mainly responsible for paracellular calcium absorption in the intestine [10,25]. Transcellular calcium absorption is dominant in the duodenum of rodents and humans as this segment exhibits the highest expression of the transcellular transporters [6] compared to the jejunum and ileum. However, there is a paucity of information regarding the relative segmental expression and functional absorption profile of the paracellular calcium transport pathway in the three segments of the small intestine of rodents

and humans. Additionally, due to the difficulty in studying the mechanisms of calcium absorption using fresh human intestinal tissues, human Caco-2 cells are continually employed as a good model to study ion transport processes in the human small intestine.

Caco-2 cells are known to exhibit most of the absorptive phenotype of the human small intestine including a well-developed tight junction when fully differentiated after 21 days in culture [389,390]. Numerous *in vitro* studies have used of Caco-2 cells to investigate the transcellular and paracellular mechanisms of calcium absorption, and the impact of $1,25(OH)_2D_3$ in regulating these mechanisms [25,271,272,391–393]. Although these studies have considered Caco-2 cells as a good model for investigating small intestinal calcium absorption, no study has identified the specific small intestinal segment in humans that is most comparable to Caco-2 cells. There is also a paucity of information regarding how the mRNA expression of the small intestinal calcium transporters, and claudin-2 and -12 compare with the expression levels in Caco-2 cells. Investigating and comparing the mRNA expression of the transcellular and paracellular calcium transport proteins in human intestinal biopsies and Caco-2 cells in the current study will provide some insight into the specific intestinal segment Caco-2 cells represent.

2.1.1. Aims

The aim of this chapter was to investigate the functional absorption profile of paracellular calcium absorption in the duodenum, jejunum, and ileum and to investigate the underlying mechanisms responsible for the potential differences. Second, was to compare the expression profile of the transcellular and paracellular

calcium transport proteins in parental Caco-2 cells with the human duodenum and ileum to determine which segment parental Caco-2 cells are most comparable to.

2.2. Materials and Methods

2.2.1. Ethics

All procedures were carried out in accordance with the UK Animals Scientific Procedures Act, 1986, Amendment regulations 2012. Protocols were approved by the University College London (Royal Free Campus) Comparative Biology Unit (CBU) and the Animal Welfare and Ethical Review Body (AWERB) committee and carried out according to the project licence PPL 14178. For the human tissue experiments, all volunteers gave written consent, and the study was approved by the Regional Ethical Review Board of Gothenburg, Sweden.

2.2.2. Animals and diet

Male Sprague Dawley rats, age 6-8 weeks (180-200g) were purchased from Charles River Laboratories (Harlow, UK) and transported to the Royal Free Campus Comparative Biology Unit (CBU). A maximum of 3 rats were housed in a cage under a 12-hour light/12-hour dark cycle and allowed to acclimatise for 4 days while given *ab libitum* access to a standard RM1 diet (Special Diet Services, Witham,UK) and water. Following this, the animals were fed a control diet (TD. 80394) containing 48ppm iron, 0.52% calcium and 0.54% phosphorus (Harlan Laboratories, Inc. Madison, WI, USA) for 2 weeks, which was consistent with the diets of the control animals in the experiments reported in Chapter 3.

2.2.3. *In vivo* calcium uptake experiments and intestinal tissue collection in rats.

Following the 2-week dietary regimen, intestinal calcium absorption was measured using an *in situ* intestinal loop technique. The animals were weighed and anesthetised with an intraperitoneal injection of 45mg/kg of pentobarbitone sodium (Pentoject, Animal Care Ltd., Kent, UK). The depth of anaesthesia was confirmed and monitored by checking the reflexes (corneal, tail pinch and pedal withdrawal). Once deep anaesthesia was confirmed, the femoral artery was cannulated for blood collection. In each anesthetised animal, a 5cm long segment of the duodenum (beginning 2cm distal to the pylorus), jejunum (5cm distal to the ligament of Trietz), or ileum (5cm proximal from the ileocecal junction) was isolated, and the lumen was flushed with warm 0.9% saline, followed by air. Subsequently, 450µl of uptake solution containing 16mM sodium-HEPES, 140mM NaCl, 3.5mM KCl, 100mM $CaCl_2$ (pH 7.4) and 0.37MBq ^{45}Ca (PerkinElmer, Bucks, UK) was then instilled into the lumen and the segment was tied off. The chosen volume of buffer ensured that the intestinal segment was filled with the buffer whilst preventing distention. To determine the amount of ^{45}Ca absorbed from the isolated segment, 500µl of blood was collected at 10-minute intervals for a duration of 30 minutes via the femoral artery and centrifuged at 5,000xg for 10 minutes to obtain the plasma, and the activity of ^{45}Ca was subsequently measured using a scintillation counter (Tri-Carb 2900TR; Perkin Elmer). The proportion of ^{45}Ca transferred into 1ml of plasma per 5cm of the segment was calculated using the amount of ^{45}Ca in the plasma and initial uptake solution, and the length of the isolated intestinal segment. Following blood

collection, the animals were killed by excising the heart and death was confirmed by cessation of breathing.

To investigate the regional expression of the calcium transport proteins, intestinal mucosa was collected from the duodenum (between the end of the pylorus to the ligament of Trietz), jejunum (ligament of Trietz to halfway along the remainder of the small intestine), and ileum (from the half-way point to the ileocecal junction). Subsequently, the mucosa was snap frozen and stored at -80^{o}C for future experiments.

2.2.4. Human tissue collection

Following an overnight fast, human tissue biopsy were collected from the small intestine of healthy adult volunteers in the endoscopy unit of the Sahlgrenska University Hospital, Gothenburg, Sweden. Biopsies of the duodenum, proximal jejunum and ileum was collected following sedation using midazolam and alfentanil. After which, the tissues were immediately placed in RNA STAT-60 (Amsbio, Abingdon, U.K) and subsequently snap-frozen in liquid nitrogen. The human tissue samples were then kindly shipped on dry ice to the Royal Free hospital, London, by Prof. Lars Fandriks' Laboratory from University of Gothenburg, Sweden, where they were used for the current study.

2.2.5. Cell culture

Parental colon adenocarcinoma cells (Caco-2 cells) were kindly gifted by Dr Havovi Chichger (Anglia Ruskin University) and used from passage 35-45. Cells were cultured in Dulbecco's-modified Eagle's medium (DMEM; Gibco, Fisher Scientific, Loughborough, UK), supplemented with 10% foetal bovine serum (FBS; Gibco,

Fisher Scientific, Loughborough, UK) and 1% penicillin/streptomycin (Sigma Aldrich, Gillingham, UK). The seeding density of the cells was 10,000 cm^{-2} and the cells were 100% confluent 3 days after seeding. Cultures were incubated at 37°C with 5%CO_2:95%O_2 and >95% humidity. At approximately 70% confluence, cells were sub-cultured by trypsinisation (Gibco, Fisher Scientific, Loughborough, UK) and the medium was changed every 2 days for a duration of 21 days.

2.2.6. RNA extraction and cDNA synthesis

RNA was extracted from rat intestinal mucosa, human intestinal biopsies and Caco-2 cells using TRIzol reagent according to manufacturer's instructions (Life Technologies, Paisley, UK). The quality and concentration of the RNA was then quantified using a Denovix (DS-11) spectrophotometer (Delaware, USA) and 1 µg of the extracted RNA was treated with deoxyribonuclease I (Invitrogen Life Technologies, Paisley, UK) to remove any DNA contamination according to manufacturer's instructions. Subsequently, using a cDNA synthesis kit (PCR Biosystems Ltd, London, UK), complementary DNA (cDNA) was synthesised by the reverse transcription and a corresponding negative control (without reverse transcriptase) was prepared following the manufacturer's instructions.

2.2.7. Reverse-transcription polymerase chain reaction

The mRNA expression of the genes of interest was detected and analysed by real-time polymerase chain reaction (RT-PCR) using a 2x qPCRBIO SyGreen kit (PCR Biosystems Ltd, London, UK) and primers specific for rat (Table 2.1) and human (Table 2.2) samples. The primers were either purchased from Qiagen (UK) or ThermoFisher Scientific or predesigned sequences were sent to Sigma-Aldrich to be

manufactured. Using a Light Cycler 96 instrument (Roche Diagnostics, East Sussex, UK), cycling conditions were set to the following: preincubation at 95°C for 10 minutes and a 3-step amplification consisting of: 95°C for 10 seconds (separation of DNA strands), 60°C for 10 seconds (to promote primer annealing) and 72°C for 10 seconds (to promote primer extension by DNA polymerase). A total of 35 or 45 cycles of the amplification process were carried out followed by a melting step consisting of 95°C for 10 seconds, 60°C for 60 seconds and 97°C for 1 second to terminate the reaction. The mRNA expression of the desired gene was expressed as the ratio of the gene of interest to β-actin using the Light Cycler 96 analysis software.

Table 2.1. Rat-specific primers. Primers were obtained from Qiagen, UK, and specific primer sequences were not given, however, information regarding sequence can be obtained using the catalogue number of each primer.

Primer name	**Catalogue number**
Claudin-2	QT00451836
Claudin-12	QT01607319
Claudin-15	QT01584604
TRPV6	QT00185255
Calbindin-D9K	QT00381458
PMCA1	QT00182210
NCX1	QT00456323
β-actin	QT00193473

Table 2.2. Human-specific primers. Primers were either obtained from Qiagen, ThermoFisher Scientific or predesigned primer sequences were used to make the primer by Sigma-Aldrich

Human Primers	**Catalogue number**	**Forward sequence**	**Reverse sequence**
TRPV6	QT00040096	-	-
Calbindin-D9K	QT00000329	-	-
PMCA1	QT00087045	-	-
NCX1	QT02432633		
Claudin-2	Hs00252666_s1	-	-
Claudin-12	QT01012186	-	-
β-actin	-	AACAAGATGAGATTGGCATGG	AGTGGGGTGGCTTTTAGGAT

2.2.8. Intestinal brush border membrane vesicles

Intestinal brush border membrane vesicles were prepared from snap frozen duodenum, jejunum and ileum mucosa using $MgCl_2$ as described previously [394]. Mucosa tissue was weighed and mixed with homogenising buffer (28ml/g of tissue) containing 50mM mannitol, 2mM 4-(2-hydroxyethtl)-1-piperazineethanesulfonic acid (HEPES), pH 7.1. The intestinal mucosa was then homogenised three times for 20 seconds each with 5 second intervals using an Ultraturax homogeniser (Jankee & Kunkel, FRG, UK) at half speed. A portion of the homogenate sample was collected and stored for protein quantification and Western blotting. $MgCl_2.6H_2O$ was added to the remaining homogenate to make up a final concentration of 10mM, which was

stirred on ice for 20 minutes, and centrifuged at 4600xg for 10 minutes. The resultant pellet containing nuclei, cell debris and non-microvilli contaminating membranes was discarded and supernatant was re-centrifuged at 41600xg for 30 minutes. Subsequently, the pellet was re-suspended in 20ml/g of resuspension buffer containing 300mM mannitol, 20mM HEPES, 0.1mM $MgSO_4$, pH 7.2 using a 5ml syringe and a 21G needle. Following resuspension, the sample was then centrifuged for 15 minutes at 9300xg, to obtain a supernatant. The supernatant was collected and subjected to a final centrifugation step for 30 minutes at 41600xg to obtain the brush border (microvilli) vesicles (BBMV), which was re-suspended in the appropriate volume of resuspension buffer to a protein concentration of between 3 – 6mg/ml. All buffers used for the brush border preparation were supplemented with EDTA-free protease inhibitor that inhibits a broad spectrum of serine and cysteine proteases (Roche Life Sciences, West Sussex, UK) to prevent protein degradation and the protein concentration of the homogenate and BBMV samples was determined using a Bradford assay [395].

2.2.9. Western blotting

Intestinal BBMV or homogenate samples (50 and 100µg, respectively) were solubilised in 2xLaemmli buffer (Bio-rad, USA) and loaded onto a 10% SDS-polyacrylamide gel (used to detect proteins >30kDa) or a 16% gel (for proteins <30kDa). The loaded samples were then separated by gel electrophoresis using a running buffer (containing 25mM TRIS- Base, 200mM glycine and 0.1% (v/v) SDS) at 40mA and transferred to a polyvinylidene difluoride (PVDF) membrane at 15V for 1 hour 15 minutes or 10V for 25 minutes for a 10% or 16% gel, respectively. Non-specific proteins were blocked using 6% fat-free milk in PBS-Tween (0.1% Tween-

20) for 1 hour at room temperature and incubated with a primary antibody (raised in mouse or rabbit) specific to the protein of interest overnight at 4^{o}C. Following a 15-minute and a 3x 5-minute wash in PBS-Tween, the proteins were incubated with either an anti-mouse (1:500 dilution, Sigma Aldrich, Dorset, UK) or an anti-rabbit (1:2000 dilution, GE Healthcare, Buckinghamshire, UK) HRP-conjugated secondary antibody for 1 hour. Following this, the membrane was washed as previously described and the protein of interest was detected using a chemiluminescence solution (ECL, containing 2.5mM 3- aminophthalhydrazide, 0.4mM p-coumaric acid, 100mM Tris-HCl, 200mM NaCl, 30% hydrogen peroxide, pH 8.5) and a c600 azure imager. Subsequently, the membranes were stripped of the bound antibody using a stripping buffer (Thermoscientific, Hemel, Hempstead, UK), blocked in 6% fat-free milk for 1 hour and re-probed for β-actin following the steps previously described. The ratio of the protein of interest to β-actin band volume was measured for each sample using ImageJ software and presented in arbitrary units (a.u). The antibodies used along with their optimal dilution factors are listed in **Table 2.3**.

Table 2.3. Primary antibodies used for Western blotting

Protein of interest (Concentration)	**Company**	**Catalogue number**	**Dilution**	**Species**
Claudin-2 (0.5mg/ml)	Thermofisher	12H12	1.1000	Mouse monoclonal
Claudin-12 (0.25mg/ml)	Thermofisher	38-8200	1:500	Rabbit polyclonal
β-actin (HRP-conjugated) (1.0mg/ml)	Proteintech	HRP-60008	1:2000	Mouse monoclonal

2.2.10. Statistical analysis

Data are presented as the mean ± standard error of mean (SEM). Statistical analysis was carried out using GraphPad prism software 9.0. Where possible, unpaired Student's t-test and one-way ANOVA with Tukey multiple comparisons test were used to analyse differences between two groups, and three or more groups respectively. Statistical significance was represented by *p<0.05, **p<0.01, ***p<0.001 and ****p<0.0001.

2.3. Results

2.3.1. Segmental differences in calcium absorption across the small intestine

Although the segmental differences in transcellular calcium absorption across the small intestine have been extensively studied, little is known about the differences in the paracellular calcium transport pathway. To investigate this, *in vivo* uptake experiments were conducted using 100mM $CaCl_2$ (a concentration that favours the paracellular calcium pathway) and ^{45}Ca over a 30-minute period. The results showed that calcium absorption was highest in the duodenum and lowest in the ileum (**Figure 2.1A**). To investigate the differences in the rate of calcium absorption in each segment of the small intestine, the amount of calcium absorbed was divided by the duration of the experiment (30 minutes). As expected, the result showed that the highest rate of calcium absorption occurred in the duodenum, followed by the jejunum, while the lowest rate of calcium absorption was seen in the ileum (**Figure 2.1B**). These results suggest that the duodenum has the highest capacity for calcium transport.

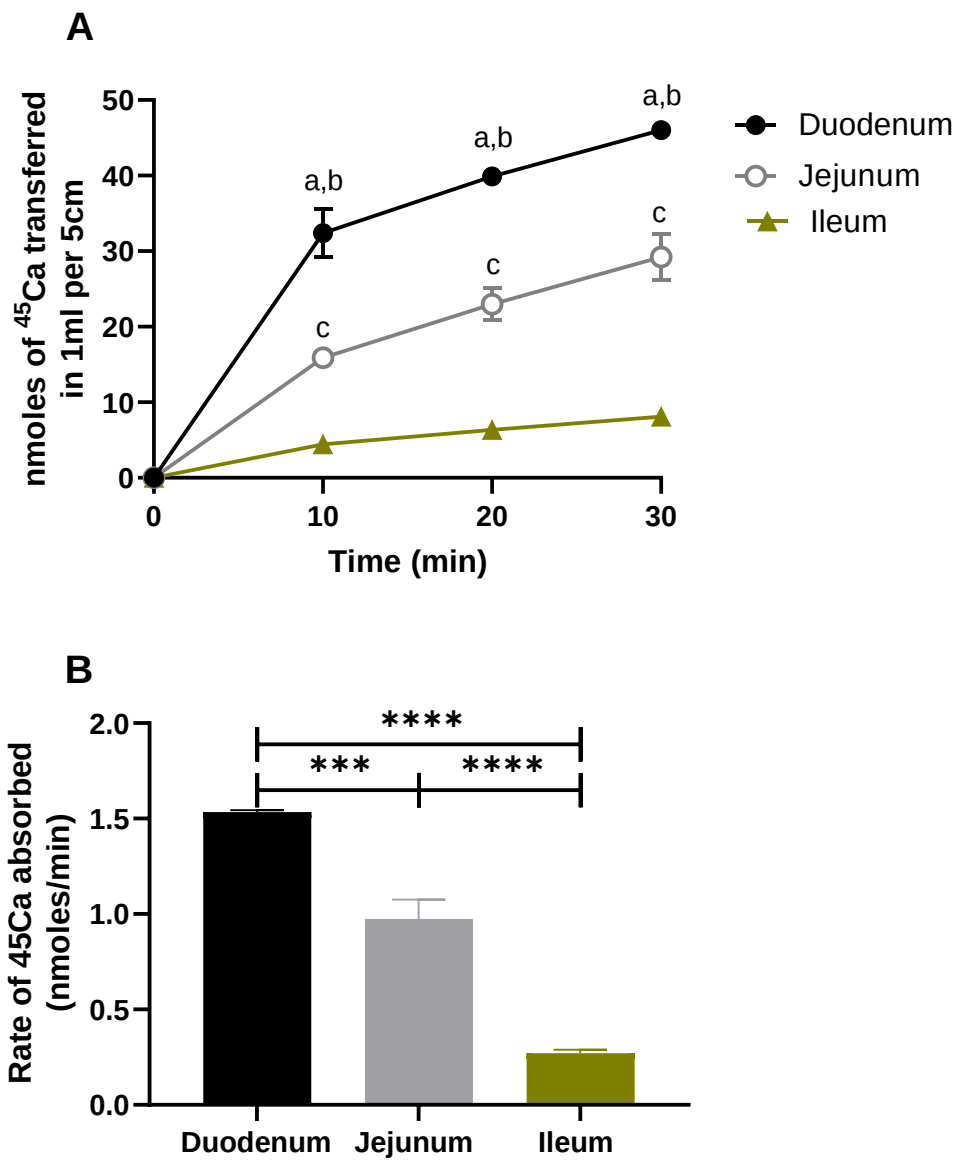

Figure 2.1. Segmental differences in intestinal calcium absorption *in vivo*. A: Calcium absorbed from intestinal luminal solution (containing 100 mM $CaCl_2$ and ^{45}Ca), instilled into the duodenum, jejunum or ileum, was determined after 10, 20 and 30 minutes, using *in situ* intestinal loop technique. Data were analysed using a two-way ANOVA, with Bonferroni's multiple comparisons post-test used to compare differences between segments at different time-points. a-c indicates comparisons with P<0.0001. a represents duodenum *Vs* jejunum, b represents duodenum *Vs* ileum and c = jejunum *Vs* ileum, at each time-point, n=4-6 rats per intestinal segment or time-point. **B**: Rate of calcium absorbed in the duodenum, jejunum, and ileum over a 30-minute period. Values are expressed as mean ± SEM. Data were analysed using one-way ANOVA ***P<0.001, ****P<0.0001, n=4-6 rats in each group.

2.3.2. Intestinal expression profile of transcellular calcium transporters

To understand the mechanisms responsible for the differences in calcium absorption across the small intestine, the relative mRNA expression of the proteins involved in transcellular calcium absorption was investigated in the duodenum, jejunum, and ileum. The mRNA expression of TRPV6, which is the protein responsible for calcium entry into enterocytes across the BBM, was relatively higher in the duodenum, while expression was barely detectable in the jejunum and ileum (**Figure 2.2**). Additionally, there was no significant difference in TRPV6 expression between the jejunum and ileum (**Figure 2.2**). Similarly, the mRNA expression of the cytosolic calcium binding protein Calbindin-D9k, and the calcium exporter protein PMCA1 were significantly higher in the duodenum compared to the jejunum and ileum, with similar levels of these transporters seen in the jejunum and ileum (**Figure 2.2**). Interestingly, the pattern of expression of these transcellular transporter's mirrors that of the *in vivo* calcium uptake where calcium flux was greatest in the duodenum. The expression profile of NCX1, another calcium exporter, was shown to be lowest in the jejunum, with the duodenum and ileum showing a similar expression profile (**Figure 2.2**).

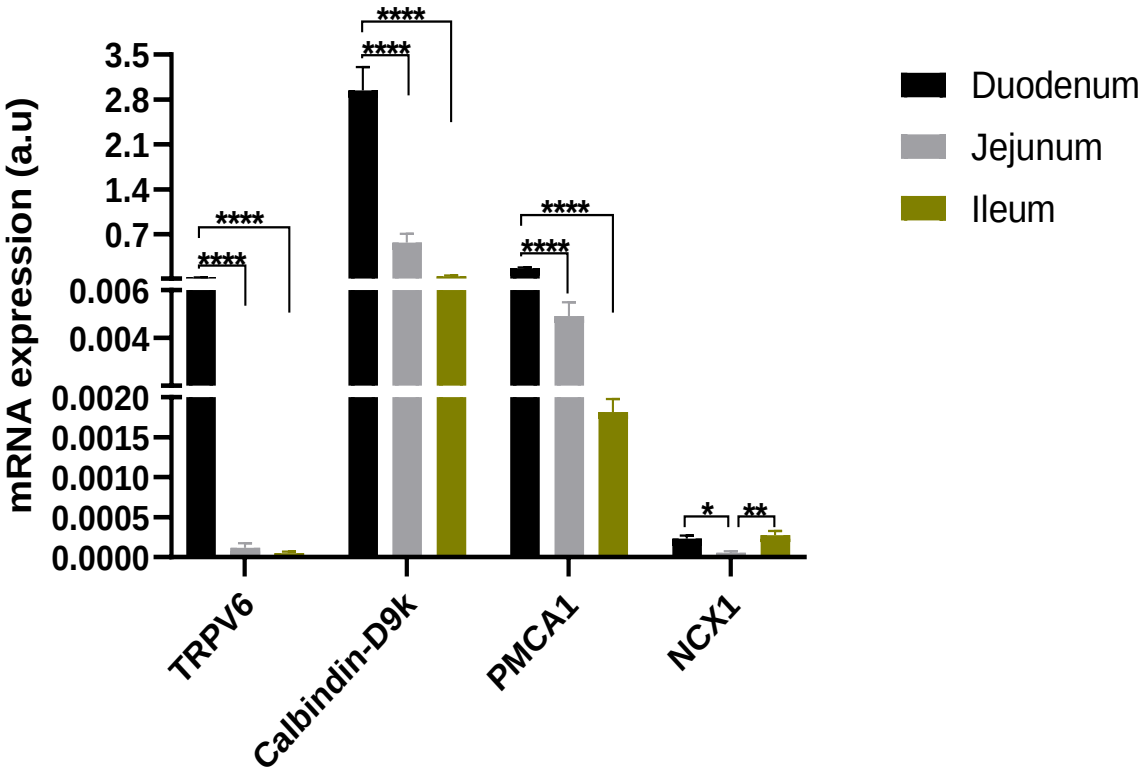

Figure 2.2. Segmental mRNA expression profile of rat transcellular calcium transport genes. mRNA expression of TRPV6, Calbindin-D9k, PMCA1 and NCX1 in the duodenum, jejunum, and ileum was determined using RT-PCR. Duplicate PCR reactions were performed for each sample and the mRNA expression of each gene of interest (TRPV6, Calbindin-D9k, PMCA1 and NCX1) was expressed as a ratio of the gene to β-actin, indicated in arbitrary unit (a.u). Data are expressed as mean ± SEM and the difference between groups was analysed using a one-way ANOVA, *P<0.05, **P<0.01, ****P<0.0001, n=6-7 rats per group.

2.3.3. Intestinal expression profile of claudin-2, -12 and -15

In addition to the transcellular pathway, the paracellular pathway is also known to contribute to calcium absorption. Therefore, the mRNA and protein levels of claudin-2 and -12, known to be the major mediators of paracellular calcium absorption were measured [25]. Although calcium absorption was significantly different between the 3 segments of the small intestine, there were no significant differences in the mRNA

expression (**Figure 2.3**) and protein levels (**Figure 2.4**) of claudin-2 and -12. Even though there were no significant segmental differences in claudin-2 and -12 protein levels (**Figure 2.4**), the protein levels (mean values) of these claudins appeared to be the highest in the duodenum (**Figure 2.4**). This may potentially contribute to the high levels of calcium absorption in the duodenum. Interestingly, the regional profile for claudin-15 mRNA mirrors that of the total transepithelial calcium absorption *in vivo*, with the highest levels of claudin-15 mRNA detected in the duodenum (**Figure 2.5**). Even though there is no direct evidence implicating claudin-15 in mediating intestinal calcium absorption, this claudin has been speculated to mediate paracellular calcium transport [128]. This speculation and the regional profile for claudin-15 in the current study suggest that this claudin may be responsible for the significantly higher rate of duodenal calcium absorption in the current study.

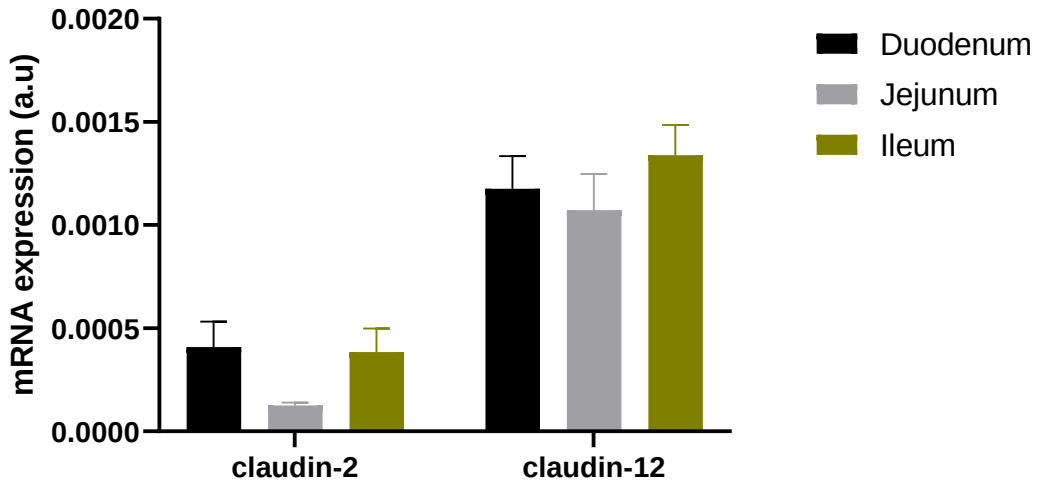

Figure 2.3. Segmental mRNA expression profile of rat claudin-2 and -12. mRNA expression of claudin-2 and -12 in the duodenum, jejunum, and ileum of rats was determined using RT-PCR. Duplicate PCR reactions were performed for each sample and the mRNA expression of each gene of interest (claudin-2 and -12) was expressed as a ratio of the gene to β-actin, indicated in arbitrary unit (a.u). Data are expressed as mean ± SEM and the difference between groups was analysed using a one-way ANOVA, n=6-7 rats per group.

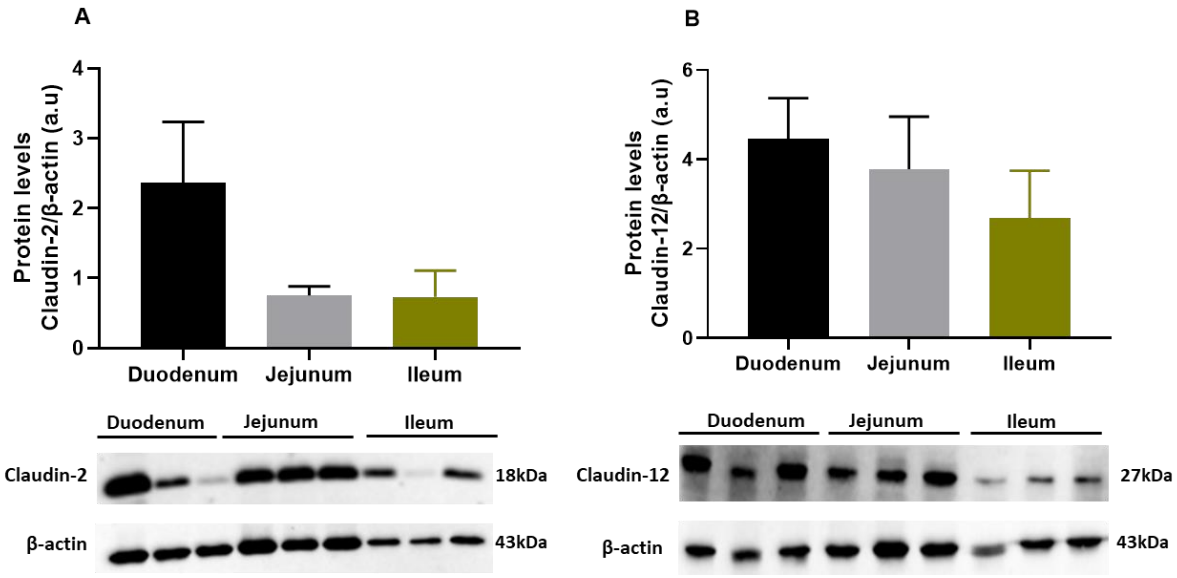

Figure 2.4. Segmental profile of rat claudin-2 and -12 protein. Protein levels of claudin-2 (A) and -12 (B) in the duodenum, jejunum, and ileum of rats were determined using Western blot. The abundance of claudin-2 and -12 protein is given as the ratio of their band density to β-actin, expressed in arbitrary units (a.u). Data are expressed as mean ± SEM and the difference between groups was analysed using a one-way ANOVA, n=5-6 rats per group. Western blot representative image of claudin-2 and -12 in the duodenum, jejunum and ileum are shown below each graph (n=3 rats).

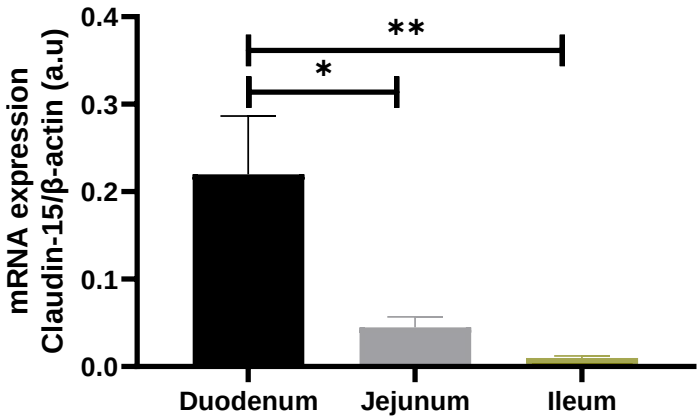

Figure 2.5. Segmental mRNA expression profile of rat claudin-15. mRNA expression of claudin-15 in the duodenum, jejunum, and ileum of rats was determined using RT-PCR. Duplicate PCR reactions were performed for each sample and the mRNA expression of claudin-15 was expressed as a ratio of its gene expression to β-actin, indicated in arbitrary unit (a.u). Data are expressed as mean ± SEM and the difference between groups was analysed using a one-way ANOVA, n=5-6 rats in each group.

2.3.4. Intestinal expression profile of human transcellular calcium transporters and Caco-2 cells

The mRNA expression of TRPV6, calbindin-D9k, PMCA1, NCX1, claudin-2 and -12, was measured in the duodenum and ileum of human intestinal biopsies. Like in the rat small intestine, the mRNA expression of PMCA1 and calbindin-D9k was significantly higher in the human duodenum compared to the ileum (**Figure 2.6**). Additionally, TRPV6 mRNA was undetected in the ileum but was present in the duodenum, while NCX1 expression was barely detected in both the duodenum and ileum of humans (**Figure 2.6**). With the assumption that the mRNA expression translates to protein, the result suggests that transcellular calcium absorption is higher in the human duodenum compared to the ileum. Furthermore, the mRNA

expression of claudin-2 and -12 were comparable in the duodenum and ileum (**Figure 2.7**).

As it is not possible to investigate calcium absorption in human biopsies, a human cellular model of the small intestine is required. Several studies have identified Caco-2 cells as a suitable model for the small intestine [390,396–398], therefore the relative mRNA expression of proteins involved in calcium absorption was measured using RT-PCR to determine whether Caco-2 could be suitable for investigating calcium absorption. The major transcellular calcium proteins, TRPV6, calbindin-D9k and PMCA1, and claudin-2 and -12, known to mediate paracellular calcium absorption, were detected in Caco-2 cells cultured for 21 days (**Figure 2.8**). Interestingly, NCX1 mRNA was not detected in Caco-2 cells cultured for 21 days (**Figure 2.8**), an observation that was similar to the extremely low levels of NCX1 mRNA in both the duodenum and ileum of humans (**Figure 2.6**). Since TRPV6 mRNA was detected in both the human duodenum and Caco-2 cells, it is possible that Caco-2 cells may be a suitable model for investigating the mechanisms of calcium absorption in the human duodenum.

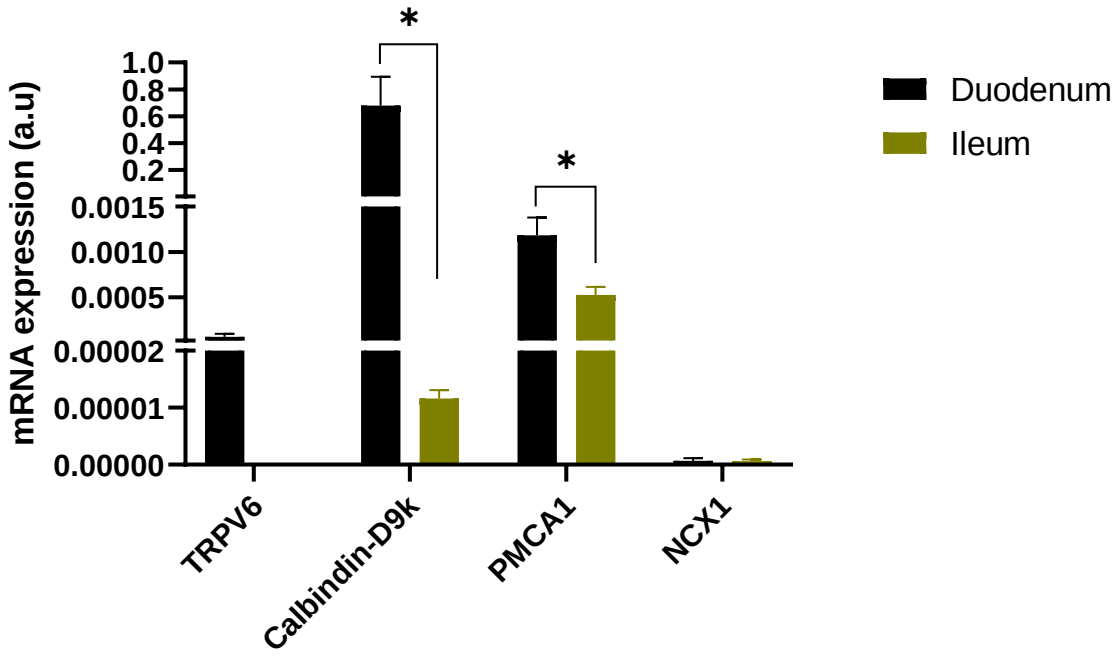

Figure 2.6. Segmental mRNA expression profile of human transcellular calcium transport genes. mRNA expression of TRPV6, Calbindin-D9k, PMCA1 and NCX1 in human duodenal and ileal biopsies was determined using RT-PCR. Duplicate PCR reactions were performed for each sample (a single biopsy from 1 donor) and the mRNA expression of each gene of interest was expressed as a ratio of the gene to β-actin, indicated in arbitrary unit (a.u). Data are expressed as mean ± SEM and the difference between groups was analysed using unpaired t-test. *P<0.05, n=4-5 donors.

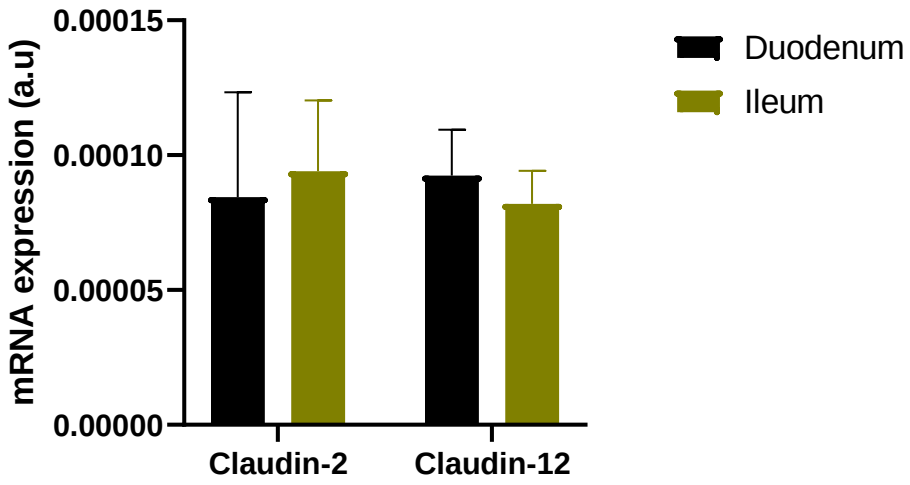

Figure 2.7. Segmental mRNA expression profile of human claudin-2 and -12. mRNA expression of claudin-2 and -12 in human duodenal and ileal biopsies was determined using RT-PCR. Duplicate PCR reactions were performed for each sample (a single biopsy from 1 donor) and the mRNA expression of each gene of interest was expressed as a ratio of the gene to β-actin, indicated in arbitrary unit (a.u). Data are expressed as mean ± SEM and the difference between groups was analysed using unpaired t-test, n=4-5 donors.

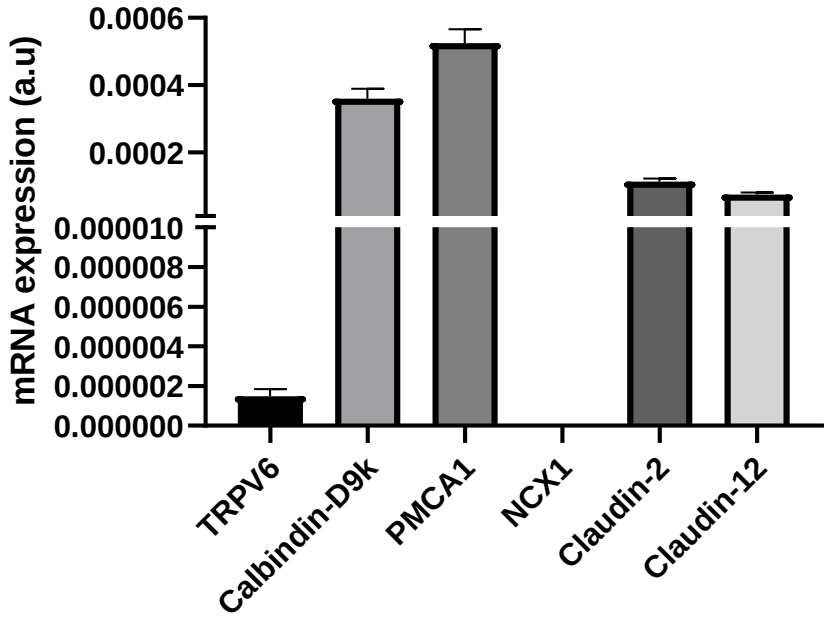

Figure 2.8. Relative mRNA expression of calcium transport genes in Caco-2 cells. mRNA expression of TRPV6, Calbindin-D9k, PMCA1, NCX1, Claudin-2 and -12 in parental Caco-2 cells. Duplicate PCR reactions were performed for each sample and the mRNA expression of each gene of interest was expressed as a ratio of the gene to β-actin, indicated in arbitrary unit (a.u). Data are expressed as mean ± SEM, n=3 independent experiments.

2.4. Discussion

2.4.1. Segmental differences in calcium absorption and the potential contribution of the duodenum, jejunum, and ileum to overall calcium absorption in rats

The small intestine is known to be the major site for calcium absorption where about 90% of absorption occurs and is determined by various factors including intestinal sojourn time, mucosal permeability and calcium solubility [208]. Although it has been established that calcium absorption occurs in all 3 segments of the small intestine, studies investigating the segmental differences in calcium absorption *in vivo* using physiologically relevant calcium concentrations (that would be expected post-

prandially) are limited. For example, one of the earliest studies investigating net calcium flux across the different segments of the small intestine in rats using Lucite hemi-chambers, showed that the duodenum was the only segment where net absorption occurs, while net calcium secretion was observed in the jejunum and ileum [399]. Although this study suggests that the duodenum is the major site for calcium absorption, it should be noted that the experiments were conducted *in vitro,* using an uptake buffer with a low calcium concentration (1.25mM) and in the absence of an electrochemical gradient. These factors predominantly favour the active transcellular calcium transport pathway rather than the passive paracellular calcium absorption pathway. Contrary to these conditions, during the post-prandial phase, when maximal calcium absorption takes place, a large calcium concentration gradient and a negative transepithelial potential difference are expected [24], which will favour the paracellular pathway.

To mimic post-prandial conditions, the current study used a calcium concentration of 100mM to investigate and compare total transepithelial calcium absorption in different segments of the small intestine. Consistent with previous findings [216,399], the duodenum showed the highest amount of total calcium absorption, while absorption was the lowest in the ileum. Since 100mM of calcium favours the paracellular pathway, this pathway is likely responsible for the significantly higher amounts of calcium absorbed in the duodenum. This suggests that the rate of paracellular calcium absorption is highest in this segment compared to the jejunum and ileum. A limitation of the current study is the amount of time the uptake buffer spends in each segment of the small intestine, which is not expected to occur under physiological settings. For instance, unlike the current study where calcium was instilled for 30

minutes, during normal feeding, chyme is expected to spend considerably less time in the duodenum (about 2.5mins) compared to the jejunum (about 43mins) and ileum (about 141mins) [213]. Based on the differences in intestinal transit time in each segment, the ileum, where chyme stays the longest, has been speculated to contribute the most to net calcium absorption despite the high capacity for calcium absorption in the duodenum [213]. Nevertheless, to date, no study has been able to directly measure the relative contribution of the intestinal segments to calcium absorption while simultaneously accounting for all the factors influencing absorption. Therefore, whether the duodenum is the major site for calcium absorption remains uncertain. However, what the findings of the current study tell us is that the duodenum has the highest capacity for calcium absorption under high luminal calcium concentrations. Similar to the widely accepted dogma that transcellular calcium absorption is highest in the duodenum (discussed in **section 1.3**), the findings of this study indicate that the rate of paracellular calcium absorption is also highest in this segment compared to the jejunum and ileum. Thus, the duodenum may be a key segment for controlling total transepithelial calcium absorption in the small intestine.

2.4.2. Mechanisms underlying the segmental differences in calcium absorption in the rat small intestine.

To understand the mechanisms responsible for the segmental differences in calcium absorption seen in the current study, the expression of the proteins involved in intestinal calcium absorption were investigated. While previous studies have investigated the mRNA expression profile of proteins involved in calcium absorption in mice [23,137,400], there is a paucity of information in rats. In agreement with studies

in mice [23,55,106,400,401], the relative mRNA expression of TRPV6, calbindin-D9k and PMCA1 in rats demonstrate a proximal-distal gradient, with high levels of expression in the duodenum and low levels in the ileum. Collectively, this expression profile supports the finding that transcellular calcium absorption predominantly occurs in the duodenum of rats [402]. Additionally, since the expression profile mirrors the segmental differences in intestinal calcium absorption, it is possible that TRPV6, calbindin-D9k and PMCA1 contribute to the differences in calcium absorption across the segments of the small intestine. Interestingly, the mRNA expression profile of NCX1 in rats does not follow the same proximal-distal gradient as the other transcellular calcium transport proteins. Therefore, NCX1 is unlikely to contribute to the segmental differences in intestinal calcium absorption seen in the rats. In addition, there is evidence that NCX1 contributes approximately 15-20% of total basolateral calcium extrusion into plasma, with PMCA1 accounting for a greater proportion of basolateral calcium extrusion [16].

Compared to the other transcellular calcium transport proteins, knockout studies [93] and experiments involving PMCA1 inhibition [403] have shown that this protein is the major transcellular calcium transporter. These studies demonstrated a significant reduction in calcium absorption following PMCA1 inhibition [403] and a decrease in bone mineral density in PMCA1 knockout mice, which is indicative of dysregulated calcium balance [93]. Taken together, PMCA1 may be the most important transcellular calcium transporter contributing to the segmental differences in total calcium absorption in the rat small intestine seen in the current study. However, at 100mM of calcium employed in this study, the proteins involved in transcellular calcium

absorption pathway are expected to be saturated, thus, most of the calcium absorbed would likely be mediated via the paracellular pathway [10].

Regarding the paracellular calcium transport pathway, the pore-forming claudin-2 and -12 have been demonstrated to be responsible for mediating this pathway [25]. Although claudin-15 has been speculated to play a role in mediating paracellular calcium absorption [24], there is currently no direct evidence to show that this claudin is a calcium-specific pore *in vivo*. The findings of the current study showed no significant differences in the segmental expression of claudin-2 and -12 in the small intestine, though a trend for higher protein levels of claudin-2 was observed in the duodenum compared to the jejunum and ileum. Since the paracellular pathway is known to be the dominant pathway under high luminal calcium levels [6], at 100mM of calcium, claudin-2 may potentially contribute to the segmental differences in calcium absorption. In addition to the passive paracellular movement of calcium down its concentration gradient via claudin-2 and -12 pores, paracellular calcium transport has also been reported to occur via a solvent drag mechanism [22,164].

There are a number of sodium-dependent transport mechanisms that generate solvent drag in the intestine. Among these mechanisms, the transcellular absorption of glucose and sodium via SGLT1 [404], and sodium via NHE3 [186] create a hyperosmotic gradient, resulting in the movement of water and dissolved solutes, including calcium, into the circulation. Importantly, there is evidence that claudin-15 plays a role in maintaining luminal sodium homeostasis necessary to drive sodium-dependent nutrient transport via SGLT1 and NHE3 in the small intestine [199]. This role of claudin-15 on sodium-mediated transport processes suggests that the

segmental profile of claudin-15 may be a major determinant of the degree of glucose and sodium absorption, and thus, the magnitude of solvent drag in different intestinal segments. Interestingly, the claudin-15 expression profile shows a proximal-distal gradient in the small intestine, with the highest levels seen in the duodenum. Since the expression profile of claudin-15 mirrors the segmental differences in total transepithelial calcium absorption in the current study, it is possible that this claudin may be responsible for the higher rate of calcium absorption in the duodenum via the solvent drag mechanism. This suggests that claudin-15 may be an important mediator of paracellular calcium absorption via solvent drag.

2.4.3. Mechanisms of small intestinal calcium absorption in humans

Due to the limitations of human experimentation, rodents are commonly used as *in vivo* models to further understand physiological mechanisms in humans. With the availability of human cell lines, translational studies investigating the mechanisms underlying physiological processes in humans are now being conducted *in vitro*. In the current study, the mRNA expression profile of proteins involved in intestinal calcium absorption were investigated in human intestinal biopsies and compared to Caco-2 cells to determine whether this cell line is a good model for investigating the mechanisms of calcium absorption. Additionally, the segmental expression profile of these calcium transport proteins, and the differential rate of calcium absorption in the rat small intestine was used to predict potentially novel mechanisms underlying paracellular calcium absorption in humans. Using human duodenal and ileal biopsies, the mRNA expression of all the proteins involved in transcellular calcium absorption was significantly higher in the duodenum compared to the ileum, except NCX1 expression, which was comparable in both segments. Additionally, the mRNA

expression of claudin-2 and -12 was similar in both segments. Due to insufficient human tissue, claudin-15 mRNA expression profile and the protein levels of the calcium transport proteins were not investigated in the current study. However, as described in **section 1.2.6.2 and figure 1.8**, the expression profile for claudin-15 in the human small intestine [138] was shown to be similar to the findings of this study in rats, with higher expression in the duodenum compared to the ileum. Taken together, the expression profile of the proteins involved in intestinal calcium transport in humans is consistent with the rats used in the current study. Therefore, in keeping with the calcium uptake data and the solvent drag speculation in the rat duodenum, it is possible that the higher expression of claudin-15 in the human duodenum compared to the ileum may potentially drive solvent drag-mediated paracellular calcium absorption in the duodenum of humans. This mechanism, in addition to the calcium transport function of claudin-2 and -12 may make the human duodenum an important segment for calcium absorption and therefore, a good target for controlling calcium absorption in humans.

The challenge of conducting functional uptake experiments to measure paracellular calcium flux using human tissue, means it is imperative to validate an alternative human model, Caco-2 cells, which is commonly used as a model of the human small intestine (32). The endogenous expression of key proteins involved in calcium absorption in Caco-2 cells as demonstrated in the current study makes this cell line a suitable human model for investigating the mechanisms underlying transepithelial calcium absorption. While Caco-2 cells express the proteins involved in both transcellular and paracellular calcium transport as seen in the human duodenum, TRPV6, the major apical calcium transporter was undetected in the human ileum.

Based on this finding, it is hypothesised that Caco-2 cells are a good model to study both transcellular and paracellular calcium transport mechanisms in the duodenum. To support this hypothesis, high levels of the iron transporter, DMT1 (that is known to be most highly expressed in the duodenal segment of the human small intestine [405]), are endogenously expressed in Caco-2 cells used in the current study (**Figure 4.2A and 4.5**).

2.5. Conclusion

There are significant segmental differences in total transepithelial calcium absorption across the rat small intestine at 100 mM of luminal calcium, a concentration that would be expected to favour paracellular calcium absorption. Under this condition, the duodenum has the highest capacity for calcium absorption, while the ileum appears to have the lowest capacity. The regional expression of claudin-15 mirrored the *in vivo* calcium absorption profile, suggesting that claudin-15 may be responsible for the segmental differences in intestinal calcium absorption. Based on the comparable expression levels of the proteins involved in calcium absorption in rat and human small intestine, the rat appears to be a good model to investigate the mechanisms of calcium transport in humans *in vivo.* Moreover, the endogenous expression of both the transcellular and paracellular calcium transport proteins in Caco-2 cells makes this cell line a good *in vitro* model of the human duodenum.

Chapter 3 - Impact of diet-induced iron deficiency on calcium homeostasis

3.1. Introduction

Iron deficiency is the most common micronutrient deficiency worldwide, which can be seen in all population subgroups; however, young children (<5years), menstruating and pregnant women are most affected due to high iron demand [406]. Several causes of iron deficiency have been identified, such as diseases linked to malabsorption (e.g. coeliac disease), duodenal resection, malnutrition, chronic kidney disease and pregnancy [407]. Prolonged iron deficiency is commonly associated with anaemia as iron serves as a crucial co-factor in the oxygen transport function of haemoglobin and myoglobin. Unlike most micronutrients, there is no known renal excretory mechanism for iron, therefore, the maintenance of iron homeostasis appears to solely rely on intestinal iron absorption and iron release from its cellular stores (such as hepatocytes and macrophages)[323], which are controlled by the master regulatory hormone, hepcidin. This liver-derived peptide hormone inhibits intestinal iron absorption by inhibiting the transcription of the iron importer (DMT1) [363]. Additionally, hepcidin is also known to reduce intestinal iron absorption and iron release from its stores by binding to the iron exporter (FPN) and targeting this protein for lysosomal degradation [408]. Interestingly, recent studies have suggested a link between hepcidin and intestinal calcium absorption [371,383], and that iron deficiency may be a risk factor for osteoporosis [384]. Since calcium is a major component of bone mineral hydroxyapatite, it is possible that intestinal calcium absorption, which is necessary for bone development may also be impacted during iron deficiency. In support of this hypothesis, two studies have investigated the impact of iron deficiency on intestinal calcium absorption. While the study conducted by Campos *et. al* [409] reported an increase in intestinal calcium absorption in response

to diet-induced iron deficiency, Katsumata *et.al* [385] reported a decrease in intestinal calcium absorption. The discrepancy in these findings may have resulted from differences in the composition of the iron diets, the age of the animals and the length of treatment, resulting in variations in the severity of iron deficiency. Importantly, no study has been designed to systematically determine the impact of iron deficiency on calcium absorption across the different segments of the small intestine and the potential underlying mechanisms. Understanding these mechanisms will be essential in identifying an intestinal segment-specific (e.g., duodenum-specific) modulator of calcium absorption.

3.1.1. Aims:

Based on the link between iron and calcium transport processes (discussed in **Chapter 1, section 1.7**) and because iron absorption mainly occurs in the duodenum [329–333], it is hypothesised that iron deficiency will have differential impact on calcium absorption across the 3 segments of the small intestine. Therefore, the aim of this chapter is to investigate the impact of diet-induced iron deficiency on calcium absorption across the different segments of the small intestine using *in vivo* uptake techniques and to investigate the underlying mechanisms using quantitative PCR and Western blotting. Additionally, the impact of iron deficiency on renal calcium excretion, the levels of renal calcium transporters, and bone turnover was examined to determine the physiological impact of iron deficiency on the other mechanisms of calcium homeostasis.

3.2. Methods

3.2.1. Animals

Male Sprague-Dawley rats were purchased and housed as previously described in **section 2.2.2**. Following acclimatisation, the rats were divided into an iron-deficient group or control group where the animals were fed an iron-deficient diet (TD. 80396, Harlan Laboratories, Inc. Madison, WI, USA) containing 2-6ppm of iron or a matched control diet (TD. 80394), containing 48ppm of iron, for 2 weeks as previously reported [410]. At the end of the 2-week period, animals were individually housed in metabolic cages for 16 hours, where they were given *ad libtum* access to water and their respective diets.

3.2.2. Blood and urine biochemistry

Following the 2-week dietary regimen, the urine of the animals was collected using metabolic cages over a 16-hour period. The rats were then anesthetised with pentobarbitone as described in **section 2.2.3**, and blood was collected via femoral artery cannulation or cardiac puncture and put into 1.5ml microfuge tubes and EDTA tubes (to prevent coagulation) for the isolation of serum and plasma, respectively. The blood collected in microfuge tubes was allowed to clot for at least 1 hour and then centrifuged at 1,000xg for 10 minutes and serum was collected. The blood collected in EDTA tubes was centrifuged at 5,000xg for 10 minutes to obtain the plasma fraction. Additionally, urine samples were collected, and the volumes measured. The serum or plasma, and urine were used for a range of biochemical tests described in the subsequent subheadings to investigate the impact of iron deficiency on iron and calcium homeostasis.

3.2.2.1. Blood iron markers

To confirm that the 2-week dietary regimen successfully induced iron deficiency in the rats, haematocrit levels were measured using a micro-haematocrit reader. This was achieved by using non-haemolysed blood collected via the femoral artery in heparinised glass capillary tubes and centrifuged in a micro-haematocrit centrifuge (Hawksley, England) for 2 minutes.

Serum iron and unsaturated iron binding capacity (UIBC) were measured using a colorimetric assay kit (Pointe Scientific Inc. Canton, MI, USA) according to the manufacturer's instructions. The principle of the iron assay is based on the knowledge that ferric iron (Fe^{2+}) in serum is bound to transferrin which dissociates at an acid pH and is reduced to ferrous iron (Fe^{3+}). Fe^{3+} reacts with ferrozine to form a violet colour and the absorbance is measured at a wavelength of 560nm using a spectrophotometer (Denovix-DS-11, Delaware, USA). The UIBC is determined by adding a known amount of ferrous iron to the serum which binds to the unsaturated sites of transferrin at an alkaline pH. The unbound ferrous iron then reacts with ferrozine to produce the violet colour and the absorbance is measured at the same wavelength. The UIBC is calculated as the difference between the Fe^{3+} added and the unbound serum iron measured.

In addition to iron levels, ferritin levels in plasma were measured using a rat-specific ELISA kit (Abcam, Cambridge, UK) according to the manufacturer's instructions. The principle of this assay relies on the use of 2 monoclonal antibodies specific to ferritin. The first anti-ferritin antibody is immobilised on the microwell plate, while the second antibody, specific to a different region of ferritin, is conjugated with horseradish

peroxidase (HRP). The standards and samples simultaneously bind to both antibodies, after which the wells were washed and decanted to remove unbound HRP-conjugated antibodies. Following this, a chromogenic reagent (TMB substrate) is added to react with the HRP to produce a colour and the absorbance is measured by a microplate reader at 450nm within 20 minutes after the addition of a stop solution. The intensity of the colour measured is directly proportional to the amount of ferritin in the sample.

3.2.2.2. Serum and urinary calcium levels

To investigate the impact of the dietary regimen on calcium homeostasis, serum and urine calcium levels were measured using a colorimetric calcium assay kit (GeneTex, Hsinchu City, Taiwan) according to the manufacturer's instruction. The principle of this assay relies on the binding of calcium ions to o-cresolphthalein which forms a chromogenic complex and the optical density (O.D) can be measured at 575nm using a spectrophotometer (Denovix-DS-11, Delaware, USA).

3.2.2.3. Serum CTX-1 levels

In addition to the intestine and kidney, bone is also known to contribute to calcium homeostasis. This predominantly occurs via bone resorption and formation. Therefore, a marker of bone resorption, carboxy terminal telopeptide of type I collagen (CTX-1), was measured in the serum using an ELISA kit (Cloud-Clone Corp., USA), according to the manufacturer's instruction. The principle of the CTX-1 kit employs a competitive enzyme immunoassay technique using an anti-CTX-1 antibody coated in the microtiter plate and a CTX-1-HRP conjugate. The sample and CTX-1-HRP conjugate are added to the plate for competitive binding to the antibody.

Following this, a substrate for the HRP enzyme is added and the reaction between the HRP and the substrate produces a blue complex. The O.D of the blue complex was measured at 450nm using a microplate reader (Multimode Detector, Beckman Coulter). The O.D or intensity of the colour measured, is inversely proportional to the amount of CTX-1 in the sample.

3.2.2.4. Plasma osteocalcin levels

In addition to the measurement of the bone resorption marker, CTX-1, the bone formation marker, osteocalcin was also measured in the plasma using an ELISA kit (Signalway Antibody, USA), according to the manufacturer's instructions. The principle of the assay is also based on the sandwich ELISA principle where the microtiter plates are coated with an osteocalcin-specific antibody. Standards or plasma samples are then added to the wells to bind to the antibody. Unbound samples are then washed away, and a biotin-conjugated detection antibody is added, which binds to the osteocalcin antigen. Following washing, an avidin-HRP conjugate is added which binds to the biotin. A chromogenic 3,3′,5,5′-Tetramethylbenzidine (TMB) substrate is then added, which reacts with HRP to form a coloured complex. The O.D of the coloured complex was measured at 450nm using a microplate reader (Multimode Detector, Beckman Coulter). The O.D or intensity of the colour, is directly proportional to the amount of osteocalcin in the standard or sample.

3.2.3. *In vivo* calcium uptake experiments.

To understand the impact of the 2-week dietary treatment on intestinal calcium absorption, the *in vivo* ligated loop technique, described in **Section 2.2.3**, was

conducted in each small intestinal segment of the control animals, and compared to the iron-deficient animals. Calcium uptake experiment was carried out using a solution containing 100mM calcium, in which paracellular calcium absorption is expected to be the dominant pathway.

3.2.4. RNA extraction, cDNA synthesis and RT-PCR

To understand the cellular mechanisms underlying any changes in calcium absorption, RNA was extracted from the duodenum, jejunum and ileum of the control and iron-deficient animals using TRI-zol reagent and quantified as described in **section 2.2.6**. Additionally, RNA was extracted from the kidney to test potential changes in the expression of renal calcium transporters in response to iron deficiency. Following RNA extraction, cDNA was synthesised from the RNA samples as described in **section 2.2.6** and RT-PCR as described in **section 2.2.7**, was used to examine the impact of iron deficiency on the mRNA expression of genes involved in renal calcium reabsorption, intestinal calcium and iron absorption using rat-specific primers purchased from Qiagen (UK) listed in **Table 3.1.**

Table 3.1: Rat-specific primers used for PCR experiment

Rat Primers	Catalogue number
DMT1	QT00182623
TRPV5	QT00184590
TRPV6	QT00185255
Calbindin-D9k	QT00381458
Calbindin-D28k	QT00180159
PMCA1	QT00182210
NCX1	QT00456323
Claudin-2	QT00451836
Claudin-12	QT01607319
Claudin-15	QT01584604
Claudin-16	QT02562168
Claudin-19	QT00440769

3.2.5. Intestinal brush border membrane vesicles

Brush border membrane vesicles were prepared from the mucosa of the duodenum, jejunum and ileum as described in **section 2.2.8.**

3.2.6. Renal brush border membrane vesicles

Harvested kidneys were placed on an ice-cold glass surface and the surrounding fat tissue and capsule were removed and the decapsulated kidney was cut into smaller pieces, snap frozen in liquid nitrogen and stored at -80^{o}C for future experiments. The method used for the preparation of renal brush border membrane vesicles has been previously described [411]. 1g of excised kidney tissue was homogenised on ice in

20ml of buffer containing 300mM mannitol, 5mM ethylene glycol-bis (2-aminoethyl)-N, N, N', N',-tetra acetic acid (EGTA) and 12mM Tris-HCl (pH 7.4) for 2 minutes using an Ultra Turrax homogeniser (Janke & Kunkel, FRG) at half speed on ice. Subsequently, 28ml of distilled water was added, and a 1ml aliquot of the homogenate was then collected and stored at -20^{o}C for protein quantification and Western blot experiments. An appropriate volume of $MgCl_2$ was added to the remaining homogenate solution to make a final concentration of 12mM and stirred on ice at low speed for 15 minutes. The suspension was then centrifuged at 2000xg for 15 minutes (4°C), the pellet was discarded, and the supernatant was re-centrifuged at 33000xg for a further 30 minutes (4°C). The resultant pellet was re-suspended in 14ml/g of resuspension buffer 1 containing 150mM mannitol, 2.5mM EGTA and 6mM Tris-HCl (pH 7.4) and homogenised using a hand operated glass-Teflon homogeniser. $MgCl_2$ was then added to the homogenate to give a final concentration of 12mM, stirred on ice at low speed for 15 minutes and then centrifuged at low and high speed as described above. The resultant pellet was then re-suspended in 14ml/g of resuspension buffer 2 containing 300mM mannitol, 2.5mM EGTA, and 12mM Tris-HCl (pH 7.4), using the glass homogeniser, and centrifuged at 33000xg for 30 minutes (4°C) to obtain a pellet of purified BBM vesicles. The pellet was finally re-suspended in resuspension buffer 2 using a 1ml syringe with a 21g needle. Protease inhibitors (Roche Life Sciences, West Sussex, UK) were added to all buffers immediately before use.

3.2.7. Western blotting

In addition to the impact of diet-induced iron deficiency on the mRNA expression of iron and calcium transporters, the impact of the dietary regimen on the protein level

of these transporters were also investigated in renal and intestinal tissue. This was done by Western blotting as described in **section 2.2.9**. The details of the transporters investigated are listed in **Table 3.3**. For primary antibodies raised in goat, an anti-goat secondary antibody at 1:1000 dilution was used (Santa. Cruz, sc-2033). Details of anti-mouse and anti-rabbit secondary antibodies are stated in **section 2.2.9**.

Table 3.2: Primary antibodies used for Western blot experiment

Protein of interest (Concentration)	**Company**	**Catalogue number**	**Dilution**	**Species**
DMT1 (1mg/ml)	Alpha Diagnostic Int.	NRAMP24-A	1:500	Rabbit polyclonal
TRPV5 (0.5mg/ml)	Abcam	ab77351	1:1000	Goat polyclonal
TRPV6 (0.75mg/ml)	Alamone	Acc-036	1:200	Rabbit polyclonal
PMCA1 (0.2mg/ml)	Santa. Cruz	Sc.271917	1:1000	Mouse monoclonal
NCX1 (1mg/ml)	Abcam	ab2869	1:200	Rabbit polyclonal
Calbindin-D9k (1mg/ml)	Signalway Antibodies	46158	1:500	Rabbit polyclonal
Calbindin-D28k (0.2mg/ml)	Santa. Cruz	Sc-365360	1:500	Rabbit polyclonal
Claudin-2 (0.5mg/ml)	Thermofisher	12H12	1.1000	Mouse monoclonal
Claudin-12 (0.25mg/ml)	Thermofisher	38-8200	1:500	Rabbit polyclonal
Claudin-15 (0.25mg/ml)	Thermofisher	38-9200	1:200	Rabbit polyclonal

3.2.8. Statistical analysis:

Data are presented as the mean ± standard error of mean (SEM). Statistical analysis was performed as previously described in **section 2.2.10**. Statistical significance was represented as *p<0.05, **p<0.01, ***p<0.001 and ****p<0.0001.

3.3. Results

3.3.1. Blood iron markers

The level of the markers of iron status, haematocrit, serum iron, UIBC and plasma ferritin levels, were measured to confirm iron deficiency following the 2-week dietary regimen in rats. Additionally, the weight of the animals was measured. As expected, haematocrit levels were significantly lower in the iron-deficient group (**Figure 3.1A**). Similarly, serum iron and plasma ferritin were significantly lower, while serum UIBC was significantly higher in the iron-deficient animals compared to the control (**Figure 3.1B-D**). These findings confirm that the 2-week dietary regimen was sufficient to induce iron deficiency in the rats. Additionally, there was no significant difference between the weight of the animals in the control group (350.8 ± 4.594g) and the iron-deficient group (337.9 ± 6.255g) suggesting that both diets had similar impact on the growth rate of the animals. The rats showed the expected intestinal adaptation to diet-induced iron deficiency demonstrated by increased DMT1 mRNA expression and protein levels in the iron-deficient animals compared to the control animals (**Figure 3.2**).

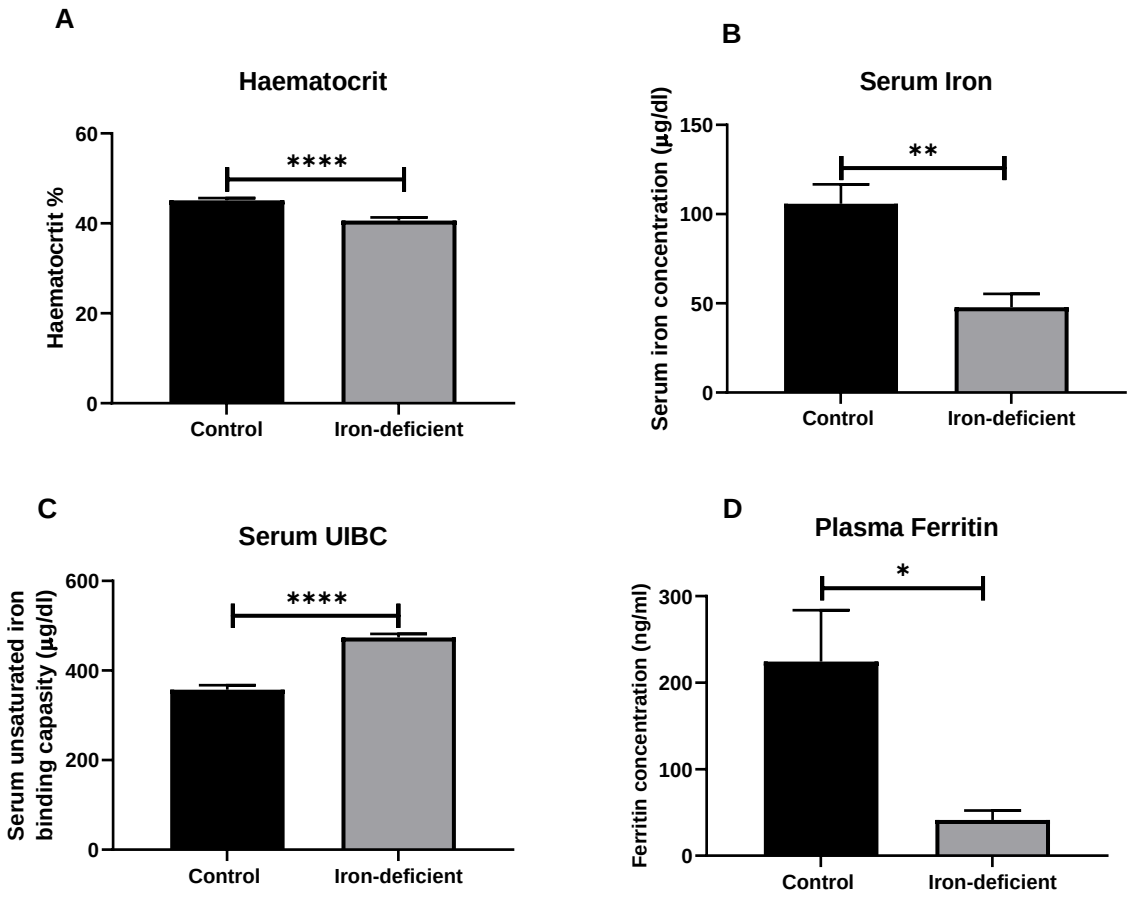

Figure 3.1. Effect of iron deficiency on markers of iron status. Data are expressed as Mean ± SEM and statistical analysis using unpaired t test was used to compare control and iron-deficient animals. **A:** Haematocrit, ****P<0.0001, n=19-20. **B:** Serum iron, **P<0.01, n=6-8. **C:** Serum UIBC, ****P<0.0001, n=8-9. **D:** Plasma ferritin, *P<0.05, n=5-6.

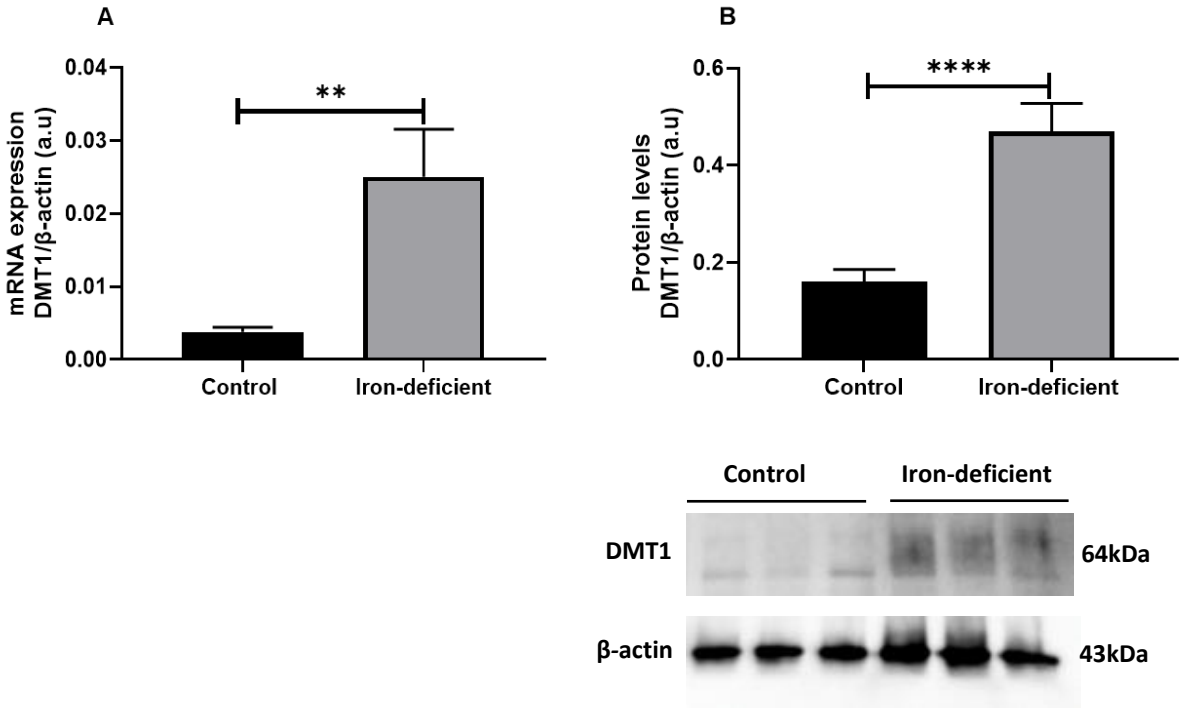

Figure 3.2. Effect of iron deficiency on the duodenal DMT1. A: mRNA expression of DMT1 in control versus iron-deficient animals was determined using RT-PCR. Duplicate PCR reactions were performed for each sample and the mRNA expression of DMT1 was expressed as a ratio of the gene to β-actin, indicated in arbitrary unit (a.u). **B**: Protein levels of DMT1 in control versus iron-deficient animals was determined using Western blot. Western blot representative image of DMT1 in control and iron-deficient animals is shown below (n=3 rats). The abundance of DMT1 protein is given as the ratio of its band density to β-actin, expressed in arbitrary units (a.u). Data are expressed as mean ± SEM and the difference between groups was analysed using unpaired t test **P<0.01 and ****P<0.0001, n=8-9 rats.

3.3.2. Effect of iron deficiency on intestinal calcium uptakes

To investigate the impact of diet-induced iron deficiency on intestinal calcium absorption, *in vivo* uptake experiments using 100mM $CaCl_2$ and ^{45}Ca were conducted in the duodenum, jejunum, and ileum of the iron-deficient and control animals over a 30-minute period. Interestingly, iron deficiency significantly increased transepithelial calcium absorption in the

duodenum (**Figure 3.3A**), while having no significant impact on calcium absorption in the jejunum (**Figure 3.3B**) and ileum (**Figure 3.3C**).

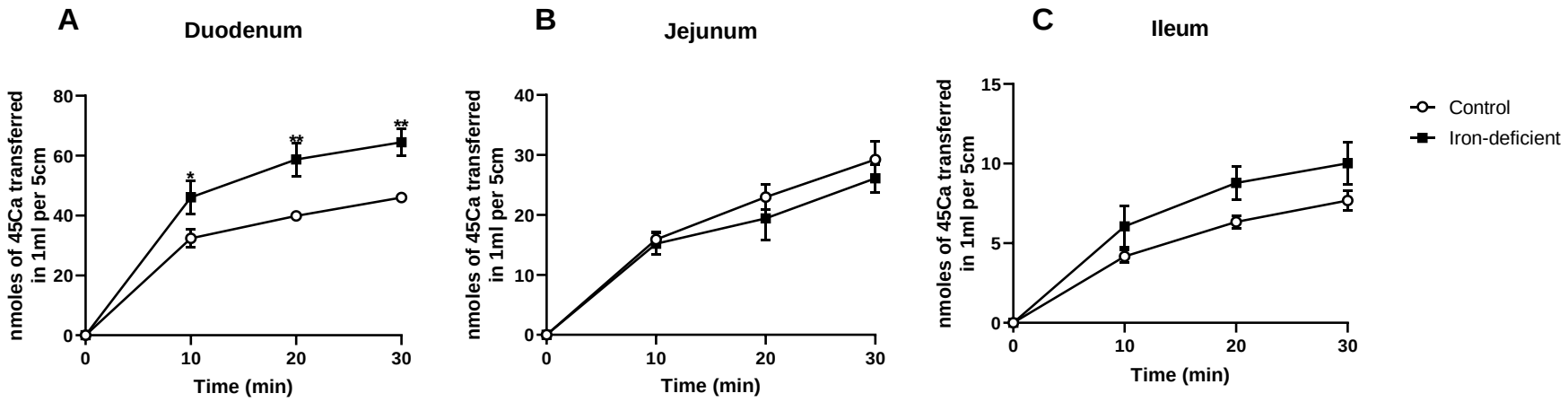

Figure 3.3. Effect of iron deficiency on intestinal calcium absorption. *In vivo* absorption of 100 mM $CaCl_2$ and ^{45}Ca across the duodenum (**A**), jejunum (**B**), and ileum (**C**) in control versus iron-deficient animals was determined using *in situ* intestinal loop technique after 10, 20 and 30 minutes. Data were analysed using two-way ANOVA with Bonferroni multiple comparisons post-hoc test to compare differences between groups. *P<0.05, **P<0.01, n=4-6 rats per group.

3.3.3. Effect of iron deficiency on transcellular calcium transporters

Since the transcellular pathway is known to contribute to overall calcium absorption, the mRNA levels of the proteins involved in this pathway were measured in all three segments of the rat small intestine in response to iron deficiency. Although calcium absorption increased significantly in the duodenum, the mRNA expression of TRPV6, PMCA1 and NCX1 were unaffected by iron deficiency (**Figure 3.4A, C and D**). Surprisingly, duodenal calbindin-D9k expression was downregulated (**Figure 3.4B**) in iron-deficient animals despite the increase in duodenal calcium absorption. Furthermore, a decrease in jejunal PMCA1 (**Figure 3.4C**) was observed in the iron-deficient group, although this has no significant functional impact on jejunal calcium absorption. In the ileum, diet-induced iron deficiency had no impact on the levels of the transcellular calcium transporters investigated in this study (**Figure 3.4A-D**).

To investigate the impact of iron deficiency on the protein levels of TRPV6, calbindin-D9k, PMCA1 and NCX1 in the duodenum, Western blotting was carried out. In keeping with the mRNA expression data, the results showed that calbindin-D9k was significantly lower in the iron-deficient group (**Figure 3.5B**), while TRPV6, PMCA1 and NCX1 were not affected (**Figure 3.5A, C and D**). The downregulation of calbindin-D9k as well as the unchanged levels of the other transcellular calcium transporters in the duodenum, suggest that the transcellular calcium transport pathway may not be responsible for the increase in duodenal calcium absorption observed during iron deficiency.

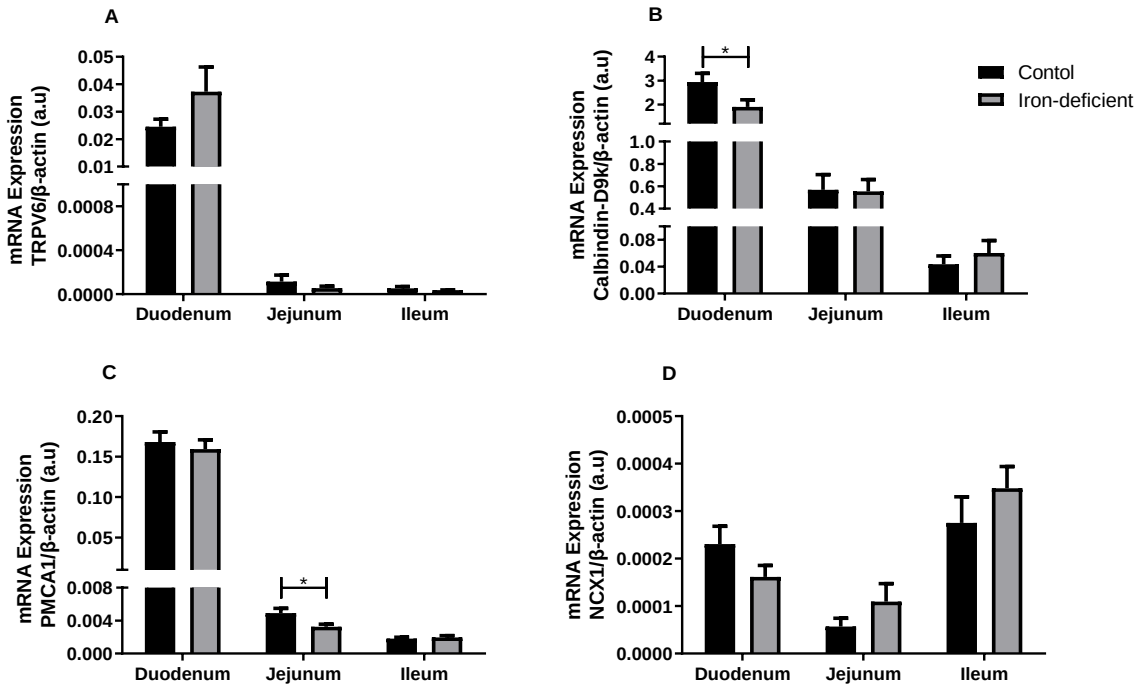

Figure 3.4. Effect of iron deficiency on the mRNA expression of transcellular calcium transporters. mRNA expression of TRPV6 (**A**), Calbindin-D9k (**B**), PMCA1 (**C**) and NCX1 (**D**) in the duodenum, jejunum, and ileum of control versus iron-deficient rats was determined using RT-PCR. Duplicate PCR reactions were performed for each sample and the mRNA expression of each gene of interest is expressed as a ratio of the gene to β-actin, indicated in arbitrary unit (a.u). Data are expressed as Mean ± SEM and the difference between groups was analysed using unpaired t test. *P<0.05, n=6-10 rats per group.

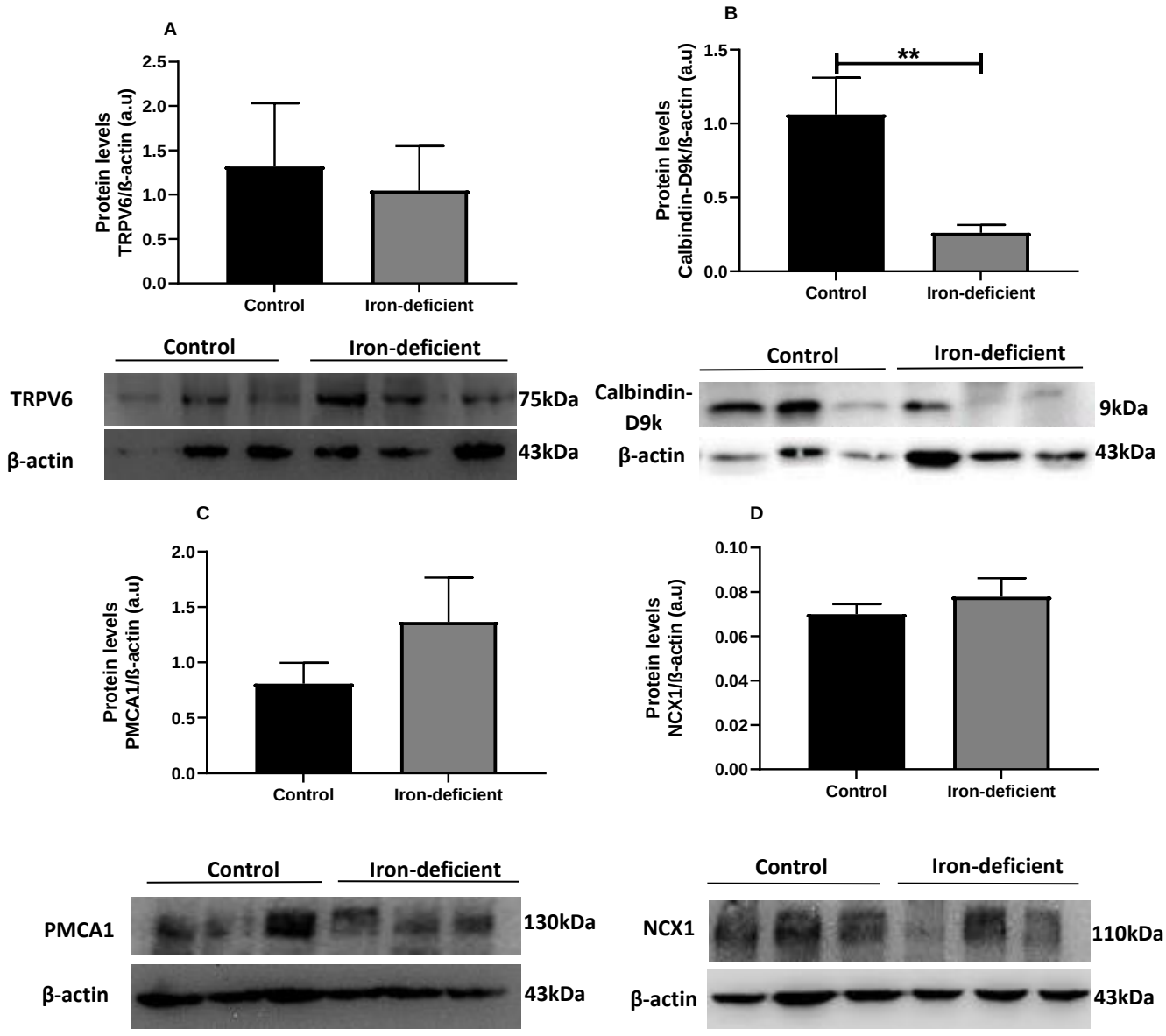

Figure 3.5. Effect of iron deficiency on the transcellular calcium transport protein levels. Protein level of TRPV6 (**A**), Calbindin-D9k (**B**), PMCA1 (**C**) and NCX1 (**D**) in the duodenum of control and iron-deficient rats was determined using Western blot. Western blot representative image of the proteins of interest in control and iron-deficient animals is shown below each graph (n=3 rats). The abundance of each protein of interest is given as the ratio of its band density to β-actin, expressed in arbitrary units (a.u). Data are expressed as mean ± SEM and the difference between groups was analysed using unpaired t test **P<0.01, n=6-8 rats per group.

3.3.4. Iron deficiency impacts claudin-2 expression in the duodenum

Given that the paracellular calcium pathway is dominant under a normal or high calcium diet, 100 mM $CaCl_2$ solution in uptake studies were used to reflect this [216]. In keeping with this knowledge, the mRNA expression and protein levels of claudin-2 and -12, known to be the major mediators of paracellular calcium transport [25] were examined in the small intestine. Additionally, based on the potential effects of claudin-15 on calcium absorption discussed in **section 2.4.2**, the mRNA expression and protein levels of this claudin were investigated. The results showed that iron deficiency significantly upregulated claudin-2 mRNA and protein levels in the duodenum (**Figure 3.6A** and **Figure 3.7A**), while having no impact on the expression of claudin-2 in the jejunum and ileum (**Figure 3.6A** and **Figure 3.7B and C**). Furthermore, the mRNA and protein levels of duodenal claudin-12 (**Figure 3.6B** and **Figure 3.8**) and claudin-15 (**Figure 3.9**) were unaffected by iron deficiency. Since claudin-2 is known to increase calcium permeability [25,159], it is hypothesised that the increase in calcium absorption in the iron-deficient animals may be mediated by claudin-2.

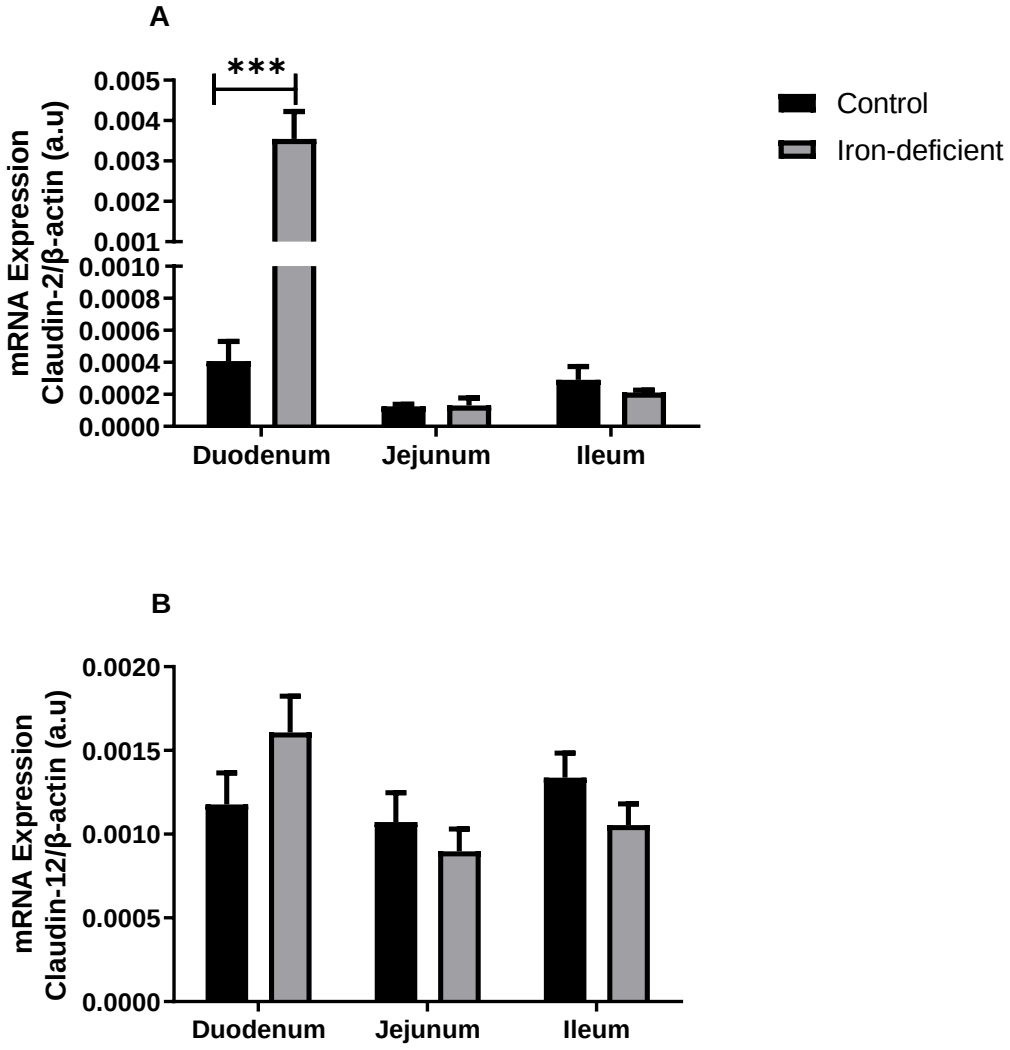

Figure 3.6. Effect of iron deficiency on the mRNA expression of the pore-forming calcium-permeable claudins. Claudin-2 (**A**) and claudin-12 (**B**) mRNA expression in the duodenum, jejunum, and ileum of control versus iron-deficient rats was determined using RT-PCR. Duplicate PCR reactions were performed for each sample and the mRNA expression of each gene of interest is expressed as a ratio of the gene to β-actin, indicated in arbitrary unit (a.u). Data are expressed as Mean ± SEM and the difference between groups was analysed using unpaired t test. ***P<0.001, n=4-6 rats per group.

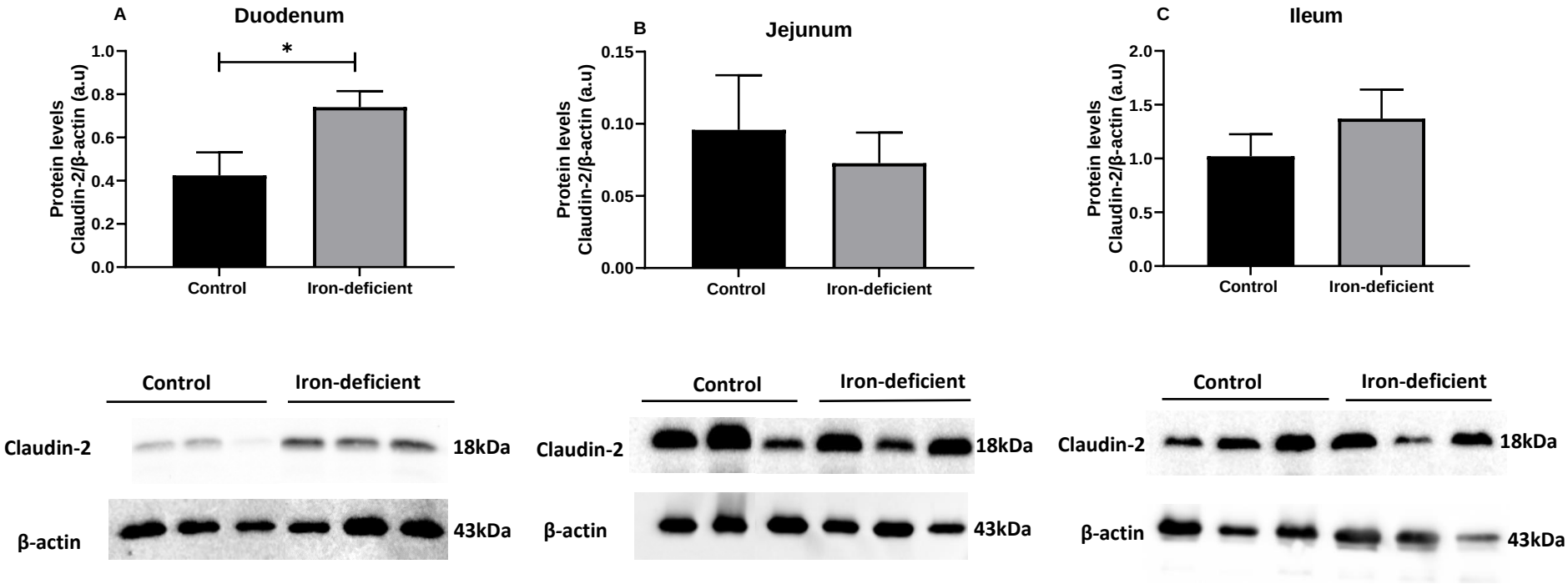

Figure 3.7. Effect of iron deficiency on the protein level of claudin-2. Protein level of claudin-2 in the duodenum (**A**), jejunum (**B**), and ileum (**C**) of control versus iron-deficient animals was determined using Western blot. Western blot representative image of claudin-2 in control and iron-deficient animals is shown below each graph (n=3 rats). The abundance of claudin-2 protein is given as the ratio of its band density to β-actin, expressed in arbitrary units (a.u). Data are expressed as mean ± SEM and the difference between groups was analysed using unpaired t test, *P<0.05 n=6-8 rats per group.

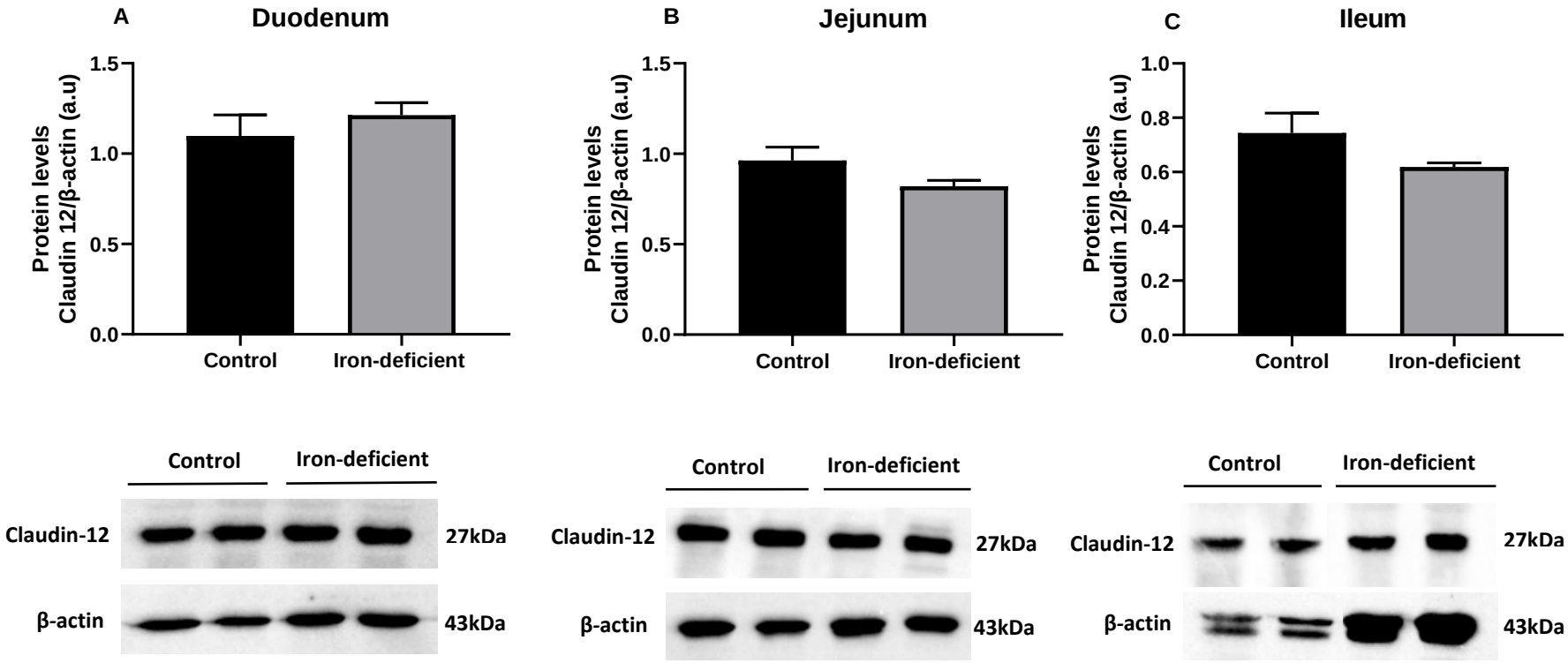

Figure 3.8. Effect of iron deficiency on the protein level of claudin-12. Protein level of claudin-12 in the duodenum (**A**), jejunum (**B**), and ileum (**C**) of control versus iron-deficient animals was determined using Western blot. Western blot representative image of claudin-12 in control and iron-deficient animals is shown below each graph (n=2 rats). The abundance of claudin-12 protein is given as the ratio of its band density to β-actin, expressed in arbitrary units (a.u). Data are expressed as mean ± SEM and the difference between groups was analysed using unpaired t test, n=4-6 rats per group.

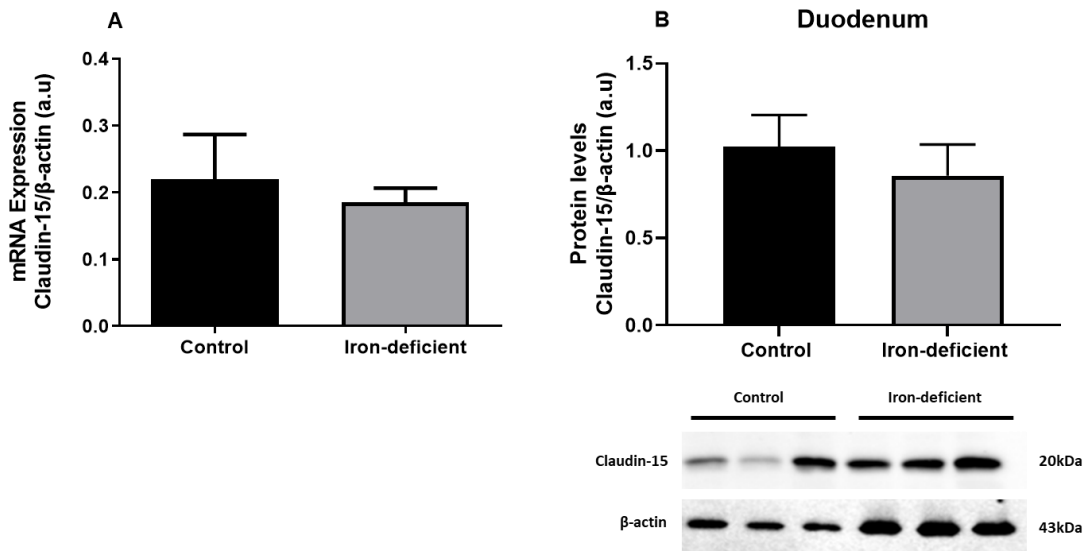

Figure 3.9. Effect of iron deficiency on duodenal claudin-15. mRNA expression of claudin-15 in control versus iron-deficient animals was determined using RT-PCR. Duplicate PCR reactions were performed for each sample and the mRNA expression of claudin-15 was expressed as a ratio of the gene to β-actin, indicated in arbitrary unit (a.u). **B**: Protein levels of claudin-15 in control versus iron-deficient animals was determined using Western blot. Western blot representative image of claudin-15 in control and iron-deficient animals is shown below the graph (n=3 rats). The abundance of claudin-15 protein is given as the ratio of its band density to β-actin, expressed in arbitrary units (a.u). Data are expressed as mean ± SEM and the difference between groups was analysed using unpaired t test, n=6-8 rats per group.

3.3.5. Iron deficiency had no impact on serum calcium levels and urinary calcium excretion

Following the 2-week dietary treatment, serum and urine calcium levels were measured to investigate the impact of iron deficiency on calcium status and renal calcium excretion. The results demonstrated that iron deficiency had no significant impact on serum calcium levels (**Figure 3.10A**). Likewise, urine calcium levels were unaffected by iron deficiency suggesting that iron deficiency had no impact on renal calcium excretion (**Figure 3.10B**).

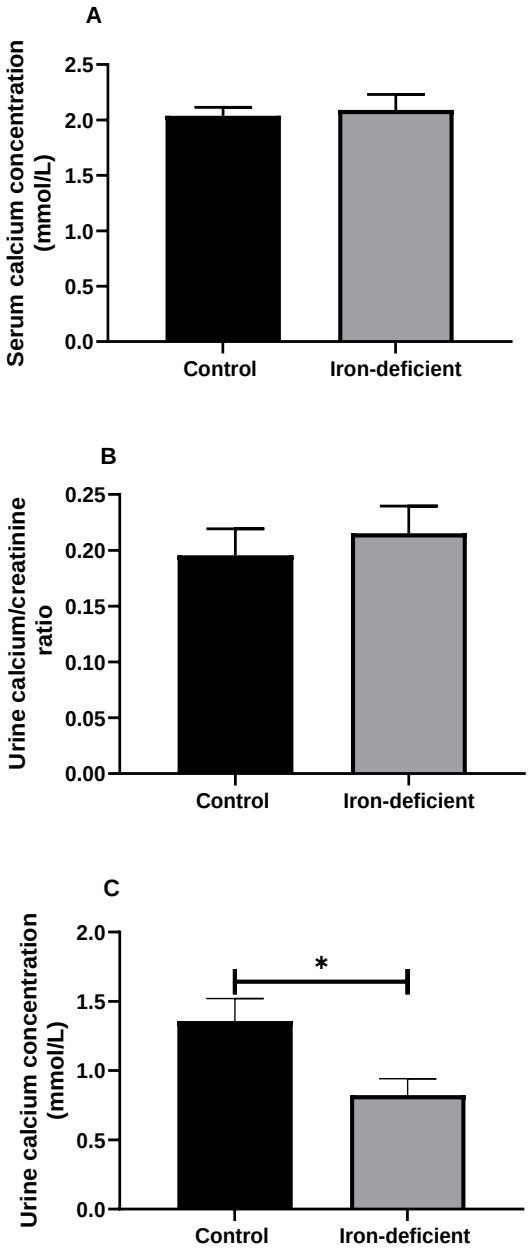

Figure 3.10. Effect of iron deficiency on serum and urinary calcium levels. Serum calcium (**A**), urine calcium/creatinine levels (**B**) and urinary calcium concentration **(C)** of control versus iron-deficient rats. Data are expressed as Mean ± SEM and the difference between groups was analysed using unpaired t test, *P<0.05, n=7-12 rats per group.

3.3.6. Effect of iron deficiency on renal calcium transporters and claudins

The impact of iron deficiency on the expression of the proteins involved in renal calcium reabsorption was investigated by PCR and Western blotting experiments. The results showed that iron deficiency significantly upregulated

renal claudin-2 protein levels (**Table 3.3 and Figure 3.11**) but had no impact on the mRNA expression and protein levels of other calcium transport proteins (**Table 3.3**). Based on the lack of change in urinary calcium levels in response to iron deficiency, the physiological impact of the changes in claudin-2 protein on calcium homeostasis is uncertain.

Table 3.3. Impact of iron deficiency on the mRNA and protein levels of the renal calcium transporters. The mRNA expression and protein levels of the renal calcium transporters were determined using RT-PCR and Western blot. The mRNA or protein expression of the transporter of interest are presented as the ratio of the transporter normalised to β-actin, expressed in arbitrary unit (a.u). Data are presented as mean ± SEM and unpaired t test was used to compare the difference between the control and iron-deficient groups for each transporter of interest, ** P<0.01, n=5-6 rats per group. ND = not determined, UD = undetected due to non-specificity of the antibody used).

	mRNA (a.u)		**Protein (a.u)**	
	Control	Iron-deficient	Control	Iron-deficient
TRPV5	0.003 ± 0.0008	0.004 ± 0.0004	UD	UD
Calbindin-D28k	0.32 ± 0.07	0.43 ± 0.06	1.02 ± 0.15	0.53 ± 0.15
PMCA1	0.02 ± 0.003	0.03 ± 0.01	1.44 ± 0.25	1.34 ± 0.12
NCX1	0.027 ± 0.004	0.02 ± 0.004	0.48 ± 0.05	0.39 ± 0.03
Claudin-2	0.005 ± 0.0005	0.01 ± 0.0006	0.49 ± 0.10	1.31 ± 0.17**
Claudin-12	0.01 ± 0.002	0.01 ± 0.001	0.94 ± 0.14	0.91 ± 0.22
Claudin-16	0.28 ± 0.11	0.20 ± 0.03	ND	ND
Claudin-19	0.032± 0.01	0.03 ± 0.01	ND	ND

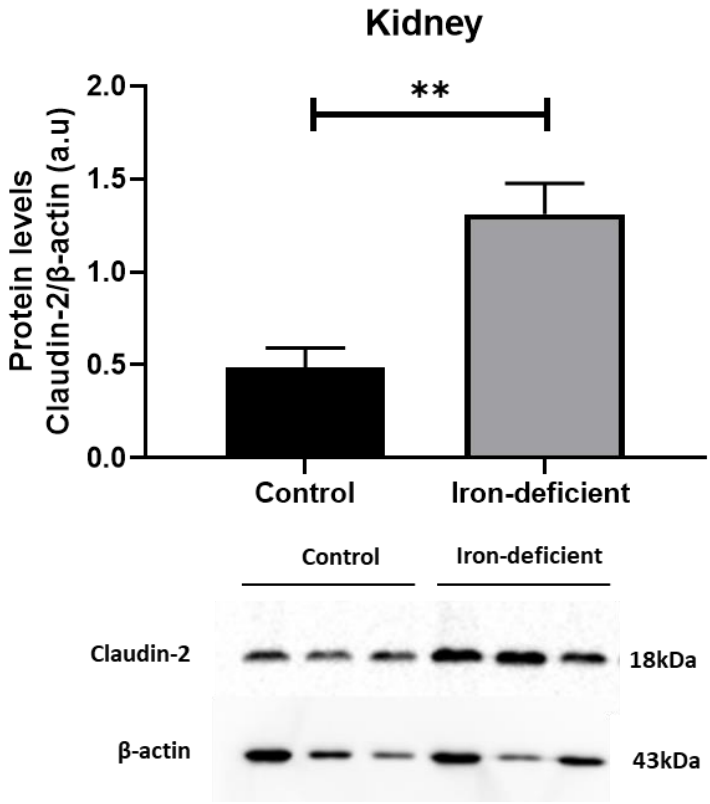

Figure 3.11. Effect of iron deficiency on renal claudin-2 protein levels. Protein levels of claudin-2 in control versus iron-deficient animals was determined using Western blot. Western blot representative image of claudin-2 in control and iron-deficient animals is shown below the graph (n=3 rats). The abundance of claudin-2 protein is given as the ratio of its band density to β-actin, expressed in arbitrary units (a.u). Data are expressed as mean ± SEM and the difference between groups was analysed using unpaired t test, ** P<0.01, n=6 rats per group.

3.3.7. Iron deficiency has no impact on markers of bone turnover

In addition to the small intestine and kidney, the bone also plays a role in the regulation of calcium balance. Therefore, the impact of iron deficiency on the marker of bone resorption, CTX-1, and bone formation, osteocalcin, in the serum and plasma respectively were investigated using ELISA. The results showed that the levels of CTX-1 and osteocalcin were unchanged in response to iron deficiency (**Figure 3.12**), suggesting that iron deficiency has no impact on bone turnover.

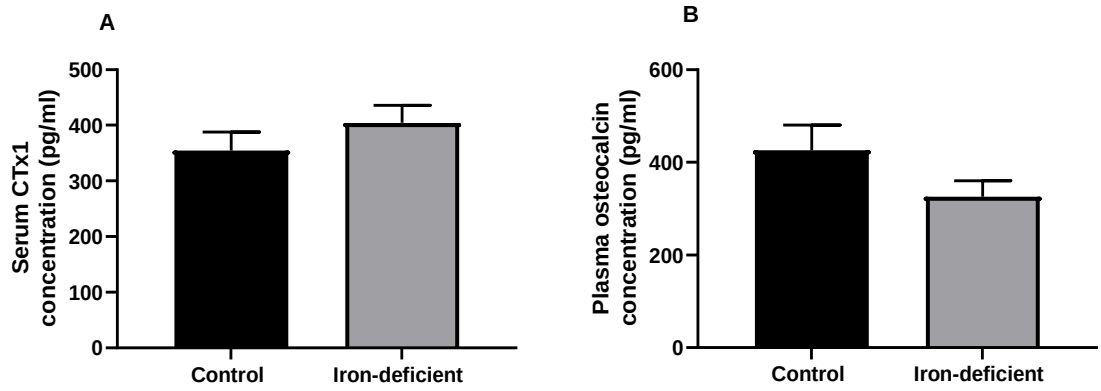

Figure 3.12. Effect of iron deficiency on markers of bone turnover. Serum CTX-1 (**A**) and Plasma Osteocalcin concentration (**B**) in control versus iron-deficient rats. Data are expressed as Mean ± SEM and the difference between groups was analysed using unpaired t test, n=7-8 rats per group.

3.4. Discussion

Previous studies have demonstrated a link between iron deficiency, osteoporosis and the mechanisms involved in calcium homeostasis [385,388,409,412]. For instance, a nationwide population based longitudinal study in Taiwan, showed that individuals with a history of iron deficiency anaemia (IDA) are nearly 2 times more likely to develop osteoporosis compared to gender and age-matched individuals without IDA [412]. This is supported by the reduction in bone mineral density and content of the femur bone of iron-deficient rats, making them more susceptible to osteoporosis [385,388]. Additionally, iron deficiency has also been shown to affect the mechanisms involved in calcium homeostasis including calcium absorption and excretion, and the levels of the calcium regulatory hormones; parathyroid hormone (PTH) and 1,25 dihydroxy vitamin D_3 ($1,25(OH)_2D_3$) in rats [385,409]. These findings demonstrate a clear link between iron and calcium homeostasis; however, the underlying mechanisms are poorly understood. Therefore, in the current study, the impact of diet-induced iron deficiency on calcium homeostasis

and the underlying mechanisms were investigated in rats. Using *in vivo* uptake techniques, diet-induced iron deficiency increased total transepithelial calcium absorption in the duodenum but had no impact in the jejunum and ileum. The increase in duodenal calcium absorption was associated with upregulated levels of claudin-2 in this intestinal segment. Additionally, urinary calcium excretion and circulating levels of osteocalcin and CTX-1 were unchanged in iron deficiency, indicating that renal calcium handling and bone turnover were unaffected in the iron-deficient animals. Although the increase in duodenal calcium absorption in response to iron deficiency had no impact on serum calcium levels, the increase in both intestinal and renal claudin-2 protein levels highlight a key role for iron as an important regulator of epithelial calcium transport.

Previous findings have reported conflicting results on the impact of diet-induced iron deficiency on intestinal calcium handling where Campos *et. al.*[409] showed an increase in apparent calcium absorption (calcium intake minus faecal calcium excretion) in contrast to Katsumata *et. al* [385], who reported a decrease in response to diet-induced iron deficiency. Although the strain and the age of the rats used in both studies were the same, the composition of the amount of iron in the iron-deficient diets and the duration of treatment differed. While the rats in Campos' study were fed an iron-deficient diet containing 4.4mg/kg of iron for 40 days, while an iron-deficient diet containing 0mg/kg of iron over a duration of 28 days was employed to induce iron deficiency in Katsumata's study. These conditions resulted in ~48% and ~82% reduction in haematocrit levels in Campos' and Katsumata's study respectively, demonstrating a considerably higher degree of iron deficiency in Katsumata's study compared to Campos' study [385,409]. Based on these findings, it is speculated that variations in the severity of nutritional ferropenic anaemia may have opposing effects on calcium homeostasis,

whereby, a more severe form of iron deficiency decreases calcium absorption, while a mild or moderate form increases calcium absorption. Consistent with this hypothesis, the mild form of iron deficiency in the current study (characterised by ~10% reduction in haematocrit levels) increased duodenal calcium absorption. Although apparent calcium absorption measured in previous studies provides information about the sum of absorption and secretion of calcium ions across the entire gastrointestinal tract, the *in vivo* uptake technique used in the current study identifies the impact of iron deficiency on specific intestinal segments. Therefore, based on the findings of the current study, mild iron deficiency appears to have a localised effect on calcium absorption across the duodenum, which is the major segment for iron absorption. This highlights a potentially novel mechanism linking iron and calcium absorption. To investigate this mechanism further, the impact of iron deficiency on the mRNA expression of the key components of transcellular and paracellular calcium absorption were measured. Since the duodenum has been established as the major small intestinal segment for transcellular calcium absorption, the protein levels of the transcellular calcium transport proteins were investigated further in this segment. Interestingly, none of the transcellular calcium transport proteins were affected by iron deficiency across the different segments of the small intestine, except for the calcium binding protein, calbindin-D9k (*S100A9*), which was inhibited by iron deficiency. In support of this finding, a gene chip analysis investigating genetic responses to iron deficiency also showed a decrease in the *S100A9* gene in the duodenum of rats [413] indicating that changes in iron transport potentially regulates calbindin-D9k. Interestingly, increased DMT1 levels have been reported to be associated with a reduction in active (transcellular) calcium absorption [372], a process that is hypothesised to be mediated by calbindin-D9k [12,414]. In the current study, downregulated levels of

calbindin-D9k in response to iron deficiency was associated with increased levels of DMT1. Taken together, these findings suggest a link between DMT1 and calbindin-D9K, however, the mechanism underlying this link is currently unknown.

During iron deficiency, DMT1 is upregulated as an adaptation to increase intestinal iron absorption. In addition to its ability to co-transport hydrogen ions with other divalent metal ions, DMT1 can also operate as a proton (H^+) uniporter [349]. In keeping with this, increased intracellular H^+ has been reported following the upregulation of DMT1 [341,349,415]. There is evidence that the DMT1-mediated increase in intracellular H^+ reduces transcellular calcium absorption in the duodenum [383]. This decrease in transcellular calcium absorption has been speculated to be due to the inhibition of calbindin-D9k expression and function, caused by a decrease in the calcium binding affinity of calbindin-D9k at low pH [416]. Therefore, this mechanism is potentially responsible for the low levels of calbindin-D9k seen in response to diet-induced iron deficiency in the current study. Even though the levels of calbindin-D9k were downregulated in response to iron deficiency, it is also possible that this change in calbindin-D9k may have little or no impact on total transepithelial calcium transport. This is based on the evidence that under normal or a high dietary calcium condition, paracellular calcium transport predominantly determines the total transepithelial calcium absorption in the small intestine [6]. Therefore, in the current study, where a high concentration of calcium in the uptake buffer was employed, the paracellular calcium pathway is most likely responsible for any changes in total transepithelial calcium absorption. Thus, proteins involved mediating paracellular calcium transport may be playing a more important role in diet-induced iron deficiency. In addition to the intracellular calcium buffering and translocation function of

calbindin-D9k, this protein has also been suggested to be involved in the crosstalk between the transcellular and paracellular calcium pathway [12]. Hwang *et.al* [417] demonstrated an increase in claudin-2 and -15 mRNA and protein expression in calbindin-D9k knockout mice fed a normal calcium diet. Therefore, it is possible that the downregulation of duodenal calbindin-D9k in the rats following iron deficiency in the current study may play a role in increasing the levels of claudins involved in paracellular calcium absorption. Alternatively, increased levels of claudins involved in paracellular calcium absorption following calbindin-D9k downregulation may be a compensatory mechanism to maintain duodenal calcium absorption in the absence of calbindin-D9k.

Iron deficiency enhanced the mRNA expression and protein levels of claudin-2 only in the duodenum, which is consistent with the finding from a gene chip analysis in iron-deficient rats [413], while claudin-12 protein levels in the iron-deficient rat duodenum were unaffected. Since claudin-2 is known to be a pore-forming claudin mediating paracellular calcium flux, the upregulation of this protein is likely responsible for the increase in duodenal calcium absorption in response to iron deficiency. Due to the potential involvement of claudin-15 in paracellular calcium absorption via solvent drag as previously mentioned in **section 1.2.7**, the effect of iron deficiency on this protein was also measured. The finding that iron deficiency had no impact on duodenal claudin-15 in the current study suggests that the speculated claudin-15-mediated calcium absorption via solvent drag may not be responsible for the increase in duodenal calcium absorption in response to iron deficiency.

To understand the physiological impact of iron deficiency on calcium homeostasis, the serum and urinary calcium levels were measured. Although

diet-induced iron deficiency significantly enhanced duodenal calcium absorption, there was no change in urinary calcium excretion or serum calcium levels. The findings that serum calcium levels were unchanged in iron deficiency in the current study is consistent with the findings of Campos *et. al* [409], which also showed a lack of change in serum calcium levels, despite the increase in apparent calcium absorption (the difference between dietary calcium intake and faecal calcium excretion) in response to iron deficiency. However, in contrast to the findings of the current study, Campos *et. al* [409] also demonstrated a significant increase in urinary calcium excretion in iron-deficient animals, highlighting the contribution of the kidney in maintaining normal serum calcium levels in these animals. The differences between the current study and that of Campos *et al.* [409] may be explained by the magnitude of calcium absorbed. While Campos *et. al* reported ~61% increase in apparent calcium absorption in response to moderate iron deficiency, the relatively milder form of iron deficiency in the current study increased duodenal calcium absorption by ~34%. This suggests that the considerably higher amount of calcium absorbed in response to iron deficiency may be responsible for the changes in renal calcium excretion in the study conducted by Campos *et. al* [409] compared to the current study.

Furthermore, while the current study focused on the impact of iron deficiency on calcium absorption in the small intestine, Campos *et. al* [409] investigated calcium absorption across the entire gastrointestinal tract. Therefore, the other intestinal segments known to contribute to total calcium absorption such as the caecum and colon [6] may have partly contributed to the higher level of calcium absorption reported by Campos *et.al* [409]. Nonetheless, due to the relatively shorter intestinal transit time in the duodenum compared to the other segments of the small intestine [213], the increase in the amount of calcium absorbed in the duodenum in

the current study may not be significant enough to alter serum calcium levels and consequently, urinary calcium excretion.

Since urinary calcium levels were unaffected by iron deficiency, it is predicted that the renal calcium transporters would also be unaffected. While this was true for the renal transcellular calcium proteins, claudin-2 protein levels were enhanced by iron deficiency suggesting that iron deficiency may have a direct impact on claudin-2. Based on a previous finding reporting hypercalciuria in claudin-2-deficient mice [159], the upregulation of claudin-2 in the current study was expected to cause a reduction in urine calcium excretion. However, this was not apparent. The lack of change in the amount of calcium excreted (Ca/Cr) despite the increase in renal claudin-2 levels, may be attributed to the amount of calcium in the diet of the animals. For instance, the amount of calcium present in the lumen of the small intestine when the rats were fed a normal calcium diet, may have been insufficient to significantly impact either serum or urine calcium levels despite the increase in claudin-2.

Apart from changes in renal calcium reabsorption, it is possible that the calcium reservoir in bone may also adapt to changes in intestinal calcium absorption by altering the amount of calcium stored in the exchangeable calcium labile pool of the bone or by altering bone turnover [418]. For the latter reason, the markers of bone formation (osteocalcin) and resorption (CTX-1) were measured. Contrary to previous findings where severe iron deficiency impacts the markers of bone turnover [385,388], there were no changes in these markers in the current study. However, it is important to note that this measurement gives no indication of the contribution of the bone labile calcium pool, which is more difficult to determine. Therefore, it is possible that the regulation of the calcium labile pool may

contribute to the maintenance of serum calcium levels as a potential adaptation to the increase in duodenal calcium absorption in the current study.

In addition to the contribution of the kidney and the bone, $1,25(OH)_2D_3$, PTH and FGF23 are important hormonal components of calcium homeostasis. Previous findings demonstrating altered calcium absorption in response to severe iron deficiency have also shown significant changes in PTH and $1,25(OH)_2D_3$ [385,409], thereby identifying these hormones as potential targets responsible for the increase in calcium absorption seen in the current study. Additionally, $1,25(OH)_2D_3$ treatment has also been demonstrated to increase claudin-2 levels in the human colonic epithelial (SKCO15) cell line via the activation of the vitamin D response element (VDRE), identified in the promoter region of the claudin-2 gene [281]. Therefore, changes in $1,25(OH)_2D_3$ levels in response to iron deficiency may also be responsible for the increase in claudin-2 levels. However, previous studies in our lab have shown that iron deficiency does not significantly impact the levels of $1,25(OH)_2D_3$, and its regulators, PTH and FGF23 [419], suggesting that the increase in duodenal calcium absorption and claudin-2 protein are not directly caused by changes in these hormones. Interestingly, a previous study in our lab showed an increase in duodenal VDR in response to diet-induced iron deficiency in rats [420]. This finding suggests that the increase in duodenal claudin-2 may be due to an increase in the expression of VDR despite unchanged levels of $1,25(OH)_2D_3$.

3.5. Conclusion

In summary, mild diet-induced iron deficiency significantly increases duodenal calcium absorption under a calcium concentration that favours the paracellular pathway. This potentially occurs via a mechanism involving claudin-2

upregulation and appears to be independent of the systemic regulators of calcium homeostasis. Although iron deficiency increased calcium absorption in the duodenum, serum and urine calcium levels, and the markers of bone turnover were unchanged in contrast to the findings of previous studies [385,409]. The varying severities of iron deficiency in the current and previous studies is likely to be the most probable cause of these differences, with more severe iron deficiency having a greater impact on calcium homeostasis compared to the milder form of iron deficiency employed in the current study. Importantly, the fact that iron deficiency impacts the levels of claudin-2 in both duodenal and renal epithelial cells suggests that the mechanisms involved in maintaining iron homeostasis may directly regulate claudin-2-mediated calcium transport in these cells.

Chapter 4 - Understanding the mechanisms underlying increased claudin-2-mediated calcium absorption in the duodenum in response to iron deficiency using Caco-2 cells.

4.1. Introduction

As briefly described in Chapter 2, Caco-2 cells are commonly used as a human model of the human small intestine. Studies indicate that a culture period of 21 days is required for this cell line to exhibit small intestine-like characteristics such as: a polarised cell monolayer with microvilli on the apical surface, established tight junctions between adjacent cells and the expression of small intestinal hydrolases, including lactase [390,398]. Although 21 days in culture allows for complete cellular differentiation and the formation of tight junctions, this also results in a very tight epithelium, which is unrepresentative of the leaky nature of the small intestine and may well be more representative of the relatively tight colonic epithelium [390]. For example, using Ussing chamber experiments, the transepithelial electrical resistance (TEER) of the different segments of the human small intestine; duodenum (45 ± 21 $\Omega.cm^2$), jejunum (34 ± 12 $\Omega.cm^2$) and ileum (37 ± 4.26 $\Omega.cm^2$), have been reported to be significantly lower than the colon (120 ± 43 $\Omega.cm^2$). Furthermore, in contrast to 21-day cultured cells, fully confluent Caco-2 cells cultured for 4 days have been shown to have a significantly lower TEER [421], suggesting that 4-day cultured cells may be more suitable for studying small intestinal paracellular calcium flux. Although, the shorter culture period may alter the expression levels of important proteins involved in calcium flux such as VDR [422], lower expression may not necessarily inhibit the function of these proteins and their response to treatments. For instance, despite the lower levels of VDR expression in 5-day cultured cells, Giuliano *et.al.* [422] demonstrated that the effect of $1,25(OH)_2D_3$ treatment on alkaline phosphatase activity (a response also observed in the rat duodenum [423]) was similar in Caco-2 cells cultured for 5 or 15 days.

The mechanisms of calcium and iron transport in Caco-2 cells have been extensively studied, and the proteins responsible for the transport of these ions (DMT1 and FPN for iron transport [424], and claudin-2, -12, TRPV6, calbindin-D9K and PMCA1 for calcium transport (**Figure 2.8**)) in the intact small intestine are endogenously expressed in this cell line. The cellular adaptations of the iron transporters to iron deficiency in Caco-2 cells have been shown to mimic the responses in the small intestine. For example, iron deficiency is characterised by the upregulation of DMT1 in the duodenum of rodents and humans, and this response is also seen in Caco-2 cells treated with the iron chelator, deferoxamine (DFO) [424,425]. DFO is a common iron chelator typically used to treat iron overload in β-thalassemia and other iron overload-related conditions in humans because it binds to iron and inhibits excess iron accumulation [426–428]. Based on this finding, DFO appears to be a good compound to investigate whether changes in iron levels may impact the mechanisms of calcium absorption in Caco-2 cells.

In addition to low iron levels, hormonal and cellular adaptations to iron deficiency also occur. Such a response includes the upregulation of the kidney-derived hormone, EPO, crucial for red blood cell production (erythropoiesis), and the transcription factor, hypoxia-inducible factor 2 (HIF-2), which are both stimulated by hypoxia and low iron levels [429,430]. In addition to erythropoiesis, EPO has also been shown to directly regulate intestinal iron absorption by stimulating the upregulation of DMT1 and FPN levels [368]. Based on the regulatory function of EPO on intestinal iron transporters, this protein was also used in the current study to investigate whether calcium absorption is impacted by changes in DMT1 levels.

More recently, the upregulation of HIF-2, in the duodenum has been reported following iron deficiency [359]. HIF-2 is identified as a regulator of intestinal iron absorption by directly stimulating the expression of the duodenal iron transporters, DMT1, DcytB and FPN [352,359]. Under iron-deficient conditions, the iron-dependent prolyl-hydroxylase domain (PHD) enzyme, known to target HIF-2α for degradation, is suppressed [358], resulting in increased transcription of the genes encoding proteins involved in iron transport including DMT1 and FPN [360]. Several drugs have been produced to increase HIF levels by inhibiting PHDs such as Molidustat and Roxadustat (FG-4592). In particular, FG-4592 increases HIF-2α levels by inhibiting the PHD, which is responsible for HIF-2α targeted degradation [431]. FG-4592 is currently used to treat anaemia in patients with CKD [431] and was used in the current study to investigate a potential relationship between HIF-2α and calcium transport in Caco-2 cells.

4.1.1. Aims

The aim of this chapter was to validate Caco-2 cells cultured for 4 days and 21 days as an appropriate cell model to investigate calcium absorption, and to use this model to test the impact of iron deficiency and the regulators of iron transport on paracellular calcium flux. To achieve this, Caco-2 cells were treated with the iron chelator, DFO, to induce cellular iron deficiency, and the impact on paracellular calcium flux and the expression of key iron transporters and claudins was investigated. Additionally, since studies have reported high levels of EPO and HIF-2α during iron deficiency [359,429,432], the direct impact of these regulators on paracellular calcium transport and the expression of the transporters mediating paracellular calcium absorption were investigated.

4.2. Methods

4.2.1. Cell culture

As previously mentioned in **Chapter 2, section 2.2.5,** parental Caco-2 cells between passage 35-45 were cultured in DMEM and supplemented with 10% fetal bovine serum and 1% penicillin/streptomycin. Cultures were incubated at 37ºC with 5%CO_2:95%O_2 and >95% humidity. At approximately 70% confluence, cells were sub-cultured by trypsinisation (Gibco, Fisher scientific, Loughborough, UK), and the media was changed three times per week.

4.2.2. Treatments

For all experiments, Caco-2 cells were cultured in Transwell inserts with polyester membranes and a pore diameter of 0.4mm. To induce iron deficiency in the cells, day 4- and day 21-cultured cells were treated in the apical compartment with either 100µM deferoxamine (DFO; Sigma Aldrich, Gillingham, UK) or 50µM ferric ammonium citrate (FAC; Sigma Aldrich, Gillingham, UK) in the iron-deficient or control group respectively for 24 hours. The concentration and duration of iron (Fe) and DFO treatment were obtained from a previous study that has shown changes in the well-established cellular adaptation to iron deficiency (e.g., changes in DMT1 levels) [424]. For erythropoietin (EPO; Biotechne, Abingdon, UK)-treated cells, day 4 and 21 cells were treated with 1u/ml, 2.5u/ml or 5u/ml of EPO in 0.1% Bovine serum albumin (BSA) in the basolateral compartment for 24 hours and compared with the control group (untreated), cultured in 0.1% BSA for the same duration. The starting concentration (1u/ml) and the duration of EPO treatment were obtained from a study by Srai *et al.* [368]. Finally, to test the impact of HIF-2α levels on calcium transport, Caco-2 cells were treated with 10µM, 50µM and 100µM of FG-4592 (Selleckchem, Cambridge, UK) in the apical compartment

for 24 hours and compared with the control group (untreated). The different concentrations of FG-4592 and the duration of treatment used were obtained from a previous study [433].

4.2.3. Measurement of transepithelial electrical resistance (TEER)

The transepithelial electrical resistance of the monolayer was measured in cells cultured on Transwell inserts using an epithelial voltohmmeter (EVOM2, World Precision Instruments, Herts, UK).

4.2.4. Ferritin assay

To determine ferritin levels in 100µM DFO-treated Caco-2 cells that were cultured for 21 days, cells were washed twice in ice-cold PBS and scraped in 100µl PBS containing an EDTA-free protease inhibitor (Roche Life Sciences, West Sussex, UK). Ferritin levels in the cell lysate were determined using a human-specific ELISA kit (Abcam, Cambridge, UK) according to the manufacturer's instructions. The principle of this assay relies on the use of 2 monoclonal antibodies specific to ferritin. The first anti-ferritin antibody is immobilised on the microwell plate, while a second antibody, ferritin-specific biotinylated detection antibody is then added. Following this, streptavidin-peroxidase complex is added, and the unbound conjugates are washed away with a wash buffer. TMB is then used to visualise the streptavidin-peroxidase enzymatic reaction, which produces a blue colour product that changes into yellow after adding the acidic stop solution. The density of yellow coloration is directly proportional to the amount of ferritin captured in the plate for each cell lysate sample.

4.2.5. Measurement of transepithelial calcium flux

To determine the effect of the treatments on paracellular transepithelial calcium flux, cells cultured on Transwell inserts following 24 hours of treatment were washed three times with warm HEPES buffer containing 140mM NaCl, 5mM KCl, 1mM $CaCl_2$, 0.5mM $MgCl_2$ and 10mM Na-HEPES. Following this, warm HEPES buffer containing 5mM glucose was added to the basolateral compartment, while uptake buffer containing 99mM $CaCl_2$, HEPES buffer and 0.37MBq of ^{45}Ca was added to the apical compartment and incubated at 37^{o}C. 100µl of basolateral solution was collected after 30 minutes and the amount of ^{45}Ca transported to the basolateral compartment was measured using a scintillation counter (Tri-Carb 2900TR; Perkin Elmer).

4.2.6. RNA extraction, cDNA production and RT-PCR

To test whether there is any relationship between duodenal DMT1, VDR, HIF-2α, with claudin-2 mRNA, duodenal mucosa was collected from rats following a 2-week dietary iron regimen as described in **section 3.2.1**. To investigate the impact of DFO treatments on the mRNA expression of iron transporters and the claudins mediating paracellular calcium transport in Caco-2, cells were scraped in TRIzol following DFO treatment. RNA was isolated and cDNA was synthesised from duodenal mucosa and Caco-2 cells as described in **section 2.2.6**. Subsequently, RT-qPCR was used to measure the mRNA expression DMT1, VDR, HIF-2α, claudin-2 in rat duodenum, Caco-2 DMT1, FPN and calcium transport proteins as described in **Chapter 2, section 2.2.7**. The rat- and human-specific primers used are listed in **Table 4.1 and 4.2** respectively.

Table 4.1. Rat-specific primers. Primers used for rat RT-PCR experiment were either obtained from Qiagen (sequences not given) or predesigned primer sequences were sent to Sigma-Aldrich where the primers were made.

Primer name	Catalogue number	Forward sequence	Reverse sequence
DMT1	QT00182623	-	-
HIF-2α	QT00192059	-	-
VDR	-	AGGCTACAAAGG TTTCTTCA	TAGCTTGGGCCT CAGACTGT
Claudin-2	QT00451836	-	-
β-actin	-	AACAAGATGAGATT GGCATGG	AGTGGGGTGGC TTTTAGGAT

Table 4.2. Human-specific primers. Primers used for RT-PCR experiment in Caco-2 cells were either obtained from Qiagen or ThermoFisher Scientific (sequences not given) or predesigned primer sequences were sent to Sigma-Aldrich where the primers were made

Primer name	Catalogue number	Forward sequence	Reverse sequence
DMT1	-	GAGCCAGTGTGTT TCTATGG	CCTAAGCCTGATA GAGCTAG
FPN	QT00094843	-	-
TRPV6	QT00040096	-	-
Calbindin-D9K	QT00000329	-	-
PMCA1	QT00087045	-	-
Claudin-2	Hs00252666_s1	-	-
Claudin-4	QT00241073	-	-
Claudin-12	QT01012186	-	-
β-actin	-	AACAAGATGAGATT GGCATGG	AGTGGGGTGGCTT TTAGGAT

4.2.7. Protein isolation and Western blotting

Treated cells were washed twice in ice-cold phosphate buffered saline (PBS) and scrapped in PBS containing an EDTA-free protease inhibitor (Roche Life Sciences, West Sussex, UK). Following this, the protein concentration was determined using the Bradford assay [395] as previously described in **section 2.2.8**. To determine the effect of DFO, EPO or FG-4592 treatment on iron transporters (DMT1+IRE and FPN), claudin-2, claudin-4, VDR and HIF-2α, Western blot experiments were carried out as previously described in **section 2.2.9** using 10-20mg of Caco-2 samples. Antibodies used for these experiments are listed in **Table 4.3**.

Table 4.3. Primary antibodies used for Western blot experiment

Protein of interest	**Company**	**Catalogue number**	**Dilution**	**Species**
DMT1+IRE (1mg/ml)	Alpha diagnostics	NRAMP22A	1:500	Rabbit polyclonal
FPN (1mg/ml)	Novus Biologicals	NBP1-21502	1:500	Mouse monoclonal
Claudin-2 (0.5mg/ml)	Thermofisher	12H12	1.1000	Mouse monoclonal
Claudin-4 (0.5mg/ml)	Thermofisher	32-9400	1:1000	Mouse monoclonal
VDR (0.2mg/ml)	Santa Cruz	Sc-13133	1:500	Mouse monoclonal
HIF-2α (1mg/ml)	Novus Biologicals	NB100-122	1:500	Rabbit polyclonal
β-actin (HRP-conjugated) (1mg/ml)	Proteintech	HRP-60008	1:2000	Mouse monoclonal

4.2.8. Statistical analysis

Data are presented as the mean ± standard error of mean (SEM). Statistical analysis was performed as previously described in **section 2.2.10**. Pearson's correlation analysis was used to examine whether there was any relationship between rat duodenal DMT1, HIF-2α, VDR, with claudin-2 mRNA expression, and whether VDR correlates with DMT1 or HIF-2α mRNA expression. Statistical significance was represented as *p<0.05, **p<0.01, ***p<0.001 and ****p<0.0001.

4.3. Results

4.3.1. Correlation analysis to identify potential regulators responsible for increased claudin-2-mediated duodenal calcium absorption in response to iron deficiency

To identify the potential regulators responsible for the increase in claudin-2-mediated calcium absorption in response to diet-induced iron deficiency in the rat duodenum, correlation analysis was carried out using the mRNA expression of DMT1, HIF-2α, VDR and claudin-2 in control and iron-deficient animals. The result showed that a significant positive correlation exists between DMT1 and claudin-2 (**Figure 4.1A**) and between HIF-2α and claudin-2 mRNA levels (**Figure 4.1B**). This suggests that there may be a relationship between HIF-2α-regulated iron transport and intestinal claudin-2 expression. Additionally, since VDR is known to be a regulator of claudin-2 [281], it is possible that the increase in claudin-2 may be induced by the upregulation of VDR in response to iron deficiency. Consistent with a previous finding in our laboratory [420], the investigation of VDR mRNA expression showed that duodenal VDR in the iron-deficient rats (0.024 ± 0.002) was significantly higher (p=0.005) than the control (0.016 ± 0.001). As

expected, with an r value of 0.8006, VDR shows the strongest correlation with claudin-2 mRNA levels (**Figure 4.1C**) suggesting that high VDR levels are associated with the high claudin-2 levels seen in the duodenum of iron-deficient animals. To test the possibility that DMT1 or HIF-2α might be impacting claudin-2 expression via VDR, correlation analysis was carried out to identify whether there is any relationship between DMT1 or HIF-2α mRNA with VDR mRNA expression. Interestingly, a significant positive correlation was seen between VDR and both DMT1 and HIF-2α (**Figure 4.1D** and **E**, respectively).

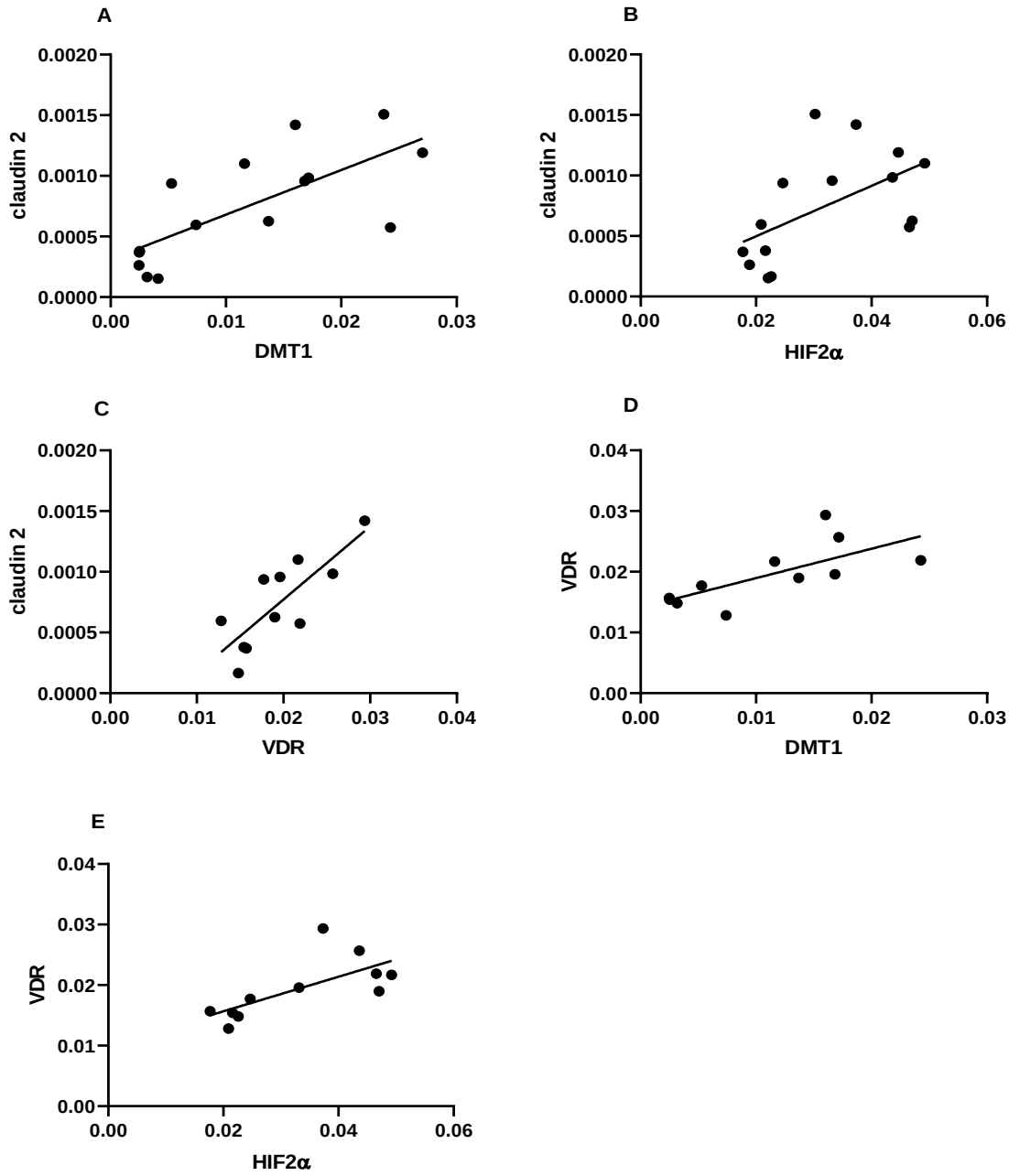

Figure 4.1. Correlation analysis of key iron and calcium transport proteins in the rat duodenum. Pearson correlations between the mRNA expression of: **A**: DMT1 and claudin-2 (r=0.7206, P<0.01), **B**: HIF-2α and claudin-2 (r=0.5475, P<0.05), **C**: VDR and claudin-2 (r=0.8006, P<0.01), **D**: DMT1 and VDR (r=0.7102, P<0.05, **E**: HIF-2α and VDR (r=0.6948, P<0.05) in the duodenum of control and iron-deficient rats. Duplicate PCR reactions were performed for each sample and the mRNA expression of each gene of interest (expressed as a ratio of the gene to β-actin) was used to perform correlation analysis as indicated in A-E, n=12-16 rats for each gene of interest.

4.3.2. mRNA expression of transporters mediating iron and calcium absorption in Caco-2 cells.

To validate the use of Caco-2 cells as a model to study the impact of iron deficiency on calcium transport, the mRNA expression of the key proteins mediating iron (DMT1 and FPN) and calcium (TRPV6, Calbindin-D9k, PMCA1, Claudin-2, and claudin-12) absorption was investigated. In addition to this, claudin-4 which is known to be the most highly expressed sealing claudin in Caco-2 cells [434] was also investigated. Although Caco-2 cells cultured for 21 days are widely accepted as a model of the small intestine, a recent study has shown that day 4 Caco-2 cells can also be used as a model for intestinal transport studies [434]. The mRNA expression of the proteins involved in iron and calcium transport as well as claudin-4 was measured in cells cultured for 4 days and compared with cells cultured for 21 days. The results showed that DMT1, FPN, Calbindin-D9k, PMCA1 and claudin-2 mRNA expression was significantly higher in Caco-2 cells cultured for 21 days compared to 4 days (**Figure 4.2A**), which is likely attributed to the increase in differentiation with time in culture [390]. Nonetheless, the proteins of interest were endogenously expressed in both 4- and 21-day cultured Caco-2 cells (**Figure 4.2A**) making both culture periods suitable for investigating changes in gene expression and protein levels. Additionally, investigation of the TEER in day 4 and 21 days cultured Caco-2 cells showed lower TEER in day 4 compared to day 21 (**Figure 4.2B**) [421]. This suggests that day 4 cultured Caco-2 cells may be more comparable to the small intestine since the small intestine is a relatively leaky epithelia (with lower TEER) than the colonic epithelia.

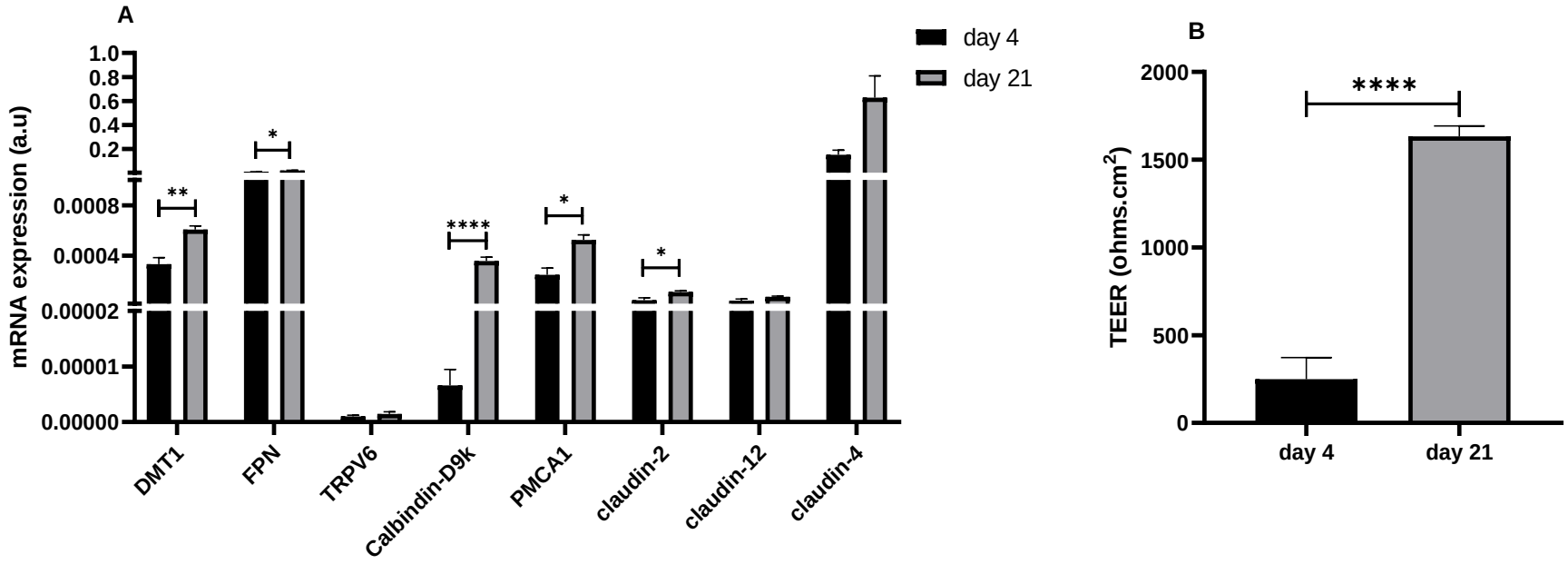

Figure 4.2. Effect of different culture periods on mRNA expression of iron and calcium transport proteins and TEER in Caco-2 cells. **A:** mRNA expression of DMT1, FPN, TRPV6, Calbindin-D9k PMCA1, claudin-2, -12 and -4, at 4- and 21-days in culture was determined using RT-PCR. Duplicate PCR reactions were performed for each sample and the mRNA expression of each gene of interest was expressed as a ratio of the gene to β-actin, indicated in arbitrary unit (a.u). **B:** TEER in 4- and 21-day cultured Caco-2 cells was measured using a voltohmmeter and expressed in ohms.cm^2. Data were analysed using unpaired t-test, *P<0.05, **P<0.01 ****P<0.0001, n=3-4 independent experiments.

4.3.3. Effect of deferoxamine (DFO) on ferritin and iron transporter levels in Caco-2 cells.

To induce iron deficiency, Caco-2 cells were treated with 100µM DFO, and ferritin levels were measured to confirm the impact of the DFO on the iron status of the cells. As expected, DFO significantly decreased ferritin levels in 21-day cultured Caco-2 cells (**Figure 4.3**) confirming that 100µM of DFO was sufficient to induce iron deficiency in the cell line. Since DMT1 and FPN are known to be upregulated during iron deficiency, the mRNA and protein levels of these transporters were measured in response to 100µM DFO. DFO treatment for 24 hours significantly upregulated DMT1 and FPN mRNA levels at 21 days (**Figure 4.4A** and **B**) and 4 days (**Figure 4.4C** and **D**) in culture. Despite significant changes in mRNA levels, the protein levels of DMT1 were unaffected by DFO treatment in both 21-day (**Figure 4.5A**) and 4-day (**Figure 4.5C**) cultured Caco-2 cells. Similarly, the protein expression of FPN was unaffected by DFO treatment in 4-day cultured Caco-2 cells (**Figure 4.5D**). Only the protein level of FPN in 21-day cultured Caco-2 cells (**Figure 4.5B**) mirrored the mRNA data in **Figure 4.4B** in response to DFO treatment.

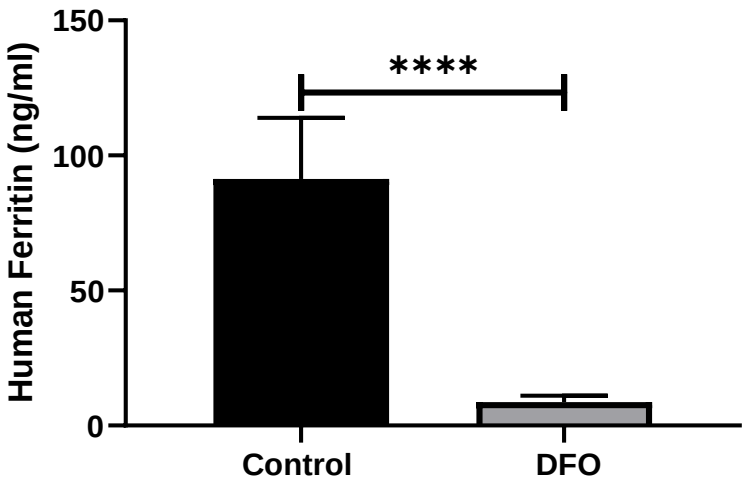

Figure 4.3. Effect of DFO on ferritin levels in 21-day cultured Caco-2 cells. Ferritin levels were measured in lysed Caco-2 cells following a 24-hour DFO (100µM) treatment or control using ELISA. Data are presented as Mean ± SEM and the difference between groups was analysed using unpaired t test. ****P<0.0001, n=6 independent experiments.

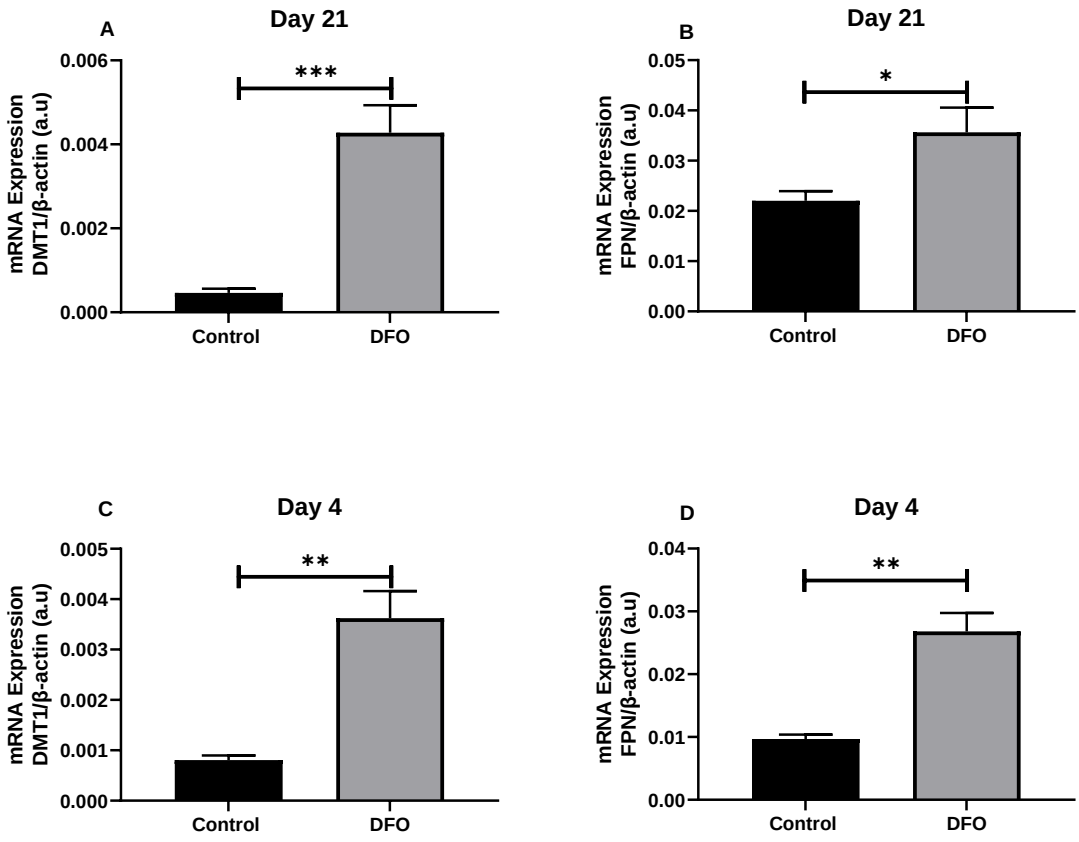

Figure 4.4. Effect of DFO on mRNA expression of iron transport genes in Caco-2 cells. mRNA expression of DMT1 (**A**) and FPN (**B**) in Caco-2 cells cultured for 21 days and the mRNA expression of DMT1 (**C**) and FPN (**D**) in Caco-2 cells cultured for 4 days, in response to a 24-hour DFO (100μM) treatment or control, was determined using RT-PCR. Duplicate PCR reactions were performed for each sample and the mRNA expression of DMT1 or FPN was expressed as a ratio of its gene to β-actin, indicated in arbitrary unit (a.u). Data are expressed as mean ± SEM and the difference between groups was analysed using unpaired t test, *P<0.05, **P<0.01, ***P<0.001, n=4-6 independent experiments.

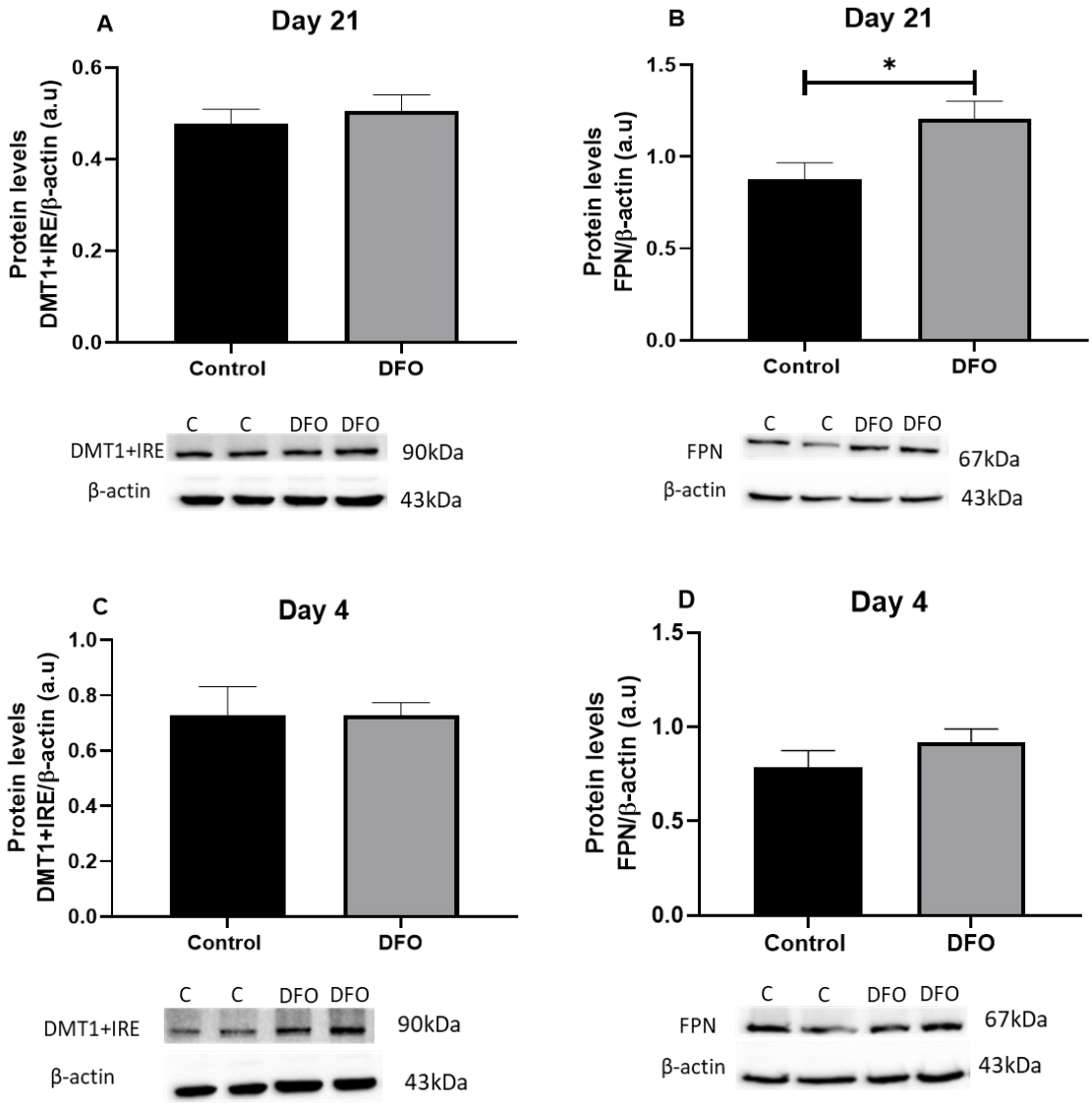

Figure 4.5. Effect of DFO on the expression of iron transport proteins in Caco-2 cells. Protein levels of DMT1 (**A**) and FPN (**B**) in Caco-2 cells cultured for 21 days and the protein expression of DMT1 (**C**) and FPN (**D**) in Caco-2 cells cultured for 4 days, in response to a 24-hour DFO (100μM) treatment or control, was determined using Western blot. Western blot representative image of DMT1 and FPN are shown below each graph (n=2 independent experiments). The abundance of DMT1 or FPN protein is given as the ratio of its band density to β-actin, expressed in arbitrary units (a.u). Data are expressed as mean ± SEM and the difference between groups was analysed using unpaired t test, *P<0.05, n=4 independent experiments.

4.3.4. Effect of DFO on mRNA expression of claudin-2, -12 and -4 in Caco-2 cells cultured for 4 and 21 days.

To investigate the impact of 100μM DFO treatment on the transporters mediating paracellular calcium absorption, mRNA levels of claudin-2 and -12 were measured in Caco-2 cells cultured for 4 and 21 days. In addition, the expression of claudin-4 was investigated. While the mRNA expression of claudin-2 was significantly lower in response to DFO in day 21 cells (**Figure 4.6A**), claudin-2 expression in day 4 cells were unchanged (**Figure 4.6D**). Interestingly, claudin-12 (**Figure 4.6B** and **E**) and claudin-4 (**Figure 4.6C** and **F**) were upregulated by DFO treatment at 21 and 4 days in culture.

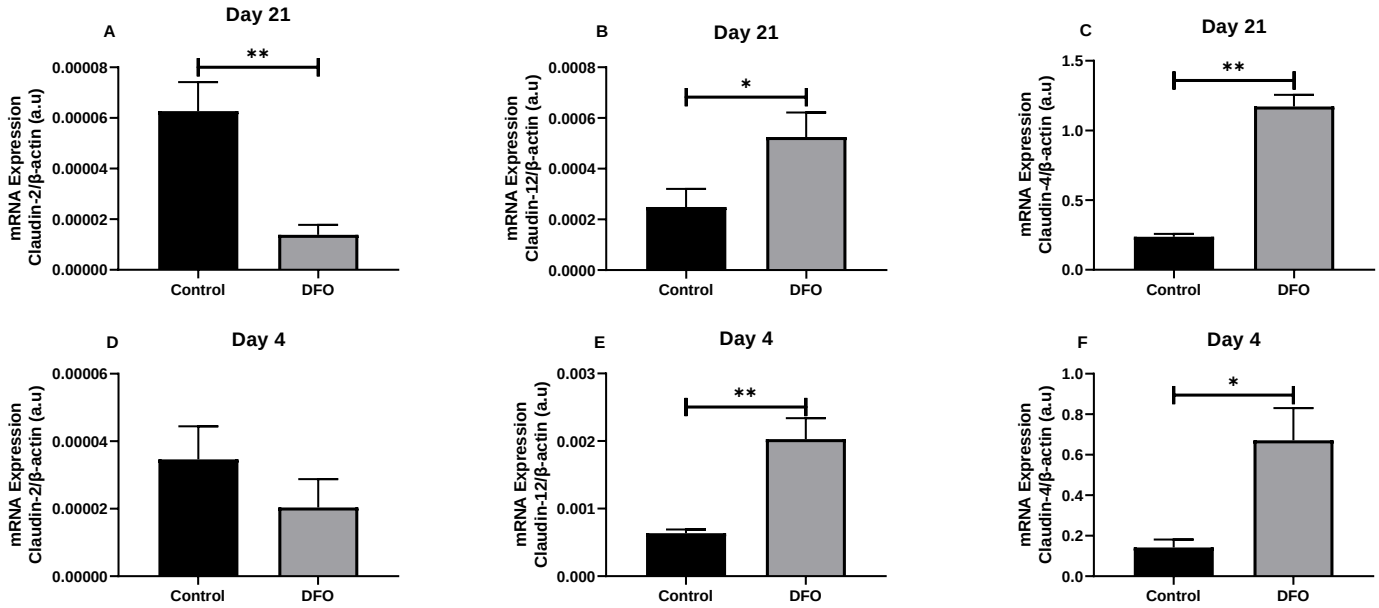

Figure 4.6. Effect of DFO on mRNA expression of claudin-2, -12 and -4 in Caco-2 cells. mRNA expression of claudin-2 (**A**) claudin-12 (**B**), claudin-4 (**C**), in Caco-2 cells cultured for 21 days, and claudin-2 (**D**) claudin-12 (**E**), claudin-4 (**F**), cultured for 4 days, in response to a 24-hour DFO (100μM) treatment or control, was determined using RT-PCR. Duplicate PCR reactions were performed for each sample and the mRNA expression of each claudin of interest was expressed as a ratio of its gene to β-actin, indicated in arbitrary unit (a.u). Data are expressed as mean ± SEM and the difference between groups was analysed using unpaired t test, *P<0.05, **P<0.01, n=4 independent experiments.

4.3.5. Effect of DFO on protein levels of claudin-2, -4, and VDR, calcium flux and TEER in Caco-2 cells cultured for 4 and 21 days.

Based on the finding of the current study that iron deficiency increased paracellular calcium absorption via claudin-2 in the rat duodenum, a mechanism potentially mediated by VDR, the effect of DFO on claudin-2 and VDR protein levels was measured. Additionally, the effect of DFO treatment on claudin-4 protein levels was investigated, as it appears to be the most highly expressed sealing claudin in Caco-2 cells [434]. Claudin-2 protein levels were unaffected by DFO treatment of 21- and 4-day cultured Caco-2 cells (**Figure 4.7A** and **D**). Although VDR and claudin-4 protein levels were also unaffected by DFO treatment of 21-day cultured Caco-2 cells (**Figure 4.7B** and **C**), these proteins were significantly upregulated by DFO in 4-day cultured Caco-2 cells (**Figure 4.7E** and **F**). Since claudin-12 is also important in mediating paracellular calcium absorption, the protein expression of this claudin would also be worth investigating. However, this was not possible due to the lack of specificity of the claudin-12 antibody (38-8200, Thermofisher) available. The transepithelial calcium flux across the Caco-2 monolayer the apical to the basolateral compartment of Transwell inserts (**Figure 4.8A** and **C**) and the transepithelial resistance (**Figure 4.8B** and **D**) were unaffected by DFO treatment in cells cultured for 21 and 4 days, respectively. This suggests that DFO-induced iron deficiency has no significant impact on claudin-2-mediated calcium flux in Caco-2 cells.

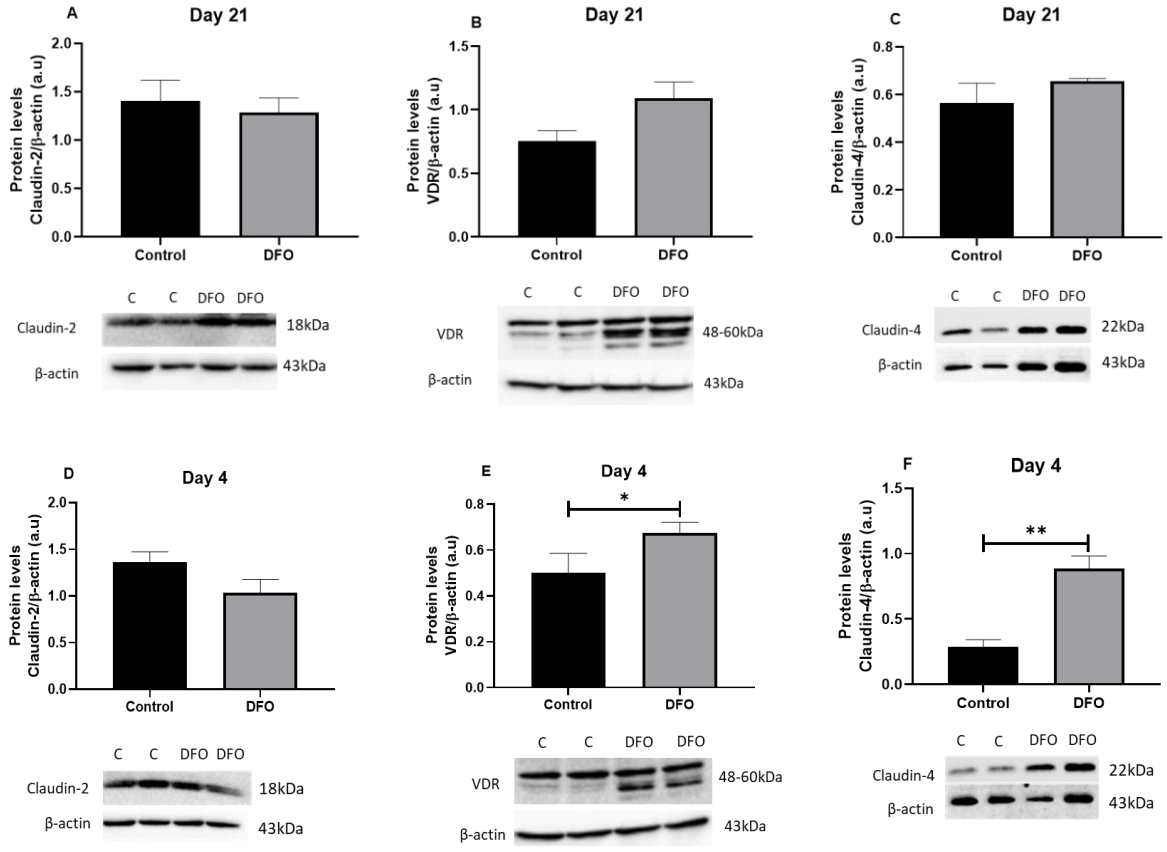

Figure 4.7. Effect of DFO on protein expression of claudin-2, -4 and VDR in Caco-2 cells. Protein expression of claudin-2 (**A**), VDR (**B**) and claudin-4 (**C**) in Caco-2 cells cultured for 21 days and of claudin-2 (**D**), VDR (**E**) and claudin-4 (**F**) in Caco-2 cells cultured for 4 days, in response to a 24-hour DFO (100µM) treatment or control, was determined using Western blot. Western blot representative image of the proteins of interest are shown below each graph (n=2 independent experiments). The abundance of each protein is given as the ratio of its band density to β-actin, expressed in arbitrary units (a.u). Data are expressed as mean ± SEM and the difference between groups was analysed using unpaired t test, *P<0.05, **P<0.01, n=4 independent experiments

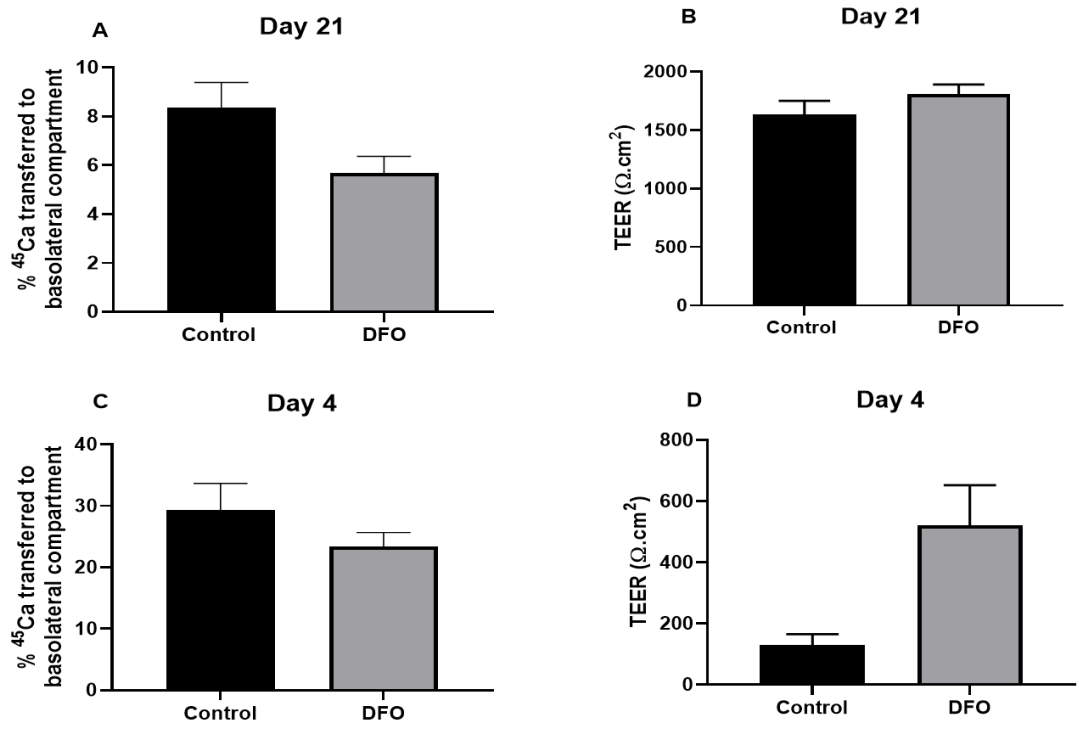

Figure 4.8. Effect of DFO on calcium flux and TEER in Caco-2 cells. Transepithelial flux of 100mM $CaCl_2$ and ^{45}Ca (**A** and **C**) and TEER (**B** and **D**) in Caco-2 cells cultured for 21 days and 4 days respectively were measured in response to a 24-hour DFO (100µM) treatment or control. Data are expressed as mean ± SEM and the difference between groups was analysed using unpaired t test, n=4 independent experiments.

4.3.6. Effect of Erythropoietin (EPO) treatment on DMT1 protein levels.

EPO is known to increase in the circulation in response to iron deficiency and has previously been shown to upregulate DMT1 [368]. In the current experiment, 1 unit (1u), 2.5 units (2.5u) and 5 units (5u) of EPO were used to treat Caco-2 cells for 24 hours, and DMT1 protein levels were investigated in cells cultured for 21 and 4 days. Although EPO had no significant effect on DMT1 protein levels in Caco-2 cells cultured for 21 days, 2.5 units of EPO produced the highest mean level of DMT1 (**Figure 4.9A**). In cells cultured for 4 days, 1 unit of EPO significantly upregulated DMT1 protein levels (**Figure 4.9B**)

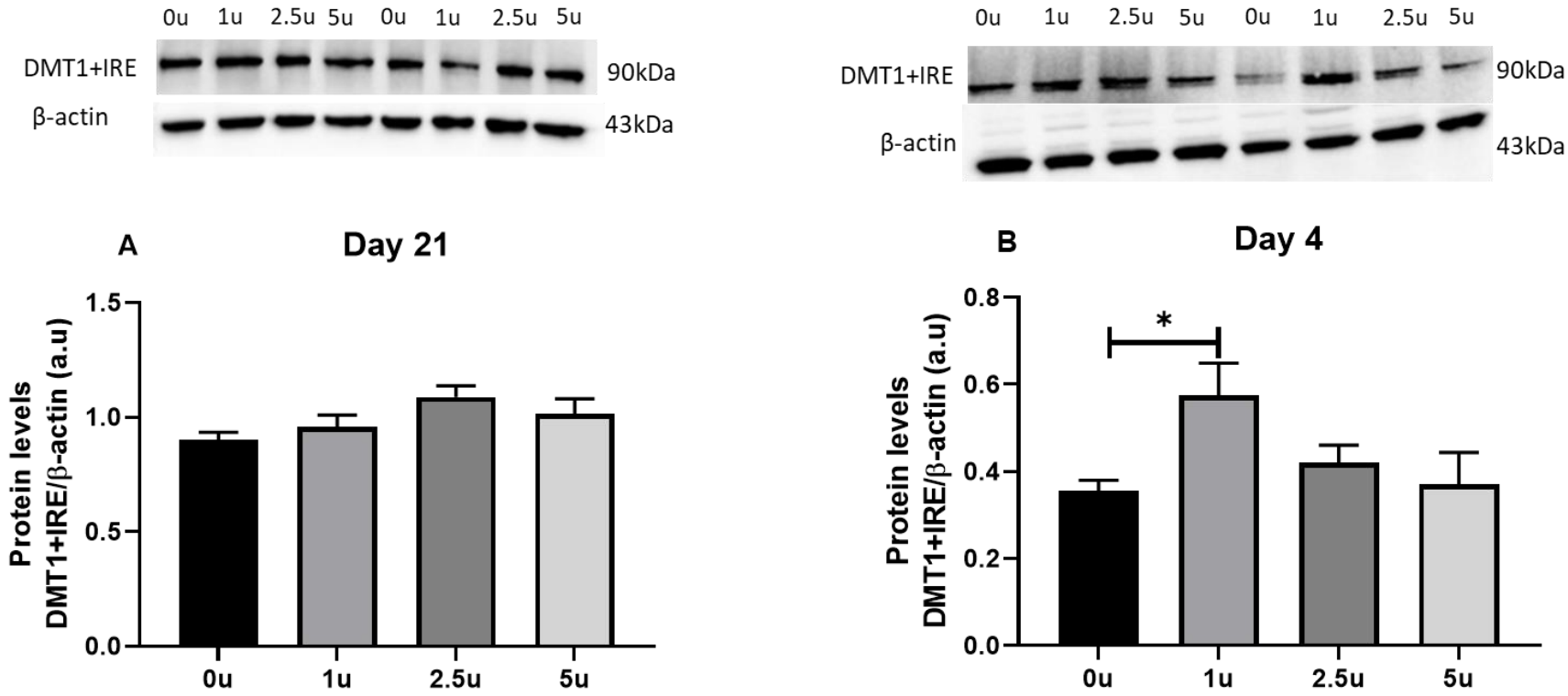

Figure 4.9. Effect of EPO on DMT1 levels in Caco-2 cells. Protein level of DMT1+IRE following control (0 unit), 1unit, 2.5 units and 5 units of EPO (for 24 hours) treatment in Caco-2 cells cultured for 21 days (**A**) and 4 days (**B**), was determined using Western blot. Western blot representative image of DMT1+IRE is shown above each graph (n=2 independent experiments). The abundance of DMT1+IRE is given as the ratio of its band density to β-actin, expressed in arbitrary units (a.u). Data are expressed as mean ± SEM and the difference between groups was analysed using a one-way ANOVA. *P<0.05, n=4 independent experiments.

4.3.7. Effect of EPO on claudin-2 and VDR protein levels, calcium flux, and TEER in day 21 and day 4 Caco-2 cells.

To investigate whether EPO had any effect on claudin-2 and VDR, the protein levels were measured in response to 2.5 units of EPO in day 21 Caco-2 cells and 1 unit of EPO in day 4 Caco-2 cells, as these were the concentrations of EPO that had the greatest effect on DMT1 protein levels. The results showed that 2.5 units of EPO treatment had no significant impact on claudin-2 (**Figure 4.10A**) and VDR (**Figure 4.10B**) protein levels in cells cultured for 21 days. Surprisingly, despite the upregulation of DMT1, claudin-2 and VDR protein levels were unaffected by 1 unit of EPO in day 4 Caco-2 cells (**Figure 4.10C** and **D**). Similarly, EPO treatment also had no significant impact on calcium uptake (**Figure 4.11A** and **C**) and TEER (**Figure 4.11B** and **D**) in 21- and 4-day cultured Caco-2 cells. This suggests that EPO, at the concentrations investigated, may not be responsible for regulating claudin-2-mediated paracellular calcium absorption during iron deficiency after 24 hours.

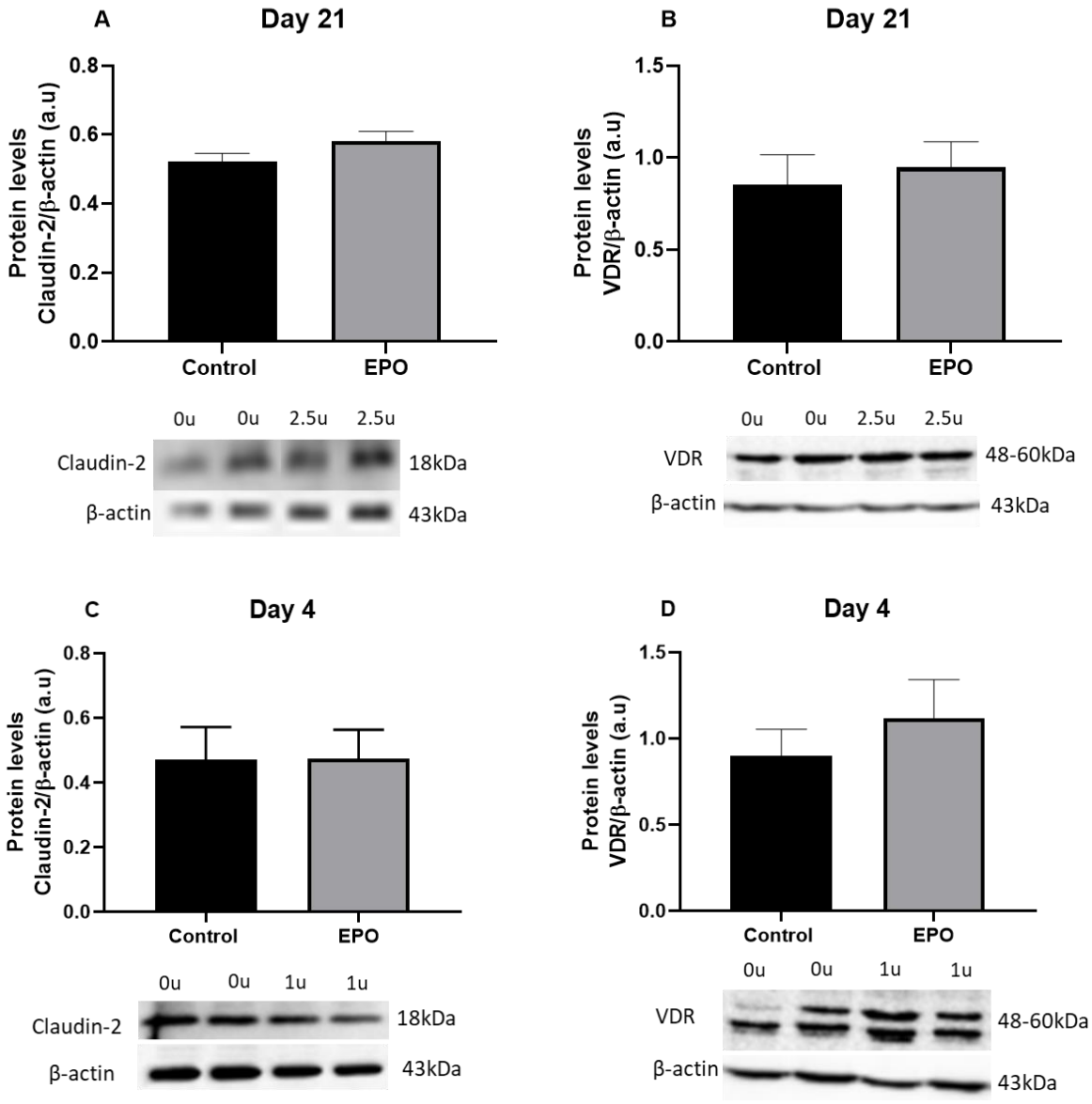

Figure 4.10. Effect of EPO on claudin-2 and VDR in Caco-2 cells. Protein level of claudin-2 (**A**) and VDR (**B**) in response to control (0 unit) or 2.5 units of EPO (for 24 hours) in Caco-2 cells cultured for 21 days, and the protein levels of claudin-2 (**C**) and VDR (**D**) in response to control (0 unit) or 1 unit of EPO (for 24 hours) in Caco-2 cells cultured for 4 days, was determined using Western blot. Western blot representative image of claudin-2 or VDR is shown below each graph (n=2 independent experiments). The abundance of claudin-2 or VDR is given as the ratio of its band density to β-actin, expressed in arbitrary units (a.u). Data are expressed as mean ± SEM and the difference between groups was analysed using unpaired t test, n=4 independent experiments.

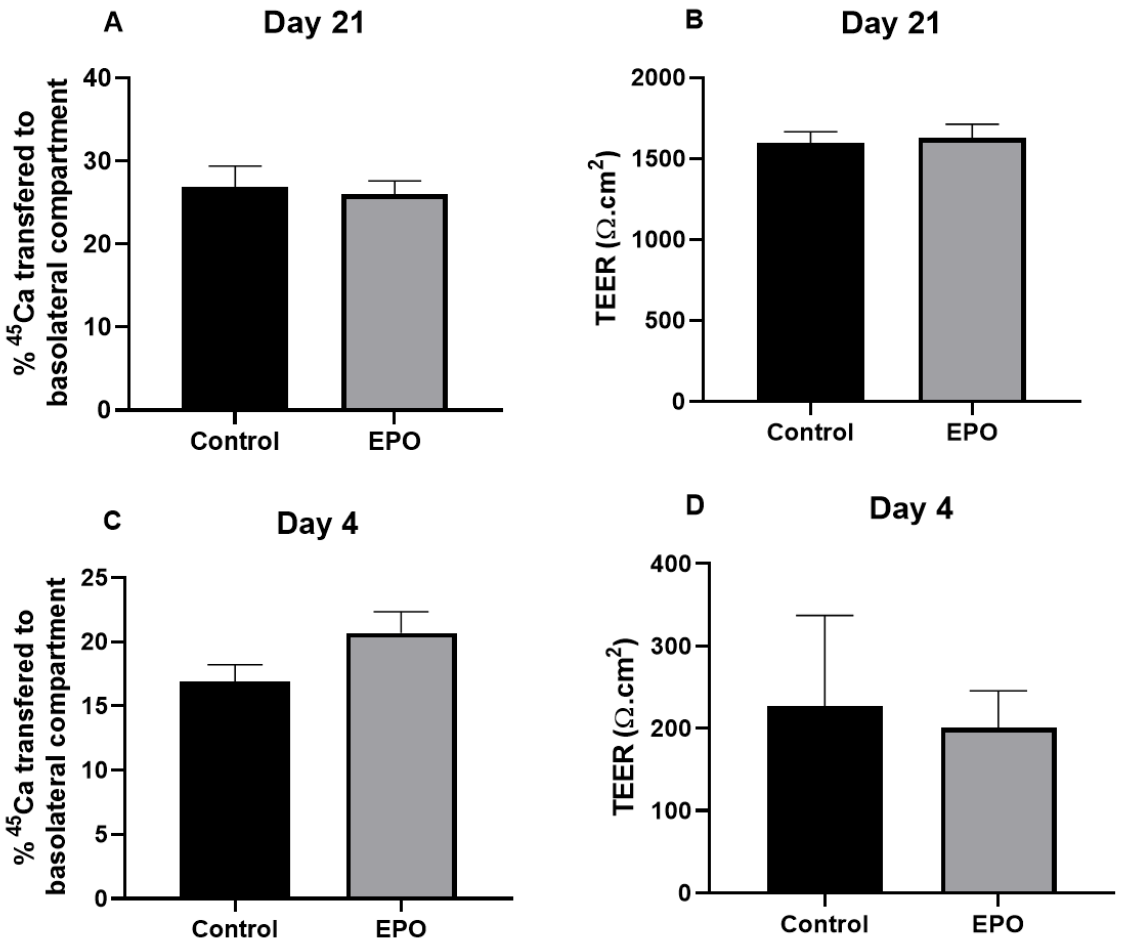

Figure 4.11. Effect of EPO on calcium flux and TEER in Caco-2 cells. Effect of control (0 unit) or 2.5 units of EPO (for 24 hours) on transepithelial flux of 100mM $CaCl_2$ and ^{45}Ca (**A**) and TEER (**B**) in Caco-2 cells cultured for 21 days, and the effect of 1 unit of EPO (for 24 hours) on transepithelial flux of 100mM $CaCl_2$ and ^{45}Ca (**C**) and TEER (**D**) in Caco-2 cells cultured for 4 days. Data are expressed as mean ± SEM and the difference between groups was analysed using unpaired t test, n=4 independent experiments.

4.3.8. Concentration-dependent effect of FG-4592 on HIF-2α protein expression in day-21 and day-4 Caco-2 cells.

To explore the potential effect of increased HIF-2α levels on claudin-2-mediated calcium absorption, Caco-2 cells were treated with increasing concentrations of FG-4592 (a HIF stabiliser) to identify the optimal concentration of the drug that will produce the highest levels of HIF-2α. The impact of 10μM, 50μM and 100μM of FG-4592 on HIF-2α protein levels was measured in day 4 and day 21 cultured Caco-2 cells after 24 hours of treatment. FG-4592 treatment resulted in a concentration-dependent increase in HIF-2α protein levels in Caco-2 cells cultured for 21 (**Figure 4.12A**) and 4 (**Figure 4.12B**) days, with the highest levels of HIF-2α observed in cells treated with 100μM of FG-4592. Based on this finding, 100μM of FG-4592 was used in subsequent experiments to investigate the impact of HIF-2α on claudin-2-mediated paracellular calcium flux in Caco-2 cells.

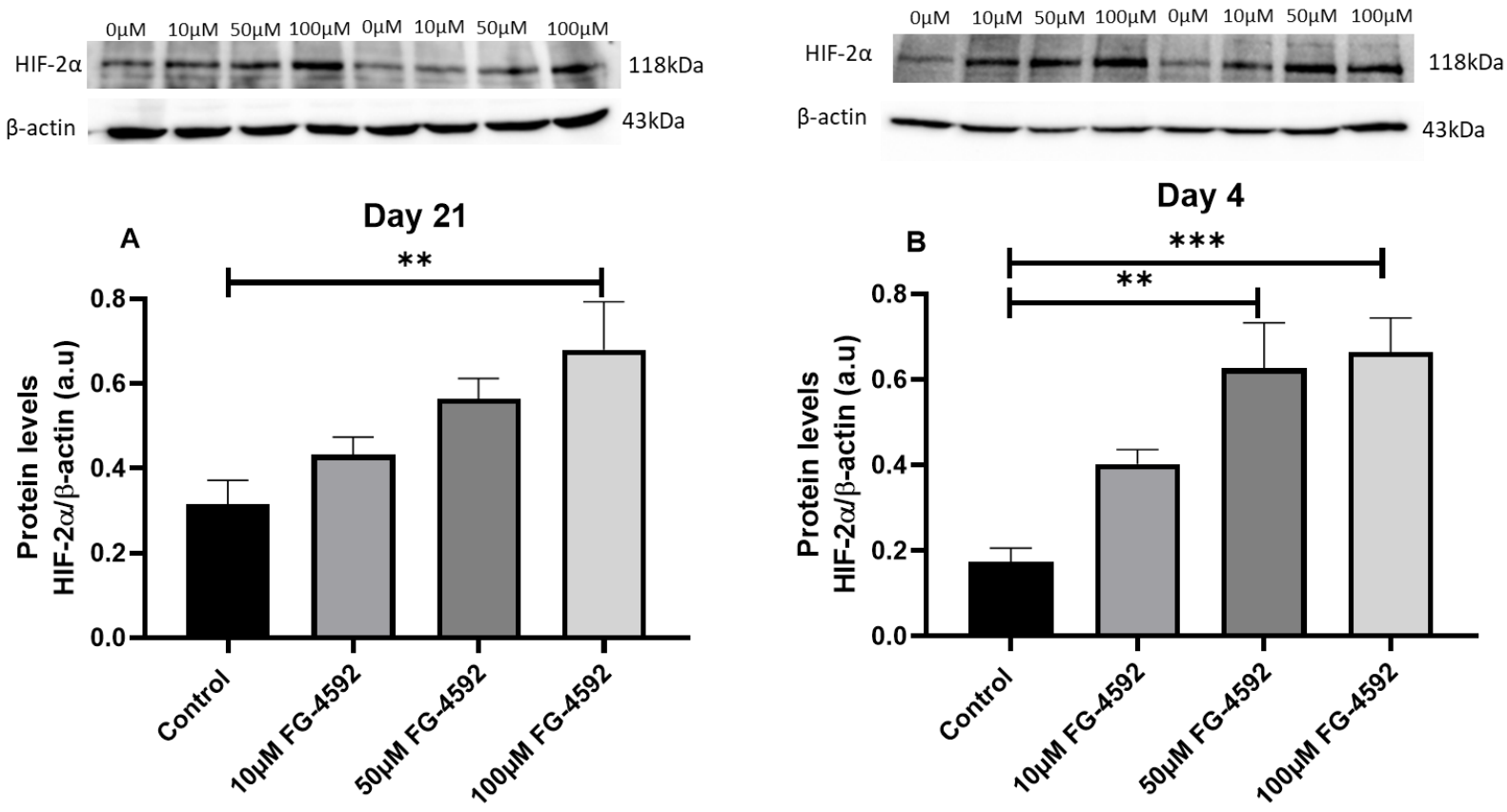

Figure 4.12. Effect of FG-4592 on HIF-2α protein levels in Caco-2 cells. Protein levels of HIF-2α in response to control (0 μM), 10 μM, 50 μM and 100 μM of FG-4592 (for 24 hours) in Caco-2 cells cultured for 21 days (A) and 4 days (B), was determined using Western blot. Western blot representative image of HIF-2α is shown above each graph (n=2 independent experiments). The abundance of HIF-2α is given as the ratio of its band density to β-actin, expressed in arbitrary units (a.u). Data are expressed as mean ± SEM and the difference between groups was analysed using a one-way ANOVA, **P<0.01, ***P<0.001 n=4 independent experiment.

4.3.9. Effect of FG-4592 on DMT1, claudin-2 and VDR protein levels, calcium flux, and transepithelial resistance in day-21 and day-4 Caco-2 cells.

Since HIF-2α is known to regulate the expression of DMT1, the effect of 100μM FG-4592 on DMT1+IRE protein levels was measured. Surprisingly, FG-4592 had no impact on DMT1 protein levels at day 21 (**Figure 4.13A**) and day 4 (**Figure 4.13D**) cultured Caco-2 cells. Additionally, despite the significant upregulation of HIF-2α in response to 100μM FG-4592, claudin-2 (**Figure 4.13B** and **E**) and VDR (**Figure 4.13C** and **F**) protein levels in 21- and 4-day cultured Caco-2 cells were also unaffected. Lastly, 100μM FG-4592 treatment on Caco-2 cells cultured for 21 and 4 days had no effect on paracellular calcium flux (**Figure 4.14A** and **C**) and TEER (**Figure 4.14B** and **D**). Taken together, these findings suggest that the increase in HIF-2α levels induced by 100μM FG-4592 may not be involved in regulating claudin-2-mediated paracellular calcium absorption in iron deficiency.

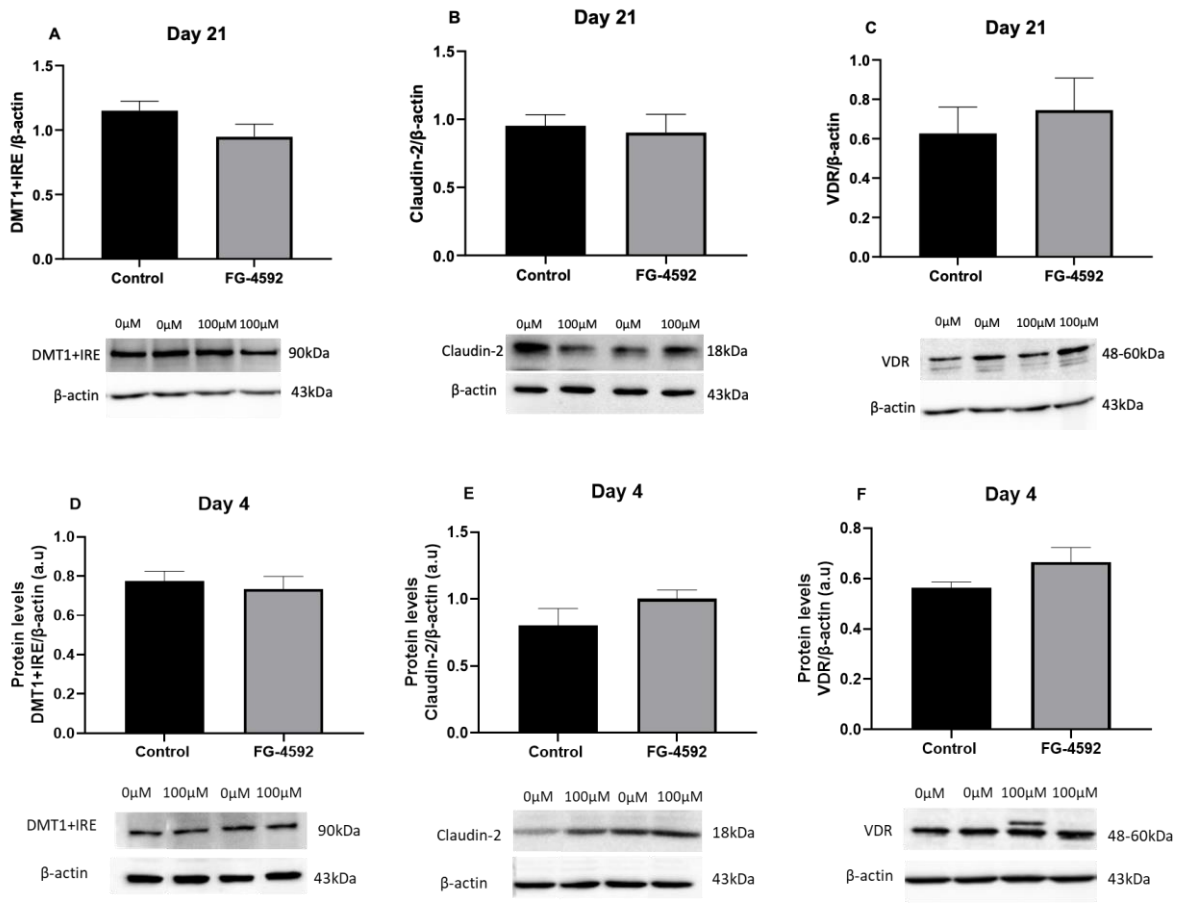

Figure 4.13. Effect of FG-4592 on DMT1+IRE, claudin-2, and VDR protein levels in Caco-2 cells. Protein levels of DMT1+IRE (**A**) claudin-2 (**B**) and VDR (**C**) in Caco-2 cells cultured for 21 days, and the levels of DMT1+IRE (**D**) claudin-2 (**E**) and VDR (**F**) in Caco-2 cells cultured for 4 days, following control (0 μM) or 100 μM FG-4592 treatment for 24 hours, was determined using Western blot. Western blot representative image of each protein of interest is shown below each graph (n=2 independent experiments). The abundance of each protein is given as the ratio of its band density to β-actin, expressed in arbitrary units (a.u). Data are expressed as mean ± SEM and the difference between groups was analysed using unpaired t test, n=3-4 independent experiment

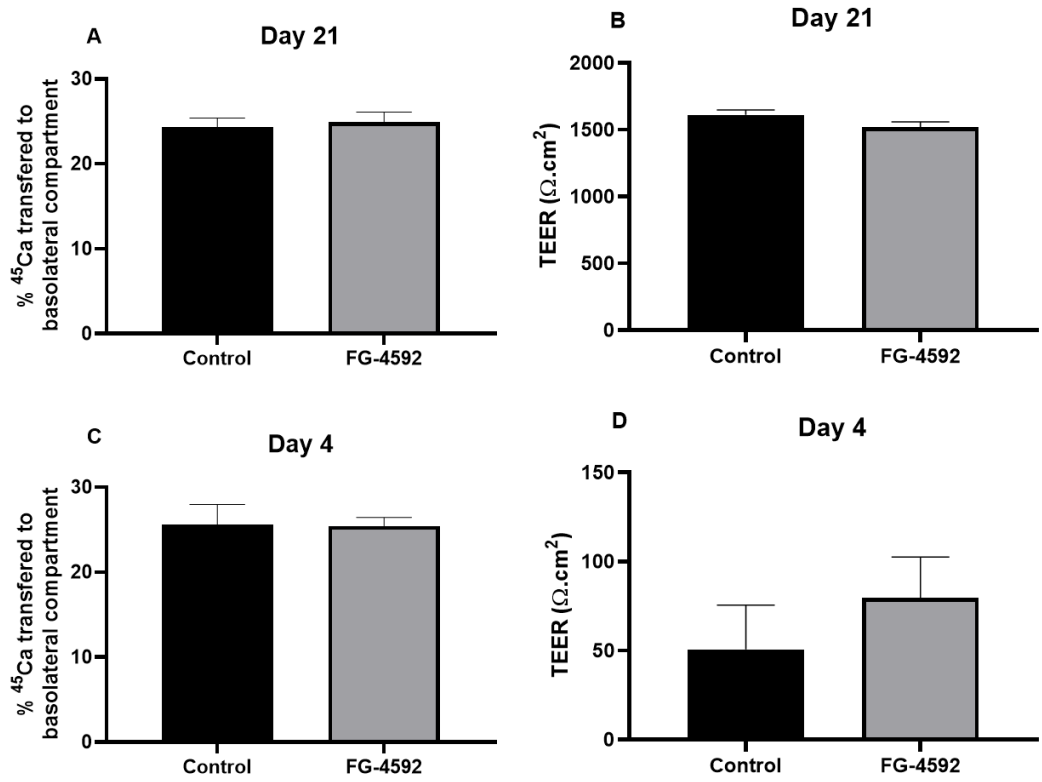

Figure 4.14. Effect of FG-4592 on calcium flux and TEER in Caco-2 cells. Transepithelial flux of 100mM $CaCl_2$ and ^{45}Ca (**A**) and TEER (**B**) in Caco-2 cells cultured for 21 days, and transepithelial flux of 100mM $CaCl_2$ and ^{45}Ca (**C**) and TEER (**D**) in Caco-2 cells cultured for 4 days, following 100µM of FG-4592 treatment for the same duration. Data are expressed as mean ± SEM and the difference between groups was analysed using unpaired t test, n=4 independent experiments.

4.4. Discussion

The findings of Chapter 3 highlight that claudin-2 is the only calcium mediating protein enhanced in the rat duodenum in response to diet-induced iron deficiency and therefore is proposed to be the most probable cause of the increase in duodenal calcium absorption. However, the mechanisms underlying the increase in claudin-2-mediated duodenal calcium transport following iron deficiency were not investigated in the previous chapter. Therefore, the purpose of this chapter was to identify and test potential mechanisms responsible for the increase in claudin-2-mediated calcium flux. To achieve this, correlation analyses were used to test whether changes in claudin-2 mRNA and its regulator, VDR, were associated with the apical iron transporter, DMT1, and the local regulator of intestinal iron absorption, HIF-2α. A positive correlation between DMT1 and claudin-2 was identified suggesting that the increase in claudin-2 mRNA may be associated with an increase in DMT1 mRNA following iron deficiency. Although the positive association between claudin-2 and DMT1 does not imply causation, it is possible that the changes in DMT1 levels may be contributing to the increase in duodenal claudin-2-mediated calcium transport seen following iron deficiency. Claudin-2 is a $1,25(OH)_2D_3$ responsive protein that has been shown to be a direct target of VDR based on the presence of a $1,25(OH)_2D_3$ response element on the promoter region of the claudin-2 gene [281]. The regulatory role of $1,25(OH)_2D_3$-VDR interaction on claudin-2 is further supported by the downregulation of claudin-2 mRNA expression and protein levels in the enterocytes of VDR knockout mice [281]. Consistent with this finding, a positive correlation between claudin-2 and VDR was observed in the current study. Since duodenal VDR mRNA expression is enhanced by iron deficiency in rats [420], it is possible that the upregulation of duodenal claudin-2 in response to iron deficiency is mediated by

the changes in VDR despite unchanged serum $1,25(OH)_2D_3$ levels. Interestingly, VDR mRNA expression positively correlated with DMT1 mRNA, suggesting that the potential impact of VDR on claudin-2 levels following iron deficiency may be linked to changes in DMT1-mediated iron transport.

There is evidence that HIF-2α plays an important cellular role in regulating iron transport [352,360] by increasing the expression of iron transporters, including DMT1, in response to iron deficiency [359]. Therefore, changes in HIF-2α may also be involved in the mechanism underlying the increase in claudin-2-mediated duodenal calcium absorption in response to iron deficiency. Based on this speculation, the correlation between HIF-2α with claudin-2 and VDR was investigated and showed that HIF-2α positively correlated with both claudin-2 and VDR. In keeping with the results of the correlation studies, the potential mechanisms responsible for the increase in calcium absorption following iron deficiency were hypothesised as follows (**Figure 4.15)**:

1. Iron deficiency increases claudin-2-mediated calcium transport via a mechanism involving VDR.
2. The increase in VDR in response to iron deficiency may be linked to the upregulated levels of DMT1 or HIF-2α seen in iron-deficient animals.
3. Increased claudin-2 following iron deficiency may be a consequence of the cellular or localised impact of high levels of DMT1 or HIF-2α on duodenal enterocytes.

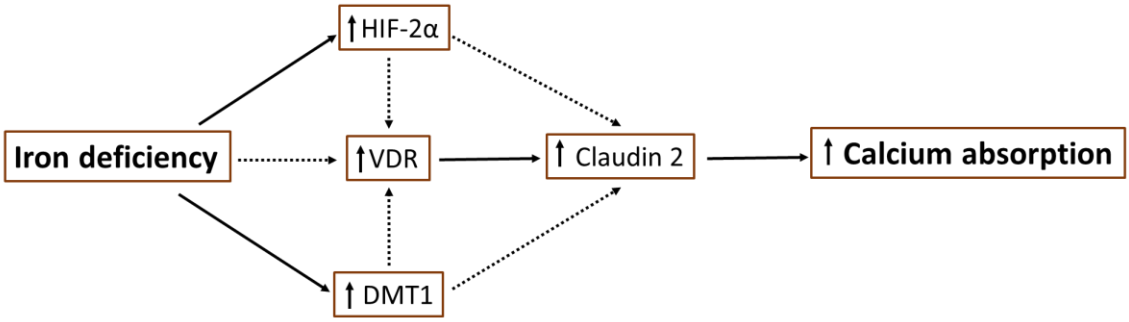

Figure 4.15. A schematic representation of the possible mechanisms underlying the duodenal increase in calcium absorption in response to diet-induced iron deficiency in rats. Dotted arrows represent hypothesised relationships, while solid arrows represent well established relationships.

To investigate these hypotheses, Caco-2 cells were employed. Before investigating the hypotheses, experiments were carried out to validate the Caco-2 cellular models used in the current study. Cells were cultured for 4 or 21 days, and the endogenous expression of the iron and calcium transporters were compared. Consistent with a previous report on DMT1 [435], the expression of the of the proteins involved in iron and calcium transport were higher in fully differentiated day-21 Caco-2 cells compared to pre-differentiated day-4 Caco-2 cells. The increase in the expression of these proteins is consistent with the higher TEER seen in fully differentiated day 21 Caco-2 cells in the current study. Although day 21 cells express higher levels of the proteins of interest, the significantly higher TEER seen in this model (indicating a very tight epithelial layer) may make it unsuitable to investigate paracellular calcium flux. In contrast, the low TEER in Caco-2 cells cultured for 4 days may be associated with a paracellular ion permeability that is more comparable to the small intestine. Importantly, both day 4 and day 21 cultured Caco-2 cells endogenously express the iron and calcium transport proteins of interest. This finding validates the use of day 4 and day 21 cultured Caco-2 cellular models to investigate the

hypothesised mechanisms underlying the changes in paracellular calcium transport following iron deficiency.

Due to the potential benefit of a fully differentiated and polarised monolayer seen in 21-day cultured Caco-2 cells, and the benefit of a leakier 4-day cultured Caco-2 cell monolayer, experiments were carried out in cells cultured at both time points. To induce iron deficiency and to mimic the cellular adaptation of iron transporters in response to iron deficiency, Caco-2 cells were treated with DFO. Consistent with a previous study [424], the mRNA expression of DMT1 and FPN was upregulated in response to 100µM of DFO at both 4 and 21 days in culture. However, DMT1 protein levels at both time-points were unaffected by DFO treatment. Although the reason for this discrepancy is unclear, the iron-deficient status of the cells in the current study was confirmed by the decrease in ferritin levels, therefore, the effect of DFO on claudin-2, -12 and VDR was further investigated.

While DFO treatment significantly decreased claudin-2 mRNA in day 21 Caco-2 cells, protein levels were unaffected and therefore unlikely to impact calcium flux. Interestingly, claudin-12 mRNA expression was enhanced by this treatment in both 4- and 21-day cultured cells. However, claudin-12 protein levels were not investigated due to the lack of commercially available antibodies specific for claudin-12. The upregulation of claudin-12 mRNA suggests an increase in claudin-12-mediated calcium flux. Therefore, to assess the potential impact of enhanced claudin-12 on calcium transport, total transepithelial calcium flux was also measured in response to DFO treatment. Calcium flux was unaffected by this treatment in both day 4 and day 21 cells. Based on this finding, it is speculated that changes in claudin-12 mRNA expression don’t translate to

protein and/or that claudin-12-mediated calcium transport may not contribute to transepithelial calcium flux in the Caco-2 models used in the current study. Importantly, this result suggests that DFO-induced iron deficiency has no significant impact on paracellular calcium flux in Caco-2 cells.

Interestingly, increased VDR protein levels following DFO treatment in day 4 Caco-2 cells had no significant impact on claudin-2 protein or paracellular calcium flux. This result contradicts a previous finding that has shown increased claudin-2 protein levels in VDR overexpressing mice [173]. The discrepancy in these findings is most likely due to the absence of the VDR ligand, $1,25(OH)_2D_3$, in the culture medium used for the *in vitro* experiments in the current study. VDR interacts with $1,25(OH)_2D_3$ to increase claudin-2- and -12-mediated calcium transport [25]. Therefore, the addition of $1,25(OH)_2D_3$ to the medium used for the Caco-2 experiment, may have resulted in increased claudin-2 levels and transepithelial calcium flux in DFO-treated day 4 Caco-2 cells since VDR was upregulated under this condition.

Furthermore, iron deficiency anaemia is characterised by increased secretion of EPO by the kidney, a feature that is known to be one of the physiological adaptations responsible for increasing DMT1-mediated iron absorption in the duodenum [436,437]. Therefore, EPO was used to stimulate this cell line to increase DMT1 protein. Surprisingly, increasing concentrations of EPO (1, 2.5 and 5u) had no significant impact on DMT1 protein levels in 21-day cultured cells, however, 1u EPO upregulated DMT1 protein in 4-day cultured Caco-2 cells. Consistent with this finding, Srai *et. al.* [368] also demonstrated an upregulation of DMT1 protein, along with other iron transporters including FPN, in response to 1u EPO in Caco-2 cells cultured for 14 days. In addition to the impact of EPO on cellular

iron transporters, previous findings have shown a relationship between human recombinant EPO (rHuEpo) and intracellular calcium levels in human bone marrow and neuroblastoma cells [438,439]. Furthermore, a retrospective study demonstrated an increase in serum calcium levels in haemodialysis patients treated with rHuEpo, suggesting that EPO may also have an impact on extracellular calcium levels [440]. Based on these reports, the effect of EPO treatment on transepithelial calcium flux, claudin-2 and VDR protein was investigated. The findings of the current study that 1u EPO had no impact on claudin-2, VDR or paracellular calcium flux, suggest that this hormone may not be involved in the increase in transepithelial calcium transport in response to iron deficiency. Importantly, it is worth noting that 1u EPO induced DMT1 upregulation in day 4 Caco-2 cells and under this condition, VDR, claudin-2 or paracellular calcium flux were unchanged. This finding suggests that increased DMT1 protein may not be responsible for the increase in duodenal calcium absorption following iron deficiency in the rat.

Another iron regulatory protein affected during iron deficiency is HIF-2α, a transcription factor that is upregulated during iron deficiency anaemia [432]. This transcription factor is also known to regulate the expression of several iron transporters such as DMT1, duodenal cytochrome b and FPN. Furthermore, the HIF protein family has also been reported to be involved in the regulation of epithelial tight junction permeability [441] and therefore, may be involved in iron deficiency-induced calcium absorption. Using a PHD inhibitor, FG-4592, HIF-2-α protein was enhanced, and the impact of this treatment on DMT1, claudin-2 and VDR protein levels and transepithelial calcium flux was investigated in Caco-2 cells. Increased HIF-2α protein following FG-4592 treatment had no significant effect on DMT1, claudin-2, VDR or transepithelial calcium flux in Caco-2 cells,

suggesting that the upregulation of HIF-2α may not be directly involved in the increase in duodenal calcium absorption during iron deficiency in rats.

Finally, in Caco-2 cells, claudin-4 has been shown to be the most highly expressed tight-junction-forming claudin [434] and this claudin has also been shown to act as a sodium barrier [442,443], a function that may inhibit solvent drag-mediated paracellular calcium transport. Based on these properties of claudin-4, the impact of DFO on this claudin was also investigated. Following DFO treatment, claudin-4 protein levels were upregulated only in day 4 cultured Caco-2 cells. A finding that may potentially inhibit solvent drag-induced calcium flux in this model. Since paracellular calcium flux in day-4 Caco-2 cells was unchanged in response to DFO treatment, the potential impact of claudin-4 upregulation on solvent drag-induced calcium flux is uncertain. Additional studies will be required to confirm the direct impact of claudin-4 on paracellular calcium flux in Caco-2 cells.

4.5. Conclusion

DFO-induced iron deficiency has no significant impact on transepithelial calcium flux and claudin-2 levels in Caco-2 cells. However, the upregulation of VDR in iron-deficient Caco-2 cells, which was similar to the observation in the duodenum of iron-deficient rats [420], suggests that an increase in VDR signalling may be responsible for increased claudin-2-mediated calcium absorption following iron deficiency. The EPO-induced increase in DMT1, and FG-4592-induced increase in HIF-2α, had no impact on paracellular calcium flux, claudin-2 or VDR levels in Caco-2 cells. This suggests that increased DMT1 or high levels of HIF-2α following iron deficiency is unlikely to be responsible for the increase in duodenal calcium absorption observed in rats.

Chapter 5 - General Discussion

5.1. Aims of experiments

Previous studies investigating the contribution of the duodenum to overall intestinal calcium absorption have shown that, while the capacity for calcium absorption is highest in this segment [216,269], it has also been estimated to mediate only a small proportion (8-15%) of overall calcium absorption [204]. With previous findings suggesting that the bioavailability of calcium is highest in the duodenum, together with the evidence that this segment has the highest capacity of calcium absorption, the basis for estimating the contribution of each segment to overall calcium absorption is worth revisiting. A proper understanding of the contribution of each segment, particularly the duodenum, will be essential to determine whether this segment will be a reliable target for controlling overall intestinal calcium absorption. What is currently known is that the duodenum predominantly mediates transcellular calcium transport, and that paracellular calcium transport occurs in all segments of the small intestine [216,217]. However, there is currently limited information as to why the duodenum exhibits the highest capacity for calcium absorption, even at a high luminal calcium concentration where the paracellular calcium transport pathway is dominant. Therefore, the first aim of the current study was to re-examine the regional profile of calcium transport using the *in situ* intestinal loop technique and an uptake buffer with a concentration that favours the paracellular pathway i.e. 100mM. Importantly, the mechanisms underlying the differences in the regional calcium transport profile was investigated by comparing the expression of the proteins involved in calcium absorption across all segments of the small intestine. The regional expression of these calcium transport proteins was also investigated using human intestinal biopsies to test whether the findings in rats may potentially translate to humans.

In addition, increasing evidence suggests an inverse relationship between the mechanism of iron and calcium homeostasis (discussed in **Chapter 1, section 1.7**), and iron deficiency has been speculated to be a risk factor for osteoporosis [384]. Therefore, the current study also aimed to investigate the impact of diet-induced iron deficiency on calcium homeostasis and the potential mechanisms responsible for the previously reported loss of bone minerals in iron-deficient rodents and humans [385–388,444–448]. Since the duodenum is the segment where iron absorption predominantly occurs [329–333], the impact of diet-induced iron deficiency on duodenal calcium absorption and the potential underlying mechanism was investigated.

5.2. Potential contribution of the duodenum to overall calcium absorption and the mechanisms underlying the segmental calcium absorption profile

Despite the lower capacity for absorption, the rat ileum is thought to be the most important segment mediating calcium absorption due to the relatively longer intestinal transit time of chyme (~141mins) compared to the duodenum (~3mins) [213]. However, since gastric emptying in rats occurs over a 3-hour period [213], the total duodenal contact time with chyme during digestion would be considerably longer (at least 3 hours). Similarly in humans, while the duodenal transit time is relatively short compared to other segments (~15mins) [449], gastric emptying is estimated to take approximately 5 hours [450], suggesting that duodenal contact time with chyme in humans may be at least 5 hours. Therefore, the total duodenal contact time with chyme in both rodents and humans suggests that the duodenum may have a greater contribution to overall calcium absorption in the small intestine than previously reported [6].

Moreover, the experiments discussed in Chapter 2 suggest that the duodenum has the highest capacity for intestinal calcium absorption in the rat small intestine. Since the *in situ* intestinal loop technique used to investigate the regional profile of calcium absorption was conducted using 100mM of calcium, it is unlikely that the transcellular calcium pathway significantly contributes to the higher capacity of duodenal calcium absorption. Therefore, paracellular calcium transport, known to predominantly mediate calcium absorption under normal or high intestinal luminal calcium concentration (> 5mM Ca^{2+}) [451,452], is likely to be the major determinant of the higher capacity of calcium absorption in the duodenum. Based on the finding that the expression profile of claudin-15 mirrors the segmental differences in intestinal calcium absorption, it is speculated that the high expression of duodenal claudin-15 is responsible for the high capacity of calcium absorption in this segment. Unlike the widely accepted calcium mediating claudins (claudin-2 and -12), overexpression studies *in vitro* have shown that the claudin-15 pore is not selective to calcium [25]. However, this claudin is speculated to be involved in solvent drag-induced paracellular calcium flux due to its ability to mediate paracellular sodium flux and transcellular sodium-coupled transport processes involving SGLT1 and NHE3 (discussed in **Chapter 1, section 1.2.7**) [199].

Solvent drag-induced paracellular calcium flux may occur via 2 potential mechanisms (**Figure 5.1**). First, in the presence of high a luminal sodium concentration, the paracellular movement of sodium may increase the intercellular osmolarity resulting in the movement of water, and subsequently, paracellular calcium absorption via claudin-2. In addition to its role in the increasing sodium permeability [162], claudin-15 is also involved in maintaining luminal sodium levels necessary to drive sodium-coupled nutrient transport

across the enterocyte [199]. The second mechanism utilises this function of claudin-15 to enhance the classical solvent drag mechanism as described in **Chapter 1, section 1.2.7**. This involves the extrusion of intracellular sodium into the intercellular space via Na^+/K^+ATPase, that then drives the paracellular movement of water, and subsequently calcium, via claudin-2. Interestingly, claudin-15 has also been shown to mediate paracellular water transport independently of sodium [162], a function that may also contribute to passive calcium diffusion. Increased water transport via claudin-15 may increase the luminal concentration of calcium and subsequently drive passive paracellular calcium absorption via claudin-2 or -12. Taken together, these mechanisms (**Figure 5.1**) enhance the absorptive capacity of calcium in the rat small intestine, particularly the duodenum, where claudin-15 expression is most highly expressed.

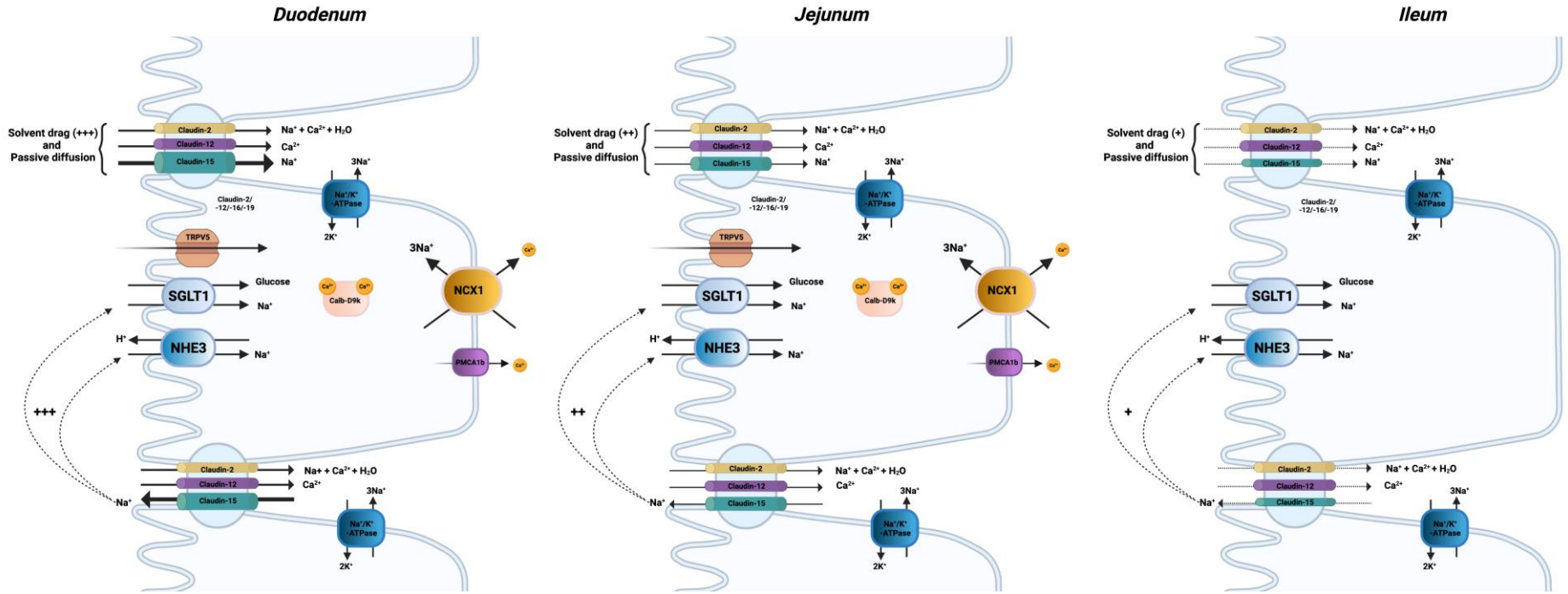

Figure 5.1. Possible mechanisms by which claudin-15 contributes to the differences in the capacity for calcium absorption across the duodenum, jejunum, and ileum. In addition to the passive diffusion of calcium via claudin-2 and -12, claudin-15 can also enhance paracellular calcium flux across claudin-2 via solvent drag. Solvent drag-induced paracellular calcium flux can either be driven by the passive diffusion of sodium via claudin-15 or via the back leak of sodium into the lumen, which drives sodium absorption via NHE3 and SGLT1 leading to increased sodium transport into the intercellular space via the Na+/K^+ATPase. These mechanisms collectively create a hyperosmolar environment that drives water along with calcium, via claudin-2 into the intercellular space. Therefore, higher levels of duodenal claudin-15 in comparison to the other segments of the small intestine are speculated to result in a higher capacity for solvent drag-induced paracellular calcium transport in the duodenum.

Furthermore, like the rat small intestine, the results of the current study demonstrate that the human duodenum also expresses higher levels of claudin-15, and proteins mediating the transcellular calcium pathway compared to the ileum. This suggests that the significantly higher calcium absorptive capacity seen in the duodenum compared to the other small intestinal segments in rats may also translate to humans. This, together with the speculation that the duodenal contact time of chyme may be longer than previously thought, highlight the importance of the duodenum to overall calcium absorption across the human small intestine. In support of this speculation, animal models and patients with dysfunctional iron metabolism, such as β-thalassaemia (with iron overload), have impaired intestinal calcium absorption and hypocalcaemia, and are at increased risk of developing bone disease [375,381,382,453,454]. Since iron absorption mainly occurs in the duodenum [329–333], it is possible that impaired calcium metabolism seen in these animals and patients may be linked to reduced calcium absorption in this segment. Indeed, in a mouse model of β-thalassaemia (β-globin knockout mice), the manifestations of dysfunctional mineral metabolism (e.g. bone loss and osteoporosis) a thought to be partly attributed to the decrease in duodenal calcium absorption [372]. The administration of hepcidin, an inhibitor of intestinal iron absorption, increases duodenal calcium absorption, and this has been speculated to effectively restore serum calcium levels in β-thalassaemia [371,372,375]. Taken together, these findings potentially highlight the importance of the duodenum to overall intestinal calcium absorption, and the interaction between duodenal calcium and iron absorption.

5.3. Effect of iron deficiency on calcium homeostasis

Because of the link between the regulators of iron and calcium metabolism (discussed in **Chapter 1, section 1.7**), and the evidence that iron deficiency is a risk factor for osteoporosis (reviewed in detail in [384]), the impact of diet-induced iron deficiency on the mechanisms of calcium homeostasis was investigated. Previous studies have reported conflicting findings demonstrating changes in intestinal calcium absorption and PTH during iron deficiency [385,387,409]. While Campos *et al.* [409] demonstrated an increase in intestinal calcium absorption and PTH levels, a finding consistent with that of Diaz-Castro *et al.* [387], Katsumata and colleagues [385] showed a reduction in calcium absorption and PTH levels during iron deficiency. Because of this discrepancy and the lack of information on the impact of iron deficiency on calcium absorption across each segment of the small intestine, the current study focused on investigating transepithelial calcium absorption in the duodenum, jejunum and ileum of rats following a 2-week administration of an iron-deficient or a control diet. In addition, the changes in the calcium regulatory hormones, renal calcium handling and markers of bone turnover were also investigated in these animals. Diet-induced iron deficiency enhanced duodenal calcium absorption but had no impact on jejunal and ileal calcium absorption. This finding suggests that the previously reported increase in overall calcium absorption following iron deficiency [409] may be due to increased duodenal calcium absorption. Interestingly, iron deficiency increased claudin-2 protein in the duodenum and kidney, but had no impact on serum calcium levels, urinary calcium excretion, the markers of bone turnover (CTX-1 and osteocalcin) or PTH and $1,25(OH)_2D_3$ levels. The lack of change in serum calcium levels following iron deficiency in the current study was surprising based on the result

that both duodenal and renal claudin-2 protein were upregulated in the iron-deficient animals. It is possible that the normal amount of dietary calcium (~0.52% by weight of diet) in the iron-deficient diet may not be sufficient to demonstrate the physiological impact of the observed changes in duodenal and renal claudin-2 on serum calcium levels. Therefore, further studies investigating the impact of iron deficiency on calcium homeostasis in rats should be carried out using an iron-deficient diet containing a higher calcium concentration (~1.5%). These studies may demonstrate the potential physiological impact of increased renal and intestinal claudin-2 on calcium homeostasis following iron deficiency. The findings from these studies may confirm the role of iron deficiency as a regulatory of calcium homeostasis.

In keeping with the finding of the current study that iron deficiency has no impact on serum calcium levels, Katsumata *et al.* [385] and Campos *et al.* [409] both showed the same unchanged serum calcium levels in iron deficient rats, even though their findings on intestinal calcium absorption were conflicting. Additionally, bone mineral density or calcium content, which was not measured in the current study, appears to be consistently lower in the iron-deficient animals in previous studies [385,387,409]. Since iron deficiency increased intestinal calcium absorption in both the current study and that of Campos *et al.* [409], clues may be taken from the latter to understand how iron deficiency may be causing osteoporosis, despite the increase in calcium absorption and unchanged serum calcium levels. Campos *et al.* [409] investigated the levels of calcium and phosphorus in the spleen, liver, sternum and femur during a 40-day period, and showed that while calcium and phosphorus levels in the femur decreased, the levels of these ions were considerably higher in the liver and spleen of iron-deficient animals. Interestingly, there was ~50% more calcium in the liver and 25% less calcium in the femur of

iron-deficient animals compared to control animals at day 20 of the dietary regimen. These findings, together with increased phosphorus deposition in the spleen and liver during iron deficiency [409], suggest that abnormal calcium and phosphorus storage in the liver and spleen may potentially make these minerals unavailable for bone formation. This may be responsible for the low levels of bone minerals in iron deficiency [409], thus, potentially leading to osteopenia and osteoporosis. How iron deficiency impacts calcium and phosphate redistribution in the liver and spleen is unclear, and whether this is linked to changes in calcium and phosphate transport proteins in these organs remains to be determined.

Nevertheless, while the upregulation of duodenal claudin-2 may be responsible for the increase in duodenal calcium absorption following diet-induced iron deficiency, the physiological impact of increased renal claudin-2 levels is unclear since urinary calcium excretion and serum calcium levels were unchanged. Even though this finding suggests that the iron deficiency-induced increase in claudin-2 protein has no impact on calcium homeostasis, it does provide the first evidence demonstrating that iron can regulate an important paracellular calcium transport protein in the intestine and renal proximal tubules. This finding potentially has significant clinical implications for patients with intestinal calcium malabsorption (discussed in **Chapter 5, section 5.4**) and disorders associated with abnormal urinary calcium loss. For example, recent evidence suggests that the loss of functional claudin-2 in mice and humans is associated with kidney stone formation [159]. In the current study, even though total urinary calcium excretion (indicated by calcium/creatinine ratio) was unchanged in response to iron deficiency, urinary calcium concentration was shown to be significantly lower in the iron-deficient animals (**Figure 3.10C**). Interestingly, therapies that increase claudin-2-mediated proximal tubular calcium reabsorption have been speculated

to be effective in reducing the incidence of kidney stones by decreasing calcium delivery to the renal papilla [455]. Additional studies are required to investigate the mechanisms underlying the impact of iron deficiency on the levels of renal claudin-2 protein as this may potentially be important for generating new therapies for the prevention of kidney stones in recurrent or high-risk stone formers.

5.4. Understanding the mechanisms underlying duodenal calcium absorption in response to iron deficiency

The current study is the first to demonstrate that diet-induced iron deficiency increases calcium absorption in the duodenum. Of all the transcellular and paracellular calcium transport proteins investigated, only claudin-2 was shown to be significantly upregulated. While the major hormones involved in regulating intestinal calcium absorption and homeostasis, $1,25(OH)_2D_3$ and PTH, were unchanged, duodenal VDR was upregulated. Based on these findings, it is speculated that diet-induced iron deficiency increases duodenal calcium absorption via VDR-induced claudin-2 upregulation. How iron deficiency upregulates VDR, and claudin-2 is unclear, but the findings of this thesis suggest that diet-induced iron deficiency locally impacts paracellular calcium transport in duodenum but not in the jejunum or ileum. Therefore, it is hypothesised that the mechanisms involved in iron transport may be impacting calcium transport via the paracellular pathway. To investigate this hypothesis, Caco-2 cells were treated with DFO, EPO and a HIF-2 stabiliser, FG-4592, and paracellular calcium flux was investigated. Even though these treatments had no impact on paracellular calcium flux and the protein levels of claudin-2, DFO significantly upregulated VDR protein levels. VDR is known to interact with circulating $1,25(OH)_2D_3$ to upregulate claudin-2 and thus, paracellular calcium transport, an

effect that is demonstrated *in vivo* in the duodenum of iron-deficient rats in the current study. In the *in vitro* experiment using Caco-2 cells, the culture medium contained essential nutrients and minerals, but lacked $1,25(OH)_2D_3$, which is expected to be in the systemic circulation that bathe enterocytes *in vivo*. Therefore, it is possible that the lack of $1,25(OH)_2D_3$ in the Caco-2 culture medium may be responsible for the lack of change in claudin-2 levels and paracellular flux. VDR upregulation following DFO treatment in Caco-2 cells may likely increase claudin-2 expression and paracellular calcium flux in the presence of $1,25(OH)_2D_3$. To confirm this, further experiments are required to investigate the impact of DFO treatment on claudin-2 levels in the presence of different concentrations of $1,25(OH)_2D_3$.

DFO is an iron chelator that has been shown to reduce intracellular iron levels. Consistent with this finding, significantly lower levels of ferritin were detected in Caco-2 cells following DFO treatment. It is possible that changes in intracellular iron levels may be associated with VDR upregulation in response to iron deficiency. In support of this hypothesis, there is evidence that therapies targeting iron homeostasis or iron deprivation are associated with increased VDR signalling, and that $1,25(OH)_2D_3$ and iron chelating agents act synergistically to amplify VDR targeted genes [456]. In keeping with these reports, low dietary iron content would result in low intracellular iron, and this may be responsible for the increase in duodenal VDR, and claudin-2 seen in the iron-deficient rats of the current study. To understand how intracellular iron impacts overall intestinal calcium absorption, clues can be taken from studies investigating changes in calcium absorption in animal models and humans with conditions associated with iron hyperabsorption or iron overload e.g. β-thalassemia [371,372,375,381]. Mice and humans with β-thalassemia have been shown to exhibit dysfunctional calcium

metabolism and bone abnormalities [375–380]. The iron overload in β-thalassaemic mice has been suggested to be responsible for calcium malabsorption [375], and the administration of an acute treatment of 1,25$(OH)_2D_3$ (3-days) did not effectively restore calcium absorption in these animals [371]. However, a 7-day treatment of 1,25$(OH)_2D_3$ restored intestinal calcium absorption in these mice [371]. Interestingly, unlike 1,25$(OH)_2D_3$, acute hepcidin treatment completely rescued intestinal calcium absorption [371], thus, suggesting that iron overload in β-thalassaemic mice results in the inhibition of 1,25$(OH)_2D_3$-VDR signalling, and the correction of iron overload by hepcidin upregulates this signalling pathway. While these studies focused on the transcellular calcium transport pathway, the paracellular calcium transport pathway was also significantly inhibited in conditions associated with iron overload [371]. However, the impact of hepcidin treatment on paracellular calcium flux in β-thalassaemic mice was not investigated. Importantly, the findings regarding the impact of iron overload and hepcidin on the transcellular calcium transport pathway, together with the increase in paracellular calcium flux in iron-deficient animals in the current study, suggest that intracellular iron may regulate overall intestinal calcium transport via both pathways. Although the results of the current study suggest that the increase in paracellular calcium absorption following iron deficiency may be due to VDR-induced claudin-2 upregulation, additional experiments are required to examine the impact of intracellular iron on paracellular calcium flux. Future experiments in DFO-treated Caco-2 cells in the presence of 1,25$(OH)_2D_3$ could be used to delineate the impact of low iron levels on the 1,25$(OH)_2D_3$-VDR signalling pathway.

The findings of the current study highlight a potentially novel mechanism linking iron deficiency, VDR, claudin-2 and transepithelial calcium absorption. It is

hypothesised that low intracellular iron upregulates VDR (directly or indirectly via the activation of unknown intracellular mechanisms) to increase claudin-2 and transepithelial calcium absorption via the paracellular pathway (**Figure 5.2**). Targeting intracellular iron levels by hepcidin or a DMT1 inhibitor has recently been speculated to be a potential therapy for correcting intestinal calcium malabsorption, osteopenia and osteoporosis in patients with β-thalassaemia [375]. While this approach is beneficial for β-thalassaemic patients with iron overload, inhibiting iron absorption to correct intestinal calcium absorption might not be practical in other clinical conditions (e.g., iron-deficient patients with hypocalcaemic rickets). Therefore, understanding the cellular mechanisms by which intracellular iron impacts VDR, claudin-2 or transepithelial calcium transport may be essential for the treatment of dysfunctional calcium metabolism where intestinal iron absorption needs to be preserved.

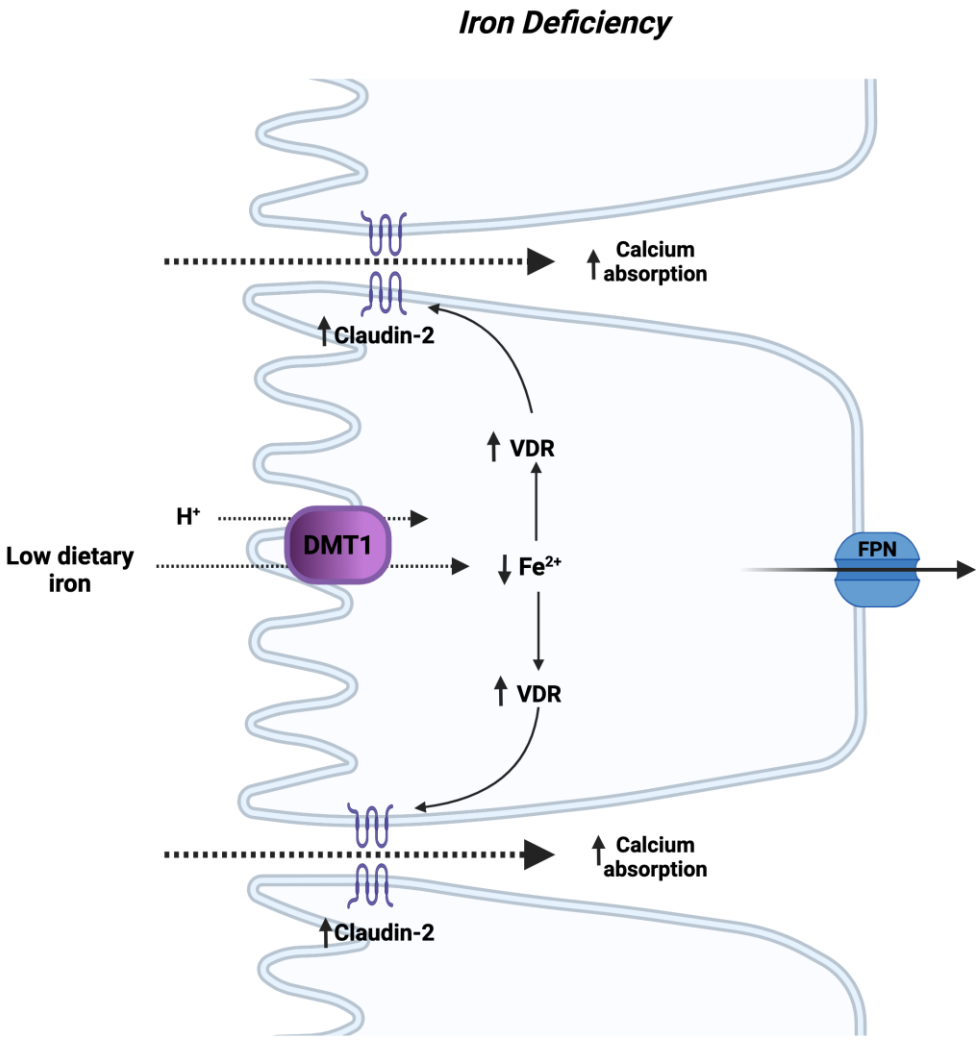

Figure 5.2. Hypothetical model describing the mechanism underlying the role of intracellular iron in regulating duodenal calcium absorption. During iron deficiency, low dietary iron decreases intracellular iron levels, which drives VDR upregulation. Increased VDR levels enhance the 1,25$(OH)_2D_3$-VDR signalling pathway leading to the upregulation of claudin-2 and paracellular calcium transport.

5.5. Conclusion

The findings of the current study suggest that the high capacity for calcium absorption under high luminal calcium conditions in the duodenum of rodents, may be due to claudin-15-mediated calcium absorption via solvent drag. This finding implicates solvent drag as a key mechanism for intestinal calcium absorption in rodents. As there is a similar segmental expression profile of rodent

and human claudin-15, solvent drag may also be an important mechanism for intestinal calcium absorption in humans, at least in the duodenum. The finding that diet-induced iron deficiency increases duodenal calcium absorption, and duodenal and renal claudin-2 levels, identifies a potentially important role of iron in regulating claudin-2-mediated calcium transport. While this regulatory role of iron appears to involve VDR in the duodenum, the mechanism underlying the changes in renal claudin-2 levels following iron deficiency is yet to be determined. This study is the first to report changes in duodenal and renal claudin-2 protein in iron-deficient conditions, and a complete understanding of the underlying cellular mechanism may be clinically beneficial for conditions associated with dysfunctional calcium metabolism.

5.6. Future Direction

5.6.1. To confirm the role of claudin-15 in mediating solvent drag-induced paracellular calcium absorption via claudin-2

One of the key findings of the current study is that claudin-15 may be responsible for the significant segmental differences in paracellular calcium absorption between the duodenum and other small intestinal segments in rats. The speculation that claudin-15 may be mediating solvent drag-induced calcium absorption via claudin-2 can be further investigated using duodenal segments collected from mice with knockout of claudin-2 or claudin-15 or double knockout of claudin-2 and -15. Paracellular calcium flux can be examined using the duodenal segments from these animals in Ussing chamber as previously described [164]. For this experiment, calcium uptake solution containing 1.25 – 100 mM of calcium would be used. Uptake solution with the same composition of calcium, glucose and other electrolytes would be put on both sides of the Ussing

chamber to eliminate a concentration gradient, and Trifluoperazine would be added to the serosa side to block transcellular calcium transport. Radioactive ^{45}Ca would be added to the mucosa side of the Ussing chamber and paracellular calcium flux investigated by collecting a given volume of samples from the serosa side at regular time intervals to measure the amount of calcium transferred from the mucosa to the serosa side via solvent drag. The result obtained from claudin-2 or claudin-15 knockout mice or mice with double knockout of these genes would be compared with wild-type mice to delineate the contribution of these claudins to solvent-drag induced calcium absorption in the duodenum.

5.6.2. To test the contribution of the duodenum to overall calcium absorption using duodenal bypass experiments

Although the duodenum was shown to have the highest capacity for overall calcium absorption in the current study, the contribution of this segment to total intestinal calcium absorption has remained a debate over the years. To extend the findings presented in this thesis, duodenal bypass surgery could be carried out in rats, and calcium homeostasis in these animals under different dietary calcium content (low, normal, and high calcium diet) may then be investigated to further understand the importance of the duodenum to overall intestinal calcium absorption. Similar studies could be conducted following jejunal or ileal resection in rodents. The findings from these studies will likely identify the physiological importance of each small intestinal segment to total intestinal calcium absorption, thus, indicating the most important intestinal segment that can be targeted to regulate overall calcium absorption.

5.6.3. Studies in iron-deficient animals using different dietary levels of calcium to identify the exact role of iron deficiency on calcium homeostasis.

In the current study, diet-induced iron deficiency had no significant impact of serum calcium levels, even though there was a significant increase in intestinal calcium absorption in rats. The increase in intestinal calcium absorption seen in iron-deficient animals was shown using an uptake solution containing 100 mM of calcium that was instilled into the intestine for 30 minutes, while serum calcium levels were measured in animals that were placed on a normal calcium diet for 2 weeks in the current study. Additional studies involving the administration of a high calcium solution to iron-deficient or control animals over a longer duration (> 30 minutes) would be important to understand the impact of iron deficiency on the long-term regulation of calcium homeostasis following a high calcium challenge. To investigate changes in calcium homeostasis following iron deficiency under a long-term high calcium challenge, animals could be gavaged with a solution containing 100 mM calcium (as used in the current study) for 3 – 7 days, and serum and urinary calcium levels can then be analysed daily in iron-deficient versus control animals. This study could potentially identify the precise impact of iron deficiency on calcium homeostasis following a calcium challenge and may also demonstrate whether the role of the kidney in maintaining calcium homeostasis is impacted in the iron-deficient animals since renal claudin-2 levels were shown to be significantly upregulated in these animals.

5.6.4. Effect of iron deficiency on claudin-2-mediated calcium transport in renal proximal tubular epithelial cells (RPTECs).

One of the clinically important findings of the current study was the finding that iron deficiency upregulates renal claudin-2 protein levels leading to a consequent

reduction in the concentration of calcium in urine. This finding is speculated to be clinically beneficial for patients with kidney stones as targeting proximal tubular calcium transport via claudin-2 may significantly alter urinary calcium concentration. To confirm whether proximal tubular calcium transport is impacted following iron deficiency, transepithelial calcium flux using ^{45}Ca may be conducted in RPTECs cultured under iron-deficient conditions. Immunohistochemical techniques may then be used to investigate the expression and cellular localisation of claudin-2 following iron deficiency in this cell line. Additional transepithelial calcium flux experiment in iron-deficient RPTECs with or without claudin-2 knockdown may be used to confirm whether iron deficiency directly impacts paracellular calcium flux in RPTECs via claudin 2. Importantly, investigating the cellular mechanisms by which iron deficiency impacts calcium flux in RPTECs is essential as this could be explored for the generation of new therapies to prevent or manage kidney stones in recurrent or high-risk stone formers.

5.6.5. The role of intracellular iron in controlling epithelial calcium transport

The findings from the current study suggest that low intracellular iron levels may be responsible for the upregulation of claudin-2 and consequently increasing calcium transport in the duodenum. This mechanism may potentially be responsible for the increase in renal claudin-2 in the iron deficient animals that are characterised with low systemic iron levels. To investigate this hypothesis linking intracellular iron to claudin-2-mediated calcium transport *in vivo*, intracellular iron levels may be reduced by injecting rats with hepcidin or a novel DMT1 inhibitor [457] to reduce iron levels in duodenal enterocytes and renal proximal tubular cells. The investigation of apparent calcium absorption in the

intestine, urinary calcium excretion and serum calcium levels may then be investigated in these animals following the administration of solutions containing different concentration of calcium. The findings of this work could confirm whether intracellular iron is a good target for regulating intestinal calcium absorption or renal calcium transport *in vivo*. To investigate the potential translatability of intracellular iron as a target for controlling calcium transport (especially the physiologically important paracellular pathway) in intestinal enterocyte, studies in Caco-2 cells treated with DFO, hepcidin or a DMT1 inhibitor in the presence of $1,25(OH)_2D_3$ could be conducted. Similar studies using DFO or a DMT1 inhibitor could be conducted in human RPTECs to test whether the findings in rats translate to humans.

References

1. Peacock, M. Calcium metabolism in health and disease. *Clin. J. Am. Soc. Nephrol.* **5**, 23–30 (2010).
2. Pu, F., Chen, N. & Xue, S. Calcium intake, calcium homeostasis and health. *Food Sci. Hum. Wellness* **5**, 8–16 (2016).
3. Veldurthy, V. *et al.* Vitamin D, calcium homeostasis and aging. *Bone Research* vol. 4 1–7 (2016).
4. Guerini, D. The Ca2+ pumps and the Na+/Ca2+ exchangers. *BioMetals* **11**, 319–330 (1998).
5. Costiniti, V. *et al.* Calcium Transport in Specialized Dental Epithelia and Its Modulation by Fluoride. *Front. Endocrinol. (Lausanne).* **12**, 977 (2021).
6. Bronner, F. & Pansu, D. Nutritional aspects of calcium absorption. *J. Nutr.* **129**, 9–12 (1999).
7. Granjon, D., Bonny, O. & Edwards, A. A model of calcium homeostasis in the rat. *Am. J. Physiol. Renal Physiol.* **311**, F1047–F1062 (2016).
8. Underland, L., Markowitz, M. & Gensure, R. Calcium and phosphate hormones: Vitamin D, parathyroid hormone, and fibroblast growth factor 23. *Pediatr. Rev.* **41**, 3–11 (2020).
9. Hoenderop, J. G. J., Nilius, B. & Bindels, R. J. M. Calcium absorption across epithelia. *Physiol. Rev.* **85**, 373–422 (2005).
10. Bronner, F. Mechanisms of intestinal calcium absorption. *J. Cell. Biochem.* **88**, 387–393 (2003).
11. Khanal, R. C. & Nemere, I. Regulation of Intestinal Calcium Transport. *Annu. Rev. Nutr.* **28**, 179–196 (2008).
12. Diaz de Barboza, G., Guizzardi, S. & Tolosa de Talamoni, N. Molecular aspects of intestinal calcium absorption. *World J. Gastroenterol.* **21**,

7142–7154 (2015).

13. Bronner, F. Calcium Absorption — A Paradigm for Mineral Absorption. *J. Nutr.* **128**, 917–920 (1998).

14. Friedman, P. A. Mechanisms of renal calcium transport. *Exp. Nephrol.* **8**, 343–350 (2000).

15. Hoenderop, J. G. J., Nilius, B. & Bindels, R. J. M. Molecular Mechanism of Active Ca^{2+} Reabsorption in the Distal Nephron. *Annu. Rev. Physiol.* **64**, 529–549 (2002).

16. Ghijsen, W. E. J. M., de Jong, M. D. & van Os, C. H. Kinetic properties of Na^{+}/Ca^{2+} exchange in basolateral plasma membranes of rat small intestine. *Biochim. Biophys. Acta. Biomembr* **730**, 85–94 (1983).

17. Bindels, R. J. M., Ramakers, P. L. M., Dempster, J. A., Hartog, A. & van Os, C. H. Role of Na^{+}/Ca^{2+} exchange in transcellular Ca^{2+} transport across primary cultures of rabbit kidney collecting system. *Pflügers Arch. Eur. J. Physiol.* **420**, 566–572 (1992).

18. Van Baal, J. *et al.* Localization and regulation by vitamin D of calcium transport proteins in rabbit cortical collecting system. *Am. J. Physiol. Physiol.* **271**, F985–F993 (1996).

19. Kellett, G. L. Alternative perspective on intestinal calcium absorption: Proposed complementary actions of Cav1.3 and TRPV6. *Nutr. Rev.* **69**, 347–370 (2011).

20. Nemere, I. Vesicular calcium transport in chick intestine. *J. Nutr.* **122**, 657–661 (1992).

21. Larsson, D. & Nemere, I. Vectorial transcellular calcium transport in intestine: Integration of current models. *J. Biomed. Biotechnol.* **2002**, 117–119 (2002).

22. Charoenphandhu, N. & Krishnamra, N. Prolactin is an important regulator of intestinal calcium transport. *Can. J. Physiol. Pharmacol.* **85**, 569–581 (2007).

23. Rievaj, J., Pan, W., Cordat, E. & Alexander, R. T. The Na^+/H^+ exchanger isoform 3 is required for active paracellular and transcellular Ca^{2+} transport across murine cecum. *Am. J. Physiol. Gastrointest. Liver Physiol.* **305**, G303—G313 (2013).

24. Beggs, M. R. & Alexander, R. T. Intestinal absorption and renal reabsorption of calcium throughout postnatal development. *Exp. Biol. Med.* **242**, 840–849 (2017).

25. Fujita, H. *et al.* Tight junction proteins claudin-2 and -12 are critical for vitamin D-dependent Ca^{2+} absorption between enterocytes. *Mol. Biol. Cell* **19**, 1912–1921 (2008).

26. Plain, A. *et al.* Claudin-12 knockout mice demonstrate reduced proximal tubule calcium permeability. *Int. J. Mol. Sci.* **21**, 2074 (2020).

27. Beggs, M. R. *et al.* Claudin-2 and claudin-12 form independent, complementary pores required to maintain calcium homeostasis. *Proc. Natl. Acad. Sci. U. S. A.* **118**, e2111247118 (2021).

28. Luis Negri, A. Role of claudins in renal calcium handling. *Nefrología* **35**, 347–352 (2015).

29. Venkatachalam, K. & Montell, C. TRP channels. *Annu. Rev. Biochem.* **76**, 387–417 (2007).

30. Müller, D. *et al.* Molecular cloning, tissue distribution, and chromosomal mapping of the human epithelial Ca^{2+} channel (ECAC1). *Genomics* **67**, 48–53 (2000).

31. Stumpf, T. *et al.* The human TRPV6 channel protein is associated with

cyclophilin B in human placenta. *J. Biol. Chem.* **283**, 18086–18098 (2008).

32. den Dekker, E., Hoenderop, J. G. J., Nilius, B. & Bindels, R. J. M. The epithelial calcium channels, TRPV5 & TRPV6: From identification towards regulation. *Cell Calcium* **33**, 497–507 (2003).
33. Nilius, B. *et al.* The single pore residue Asp542 determines Ca^{2+} permeation and Mg^{2+} block of the epithelial Ca^{2+} channel. *J. Biol. Chem.* **276**, 1020–1025 (2001).
34. Peng, J. Bin *et al.* Human calcium transport protein CaT1. *Biochem. Biophys. Res. Commun.* **278**, 326–332 (2000).
35. Peng, J. Bin, Brown, E. M. & Hediger, M. A. Structural conservation of the genes encoding CaT1, CaT2, and related cation channels. *Genomics* **76**, 99–109 (2001).
36. Hoenderop, J. G. J. *et al.* Function and expression of the epithelial Ca^{2+} channel family: comparison of mammalian ECaC1 and 2. *J. Physiol.* **537**, 747–761 (2001).
37. Yelshanskaya, M. V., Nadezhdin, K. D., Kurnikova, M. G. & Sobolevsky, A. I. Structure and function of the calcium-selective TRP channel TRPV6. *J. Physiol.* **599**, 2673–2697 (2021).
38. Nijenhuis, T., Hoenderop, J. G. J., Van Der Kemp, A. W. C. M. & Bindels, R. J. M. Localization and regulation of the epithelial Ca^{2+} channel TRPV6 in the kidney. *J. Am. Soc. Nephrol.* **14**, 2731–2740 (2003).
39. Vennekens, R. *et al.* Permeation and gating properties of the novel epithelial Ca^{2+} channel. *J. Biol. Chem.* **275**, 3963–3969 (2000).
40. Bianco, S. D. C. *et al.* Marked disturbance of calcium homeostasis in mice with targeted disruption of the Trpv6 calcium channel gene. *J. Bone*

Miner. Res. **22**, 274–285 (2007).

41. Benn, B. S. *et al.* Active intestinal calcium transport in the absence of transient receptor potential vanilloid type 6 and calbindin-D9k. *Endocrinology* **149**, 3196–3205 (2008).

42. Cui, M., Li, Q., Johnson, R. & Fleet, J. C. Villin promoter-mediated transgenic expression of transient receptor potential cation channel, subfamily V, member 6 (TRPV6) increases intestinal calcium absorption in wild-type and vitamin D receptor knockout mice. *J. Bone Miner. Res.* **27**, 2097–2107 (2012).

43. Hoenderop, J. G. J. *et al.* Renal Ca^{2+} wasting, hyperabsorption, and reduced bone thickness in mice lacking TRPV5. *J. Clin. Invest.* **112**, 1906–1914 (2003).

44. Balesaria, S., Sangha, S. & Walters, J. R. F. Human duodenum responses to vitamin D metabolites of TRPV6 and other genes involved in calcium absorption. *Am. J. Physiol. - Gastrointest. Liver Physiol.* **297**, 1193–1197 (2009).

45. Weber, K., Erben, R. G., Rump, A. & Adamski, J. Gene structure and regulation of the murine epithelial calcium channels ECaC1 and 2. *Biochem. Biophys. Res. Commun.* **289**, 1287–1294 (2001).

46. Van de Graaf, S. F. J. *et al.* Functional expression of the epithelial Ca^{2+} channels (TRPV5 and TRPV6) requires association of the S100A10-annexin 2 complex. *EMBO J.* **22**, 1478–1487 (2003).

47. van de Graaf, S. F. J., Chang, Q., Mensenkamp, A. R., Hoenderop, J. G. J. & Bindels, R. J. M. Direct Interaction with Rab11a Targets the Epithelial Ca 2+ Channels TRPV5 and TRPV6 to the Plasma Membrane. *Mol. Cell. Biol.* **26**, 303–312 (2006).

48. de Groot, T. *et al.* Molecular mechanisms of calmodulin action on TRPV5 and modulation by parathyroid hormone. *Mol. Cell. Biol.* **31**, 2845–2853 (2011).

49. Niemeyer, B. A., Bergs, C., Wissenbach, U., Flockerzi, V. & Trost, C. Competitive regulation of CaT-like-mediated Ca^{2+} entry by protein kinase C and calmodulin. *Proc. Natl. Acad. Sci. U. S. A.* **98**, 3600–3605 (2001).

50. Heizmann, C. W., Fritz, G. & Schäfer, B. W. S100 proteins: structure, functions and pathology. *Front. Biosci.* **7**, d1356-1368 (2002).

51. Christakos, S., Mady, L. J. & Dhawan, P. Calbindin-D28K and calbindin-D9K and the epithelial calcium channels TRPV5 and TRPV6. in *Vitamin D: Fourth Edition* (ed. Feldman, D.) 343–359 (Academic Press, 2018).

52. Schwaller, B. Cytosolic Ca^{2+} buffers. *Cold Spring Harb. Perspect. Biol.* **2**, a004051 (2010).

53. Nägerl, U. V., Novo, D., Mody, I. & Vergara, J. L. Binding kinetics of calbindin-D28k detemined by flash photolysis of caged Ca^{2+}. *Biophys. J.* **79**, 3009–3018 (2000).

54. Bindels, R. J. M., Timmermans, J. A. H., Hartog, A., Coers, W. & Van Os, C. H. Calbindin-D9k and parvalbumin are exclusively located along basolateral membranes in rat distal nephron. *J. Am. Soc. Nephrol.* **2**, 1122–1129 (1991).

55. Perret, C., Desplan, C. & Thomasset, M. Cholecalcin (a 9-kDa cholecalciferol-induced calcium-binding protein) messenger RNA: Distribution and induction by calcitriol in the rat digestive tract. *Eur. J. Biochem.* **150**, 211–217 (1985).

56. Lee, G. S. *et al.* Expression of human Calbindin-D9k correlated with age, vitamin D receptor and blood calcium level in the gastrointestinal tissues.

Clin. Biochem. **36**, 255–261 (2003).

57. Wasserman, R. H. & Taylor, A. N. Vitamin D3-induced calcium-binding protein in chick intestinal mucosa. *Science* **152**, 794–796 (1966).

58. Okano, T., Eric, D. & Lawson, M. Chick 28 000 Mr vitamin D-dependent calcium-binding protein in intestine, kidney and cerebellum. Purification using chromatofocusing. *J. Chromatogr. A* **448**, 145–156 (1988).

59. Roth, J., Brown, D., Norman, A. W. & Orci, L. Localization of the vitamin D-dependent calcium-binding protein in mammalian kidney. *Am. J. Physiol. Renal Physiol.* **243**, F243–F252 (1982).

60. Georgas, K. *et al.* Use of dual section mRNA in situ hybridisation/immunohistochemistry to clarify gene expression patterns during the early stages of nephron development in the embryo and in the mature nephron of the adult mouse kidney. *Histochem. Cell Biol.* **130**, 927–942 (2008).

61. Ingersoll, R. J. & Wasserman, R. H. Vitamin D3-induced Calcium-binding Protein. *J. Biol. Chem.* **246**, 2808–2814 (1971).

62. Christakos, S. & Liu, Y. Biological actions and mechanism of action of calbindin in the process of apoptosis. *J. Steroid Biochem. Mol. Biol.* **89–90**, 401–404 (2004).

63. Ahn, C. *et al.* The protective role of calbindin-D9k on endoplasmic reticulum stress-induced beta cell death. *Int. J. Mol. Sci.* **20**, 5317 (2019).

64. Feher, J. J., Fullmer, C. S. & Wasserman, R. H. Role of facilitated diffusion of calcium by calbindin in intestinal calcium absorption. *Am. J. Physiol. - Cell Physiol.* **262**, C517—C526 (1992).

65. Ebel, J. G., Taylor, A. N. & Wasserman, R. H. Vitamin D-induced calcium-binding protein of intestinal mucosa. Relation to vitamin D dose level and

lag period. *Am. J. Clin. Nutr.* **22**, 431–436 (1969).

66. Roche, C., Bellaton, C., Pansu, D., Miller, A. & Bronner, F. Localization of vitamin D-dependent active Ca^{2+} transport in rat duodenum and relation to CaBP. *Am. J. Physiol. - Gastrointest. Liver Physiol.* **251**, G314–G320 (1986).
67. Panda, D. K. *et al.* Targeted ablation of the 25-hydroxyvitamin D 1α-hydroxylase enzyme: Evidence for skeletal, reproductive, and immune dysfunction. *Proc. Natl. Acad. Sci. U. S. A.* **98**, 7498–7503 (2001).
68. Van Abel, M. *et al.* Coordinated control of renal Ca2+ transport proteins by parathyroid hormone. *Kidney Int.* **68**, 1708–1721 (2005).
69. Lee, G. S. *et al.* Phenotype of a calbindin-D9k gene knockout is compensated for by the induction of other calcium transporter genes in a mouse model. *J. Bone Miner. Res.* **22**, 1968–1978 (2007).
70. Zheng, W. *et al.* Critical role of calbindin-D28k in calcium homeostasis revealed by mice lacking both vitamin D receptor and calbindin-D28k. *J. Biol. Chem.* **279**, 52406–52413 (2004).
71. Dupret, J. M. *et al.* Transcriptional and post-transcriptional regulation of vitamin D-dependent calcium-binding protein gene expression in the rat duodenum by 1,25-dihydroxycholecalciferol. *J. Biol. Chem.* **262**, 16553–16557 (1987).
72. Darwish, H. M. & DeLuca, H. F. Identification of a 1,25-dihydroxyvitamin D3-response element in the 5′-flanking region of the rat calbindin D-9k gene. *Proc. Natl. Acad. Sci. U. S. A.* **89**, 603–607 (1992).
73. Li, Y. C., Pirro, A. E. & Demay, M. B. Analysis of vitamin D-dependent calcium-binding protein messenger ribonucleic acid expression in mice lacking the vitamin D receptor. *Endocrinology* **139**, 847–851 (1998).

74. Lee, G. S., Choi, K. C. & Jeung, E. B. Glucocorticoids differentially regulate expression of duodenal and renal calbindin-D9k through glucocorticoid receptor-mediated pathway in mouse model. *Am. J. Physiol. Endocrinol. Metab.* **290**, 299–307 (2006).

75. Nijenhuis, T., Hoenderop, J. G. J. & Bindels, R. J. M. Downregulation of Ca^{2+} and Mg^{2+} Transport Proteins in the Kidney Explains Tacrolimus (FK506)-Induced Hypercalciuria and Hypomagnesemia. *J. Am. Soc. Nephrol.* **15**, 549–557 (2004).

76. Gill, R. K. & Christakos, S. Identification of sequence elements in mouse calbindin-D28k gene that confer 1,25-dihydroxyvitamin D3- and butyrate-inducible responses. *Proc. Natl. Acad. Sci. U. S. A.* **90**, 2984–2988 (1993).

77. Varghese, S. *et al.* Transcriptional regulation and chromosomal assignment of the mammalian calbindin-D28k gene. *Mol. Endocrinol.* **3**, 495–502 (1989).

78. Bronner, F. Mechanisms and functional aspects of intestinal calcium absorption. in *Journal of Experimental Zoology* vol. 300A 47–52 (2003).

79. Axelsen, K. B. & Palmgren, M. G. Evolution of substrate specificities in the P-type ATPase superfamily. *J. Mol. Evol.* **46**, 84–101 (1998).

80. Strehler, E. E. & Zacharias, D. A. Role of alternative splicing in generating isoform diversity among plasma membrane calcium pumps. *Physiol. Rev.* **81**, 21–50 (2001).

81. Krebs, J. The plethora of PMCA isoforms: Alternative splicing and differential expression. *Biochim.Biophys.Acta.Mol.Cell Res* **1853**, 2018–2024 (2014).

82. Stauffer, T. P., Hilfiker, H., Carafoli, E. & Strehler, E. E. Quantitative

analysis of alternative splicing options of human plasma membrane calcium pump genes. *J. Biol. Chem.* **268**, 25993–26003 (1993).

83. Keeton, T. P., Burk, S. E. & Shull, G. E. Alternative splicing of exons encoding the calmodulin-binding domains and C termini of plasma membrane Ca^{2+}-ATPase isoforms 1, 2, 3, and 4. *J. Biol. Chem.* **268**, 2740–2748 (1993).

84. Freeman, T. C., Howard, A., Bentsen, B. S., Legon, S. & Walters, J. R. F. Cellular and regional expression of transcripts of the plasma membrane calcium pump PMCA1 in rabbit intestine. *Am. J. Physiol. - Gastrointest. Liver Physiol.* **269**, G126—G131 (1995).

85. Armbrecht, H. J., Boltz, M. A. & Wongsurawat, N. Expression of plasma membrane calcium pump mRNA in rat intestine: effect of age and 1,25-dihydroxyvitamin D. *Biochim. Biophys. Acta. Biomembr* **1195**, 110–114 (1994).

86. Howard, A., Legon, S. & Walters, J. R. F. Human and rat intestinal plasma membrane calcium pump isoforms. *Am. J. Physiol. - Gastrointest. Liver Physiol.* **265**, G917—G925 (1993).

87. Alexander, R. T. *et al.* Ultrastructural and immunohistochemical localization of plasma membrane Ca^{2+}-ATPase 4 in Ca^{2+}-transporting epithelia. *Am. J. Physiol. Renal Physiol.* **309**, F604–F616 (2015).

88. White, K. E., Gesek, F. A., Nesbitt, T., Drezner, M. K. & Friedman, P. A. Molecular dissection of Ca^{2+} efflux in immortalized proximal tubule cells. *J. Gen. Physiol.* **109**, 217–228 (1997).

89. Magyar, C. E., White, K. E., Rojas, R., Apodaca, G. & Friedman, P. A. Plasma membrane Ca^{2+}-ATPase and NCX1 Na^{+}/Ca^{2+} exchanger expression in distal convoluted tubule cells. *Am. J. Physiol. Renal Physiol.*

283, F29—F40 (2002).

90. Caride, A. J., Chini, E. N., Homma, S., Penniston, J. T. & Dousa, T. P. mRNA encoding four isoforms of the plasma membrane calcium pump and their variants in rat kidney and nephron segments. *J. Lab. Clin. Med.* **132**, 149–156 (1998).

91. Brini, M. & Carafoli, E. The Plasma Membrane Ca^{2+} ATPase and the plasma membrane Sodium Calcium exchanger cooperate in the regulation of cell Calcium. *Cold Spring Harb. Perspect. Biol.* **3**, 1–15 (2011).

92. Møller, J. V., Juul, B. & Le Maire, M. Structural organization, ion transport, and energy transduction of P-type ATPases. *Biochim. Biophys. Acta - Rev. Biomembr.* **1286**, 1–51 (1996).

93. Ryan, Z. C. *et al.* Deletion of the intestinal plasma membrane calcium pump, isoform 1, Atp2b1, in mice is associated with decreased bone mineral density and impaired responsiveness to 1, 25-dihydroxyvitamin D3. *Biochem. Biophys. Res. Commun.* **467**, 152–156 (2015).

94. Ehara, Y. *et al.* Reduced secretion of parathyroid hormone and hypocalcemia in systemic heterozygous ATP2B1-null hypertensive mice. *Hypertens. Res.* **41**, 699–707 (2018).

95. Okunade, G. W. *et al.* Targeted ablation of plasma membrane Ca^{2+}-ATPase (PMCA) 1 and 4 indicates a major housekeeping function for PMCA1 and a critical role in hyperactivated sperm motility and male fertility for PMCA4. *J. Biol. Chem.* **279**, 33742–33750 (2004).

96. Glendenning, P., Ratajczak, T., Dick, I. M. & Prince, R. L. Calcitriol upregulates expression and activity of the 1b isoform of the plasma membrane calcium pump in immortalized distal kidney tubular cells. *Arch.*

Biochem. Biophys. **380**, 126–132 (2000).

97. Mangialavori, I., Ferreira-Gomes, M., Pignataro, M. F., Strehler, E. E. & Rossi, J. P. F. C. Determination of the dissociation constants for Ca^{2+} and calmodulin from the plasma membrane Ca^{2+} pump by a lipid probe that senses membrane domain changes. *J. Biol. Chem.* **285**, 123–130 (2010).
98. Gabellini, N., Bortoluzzi, S., Danieli, G. A. & Carafoli, E. The human SLC8A3 gene and the tissue-specific Na^{+}/Ca^{2+} exchanger 3 isoforms. *Gene* **298**, 1–7 (2002).
99. Marshall, C. R. *et al.* CDNA cloning and expression of the cardiac Na^{+}/Ca^{2+} exchanger from Mozambique tilapia (Oreochromis mossambicus) reveal a teleost membrane transporter with mammalian temperature dependence. *J. Biol. Chem.* **280**, 28903–28911 (2005).
100. Ren, X. & Philipson, K. D. The topology of the cardiac Na^{+}/Ca^{2+} exchanger, NCX1. *J. Mol. Cell. Cardiol.* **57**, 68–71 (2013).
101. Chou, A. C., Ju, Y. Ten & Pan, C. Y. Calmodulin interacts with the sodium/calcium exchanger NCX1 to regulate activity. *PLoS One* **10**, e0138856 (2015).
102. Hilge, M., Aelen, J. & Vuister, G. W. Ca^{2+} Regulation in the Na^{+}/Ca^{2+} Exchanger Involves Two Markedly Different Ca^{2+} Sensors. *Mol. Cell* **22**, 15–25 (2006).
103. Matsuoka, S., Nicoll, D. A., He, Z. & Philipson, K. D. Regulation of the Cardiac Na^{+}-Ca^{2+} exchanger by the endogenous XIP region. *J. Gen. Physiol.* **109**, 273–286 (1997).
104. Lee, S. L., Yu, A. S. L. & Lytton, J. Tissue-specific expression of Na^{+}-Ca^{2+} exchanger isoforms. *J. Biol. Chem.* **269**, 14849–14852 (1994).
105. Quednau, B. D., Nicoll, D. A. & Philipson, K. D. The sodium/calcium

exchanger family - SLC8. *Pflugers Arch. Eur. J. Physiol.* **447**, 543–548 (2004).

106. Teerapornpuntakit, J., Dorkkam, N., Wongdee, K., Krishnamra, N. & Charoenphandhu, N. Endurance swimming stimulates transepithelial calcium transport and alters the expression of genes related to calcium absorption in the intestine of rats. *Am. J. Physiol. Endocrinol. Metab.* **296**, E775—E786 (2009).
107. Obermuller, N. *et al.* Expression of the thiazide-sensitive Na-Cl cotransporter in rat and human kidney. *Am. J. Physiol. Renal Physiol.* **269**, F900—F910 (1995).
108. Loffing, J. *et al.* Distribution of transcellular calcium and sodium transport pathways along mouse distal nephron. *Am. J. Physiol. Renal Physiol.* **281**, F1021—F1027 (2001).
109. Reeves, J. P. & Hale, C. C. The stoichiometry of the cardiac sodium-calcium exchange system. *J. Biol. Chem.* **259**, 7733–7739 (1984).
110. Blaustein, M. P. & Lederer, W. J. Sodium/calcium exchange: Its physiological implications. *Physiol. Rev.* **79**, 763–854 (1999).
111. Levi, A. J., Spitzer, K. W., Kohmoto, O. & Bridge, J. H. B. Depolarization-induced Ca entry via Na-Ca exchange triggers SR release in guinea pig cardiac myocytes. *Am. J. Physiol. - Hear. Circ. Physiol.* **266**, H1422—H1433 (1994).
112. Khuituan, P. *et al.* Fibroblast growth factor-23 negates 1,25(OH)2D 3-induced intestinal calcium transport by reducing the transcellular and paracellular calcium fluxes. *Arch. Biochem. Biophys.* **536**, 46–52 (2013).
113. Centeno, V., Picotto, G., Pérez, A., Alisio, A. & Tolosa De Talamoni, N. Intestinal Na^{+}/Ca^{2+} exchanger protein and gene expression are regulated

by 1,25(OH)2D3 in vitamin D-deficient chicks. *Arch. Biochem. Biophys.* **509**, 191–196 (2011).

114. Hoenderop, J. G. J. *et al.* Modulation of renal Ca^{2+} transport protein genes by dietary Ca^{2+} and 1,25-dihydroxyvitamin D3 in 25hydroxyvitamin D3-1α-hydroxylase knockout mice. *FASEB J.* **16**, 1398–1406 (2002).
115. Riccardi, D. *et al.* Localization of the extracellular Ca^{2+}-sensing receptor and PTH/PTHrP receptor in rat kidney. *Am. J. Physiol. Ren. Fluid Electrolyte Physiol.* **271**, F951—F956 (1996).
116. Hilgemann, D. W. Regulation and deregulation of cardiac Na^{+}-Ca^{2+} exchange in giant excised sarcolemmal membrane patches. *Nature* **344**, 242–245 (1990).
117. Li, Z. *et al.* Identification of a peptide inhibitor of the cardiac sarcolemmal Na^{+}-Ca^{2+} exchanger. *J. Biol. Chem.* **266**, 1014–1020 (1991).
118. Radhakrishnan, V. M., Gilpatrick, M. M., Parsa, N. A., Kiela, P. R. & Ghishan, F. K. Expression of Cav1.3 calcium channel in the human and mouse colon: Post-transcriptional inhibition by IFNγ. *Am. J. Physiol. - Gastrointest. Liver Physiol.* **312**, G77–G84 (2016).
119. Morgan, E. L., Mace, O. J., Helliwell, P. A., Affleck, J. & Kellett, G. L. A role for Cav1.3 in rat intestinal calcium absorption. *Biochem. Biophys. Res. Commun.* **312**, 487–493 (2003).
120. Reyes-Fernandez, P. C. & Fleet, J. C. Luminal glucose does not enhance active intestinal calcium absorption in mice: Evidence against a role for Cav1.3 as a mediator of calcium uptake during absorption. *Nutr. Res.* **35**, 1009–1015 (2015).
121. Beggs, M. R. *et al.* TRPV6 and Cav1.3 Mediate Distal Small Intestine Calcium Absorption Before Weaning. *Cell. Mol. Gastroenterol. Hepatol.* **8**,

625–642 (2019).

122. Nemere, I. & Norman, A. W. 1,25-Dihydroxyvitamin D3-mediated vesicular calcium transport in intestine: dose-response studies. *Mol. Cell. Endocrinol.* **67**, 47–53 (1989).

123. Hubbard, M. J. Calcium transport across the dental enamel epithelium. *Crit. Rev. Oral Biol. Med.* **11**, 437–466 (2000).

124. Davis, W. L., Jones, R. G. & Hagler, H. K. Calcium containing lysosomes in the normal chick duodenum: A histochemical and analytical electron microscopic study. *Tissue Cell* **11**, 127–138 (1979).

125. Nemere, I., Leathers, V. & Norman, A. W. 1,25-Dihydroxyvitamin D3-mediated intestinal calcium transport. Biochemical identification of lysosomes containing calcium and calcium-binding protein (Calbindin-D(28K)). *J. Biol. Chem.* **261**, 16106–16114 (1986).

126. Davis, W. L. & Jones, R. G. Lysosomal proliferation in rachitic avian intestinal absorptive cells following 1,25-Dihydroxycholecalciferol. *Tissue Cell* **14**, 585–595 (1982).

127. Bronner, F. Recent developments in intestinal calcium absorption. *Nutr. Rev.* **67**, 109–113 (2009).

128. Alexander, R. T., Rievaj, J. & Dimke, H. Paracellular calcium transport across renal and intestinal epithelia. *Biochem. Cell Biol.* **92**, 467–480 (2014).

129. Cochand-Priollet, B. *et al.* Altered gap and tight junctions in human thyroid oncocytic tumors: A study of 8 cases by freeze-fracture. *Ultrastruct. Pathol.* **22**, 413–420 (1998).

130. Krause, G. *et al.* Structure and function of claudins. *Biochim. Biophys. Acta. Biomembr.* **1778**, 631–645 (2008).

131. Mineta, K. *et al.* Predicted expansion of the claudin multigene family. *FEBS Lett.* **585**, 606–612 (2011).

132. Günzel, D. & Yu, A. S. L. Claudins and the modulation of tight junction permeability. *Physiol. Rev.* **93**, 525–569 (2013).

133. Furuse, M., Fujita, K., Hiiragi, T., Fujimoto, K. & Tsukita, S. Claudin-1 and -2: Novel integral membrane proteins localizing at tight junctions with no sequence similarity to occludin. *J. Cell Biol.* **141**, 1539–1550 (1998).

134. Lal-Nag, M. & Morin, P. J. The claudins. *Genome Biol.* **10**, 1–7 (2009).

135. Rahner, C., Mitic, L. L. & Anderson, J. M. Heterogeneity in expression and subcellular localization of claudins 2, 3, 4, and 5 in the rat liver, pancreas, and gut. *Gastroenterology* **120**, 411–422 (2001).

136. Fujita, H. *et al.* Differential expression and subcellular localization of claudin-7, -8, -12, -13, and -15 along the mouse intestine. *J. Histochem. Cytochem.* **54**, 933–944 (2006).

137. Holmes, J. L., Van Itallie, C. M., Rasmussen, J. E. & Anderson, J. M. Claudin profiling in the mouse during postnatal intestinal development and along the gastrointestinal tract reveals complex expression patterns. *Gene Expr. Patterns* **6**, 581–588 (2006).

138. Lameris, A. L. *et al.* Expression profiling of claudins in the human gastrointestinal tract in health and during inflammatory bowel disease. *Scand. J. Gastroenterol.* **48**, 58–69 (2013).

139. Markov, A. G., Veshnyakova, A., Fromm, M., Amasheh, M. & Amasheh, S. Segmental expression of claudin proteins correlates with tight junction barrier properties in rat intestine. *J. Comp. Physiol. B Biochem. Syst. Environ. Physiol.* **180**, 591–598 (2010).

140. Kiuchi-Saishin, Y. *et al.* Differential expression patterns of claudins, tight

junction membrane proteins, in mouse nephron segments. *J. Am. Soc. Nephrol.* **13**, 875–886 (2002).

141. Enck, A. H., Berger, U. V. & Yu, A. S. L. Claudin-2 is selectively expressed in proximal nephron in mouse kidney. *Am. J. Physiol. Physiol.* **281**, F966–F974 (2001).
142. Kirk, A., Campbell, S., Bass, P., Mason, J. & Collins, J. Differential expression of claudin tight junction proteins in the human cortical nephron. *Nephrol. Dial. Transplant.* **25**, 2107–2119 (2010).
143. Lechner, C., Mönning, U., Reichel, A. & Fricker, G. Potential and limits of kidney cells for evaluation of renal excretion. *Pharmaceuticals* **14**, 1–19 (2021).
144. Haddad, M., Lin, F., Dwarakanath, V., Cordes, K. & Baum, M. Developmental changes in proximal tubule tight junction proteins. *Pediatr. Res.* **57**, 453–457 (2005).
145. Abuazza, G. *et al.* Claudins 6, 9, and 13 are developmentally expressed renal tight junction proteins. *Am. J. Physiol. Renal Physiol.* **291**, F1132—F1141 (2006).
146. Gong, Y. *et al.* Claudin-14 regulates renal Ca^{2+} transport in response to CaSR signalling via a novel microRNA pathway. *EMBO J.* **31**, 1999–2012 (2012).
147. Oh, I. H. *et al.* Thick ascending limb claudins are altered to increase calciuria and magnesiuria in metabolic acidosis. *Am. J. Physiol. Renal Physiol.* **320**, F418–F428 (2021).
148. Simon, D. B. *et al.* Paracellin-1, a renal tight junction protein required for paracellular Mg^{2+} resorption. *Science* **285**, 103–106 (1999).
149. Weber, S. *et al.* Primary gene structure and expression studies of rodent

paracellin-1. *J. Am. Soc. Nephrol.* **12**, 2664–2672 (2001).

150. Prot-Bertoye, C. *et al.* Differential localization patterns of claudin 10, 16, and 19 in human, mouse, and rat renal tubular epithelia. *Am. J. Physiol. Renal Physiol.* **321**, F207–F224 (2021).

151. Angelow, S., El-Husseini, R., Kanzawa, S. A. & Yu, A. S. L. Renal localization and function of the tight junction protein, claudin-19. *Am. J. Physiol. Renal Physiol.* **293**, 166–177 (2007).

152. Lee, N. P. Y. *et al.* Kidney claudin-19: Localization in distal tubules and collecting ducts and dysregulation in polycystic renal disease. *FEBS Lett.* **580**, 923–931 (2006).

153. Ziemens, A. *et al.* Claudin 19 is regulated by extracellular osmolality in rat kidney inner medullary collecting duct cells. *Int. J. Mol. Sci.* **20**, 4401.1-4401.19 (2019).

154. Van Itallie, C. M. & Anderson, J. M. Claudins and epithelial paracellular transport. *Annu. Rev. Physiol.* **68**, 403–429 (2006).

155. Van Itallie, C. M., Fanning, A. S. & Anderson, J. M. Reversal of charge selectivity in cation or anion-selective epithelial lines by expression of different claudins. *Am. J. Physiol. Renal Physiol.* **285**, F1078—F1084 (2003).

156. Wongdee, K., Chanpaisaeng, K., Teerapornpuntakit, J. & Charoenphandhu, N. Intestinal Calcium Absorption. *Compr. Physiol.* **11**, 2047–2073 (2021).

157. Li, J., Zhuo, M., Pei, L., Rajagopal, M. & Yu, A. S. L. Comprehensive cysteine-scanning mutagenesis reveals claudin-2 pore-lining residues with different intrapore locations. *J. Biol. Chem.* **289**, 6475–6484 (2014).

158. Tanaka, H. *et al.* Claudin-21 Has a Paracellular Channel Role at Tight

Junctions. *Mol. Cell. Biol.* **36**, 954–964 (2016).

159. Curry, J. N. *et al.* Claudin-2 deficiency associates with hypercalciuria in mice and human kidney stone disease. *J. Clin. Invest.* **130**, 1948–1960 (2020).

160. Rosenthal, R. *et al.* Claudin-2-mediated cation and water transport share a common pore. *Acta Physiol.* **219**, 521–536 (2017).

161. Muto, S. *et al.* Claudin-2-deficient mice are defective in the leaky and cation-selective paracellular permeability properties of renal proximal tubules. *Proc. Natl. Acad. Sci. U. S. A.* **107**, 8011–8016 (2010).

162. Rosenthal, R. *et al.* Claudin-15 forms a water channel through the tight junction with distinct function compared to claudin-2. *Acta Physiol.* **228**, e13334 (2020).

163. Charoenphandhu, N. *et al.* Two-step stimulation of intestinal Ca^{2+} absorption during lactation by long-term prolactin exposure and suckling-induced prolactin surge. *Am. J. Physiol. Endocrinol. Metab.* **297**, E609—E619 (2009).

164. Tanrattana, C., Charoenphandhu, N., Limlomwongse, L. & Krishnamra, N. Prolactin directly stimulated the solvent drag-induced calcium transport in the duodenum of female rats. *Biochim. Biophys. Acta. Biomembr.* **1665**, 81–91 (2004).

165. Wongdee, K. & Charoenphandhu, N. Regulation of epithelial calcium transport by prolactin: From fish to mammals. *Gen. Comp. Endocrinol.* **181**, 235–240 (2013).

166. Dimke, H. *et al.* Activation of the Ca^{2+}-sensing receptor increases renal claudin-14 expression and urinary Ca^{2+} excretion. *Am. J. Physiol. Renal Physiol.* **304**, F761—F769 (2013).

167. Konrad, M. *et al.* Mutations in the tight-junction gene claudin 19 (CLDN19) are associated with renal magnesium wasting, renal failure, and severe ocular involvement. *Am. J. Hum. Genet.* **79**, 949–957 (2006).

168. Hou, J. *et al.* Transgenic RNAi depletion of claudin-16 and the renal handling of magnesium. *J. Biol. Chem.* **282**, 17114–17122 (2007).

169. Hou, J. *et al.* Claudin-16 and claudin-19 interaction is required for their assembly into tight junctions and for renal reabsorption of magnesium. *Proc. Natl. Acad. Sci. U. S. A.* **106**, 15350–15355 (2009).

170. Hou, J. *et al.* Claudin-16 and claudin-19 interact and form a cation-selective tight junction complex. *J. Clin. Invest.* **118**, 619–628 (2008).

171. Jaya Kausalya, P. *et al.* Disease-associated mutations affect intracellular traffic and paracellular Mg^{2+} transport function of Claudin-16. *J. Clin. Invest.* **116**, 878–891 (2006).

172. Will, C. *et al.* Targeted deletion of murine Cldn16 identifies extra- and intrarenal compensatory mechanisms of Ca^{2+} and Mg^{2+} wasting. *Am. J. Physiol. Renal Physiol.* **298**, F1152—F1161 (2010).

173. Chatterjee, I. *et al.* Overexpression of Vitamin D Receptor in Intestinal Epithelia Protects Against Colitis via Upregulating Tight Junction Protein Claudin 15. *J. Crohn's Colitis* **2021**, 1–17 (2021).

174. Sato, T. *et al.* Parathyroid hormone controls paracellular Ca^{2+} transport in the thick ascending limb by regulating the tight-junction protein Claudin14. *Proc. Natl. Acad. Sci. U. S. A.* **114**, E3344–E3353 (2017).

175. Kladnitsky, O., Rozenfeld, J., Azulay-Debby, H., Efrati, E. & Zelikovic, I. The claudin-16 channel gene is transcriptionally inhibited by 1,25-dihydroxyvitamin D. *Exp. Physiol.* **100**, 79–94 (2015).

176. Toka, H. R. New functional aspects of the extracellular calcium-sensing

receptor. *Curr. Opin. Nephrol. Hypertens.* **23**, 352–360 (2014).

177. Houillier, P. Calcium-sensing in the kidney. *Current Opinion in Nephrology and Hypertension* vol. 22 566–571 (2013).

178. Huang, Y. *et al.* Multiple Ca^{2+}-binding sites in the extracellular domain of the Ca^{2+}-sensing receptor corresponding to cooperative Ca^{2+} response. *Biochemistry* **48**, 388–398 (2009).

179. Hou, J. Claudins and mineral metabolism. *Curr. Opin. Nephrol. Hypertens.* **25**, 308–313 (2016).

180. Grosshans, B. L., Ortiz, D. & Novick, P. Rabs and their effectors: Achieving specificity in membrane traffic. *Proc. Natl. Acad. Sci. U. S. A.* **103**, 11821–11827 (2006).

181. Lu, R. *et al.* Rab14 regulation of claudin-2 trafficking modulates epithelial permeability and lumen morphogenesis. *Mol. Biol. Cell* **25**, 1744–1754 (2014).

182. Ikari, A. *et al.* Tight junctional localization of Claudin-16 is regulated by syntaxin 8 in renal tubular epithelial cells. *J. Biol. Chem.* **289**, 13112–13123 (2014).

183. Shigetomi, K. & Ikenouchi, J. Regulation of the epithelial barrier by post-translational modifications of tight junction membrane proteins. *J. Biochem.* **163**, 265–272 (2018).

184. Ikari, A. *et al.* Phosphorylation of paracellin-1 at Ser217 by protein kinase A is essential for localization in tight junctions. *J. Cell Sci.* **119**, 1781–1789 (2006).

185. Van Itallie, C. M. *et al.* Phosphorylation of claudin-2 on serine 208 promotes membrane retention and reduces trafficking to lysosomes. *J. Cell Sci.* **125**, 4902–4912 (2012).

186. Pan, W. *et al.* The epithelial sodium/proton exchanger, NHE3, is necessary for renal and intestinal calcium (re)absorption. *Am. J. Physiol. Renal Physiol.* **302**, F943–F956 (2012).

187. Lu, Z., Ding, L., Lu, Q. & Chen, Y.-H. Claudins in intestines. *Tissue Barriers* **1**, e24978 (2013).

188. Ong, M. L. D. M., Yeruva, S., Sailer, A., Nilsen, S. P. & Turner, J. R. Differential regulation of claudin-2 and claudin-15 expression in children and adults with malabsorptive disease. *Lab. Investig.* **100**, 483–490 (2020).

189. Suzuki, T., Yoshinaga, N. & Tanabe, S. Interleukin-6 (IL-6) regulates claudin-2 expression and tight junction permeability in intestinal epithelium. *J. Biol. Chem.* **286**, 31263–31271 (2011).

190. García-Hernández, V. *et al.* EGF regulates claudin-2 and -4 expression through Src and STAT3 in MDCK cells. *J. Cell. Physiol.* **230**, 105–115 (2015).

191. Balkovetz, D. F., Chumley, P. & Amlal, H. Downregulation of claudin-2 expression in renal epithelial cells by metabolic acidosis. *Am. J. Physiol. Renal Physiol.* **297**, 604–611 (2009).

192. Thongon, N. & Krishnamra, N. Apical acidity decreases inhibitory effect of omeprazole on Mg^{2+} absorption and claudin-7 and -12 expression in Caco-2 monolayers. *Exp. Mol. Med.* **44**, 684–693 (2012).

193. Pappenheimer, J. R. & Reiss, K. Z. Contribution of solvent drag through intercellular junctions to absorption of nutrients by the small intestine of the rat. *J. Membr. Biol.* **100**, 123–136 (1987).

194. Larsen, E. H., Nedergaard, S. & Ussing, H. H. Role of lateral intercellular space and sodium recirculation for isotonic transport in leaky epithelia. in

Reviews of Physiology, Biochemistry and Pharmacology (eds. Greger, R. & Rosenthal, W.) vol. 141 153–212 (2000).

195. Amerongen, H. M., Mack, J. A., Wilson, J. M. & Neutra, M. R. Membrane domains of intestinal epithelial cells: Distribution of Na^+,K^+-ATPase and the membrane skeleton in adult rat intestine during fetal development and after epithelial isolation. *J. Cell Biol.* **109**, 2129–2138 (1989).
196. Areco, V. A., Kohan, R., Talamoni, G., Tolosa De Talamoni, N. G. & Peralta López, M. E. Intestinal Ca^{2+}absorption revisited: A molecular and clinical approach. *World J. Gastroenterol.* **26**, 3344–3364 (2020).
197. Rosenthal, R. *et al.* Claudin-2, a component of the tight junction, forms a paracellular water channel. *J. Cell Sci.* **123**, 1913–1921 (2010).
198. Alexander, R. T. Claudin-15 is not a drag! *Acta Physiologica* vol. 228 e13397 (2020).
199. Tamura, A. *et al.* Loss of claudin-15, but not claudin-2, causes Na^+ deficiency and glucose malabsorption in mouse small intestine. *Gastroenterology* **140**, 913–923 (2011).
200. Tudpor, K., Charoenphandhu, N., Saengamnart, W. & Krishnamra, N. Long-term prolactin exposure differentially stimulated the transcellular and solvent drag-induced calcium transport in the duodenum of ovariectomized rats. *Exp. Biol. Med.* **230**, 836–844 (2005).
201. Tudpor, K., Teerapornpuntakit, J., Jantarajit, W., Krishnamra, N. & Charoenphandhu, N. 1,25-Dihydroxyvitamin D3 rapidly stimulates the solvent drag-induced paracellular calcium transport in the duodenum of female rats. *J. Physiol. Sci.* **58**, 297–307 (2008).
202. Charoenphandhu, N., Tudpor, K., Pulsook, N. & Krishnamra, N. Chronic metabolic acidosis stimulated transcellular and solvent drag-induced

calcium transport in the duodenum of female rats. *Am. J. Physiol. - Gastrointest. Liver Physiol.* **291**, 446–455 (2006).

203. Fleet, J. C. & Schoch, R. D. Molecular mechanisms for regulation of intestinal calcium absorption by vitamin D and other factors. *Crit. Rev. Clin. Lab. Sci.* **47**, 181–95 (2010).
204. Marcus, C. S. & Lengemann, F. W. Absorption of Ca45 and Sr85 from solid and liquid food at various levels of the alimentary tract of the rat. *J. Nutr.* **77**, 155–160 (1962).
205. Karbach, U. & Feldmeier, H. The cecum is the site with the highest calcium absorption in rat intestine. *Dig. Dis. Sci.* **38**, 1815–1824 (1993).
206. Ammann, P., Rizzoli, R. & Fleisch, H. Calcium absorption in rat large intestine in vivo: Availability of dietary calcium. *Am. J. Physiol. - Gastrointest. Liver Physiol.* **251**, G14—G18 (1986).
207. Nellans, H. N. Intestinal calcium absorption. Interplay of paracellular and cellular pathways. *Miner. Electrolyte Metab.* **16**, 101–108 (1990).
208. Wasserman, R. H. Vitamin D and the dual processes of intestinal calcium absorption. *J. Nutr.* **134**, 3137–3139 (2004).
209. Hylander, E., Ladefoged, K. & Jarnum, S. The importance of the colon in calcium absorption following small-intestinal resection. *Scand. J. Gastroenterol.* **15**, 55–60 (1980).
210. Kopic, S. & Geibel, J. P. Gastric acid, calcium absorption, and their impact on bone health. *Physiol. Rev.* **93**, 189–268 (2013).
211. Ivanovich, P., Fellows, H. & Rich, C. The absorption of calcium carbonate. *Ann. Intern. Med.* **66**, 917–923 (1967).
212. Cramer, C. F. & Copp, D. H. Progress and Rate of Absorption of Radiostrontium Through Intestinal Tracts of Rats. *Exp. Biol. Med.* **102**,

514–517 (1959).

213. Duflos, C., Bellaton, C., Pansu, D. & Bronner, F. Calcium solubility, intestinal sojourn time and paracellular permeability codetermine passive calcium absorption in rats. *J. Nutr.* **125**, 2348–2355 (1995).

214. Pansu, D., Duflos, C., Bellaton, C. & Bronner, F. Solubility and Intestinal Transit Time Limit Calcium Absorption in Rats. *J. Nutr.* **123**, 1396–1404 (1993).

215. Goss, S. L., Lemons, K. A., Kerstetter, J. E. & Bogner, R. H. Determination of calcium salt solubility with changes in pH and PCO2, simulating varying gastrointestinal environments. *J. Pharm. Pharmacol.* **59**, 1485–1492 (2010).

216. Pansu, D., Bellaton, C., Roche, C. & Bronner, F. Duodenal and ileal calcium absorption in the rat and effects of vitamin D. *Am. J. Physiol. - Gastrointest. Liver Physiol.* **7**, G695–G700 (1983).

217. Karbach, U. Segmental heterogeneity of cellular and paracellular calcium transport across the rat duodenum and jejunum. *Gastroenterology* **100**, 47–58 (1991).

218. Kraidith, K. *et al.* Direct stimulation of the transcellular and paracellular calcium transport in the rat cecum by prolactin. *Pflugers Arch. Eur. J. Physiol.* **458**, 993–1005 (2009).

219. Nellans, H. N. & Goldsmith, R. S. Transepithelial calcium transport by rat cecum: High-efficiency absorptive site. *Am. J. Physiol. - Gastrointest. Liver Physiol.* **240**, G424—G431 (1981).

220. Brommage, R., Binacua, C. & Carrié, A. L. The cecum does not participate in the stimulation of intestinal calcium absorption by calcitriol. *J. Steroid Biochem. Mol. Biol.* **54**, 71–73 (1995).

221. Favus, M. J. Evidence for absorption of ionic calcium and soluble calcium complexes by the duodenum and cecum in the rat. *Am. J. Ther.* **8**, 425–431 (2001).

222. Favus, M. J., Kathpalia, S. C. & Coe, F. L. Kinetic characteristics of calcium absorption and secretion by rat colon. *Am. J. Physiol. - Gastrointest. Liver Physiol.* **240**, G350—G354 (1981).

223. Petith, M. M., Wilson, H. D. & Schedl, H. P. Vitamin D Dependence of In Vivo Calcium Transport and Mucosal Calcium Binding Protein in Rat Large Intestine. *Gastroenterology* **76**, 99–104 (1979).

224. Luettig, J., Rosenthal, R., Barmeyer, C. & Schulzke, J. D. Claudin-2 as a mediator of leaky gut barrier during intestinal inflammation. *Tissue Barriers* **3**, e977176 (2015).

225. Blaine, J., Chonchol, M. & Levi, M. Renal control of calcium, phosphate, and magnesium homeostasis. *Clin. J. Am. Soc. Nephrol.* **10**, 1257–1272 (2015).

226. Lassiter, W. E., Gottschalk, C. W. & Mylle, M. Micropuncture study of renal tubular reabsorption of calcium in normal rodents. *Am. J. Physiol.* **204**, 771–775 (1963).

227. Moor, M. B. & Bonny, O. Ways of calcium reabsorption in the kidney. *Am. J. Physiol. Renal Physiol.* **310**, F1337–F1350 (2016).

228. Wang, X., Armando, I., Upadhyay, K., Pascua, A. & Jose, P. A. The regulation of proximal tubular salt transport in hypertension: An update. *Curr. Opin. Nephrol. Hypertens.* **18**, 412–420 (2009).

229. Walser, M. Calcium clearance as a function of sodium clearance in the dog. *Am. J. Physiol.* **200**, 1099–1104 (1961).

230. Günzel, D. *et al.* Claudin-10 exists in six alternatively spliced isoforms that

exhibit distinct localization and function. *J. Cell Sci.* **122**, 1507–1517 (2009).

231. Krug, S. M. *et al.* Claudin-17 forms tight junction channels with distinct anion selectivity. *Cell. Mol. Life Sci.* **69**, 2765–2778 (2012).
232. Rector, F. C. Sodium, bicarbonate, and chloride absorption by the proximal tubule. *Am. J. Physiol. Ren. Fluid Electrolyte Physiol.* **13**, F461—F471 (1983).
233. Hebert, S. C., Brown, E. M. & Harris, H. W. Role of the Ca^{2+}-sensing receptor in divalent mineral ion homeostasis. *J. Exp. Biol.* **200**, 295–302 (1997).
234. Toka, H. R. *et al.* Deficiency of the calcium-sensing receptor in the kidney causes parathyroid hormone-independent hypocalciuria. *J. Am. Soc. Nephrol.* **23**, 1879–1890 (2012).
235. Bernardo, J. A. F. & Friedman, P. A. Renal Calcium Metabolism. in *Seldin and Geibisch's The Kidney* (eds. Alpern, R., Caplan, M. & Moe, O.) vol. 2 2225–2247 (Academic Press, 2013).
236. Jeon, U. S. Kidney and calcium homeostasis. *Electrolyte Blood Press.* **6**, 68–76 (2008).
237. Sands, J. M. & Layton, H. E. The Physiology of Urinary Concentration: An Update. *Semin. Nephrol.* **29**, 178–195 (2009).
238. Fenton, R. A. *et al.* Acute regulation of aquaporin-2 phosphorylation at Ser-264 by vasopressin. *Proc. Natl. Acad. Sci. U. S. A.* **105**, 3134–3139 (2008).
239. Hannan, F. M., Kallay, E., Chang, W., Brandi, M. L. & Thakker, R. V. The calcium-sensing receptor in physiology and in calcitropic and noncalcitropic diseases. *Nat. Rev. Endocrinol.* **15**, 33–51 (2018).

240. Moe, S. M. Calcium homeostasis in health and in kidney disease. *Compr. Physiol.* **6**, 1781–1800 (2016).

241. Mundy, G. R. & Guise, T. A. Hormonal control of calcium homeostasis. *Clin. Chem.* **45**, 1347–1352 (1999).

242. Khanal, R. C. & Nemere, I. Endocrine regulation of calcium transport in epithelia. *Clin. Exp. Pharmacol. Physiol.* **35**, 1277–1287 (2008).

243. Felsenfeld, A. J. & Levine, B. S. Calcitonin, the forgotten hormone: Does it deserve to be forgotten? *Clin. Kidney J.* **8**, 180–187 (2015).

244. Goltzman, D., Mannstadt, M. & Marcocci, C. Physiology of the Calcium-Parathyroid Hormone-Vitamin D Axis. *Front. Horm. Res.* **50**, 1–13 (2018).

245. Silva, B. C. & Bilezikian, J. P. Parathyroid hormone: Anabolic and catabolic actions on the skeleton. *Curr. Opin. Pharmacol.* **22**, 41–50 (2015).

246. Dobnig, H. & Turner, R. T. The effects of programmed administration of human parathyroid hormone fragment (1-34) on bone histomorphometry and serum chemistry in rats. *Endocrinology* **138**, 4607–4612 (1997).

247. Bandeira, F. *et al.* Bone disease in primary hyperparathyroidism. *Arq. Bras. Endocrinol. Metabol.* **58**, 553–561 (2014).

248. Grosso, M. J. *et al.* Intermittent pth administration and mechanical loading are anabolic for periprosthetic cancellous bone. *J. Orthop. Res.* **33**, 163–173 (2015).

249. Amugongo, S. K. *et al.* Effect of sequential treatments with alendronate, parathyroid hormone (1-34) and raloxifene on cortical bone mass and strength in ovariectomized rats. *Bone* **67**, 257–268 (2014).

250. Zhou, H. *et al.* Anabolic action of parathyroid hormone on cortical and cancellous bone differs between axial and appendicular skeletal sites in

mice. *Bone* **32**, 513–520 (2003).

251. Jiang, Y. *et al.* Recombinant Human Parathyroid Hormone (1-34) [Teriparatide] Improves Both Cortical and Cancellous Bone Structure. *J. Bone Miner. Res.* **18**, 1932–1941 (2003).
252. Dunlay, R. & Hruska, K. PTH receptor coupling to phospholipase C is an alternate pathway of signal transduction in bone and kidney. *Am. J. Physiol. Ren. Fluid Electrolyte Physiol.* **258**, F223—F231 (1990).
253. De Groot, T. *et al.* Parathyroid hormone activates TRPV5 via PKA-dependent phosphorylation. *J. Am. Soc. Nephrol.* **20**, 1693–1704 (2009).
254. Tong, G. *et al.* Parathyroid hormone activates phospholipase C (PLC)-independent protein kinase C signaling pathway via protein kinase A (PKA)-dependent mechanism: A new defined signaling route would induce alternative consideration to previous conceptions. *Med. Sci. Monit.* **23**, 1896–1906 (2017).
255. Ba, J., Brown, D. & Friedman, P. A. Calcium-sensing receptor regulation of PTH-inhibitable proximal tubule phosphate transport. *Am. J. Physiol. Renal Physiol.* **285**, F1233—F1243 (2003).
256. Lupp, A. *et al.* Immunohistochemical identification of the PTHR1 parathyroid hormone receptor in normal and neoplastic human tissues. *Eur. J. Endocrinol.* **162**, 979–986 (2010).
257. Traebert, M., Völkl, H., Biber, J., Murer, H. & Kaissling, B. Luminal and contraluminal action of 1-34 and 3-34 PTH peptides on renal type IIa Na-P(i) cotransporter. *Am. J. Physiol. Renal Physiol.* **278**, F792—F798 (2000).
258. Friedman, P. A., Coutermarsh, B. A., Kennedy, S. M. & Gesek, F. A. Parathyroid hormone stimulation of calcium transport is mediated by dual

signaling mechanisms involving protein kinase A and protein kinase C. *Endocrinology* **137**, 13–20 (1996).

259. Horiuchi, N., Suda, T., Takahashi, H., Shimazawa, E. & Ogata, E. In vivo evidence for the intermediary role of 3′,5′-cyclic amp in parathyroid hormone-induced stimulation of lα,25-Dihydroxy vitamin D3 synthesis in rats. *Endocrinology* **101**, 969–974 (1977).
260. Henry, H. L. Parathyroid hormone modulation of 25-hydroxyvitamin D3 metabolism by cultured chick kidney cells is mimicked and enhanced by forskolin. *Endocrinology* **116**, 503–510 (1985).
261. Romero, G. *et al.* Parathyroid hormone receptor directly interacts with Dishevelled to regulate β-catenin signaling and osteoclastogenesis. *J. Biol. Chem.* **285**, 14756–14763 (2010).
262. Tohmonda, T. *et al.* The IRE1α-XBP1 pathway positively regulates parathyroid hormone (PTH)/PTH-related peptide receptor expression and is involved in PTH-induced osteoclastogenesis. *J. Biol. Chem.* **288**, 1691–1695 (2013).
263. Dempster, D. W. *et al.* Normal human osteoclasts formed from peripheral blood monocytes express PTH type 1 receptors and are stimulated by PTH in the absence of osteoblasts. *J. Cell. Biochem.* **95**, 139–148 (2005).
264. Liu, S. *et al.* Bovine parathyroid hormone enhances osteoclast bone resorption by modulating V-ATPase through PTH1R. *Int. J. Mol. Med.* **37**, 284–292 (2016).
265. Gil, Á., Plaza-Diaz, J. & Mesa, M. D. Vitamin D: Classic and Novel Actions. *Ann. Nutr. Metab.* **72**, 87–95 (2018).
266. Demer, L. L., Hsu, J. J. & Tintut, Y. Steroid Hormone Vitamin D: Implications for Cardiovascular Disease. *Circ. Res.* **122**, 1576–1585

(2018).

267. Khundmiri, S. J., Murray, R. D. & Lederer, E. PTH and vitamin D. *Compr. Physiol.* **6**, 561–601 (2016).

268. Zehnder, D. *et al.* Expression of 25-hydroxyvitamin D3-1α-hydroxylase in the human kidney. *J. Am. Soc. Nephrol.* **10**, 2465–2473 (1999).

269. Pérez, A. V. *et al.* Minireview on Regulation of Intestinal Calcium Absorption. *Digestion* **77**, 22–34 (2008).

270. Van Abel, M., Hoenderop, J. G. J., Van der Kemp, A. W. C. M., Van Leeuwen, J. P. T. M. & Bindels, R. J. M. Regulation of the epithelial Ca^{2+} channels in small intestine as studied by quantitative mRNA detection. *Am. J. Physiol. - Gastrointest. Liver Physiol.* **285**, G78—G85 (2003).

271. Fleet, J. C., Eksir, F., Hance, K. W. & Wood, R. J. Vitamin D-inducible calcium transport and gene expression in three Caco-2 cell lines. *Am. J. Physiol. - Gastrointest. Liver Physiol.* **283**, G618—G625 (2002).

272. Fleet, J. C. & Wood, R. J. Specific 1,25(OH)2D3-mediated regulation of transcellular calcium transport in Caco-2 cells. *Am. J. Physiol. - Gastrointest. Liver Physiol.* **276**, G958—G964 (1999).

273. Fleet, J. C. & Wood, R. J. Identification of Calbindin D-9k mRNA and Its Regulation by 1,25-Dihydroxyvitamin D3 in Caco-2 Cells. *Arch. Biochem. Biophys.* **308**, 171–174 (1994).

274. Hemmingsen, C., Staun, M., Lewin, E., Nielsen, P. K. & Olgaard, K. Effect of vitamin D metabolites and analogs on renal and intestinal calbindin-D in the rat. *Calcif. Tissue Int.* **59**, 371–376 (1996).

275. Xue, Y. & Fleet, J. C. Intestinal Vitamin D Receptor Is Required for Normal Calcium and Bone Metabolism in Mice. *Gastroenterology* **136**, 1317-1327.e2 (2009).

276. Van Cromphaut, S. J. *et al.* Duodenal calcium absorption in vitamin D receptor-knockout mice: functional and molecular aspects. *Proc. Natl. Acad. Sci. U. S. A.* **98**, 13324–13329 (2001).

277. Barsony, J., Renyi, I. & McKoy, W. Subcellular distribution of normal and mutant vitamin D receptors in living cells. Studies with a novel fluorescent ligand. *J. Biol. Chem.* **272**, 5774–5782 (1997).

278. Bikle, D. D. Vitamin D metabolism, mechanism of action, and clinical applications. *Chem. Biol.* **21**, 319–329 (2014).

279. Lemon, B. D., Fondell, J. D. & Freedman, L. P. Retinoid X receptor:vitamin D3 receptor heterodimers promote stable preinitiation complex formation and direct 1,25-dihydroxyvitamin D3-dependent cell-free transcription. *Mol. Cell. Biol.* **17**, 1923–1937 (1997).

280. Yasmin, R., Williams, R. M., Xu, M. & Noy, N. Nuclear import of the retinoid X receptor, the vitamin D receptor, and their mutual heterodimer. *J. Biol. Chem.* **280**, 40152–40160 (2005).

281. Zhang, Y. G. *et al.* Tight junction CLDN2 gene is a direct target of the Vitamin D receptor. *Sci. Rep.* **5**, 1–12 (2015).

282. Yoshida, N. *et al.* Calcitonin induces 25-hydroxyvitamin D3 1α-hydroxylase mRNA expression via protein kinase C pathway in LLC-PK1 cells. *J. Am. Soc. Nephrol.* **10**, 2474–2479 (1999).

283. Wongsurawat, N. & Armbrecht, H. J. Calcitonin stimulates 1,25-dihydroxyvitamin D production in diabetic rat kidney. *Metabolism* **40**, 22–25 (1991).

284. Matsui, T., Kuramitsu, N., Yano, H. & Kawashima, R. Suppressive Effect of Calcitonin on Intestinal Absorption of Calcium and Phosphorus in Sheep. *Endocrinol. Jpn.* **30**, 485–490 (1983).

285. Swaminathan, R., Ker, J. & Care, D. Calcitonin and intestinal calcium absorption. *J. Endocrinol.* **61**, 83–94 (1974).

286. Friedman, J., Au, W. Y. & Raisz, L. G. Responses of fetal rat bone to thyrocalcitonin in tissue culture. *Endocrinology* **82**, 149–156 (1968).

287. Hoff, A. O. *et al.* Increased bone mass is an unexpected phenotype associated with deletion of the calcitonin gene. *J. Clin. Invest.* **110**, 1849–1857 (2002).

288. Bonewald, L. F. & Wacker, M. J. FGF23 production by osteocytes. *Pediatr. Nephrol.* **28**, 563–568 (2013).

289. Guo, Y. C. & Yuan, Q. Fibroblast growth factor 23 and bone mineralisation. *Int. J. Oral Sci.* **7**, 8–13 (2015).

290. Liu, S. *et al.* Fibroblast growth factor 23 is a counter-regulatory phosphaturic hormone for vitamin D. *J. Am. Soc. Nephrol.* **17**, 1305–1315 (2006).

291. Burnett, S. A. M. *et al.* Regulation of C-terminal and intact FGF-23 by dietary phosphate in men and women. *J. Bone Miner. Res.* **21**, 1187–1196 (2006).

292. Collins, M. T. *et al.* Fibroblast growth factor-23 is regulated by 1α,25-dihydroxyvitamin D. *J. Bone Miner. Res.* **20**, 1944–1950 (2005).

293. Saito, H. *et al.* Circulating FGF-23 is regulated by 1α,25-dihydroxyvitamin D 3 and phosphorus in vivo. *J. Biol. Chem.* **280**, 2543–2549 (2005).

294. Rodríguez, M. & Rodríguez-Ortiz, M. E. FGF23 as a calciotropic hormone. *F1000Research* **4**, 1–6 (2015).

295. Quinn, S. J. *et al.* Interactions between calcium and phosphorus in the regulation of the production of fibroblast growth factor 23 in vivo. *Am. J. Physiol. Endocrinol. Metab.* **304**, E310—E320 (2013).

296. Rodriguez-Ortiz, M. E. *et al.* Calcium deficiency reduces circulating levels of FGF23. *J. Am. Soc. Nephrol.* **23**, 1190–1197 (2012).

297. Kurosu, H. *et al.* Regulation of fibroblast growth factor-23 signaling by Klotho. *J. Biol. Chem.* **281**, 6120–6123 (2006).

298. Ben-Dov, I. Z. *et al.* The parathyroid is a target organ for FGF23 in rats. *J. Clin. Invest.* **117**, 4003–4008 (2007).

299. Shimada, T. *et al.* FGF-23 is a potent regulator of vitamin D metabolism and phosphate homeostasis. *J. Bone Miner. Res.* **19**, 429–435 (2004).

300. Perwad, F., Zhang, M. Y. H., Tenenhouse, H. S. & Portale, A. A. Fibroblast growth factor 23 impairs phosphorus and vitamin D metabolism in vivo and suppresses 25-hydroxyvitamin D-1α-hydroxylase expression in vitro. *Am. J. Physiol. Renal Physiol.* **293**, 1577–1583 (2007).

301. Mace, M. L., Gravesen, E., Nordholm, A., Olgaard, K. & Lewin, E. Fibroblast Growth Factor (FGF) 23 Regulates the Plasma Levels of Parathyroid Hormone In Vivo Through the FGF Receptor in Normocalcemia, But Not in Hypocalcemia. *Calcif. Tissue Int.* **102**, 85–92 (2018).

302. Krajisnik, T. *et al.* Fibroblast growth factor-23 regulates parathyroid hormone and 1α-hydroxylase expression in cultured bovine parathyroid cells. *J. Endocrinol.* **195**, 125–131 (2007).

303. Khuituan, P. *et al.* Fibroblast growth factor-23 abolishes 1,25-dihydroxyvitamin D3-enhanced duodenal calcium transport in male mice. *Am. J. Physiol. Endocrinol. Metab.* **302**, 903–913 (2012).

304. Centeno, V., Díaz De Barboza, G., Marchionatti, A., Rodríguez, V. & Tolosa De Talamoni, N. Molecular mechanisms triggered by low-calcium diets. *Nutr. Res. Rev.* **22**, 163–174 (2009).

305. Felsenfeld, A., Rodriguez, M. & Levine, B. New insights in regulation of calcium homeostasis. *Curr. Opin. Nephrol. Hypertens.* **22**, 371–376 (2013).

306. Chattopadhyay, N. *et al.* Identification and localization of extracellular Ca^{2+}-sensing receptor in rat intestine. *Am. J. Physiol. - Gastrointest. Liver Physiol.* **274**, G122—G130 (1998).

307. Sheinin, Y. *et al.* Immunocytochemical localization of the extracellular calcium-sensing receptor in normal and malignant human large intestinal mucosa. *J. Histochem. Cytochem.* **48**, 595–601 (2000).

308. Lee, J. J. *et al.* Activation of the calcium-sensing receptor attenuates TRPV6-dependent intestinal calcium absorption. *JCI Insight* **4**, e128013 (2019).

309. Loupy, A. *et al.* PTH-independent regulation of blood calcium concentration by the calcium-sensing receptor. *J. Clin. Invest.* **122**, 3355–3367 (2012).

310. Kantham, L. *et al.* The calcium-sensing receptor (CaSR) defends against hypercalcemia independently of its regulation of parathyroid hormone secretion. *Am. J. Physiol. Endocrinol. Metab.* **297**, E915—E923 (2009).

311. Gallagher, J. C., Riggs, B. L. & Deluca, H. F. Effect of estrogen on calcium absorption and serum vitamin D metabolites in postmenopausal osteoporosis. *J. Clin. Endocrinol. Metab.* **51**, 1359—1364 (1980).

312. Nordin, B. E. C., Need, A. G., Morris, H. A., O'Loughlin, P. D. & Horowitz, M. Effect of age on calcium absorption in postmenopausal women. *Am. J. Clin. Nutr.* **80**, 998–1002 (2004).

313. Nie, X. *et al.* Estrogen Regulates Duodenal Calcium Absorption Through Differential Role of Estrogen Receptor on Calcium Transport Proteins.

Dig. Dis. Sci. **65**, 3502–3513 (2020).

314. Ajibade, D. V. *et al.* Evidence for a role of prolactin in calcium homeostasis: Regulation of intestinal transient receptor potential vanilloid type 6, intestinal calcium absorption, and the 25-hydroxyvitamin D3 1α hydroxylase gene by prolactin. *Endocrinology* **151**, 2974–2984 (2010).
315. Wallace, D. F. The Regulation of Iron Absorption and Homeostasis. *Clin. Biochem. Rev.* **37**, 51–62 (2016).
316. Anderson, G. J. & Frazer, D. M. Current understanding of iron homeostasis. *Am. J. Clin. Nutr.* **106**, 1559S-1566S (2017).
317. Ganz, T. Systemic iron homeostasis. *Physiol. Rev.* **93**, 1721–1741 (2013).
318. Yiannikourides, A. & Latunde-Dada, G. A short review of iron metabolism and pathophysiology of iron disorders. *Medicines* **6**, 85 (2019).
319. Finberg, K. E. Unraveling mechanisms regulating systemic iron homeostasis. *Hematology Am. Soc. Hematol. Educ. Progr.* **2011**, 532–537 (2011).
320. Andrews, N. C. & Schmidt, P. J. Iron Homeostasis. *Annu. Rev. Physiol.* **69**, 69–85 (2007).
321. Firkin, F. & Rush, B. Interpretation of biochemical tests for iron deficiency: diagnostic difficulties related to limitations of individual tests. *Aust. Prescr.* **20**, 74–76 (1997).
322. Ganz, T. Hepcidin and iron regulation, 10 years later. *Blood* **117**, 4425–4433 (2011).
323. Abbaspour, N., Hurrell, R. & Kelishadi, R. Review on iron and its importance for human health. *J. Res. Med. Sci.* **19**, 164–174 (2014).
324. Hunt, J. R., Zito, C. A. & Johnson, L. A. K. Body iron excretion by healthy

men and women. *Am. J. Clin. Nutr.* **89**, 1792–1798 (2009).

325. Theurl, I. *et al.* On-demand erythrocyte disposal and iron recycling requires transient macrophages in the liver. *Nat. Med.* **22**, 945–951 (2016).
326. Ganz, T. & Nemeth, E. Hepcidin and iron homeostasis. *Biochim.Biophys.Acta.Mol.Cell Res* **1823**, 1434–1443 (2012).
327. Anderson, E. R. & Shah, Y. M. Iron homeostasis in the liver. *Compr. Physiol.* **3**, 315–330 (2013).
328. Collins, J. F., Wessling-Resnick, M. & Knutson, M. D. Hepcidin regulation of iron transport. *J. Nutr.* **138**, 2284–2288 (2008).
329. Sharp, P. & Srai, S. K. Molecular mechanisms involved in intestinal iron absorption. *World J. Gastroenterol.* **13**, 4716–4724 (2007).
330. Knutson, M. D. Iron transport proteins: Gateways of cellular and systemic iron homeostasis. *J. Biol. Chem.* **292**, 12735–12743 (2017).
331. Gulec, S., Anderson, G. J. & Collins, J. F. Mechanistic and regulatory aspects of intestinal iron absorption. *Am. J. Physiol. Gastrointest. Liver Physiol.* **307**, G397-409 (2014).
332. Wheby, M. S., Jones, L. G. & Crosby, W. H. Studies on Iron Absorption. Intestinal Regulatory Mechanisms. *J. Clin. Invest.* **43**, 1433–1442 (1964).
333. Muir, A. & Hopfer, U. Regional specificity of iron uptake by small intestinal brush-border membranes from normal and iron-deficient mice. *Am. J. Physiol. - Gastrointest. Liver Physiol.* **248**, G376—G379 (1985).
334. Morgan, E. H. & Oates, P. S. Mechanisms and regulation of intestinal iron absorption. *Blood Cells. Mol. Dis.* **29**, 384–399 (2002).
335. Hooda, J., Shah, A. & Zhang, L. Heme, an essential nutrient from dietary proteins, critically impacts diverse physiological and pathological

processes. *Nutrients* **6**, 1080–1102 (2014).

336. Han, O. Molecular mechanism of intestinal iron absorption. *Metallomics* **3**, 103–109 (2011).

337. Shayeghi, M. *et al.* Identification of an intestinal heme transporter. *Cell* **122**, 789–801 (2005).

338. Donovan, A., Roy, C. N. & Andrews, N. C. The ins and outs of iron homeostasis. *Physiology* **21**, 115–123 (2006).

339. Monsen, E. R. Iron nutrition and absorption: dietary factors which impact iron bioavailability. *J. Am. Diet. Assoc.* **88**, 786–90 (1988).

340. Young, I. *et al.* Association between haem and non-haem iron intake and serum Ferritin in healthy young women. *Nutrients* **10**, 1–13 (2018).

341. Tandy, S. *et al.* Nramp2 expression is associated with pH-dependent iron uptake across the apical membrane of human intestinal Caco-2 cells. *J. Biol. Chem.* **275**, 1023–1029 (2000).

342. Shawki, A. *et al.* Intestinal brush-border Na^+/H^+ exchanger-3 drives H^+-coupled iron absorption in the mouse. *Am. J. Physiol. - Gastrointest. Liver Physiol.* **311**, G423–G430 (2016).

343. Anderson, G. J., Frazer, D. M. & McLaren, G. D. Iron absorption and metabolism. *Curr. Opin. Gastroenterol.* **25**, 129–135 (2009).

344. Valerio, L. G. Mammalian iron metabolism. *Toxicol. Mech. Methods* **17**, 497–517 (2007).

345. Yanatori, I., Yasui, Y., Tabuchi, M. & Kishi, F. Chaperone protein involved in transmembrane transport of iron. *Biochem. J.* **462**, 25–37 (2014).

346. Nishito, Y. & Kambe, T. Absorption Mechanisms of Iron, Copper, and Zinc: An Overview. *J. Nutr. Sci. Vitaminol. (Tokyo).* **64**, 1–7 (2018).

347. Wang, J. & Pantopoulos, K. Regulation of cellular iron metabolism.

Biochem. J. **434**, 365–381 (2011).

348. McKie, A. T. *et al.* A novel duodenal iron-regulated transporter, IREG1, implicated in the basolateral transfer of iron to the circulation. *Mol. Cell* **5**, 299–309 (2000).

349. Gunshin, H. *et al.* Cloning and characterization of a mammalian proton-coupled metal-ion transporter. *Nature* **388**, 482–488 (1997).

350. Galy, B., Ferring-Appel, D., Kaden, S., Gröne, H. J. & Hentze, M. W. Iron regulatory proteins are essential for intestinal function and control key iron absorption molecules in the duodenum. *Cell Metab.* **7**, 79–85 (2008).

351. Zhang, D. L., Hughes, R. M., Ollivierre-Wilson, H., Ghosh, M. C. & Rouault, T. A. A ferroportin transcript that lacks an iron-responsive element enables duodenal and erythroid precursor cells to evade translational repression. *Cell Metab.* **9**, 461–473 (2009).

352. Mastrogiannaki, M., Matak, P. & Peyssonnaux, C. The gut in iron homeostasis: Role of HIF-2 under normal and pathological conditions. *Blood* **122**, 885–892 (2013).

353. Barrett, T. D. *et al.* Prolyl hydroxylase inhibition corrects functional iron deficiency and inflammation-induced anaemia in rats. *Br. J. Pharmacol.* **172**, 4078–4088 (2015).

354. Strowitzki, M. J., Cummins, E. P. & Taylor, C. T. Protein hydroxylation by hypoxia-inducible factor (HIF) hydroxylases: Unique or ubiquitous? *Cells* **8**, 384 (2019).

355. Ramakrishnan, S. K. & Shah, Y. M. Role of Intestinal HIF-2α in Health and Disease. *Annu. Rev. Physiol.* **78**, 301–325 (2016).

356. Ivan, M. *et al.* HIFα targeted for VHL-mediated destruction by proline hydroxylation: Implications for O2 sensing. *Science* **292**, 464–468 (2001).

357. Jaakkola, P. *et al.* Targeting of HIF-α to the von Hippel-Lindau ubiquitylation complex by O2-regulated prolyl hydroxylation. *Science* **292**, 468–472 (2001).

358. Peyssonnaux, C., Nizet, V. & Johnson, R. S. Role of the hypoxia inducible factors in iron metabolism. *Cell Cycle* **7**, 28–32 (2008).

359. Shah, Y. M., Matsubara, T., Ito, S., Yim, S. H. & Gonzalez, F. J. Intestinal hypoxia-inducible transcription factors are essential for iron absorption following iron deficiency. *Cell Metab.* **9**, 152–164 (2009).

360. Mastrogiannaki, M. *et al.* HIF-2α, but not HIF-1α, promotes iron absorption in mice. *J. Clin. Invest.* **119**, 1159–1166 (2009).

361. Taylor, M. *et al.* Hypoxia-inducible factor-2α mediates the adaptive increase of intestinal ferroportin during iron deficiency in mice. *Gastroenterology* **140**, 2044–2055 (2011).

362. Brasse-Lagnel, C. *et al.* Intestinal DMT1 cotransporter is down-regulated by hepcidin via proteasome internalization and degradation. *Gastroenterology* **140**, 1261–1271 (2011).

363. Mena, N. P., Esparza, A., Tapia, V., Valdés, P. & Núñez, M. T. Hepcidin inhibits apical iron uptake in intestinal cells. *Am. J. Physiol. - Gastrointest. Liver Physiol.* **294**, 192–198 (2007).

364. Chung, B., Chaston, T., Marks, J., Srai, S. K. & Sharp, P. A. Hepcidin decreases iron transporter expression in vivo in mouse duodenum and spleen and in vitro in THP-1 macrophages and intestinal Caco-2 cells. *J. Nutr.* **139**, 1457–1462 (2009).

365. Chaston, T. *et al.* Evidence for differential effects of hepcidin in macrophages and intestinal epithelial cells. *Gut* **57**, 374–382 (2008).

366. Papanikolaou, G. & Pantopoulos, K. Systemic iron homeostasis and

erythropoiesis. *IUBMB Life* **69**, 399–413 (2017).

367. Mulachy, L. The erythropoietin receptor. *Semin. Oncol.* **28**, 19–23 (2001).
368. Srai, S. K. *et al.* Erythropoietin regulates intestinal iron absorption in a rat model of chronic renal failure. *Kidney Int.* **78**, 660–667 (2010).
369. Nicolas, G. *et al.* Hepcidin, a new iron regulatory peptide. *Blood Cells. Mol. Dis.* **29**, 327–335 (2002).
370. Kong, W. N. *et al.* Effect of erythropoietin on hepcidin, DMT1 with IRE, and hephaestin gene expression in duodenum of rats. *J. Gastroenterol.* **43**, 136–143 (2008).
371. Kraidith, K. *et al.* Hepcidin and 1,25(OH)2D3 effectively restore Ca2+ transport in β-thalassemic mice: Reciprocal phenomenon of Fe^{2+} and Ca^{2+} absorption. *Am. J. Physiol. Endocrinol. Metab.* **311**, E214–E223 (2016).
372. Charoenphandhu, N. *et al.* 1,25-Dihydroxyvitamin D3-induced intestinal calcium transport is impaired in β-globin knockout thalassemic mice. *Cell Biochem. Funct.* **31**, 685–691 (2013).
373. Benkhedda, K., L'Abbé, M. R. & Cockell, K. A. Effect of calcium on iron absorption in women with marginal iron status. *Br. J. Nutr.* **103**, 742–748 (2010).
374. Phoaubon, S., Lertsuwan, K., Teerapornpuntakit, J. & Charoenphandhu, N. Hepcidin induces intestinal calcium uptake while suppressing iron uptake in Caco-2 cells. *PLoS One* **16**, e0258433 (2021).
375. Lertsuwan, K., Wongdee, K., Teerapornpuntakit, J. & Charoenphandhu, N. Intestinal calcium transport and its regulation in thalassemia: interaction between calcium and iron metabolism. *J. Physiol. Sci.* **68**, 221–232 (2018).

376. Lertsuwan, K. *et al.* Ferrous and ferric differentially deteriorate proliferation and differentiation of osteoblast-like UMR-106 cells. *BioMetals* **31**, 873–889 (2018).

377. Punzo, F. *et al.* Iron chelating properties of Eltrombopag: Investigating its role in thalassemia-induced osteoporosis. *PLoS One* **13**, e0208102 (2018).

378. Lertsuwan, K. *et al.* Differential effects of Fe^{2+} and Fe^{3+} on osteoblasts and the effects of 1,25(OH)2D3, deferiprone and extracellular calcium on osteoblast viability under iron-overloaded conditions. *PLoS One* **15**, e0234009 (2020).

379. Dede, A. D. *et al.* Thalassemia-associated osteoporosis: a systematic review on treatment and brief overview of the disease. *Osteoporos. Int.* **27**, 3409–3425 (2016).

380. Soliman, A., Adel, A., Bedair, E. & Wagdy, M. An adolescent boy with thalassemia major presenting with bone pain, numbness, tetanic contractions and growth and pubertal delay: Panhypopituitarism and combined vitamin D and parathyroid defects. *Pediatr. Endocrinol. Rev.* **6**, 155–157 (2008).

381. Liakakos, D., Vlachos, P., Anoussakis, C., Constantinides, C. & Tsakalosos, I. Calcium metabolism in children suffering from homozygous β thalassaemia after oral administration of 47Ca. *Nuklearmedizin* **15**, 77–79 (1976).

382. Aleem, A., Al-Momen, A. K., Al-Harakati, M. S., Hassan, A. & Al-Fawaz, I. Hypocalcemia due to hypoparathyroidism in β-thalassemia major patients. *Ann. Saudi Med.* **20**, 364–366 (2000).

383. Charoenphandhu, N. *et al.* Na^+/H^+ exchanger 3 inhibitor diminishes

hepcidin-enhanced duodenal calcium transport in hemizygous β-globin knockout thalassemic mice. *Mol. Cell. Biochem.* **427**, 201–208 (2017).

384. Toxqui, L. & Vaquero, M. P. Chronic iron deficiency as an emerging risk factor for osteoporosis: A hypothesis. *Nutrients* **7**, 2324–2344 (2015).
385. Katsumata, S., Katsumata-Tsuboi, R., Uehara, M. & Suzuki, K. Severe iron deficiency decreases both bone formation and bone resorption in rats. *J. Nutr.* **139**, 238–43 (2009).
386. Katsumata, S. I., Tsuboi, R., Uehara, M. & Suzuki, K. Dietary iron deficiency decreases serum osteocalcin concentration and bone mineral density in rats. *Biosci. Biotechnol. Biochem.* **70**, 2547–2550 (2006).
387. Díaz-Castro, J. *et al.* Severe nutritional iron-deficiency anaemia has a negative effect on some bone turnover biomarkers in rats. *Eur. J. Nutr.* **51**, 241–247 (2012).
388. Medeiros, D. M., Stoecker, B., Plattner, A., Jennings, D. & Haub, M. Iron deficiency negatively affects vertebrae and femurs of rats independently of energy intake and body weight. *J. Nutr.* **134**, 3061–3067 (2004).
389. Awortwe, C., Fasinu, P. S. & Rosenkranz, B. Application of Caco-2 cell line in herb-drug interaction studies: Current approaches and challenges. *J. Pharm. Pharm. Sci.* **17**, 1–19 (2014).
390. Lea, T. Caco-2 cell line. in *The Impact of Food Bioactives on Health: In Vitro and Ex Vivo Models* (eds. Verhoeckx, K. et al.) 103–111 (Springer International Publishing, 2015).
391. Chirayath, M. V. *et al.* Vitamin D increases tight-junction conductance and paracellular Ca^{2+} transport in Caco-2 cell cultures. *Am. J. Physiol. - Gastrointest. Liver Physiol.* **274**, G389—G396 (1998).
392. Blais, A., Aymard, P. & Lacour, B. Paracellular calcium transport across

Caco-2 and HT29 cell monolayers. *Pflugers Arch.* **434**, 300–5 (1997).

393. Davies, S. L., Gibbons, C. E., Steward, M. C. & Ward, D. T. Extracellular calcium- and magnesium-mediated regulation of passive calcium transport across Caco-2 monolayers. *Biochim. Biophys. Acta. Biomembr.* **1778**, 2318–2324 (2008).
394. Kessler, M. *et al.* A modified procedure for the rapid preparation of efficiently transporting vesicles from small intestinal brush border membranes. Their use in investigating some properties of d-glucose and choline transport systems. *Biochim. Biophys. Acta. Biomembr* **506**, 136–154 (1978).
395. Bradford, M. M. A rapid and sensitive method for the quantitation of microgram quantities of protein utilizing the principle of protein-dye binding. *Anal. Biochem.* **72**, 248–254 (1976).
396. Hidalgo, I. J., Raub, T. J. & Borchardt, R. T. Characterization of the Human Colon Carcinoma Cell Line (Caco-2) as a Model System for Intestinal Epithelial Permeability. *Gastroenterology* **96**, 736–749 (1989).
397. Peterson, M. D. & Mooseker, M. S. An in vitro model for the analysis of intestinal brush border assembly. I. Ultrastructural analysis of cell contact-induced brush border assembly in Caco-2(BBe) cells. *J. Cell Sci.* **105**, 445–460 (1993).
398. Van Beers, E. H. *et al.* Lactase and sucrase-isomaltase gene expression during Caco-2 cell differentiation. *Biochem. J.* **308**, 769–775 (1995).
399. Walling, M. W. & Kimberg, D. V. Active secretion of calcium by adult rat ileum and jejunum in vitro. *Am. J. Physiol.* **225**, 415–422 (1973).
400. Chow, E. C. Y., Quach, H. P., Vieth, R. & Sandy Pang, K. Temporal changes in tissue 1α,25-dihydroxyvitamin D3, vitamin D receptor target

genes, and calcium and PTH levels after 1,25(OH)2D3 treatment in mice. *Am. J. Physiol. Endocrinol. Metab.* **304**, E977—E989 (2013).

401. Armbrecht, H. J., Boltz, M. A. & Bruns, M. E. H. Effect of age and dietary calcium on intestinal calbindin D-9k expression in the rat. *Arch. Biochem. Biophys.* **420**, 194–200 (2003).
402. Favus, M. J. Factors that influence absorption and secretion of calcium in the small intestine and colon. *Am. J. Physiol. - Gastrointest. Liver Physiol.* **248**, G147—G157 (1985).
403. Favus, M. J., Angeid-Backman, E., Breyer, M. D. & Coe, F. L. Effects of trifluoperazine, ouabain, and ethacrynic acid on intestinal calcium transport. *Am. J. Physiol. - Gastrointest. Liver Physiol.* **244**, G111—G115 (1983).
404. Chen, L., Tuo, B. & Dong, H. Regulation of intestinal glucose absorption by ion channels and transporters. *Nutrients* **8**, 1–11 (2016).
405. Koch, R. O. *et al.* Distribution of DMT 1 within the human glandular system. *Histol. Histopathol.* **18**, 1095–1101 (2003).
406. Camaschella, C. Iron deficiency. *Blood* vol. 133 30–39 (2019).
407. Jimenez, K., Kulnigg-Dabsch, S. & Gasche, C. Management of iron deficiency Anemia. *Gastroenterol. Hepatol.* **11**, 241–250 (2015).
408. Pantopoulos, K., Porwal, S. K., Tartakoff, A. & Devireddy, L. Mechanisms of mammalian iron homeostasis. *Biochemistry* **51**, 5705–5724 (2012).
409. Campos, M. S. *et al.* Interactions among iron, calcium, phosphorus and magnesium in the nutritionally iron-deficient rat. *Exp. Physiol.* **83**, 771–781 (1998).
410. Cotroneo, E. *et al.* Iron homeostasis and pulmonary hypertension: Iron deficiency leads to pulmonary vascular remodeling in the rat. *Circ. Res.*

116, 1680–1690 (2015).

411. Biber, J., Stieger, B., Haase, W. & Murer, H. A high yield preparation for rat kidney brush border membranes Different behaviour of lysosomal markers. *Biochim. Biophys. Acta. Biomembr* **647**, 169–176 (1981).
412. Pan, M. L., Chen, L. R., Tsao, H. M. & Chen, K. H. Iron deficiency anemia as a risk factor for osteoporosis in Taiwan: A nationwide population-based study. *Nutrients* **9**, 1–10 (2017).
413. Collins, J. F. Gene chip analyses reveal differential genetic responses to iron deficiency in rat duodenum and jejunum. *Biol. Res.* **39**, 25–37 (2006).
414. Bronner, F., Pansu, D. & Stein, W. D. An analysis of intestinal calcium transport across the rat intestine. *Am. J. Physiol. - Gastrointest. Liver Physiol.* **250**, G561—G569 (1986).
415. Mackenzie, B., Ujwal, M. L., Chang, M. H., Romero, M. F. & Hediger, M. A. Divalent metal-ion transporter DMT1 mediates both H^+-coupled Fe^{2+} transport and uncoupled fluxes. *Pflugers Arch. Eur. J. Physiol.* **451**, 544–558 (2006).
416. Kesvatera, T. *et al.* Calbindin D9k: A protein optimized for calcium binding at neutral pH. *Biochemistry* **40**, 15334–15340 (2001).
417. Hwang, I. *et al.* Alteration of tight junction gene expression by calcium and vitamin D-deficient diet in the duodenum of calbindin-null mice. *Int. J. Mol. Sci.* **14**, 22997–23010 (2013).
418. Pirklbauer, M. & Mayer, G. The exchangeable calcium pool: Physiology and pathophysiology in chronic kidney disease. *Nephrol. Dial. Transplant.* **26**, 2438–2444 (2011).
419. Asowata, E. O. *et al.* Diet-induced iron deficiency in rats impacts small intestinal calcium and phosphate absorption. *Acta Physiol.* **232**, e13650

(2021).

420. Olusanya, O., Asowata, E., Chichger, H. & Marks, J. Iron deficiency impacts duodenal paracellular calcium absorption via a mechanism involving claudin 2. in *Future Physiology (Liverpool, UK) Proc Physiol Soc 45, PC88* (2019).

421. Guri, A., Gülseren, I. & Corredig, M. Utilization of solid lipid nanoparticles for enhanced delivery of curcumin in cocultures of HT29-MTX and Caco-2 cells. *Food Funct.* **4**, 1410–1419 (2013).

422. Giuliano, A. R., Franceschi, R. T. & Wood, R. J. Characterization of the vitamin D receptor from the Caco-2 human colon carcinoma cell line: Effect of cellular differentiation. *Arch. Biochem. Biophys.* **285**, 261–269 (1991).

423. Krawitt, E. L. & Korson, R. Effect of vitamin D on brush border alkaline phosphatase in the rat small intestine. *Enzyme* **13**, 278–285 (1972).

424. Zoller, H., Theurl, I., Koch, R., Kaser, A. & Weiss, G. Mechanisms of iron mediated regulation of the duodenal iron transporters divalent metal transporter 1 and ferroportin 1. *Blood Cells. Mol. Dis.* **29**, 488–497 (2002).

425. Lesjak, M. *et al.* Quercetin inhibits intestinal iron absorption and ferroportin transporter expression in vivo and in vitro. *PLoS One* **9**, e102900 (2014).

426. Lombardo, T., Ferro, G., Frontini, V. & Percolla, S. High-dose intravenous desferrioxamine (DFO) delivery in four thalassemic patients allergic to subcutaneous DFO administration. *Am. J. Hematol.* **51**, 90–92 (1996).

427. Galanello, R. & Origa, R. Beta-thalassemia. *Orphanet J. Rare Dis.* **5**, 11 (2010).

428. Mobarra, N. *et al.* A review on iron chelators in treatment of iron overload

syndromes. *Int. J. Hematol. Stem Cell Res.* **10**, 239–247 (2016).

429. Jansson, L. T., Perkkio, M. V, Clemons, G., Refino, C. J. & Dallman, P. R. Erythropoietin concentration during the development and recovery from iron deficiency in the rat. *Blood* **65**, 959–963 (1985).

430. Haase, V. H. Hypoxic regulation of erythropoiesis and iron metabolism. *Am. J. Physiol. Renal Physiol.* **299**, F1—F13 (2010).

431. Haase, V. H. HIF-prolyl hydroxylases as therapeutic targets in erythropoiesis and iron metabolism. *Hemodial. Int.* **21**, S110–S124 (2017).

432. Yeh, K. yih, Yeh, M., Polk, P. & Glass, J. Hypoxia-inducible factor-2α and iron absorptive gene expression in Belgrade rat intestine. *Am. J. Physiol. - Gastrointest. Liver Physiol.* **301**, G82—G90 (2011).

433. Yeh, T. L. *et al.* Molecular and cellular mechanisms of HIF prolyl hydroxylase inhibitors in clinical trials. *Chem. Sci.* **8**, 7651–7668 (2017).

434. Shil, A. *et al.* Artificial sweeteners disrupt tight junctions and barrier function in the intestinal epithelium through activation of the sweet taste receptor, t1r3. *Nutrients* **12**, 1–19 (2020).

435. Sharp, P. *et al.* Rapid regulation of divalent metal transporter (DMT1) protein but not mRNA expression by non-haem iron in human intestinal Caco-2 cells. *FEBS Lett.* **510**, 71–76 (2002).

436. Bray, G. L., Taylor, B. & O'Donnell, R. Comparison of the erythropoietin response in children with aplastic anemia, transient erythroblastopenia, and iron deficiency. *J. Pediatr.* **120**, 528–532 (1992).

437. Joosten, E. *et al.* Serum Erythropoietin Levels in Elderly Inpatients with Anemia of Chronic Disorders and Iron Deficiency Anemia. *J. Am. Geriatr. Soc.* **41**, 1301–1304 (1993).

438. Mladenovic, J. & Kay, N. E. Erythropoietin induces rapid increases in intracellular free calcium in human bone marrow cells. *J. Lab. Clin. Med.* **112**, 23–27 (1988).

439. Assandri, R. *et al.* Erythropoietin modulates intracellular calcium in a human neuroblastoma cell line. *J. Physiol.* **516**, 343–352 (1999).

440. Saatci, U., Topaloglu, R., Ozen, S., Bakkkaloglu, A. & Besbas, N. Does erythropoietin have a beneficial effect on calcium, phosphorus and parathyroid hormone levels in pediatric hemodialysis patients? [8]. *Nephron* **67**, 371 (1994).

441. Glover, L. E. & Colgan, S. P. Epithelial barrier regulation by hypoxia-inducible factor. *Ann. Am. Thorac. Soc.* **14**, S233–S236 (2017).

442. Van Itallie, C., Rahner, C. & Anderson, J. M. Regulated expression of claudin-4 decreases paracellular conductance through a selective decrease in sodium permeability. *J. Clin. Invest.* **107**, 1319–1327 (2001).

443. Hou, J., Gomes, A. S., Paul, D. L. & Goodenough, D. A. Study of claudin function by RNA interference. *J. Biol. Chem.* **281**, 36117–36123 (2006).

444. Harris, M. M. *et al.* Dietary iron is associated with bone mineral density in healthy postmenopausal women. *J. Nutr.* **133**, 3598–3602 (2003).

445. Maurer, J. *et al.* Dietary iron positively influences bone mineral density in postmenopausal women on hormone replacement therapy. *J. Nutr.* **135**, 863–869 (2005).

446. D'Amelio, P. *et al.* Role of iron metabolism and oxidative damage in postmenopausal bone loss. *Bone* **43**, 1010–1015 (2008).

447. Blanco-Rojo, R. *et al.* Relationship between vitamin D deficiency, bone remodelling and iron status in iron-deficient young women consuming an iron-fortified food. *Eur. J. Nutr.* **52**, 695–703 (2013).

448. Toxqui, L. *et al.* Low iron status as a factor of increased bone resorption and effects of an iron and vitamin D-fortified skimmed milk on bone remodelling in young Spanish women. *Eur. J. Nutr.* **53**, 441–448 (2014).

449. Shkembi, B. & Huppertz, T. Calcium absorption from food products: Food matrix effects. *Nutrients* **14**, 1–31 (2022).

450. Hellmig, S. *et al.* Gastric emptying time of fluids and solids in healthy subjects determined by 13C breath tests: Influence of age, sex and body mass index. *J. Gastroenterol. Hepatol.* **21**, 1832–1838 (2006).

451. Charoenphandhu, N., Limlomwongse, L. & Krishnamra, N. Prolactin directly enhanced Na^+/K^+- and Ca^{2+}-ATPase activities in the duodenum of female rats. *Can. J. Physiol. Pharmacol.* **84**, 555–563 (2006).

452. Wongdee, K., Rodrat, M., Teerapornpuntakit, J., Krishnamra, N. & Charoenphandhu, N. Factors inhibiting intestinal calcium absorption: hormones and luminal factors that prevent excessive calcium uptake. *J. Physiol. Sci.* **69**, 683–696 (2019).

453. Vogiatzi, M. G. *et al.* Low bone mineral density in adolescents with β-thalassemia. *Ann. N. Y. Acad. Sci.* **1054**, 462–466 (2005).

454. Goyal, M., Abrol, P. & Lal, H. Parathyroid and calcium status in patients with thalassemia. *Indian J. Clin. Biochem.* **25**, 385–387 (2010).

455. Allison, S. J. Claudin 2: role in hypercalciuria and kidney stone disease. *Nat. Rev. Nephrol.* **16**, 252 (2020).

456. Callens, C. *et al.* Targeting iron homeostasis induces cellular differentiation and synergizes with differentiating agents in acute myeloid leukemia. *J. Exp. Med.* **207**, 731–750 (2010).

457. Montalbetti, N. *et al.* Discovery and characterization of a novel non-competitive inhibitor of the divalent metal transporter DMT1/SLC11A2.

Biochem. Pharmacol. **96**, 216–224 (2015).